STUDIES ON THE CATALYSIS AND POST TRANSLATIONAL PROCESSING OF PENICILLIN V ACYLASE

P. MANISH CHANDRA

NATIONAL CHEMICAL LABORATORY
PUNE - 411 008

MAY 2005

STUDIES ON THE CATALYSIS AND POST TRANSLATIONAL PROCESSING OF PENICILLIN V ACYLASE

THESIS SUBMITTED TO

THE UNIVERSITY OF PUNE

FOR THE DEGREE OF

DOCTOR OF PHILOSOPHY

IN

CHEMISTRY (BIOCHEMISTRY)

BY

P. MANISH CHANDRA

DIVISION OF BIOCHEMICAL SCIENCES,
NATIONAL CHEMICAL LABORATORY,
PUNE 411 008 (INDIA)

MAY 2005

DECLARATION

I hereby declare that the thesis entitled "**Studies on the catalysis and post translational processing of penicillin V acylase**" submitted for Ph.D. degree to the University of Pune has not been submitted by me to any other university for a degree or diploma.

P Manish Chandra

Biochemical sciences division
National Chemical Laboratory
Homi Bhabha Road
Pune 411 008

Date:

CERTIFICATE

Certified that the work incorporated in this thesis entitled, "**Studies on the catalysis and post translational processing of penicillin V acylase**" submitted by Mr. P Manish Chandra was carried out by the candidate under my supervision. The material obtained from other sources has been duly acknowledged in the thesis.

(Dr. C. G. Suresh) Date:

Research Guide

Dedicated to

my mentor
Dr. C. G. Suresh

ACKNOWLEDGEMENTS

A journey is easier when we travel together. Interdependence is certainly more valuable than independence. This thesis is the result of four and half years of work whereby I have been accompanied and supported by many people. It is a pleasant aspect that I have now the opportunity to express my gratitude for all of them.

The first person I would like to thank is my supervisor Dr C G Suresh. His integral view on research and his mission for providing 'only high-quality work and not less', has made a deep impression on me. I owe him lots of gratitude for having me shown this way of research. I am really glad that I came to know him in my life. I am indebted to him for valuable suggestions, hints and encouragement in all the time of research and writing of this thesis.

I feel a deep sense of gratitude for Prof Guy Dodson, who changed part of my vision and taught me the stimulating chemistry emanating from X-ray electron density of protein crystals. The happy memory of Prof Guy Dodson provides a persistent inspiration and enthusiasm for my crystallographic journey.

I am obliged to Eleanor Dodson because of her ebullience, interest and support in the most difficult part of my Ph.D. thesis (i.e. chapter 6). Her reciprocal ways of looking at X-ray crystallography through CCP4 programs have added to my understanding of the subject.

The extensive comments and the many discussions and the interactions with Dr Shama Barnabas & Dr M. Islam Khan, had a direct impact on the final form and quality of this thesis. I would like to thank them, for our many discussions and providing me advises and tips that helped me a lot in staying at the right track.

I had the pleasure to work with several people who contributed in the project dearly and have been beneficial for the presented work in this thesis. The site directed mutants used for study in this thesis are prepared by James Brannigan, Asmita Prabhune & Archana Pundle. Ever-smiling Chandra Shekhar Verma modelled the substrate in PVA and did energy minimisation. Although, I did not work with Jim directly, his advice on the overall structure and organisation of project was significantly helpful. I am very much grateful to him for his precious advice and constantly checking the progress of research.

I fall short of words to express my feelings towards Archana Pundle & Asmita Prabhune. Together, they have made an outstanding impact on my abilities to put efforts to get results. I still remember my initial days when I learnt PVA expression and purification from them. I appreciable their time to time help.

Minute details of crystallography from crystal fishing to data collection and processing were introduced to me by Johan Turkenburg. I appreciate his instant suggestions & quick reply on the problematic part of data collection & processing. Synchrotron trips with him were greatly informative.

Lots of thanks goes to Marek, Nicolas, Annabelle, Berry, Anna, Karim, James Faudi, Stefano, Szymon, Sally, Simon Grist, Simon Charnock. It was a pleasure to work with them and the other people of YSBL, York. I thank Lorraine and Dubravka for X-ray data collection of PVA mutant Cys1Gly and Cys1Ser, respectively.

I sincerely thank Prof George Sheldrick and Garib Murshudov for the instant help, whenever ShelxL or Refmac5 stucked with refinement.

My seniors at NCL helped in someway or other. There experiences were extremely useful during the course of Ph.D. Narasimha Rao, Mallikarjun, Late Mukund Katti, Aparna, Ramesh Babu, Ramchander, Bhushan, Prakash, Rachana: Thankyou very much to all.

My labmates gave me the feeling of being at home at work. Priya, Satya, Suresh Kumar, Uma, Poorva & Raamesh. Beside their company in lab, I enjoyed outing and partying with them. Additional energy and vitality for this research was provided externally through my involvement in several social activities. Many thanks for being their kids!

My colleagues from the NCL supported me in my research work. I want to thank them for their help. Many, many people have helped me not to get lost during the development of this thesis. Especially, Anish & Nitin, deserve special thanks for throughout support.

Overnight discussions with Ambrish Rathore helped me understanding and analysing the minute details of chemistry of Ntn-hydrolases. Thanks Ambrish!

I need to acknowledge Indira, Mari, Satyali, Caroline, Louise for the help in administrative work and Mr Trehan, Karanjekar, Kamte, Tim, Sally & Stuart for technical assistance.

Thanks are also due to Mike Bray, Anjanee Rao & Helen Newsome from British council and Deborah Bennett from Association of Commonwealth Universities, London for taking my care during my tenure of commonwealth fellowship at UK. Their endeavours indeed made my stay pleasant and productive.

I also express my sincere appreciation to Uddhavesh Sonawane for quick help in installation of ShelxL on PARAM-Padma. I am grateful to CDAC for providing Tera Scale Supercomputing Facility to us.

Nothing would have been possible without the blessings of my parents and my brothers. I am indebted to them for the love and support and encouragement.

I gratefully acknowledge Council of Scientific and Industrial Research, New Delhi for the award of CSIR Junior and Senior Research Fellowship. I also thank the Commonwealth for a split-site Ph.D. fellowship.

P. Manish Chandra

CONTENTS

LIST OF ABBREVIATIONS

6-APA	:	6- aminopenicillanic acid
7-ACA	:	7-aminocephalosporanic acid
7-ADCA	:	7-aminodeacetoxycephalosporanic acid
AGA	:	Aspartylglucosaminidase
AS	:	Ammonium Sulfate
AmoRe	:	Automated Molecular Replacement
ATCC	:	American Type Culture Collection
BSH	:	Bile Salt Hydrolase
BSTR	:	Batch Stirred Tank Reactor
CCD	:	Charge-Coupled Device
CCP4	:	Colloborative Computational Project No. 4
CID	:	Cumulative Intensity distribution

CPA	:	Cephalosprin Acylase
CPB	:	Citrate-Phosphate buffer
CPC	:	Cephalosporin C
DMF	:	Dimethyl formamide
DMSO	:	Dimethyl Sulfoxide
DTT	:	Dthiothreitol
DQE	:	Detective Quantum Efficiency
EDTA	:	Ethylenediaminetetraacetic acid
ESRF	:	European Synchrotron Radiation Facility, France
GAT	:	Glutamine amido transferase
GCA	:	Glutaryl 7-aminocephalosporanic acid acylase
HXT	:	1,2,6-Hexane tri-ol
HMW	:	high molecular weight
IPTG	:	Isopropyl-β-D-thiogalactopyranoside
LB	:	Luria-Bertani
lit	:	litre
m	:	metre
M	:	molar
mm	:	milli metre
MAD	:	multi-wavelength anomalous dispersion
MB	:	megabytes
MC	:	Magnesium Chloride
min	:	Minute
ML	:	Maltose
MR	:	molecular replacement
Mol. Wt./Mr	:	molecular weight
nm	:	Nano metre
NC	:	Nickel Chloride
NCS	:	non-crystallographic symmetry
NMR	:	Nuclear magnetic resonance
Ntn	:	N-terminal nucleophile
OD	:	Optical density
PAA	:	Phenoxy Acetic Acid
pac	:	Penicillin G Acylase gene
PAGE	:	poly-acrylamide gel electrophoresis
PB	:	Phosphate Buffer
PDB	:	Protein Data Bank
PEG	:	Polyethylene Glycol
PMSF	:	Phenylmethanesulfonyl fluoride
PSI-BLAST	:	Position-Specific Iterated - Basic Local Alignment Search Tool
pv	:	Penicillin V
PVA	:	penicillin V acylase
PGA	:	penicillin G acylase
Pen V	:	Penicilin V (Phenoxymethyl penicillanic acid)
Pen G	:	Penicillin G (Benzyl penicillanic acid)
pre	:	precursor
r.m.s.	:	Root Mean Square
RPBR	:	Recirculated Packed Bed Batch Reactor
rpm	:	revolution per minute
s/sec	:	second
SCB	:	Sodium Cacodylate Buffer,
SDS	:	sodium dodecyl sulfate
SRS	:	Synchrotron Radiation Source, Daresbury, UK

TFPI	:	Tissue Factor Pathway Inhibitors
TMAO	:	Trimethylamine N-oxide
Tris	:	tris-hydroxymethyl amino methane
U	:	Unit
V_m	:	Matthew's number
Å	:	Angstrom
α	:	alpha
α (h,k,l)	:	phase angle
F(hkl)	:	structure factor
σ	:	sigma
Σ	:	summation
∫	:	integration
kDa	:	kilo Dalton
°C	:	degree centigrade
µg	:	microgram
µl	:	microlitre
µM	:	micromolar

ABSTRACT

Penicillin V acylase (PVA) from *Bacillus sphaericus* is an important enzyme employed in the commercial production of 6-aminopenicillanic acid (6-APA), the precursor for a large number of semisynthetic penicillins with important therapeutic advantages. The enzyme PVA specifically hydrolyses Phenoxymethylpenicillin (Penicillin V) to yield 6-APA and the corresponding carboxylic acid. Key to this process is the ability of Penicillin acylase to selectively hydrolyze the amide bond of the side chain keeping the β-lactam amide bond intact.

Out of the two types of Penicillin acylases viz. Penicillin V acylase (PVA) and Penicillin G acylase (PGA) Penicillin G/PGA combination dominated the production of semi-synthetic penicillins because of its long history and productivity. Nevertheless, the greater stability of Penicillin V (Pen V) in aqueous solution especially at lower pH, tolerance of Pen V producing strains to higher concentrations of phenoxyacetic acid allowing higher throughput and a higher concentration of soluble 6-APA are enough reasons to encourage a shift towards processes based on Penicillin V/ PVA combination.

PVA has no detectable sequence homology with PGA although the substrates of these enzymes have related structures. PVA is a homotetramer of molecular weight 150 kDa, whereas PGA is a 90 kDa heterodimer. They showed remarkable structural similarity. The crystal structure of PVA revealed a Cysteine at the N-terminus - this is the fourth residue as per the DNA sequence - indicating the removal of three preceding amino acids during maturation through autocatalytic processing. Post-translational processing is hypothesized to be a common feature of the members of the Ntn hydrolase family.

The three-dimensional structure of PVA consists of two central anti parallel β-sheets sandwiched by helices on either side, resulting in a four layered catalytically active αββα-core structure, found in the proteins of Ntn-Hydrolase family.

The N-terminal nucleophile residue happen to be a cysteine in PVA and Glutamine amidotransferase, whereas it is a Serine in PGA while a Threonine in the Proteasomes. Since the design of the catalytic sites of PVA and PGA is similar, it is reasonable to expect that they share a common catalytic mechanism, the nucleophilic attack on the carbonyl carbon of the beta-lactam R-group carried out by the side chain of N-terminal residue. The free alpha-amino group of this residue acts as the catalytic base that reminds of His in the classical catalytic triad of serine proteases.

The thesis describes the determination of the three-dimensional structures of several selected site directed mutants of Penicillin V Acylase from *Bacillus sphaericus*. Evidence is presented that some of these active site mutations have suppressed the autoprocessing activity either partially or fully. One of the mutants of PVA could be co-crystallized with the substrate penicillin V. The study of the interactions with its substrate has provided probable reasons for the substrate specificity of PVA towards penicillin V.

Chapter One: General introduction:

This chapter presents the literature survey of the research carried out on Penicillin V acylases, especially with respect to their occurrence, properties, gene organization, related enzymes and applications. It is well established that PVA belongs to the Ntn-hydrolase family, specifically integrated with a subfamily called U34 peptidase.

Chapter Two: Materials and Methods:

This chapter describes the details of materials and methods used for the preparation of PVA mutants, their crystallization, X-ray data collection, data processing, structure solution, refinement and

analysis of the refined structure and structural comparison of all the site directed mutants. It also provides details of the materials and methods employed in the purification of PVA mutants. There was one standardized protocol available for the purification of PVA using chromatography on a hydrophobic Octyl-sepharose column. However, for the convenience of purification, some of the mutants were cloned with His-tag at the C-terminal to simplify purification procedure by employing a metal chelating Nickel column.

Hanging drop vapour diffusion technique was the method of choice for crystallizing all the PVA site directed mutants. The X-ray data were collected using CCD detectors at synchrotron sources at ESRF, France and Daresbury, UK. The x-ray images were processed using DENZO and SCALEPACK program in HKL suit. The crystal structures were solved using molecular replacement technique implemented in AMoRe program using native PVA molecule as the model. The Refmac5 program was used for structure refinement in cycles along with the program QUANTA for display and model fitting of the structure. CCP4 suite programs were used for other calculations.

Chapter Three: Crystallization and x-ray data collection of PVA mutants

Several site directed mutants of penicillin V acyalse have been prepared to study the mechanism of autoproteolysis and catalysis. The PVA site directed mutations were chosen near the active site only. None of the mutants were seriously affecting the quaternary structure but some were found not to crystallize under same crystallization conditions. Ammonium sulphate and Poly Ethylene Glycol were used as precipitants to crystallize the proteins. This chapter elucidates the crystallization conditions with different additives used for each one of the mutants.
Selecting a diffracting crystal and collecting useful x-ray diffraction data from it are critical steps in deciphering any structure. Several x-ray data sets were collected for site directed mutants in precursor form, truncated form and in complex with substrate. The data collection details along with x-ray diffraction statistics will be discussed.

Chapter Four: The studies on the Auto-Proteolytic activation of penicillin V acylase from *Bacillus sphaericus*

The gene structure of the open reading frame of PVA from *Bacillus sphaericus* shows an additional tri-peptide Met-Leu-Gly before the N-terminal Cysteine residue. This tri-peptide is processed and removed from the precursor N-terminus to unmask the nucleophilic cysteine with a free alpha-amino group. It is hypothesized that all Ntn-hydrolases share the autocatalytic post-translational processing. We have prepared specific mutants of the enzyme through site directed mutagenesis to produce an inactive form of the enzyme or to yield an unprocessed precursor. Three latter precursor type mutants Cys1Ala, Cys1Ser and Asn175Ala mutants have also been prepared and crystallized. When the structures of the corresponding mutants in the processed form were compared with those of unprocessed ones, some of the features at the active site were found to vary. This suggests the occurrence of a series of events at the scissile bond in the auto-proteolytic process. The central role of the N-terminal nucleophile residue cysteine and of Asparagine 175 of the oxyanion hole in autoproteolysis is clear from this study. The position of Cysteine at the N-terminus seems indispensable in PVA, since the mutation of this residue to Serine, another amino acid known to act as nucleophile, inactivates the enzyme and influences the autoprocessing. The role of a water molecule in autoprocessing will be discussed in detail; the presence of such a water molecule at the active site and its importance is reported in other Ntn hydrolases also.

The structural analysis of the mutants explains the mandatory requirement of cysteine at the C-terminal side of the cleavage site to create an intermediate thio (ester) bond in the place of the scissile peptide bond. By comparing with the reported mechanism of auto-proteolysis this N-S acyl shift can be considered as the first step in the initiation of auto-proteolysis that finally leads to the removal of the tri-peptide at the N-terminus and ends up in the activation of the PVA enzyme.

Chapter Five: The studies on the mechanism of activity of Penicillin V acylase

In the present study we have examined the interaction of PVA with the substrate Penicillin V to understand the binding process and to identify the residues involved. This study is also aimed at understanding the specificity of PVA for Penicillin V irrespective of the fact that Penicillin V (Phenoxymethyl penicillin) and Penicillin G (Benzyl penicillin) have related structures. The specific interaction of penicillin V with the residues at the PVA active site will be the basis for the specificity towards penicillin V. An extra oxygen in the side chain of Pen V differentiates it from Pen G. This oxygen could be contributing to the substrate specificity of PVA. Moreover, the electron withdrawing group present in the side chain can reduce electron density at the carbonyl carbon of the scissile peptide bond and could protect these penicillins from acid degradation. Thus, the electronegative oxygen in the side chain makes penicillin V more acid resistant than penicillin G. The result is that a stronger nucleophile like cysteine is required for the deacylation of Pencillin V.

The crystal structure of Cys1Gly mutant with a bound penicillin V molecule was analysed for understanding the mode of binding of the substrate in PVA.

Chapter Six: The polymorphism, pseudo symmetry and twinning in the crystals of Penicillin V Acylase

Two forms of the native penicillin V acylase have been previously reported (Suresh et al., 1999). In the first form which crystallized in the hexagonal space group $P6_5$ with unit cell parameters a = b = 208.4, c = 96.3 Å (pdb, 2PVA) the N-terminal cysteine was found oxidized into cysteinesulfonic acid. In the other form the N-terminal cysteine remained in the reduced form and the protein crystallized in the triclinic space group P1 with cell parameters a = 47.4, b = 129.6, c = 156.7, $\alpha = 88.3$, $\beta = 83.4$, $\gamma = 84.6^{o}$ (pdb, 3PVA).

The PVA site directed mutants have all crystallized in space groups different from those of the native enzyme. Interestingly, the site directed mutants, which remained as unprocessed precursors of PVA by mutation have all crystallized in Monoclinic space group $P2_1$ (e.g. precursor Cys1Ser, a = 102.64, b = 90.09, c = 102.27 Å, $\beta = 102.13^{o}$). Truncated PVA mutants prepared for co-crystallization studies with Pen V, crystallized in orthorhombic space group $P2_12_12_1$ (e.g. Cys1Gly mutant in processed form, a = 91.76, b = 130.71, c = 158.70 Å). Some other processed form of mutants had a different monoclinic cell with one large cell dimension (eg. Asn175Ala, a = 47.29, b = 379.38, c = 102.01 Å, $\beta = 93.5^{o}$).

Some of the cells are related by simple transformations but with different symmetry. In a few cases the refinement of the structure itself turned out to be challenging due to the presence of pseudo-symmetry or twinning. In this chapter, a detailed comparison of the molecular arrangement in the PVA crystals and discussion on the interaction between symmetrically related molecules in the lattice belonging to different space groups would be included.

CHAPTER - ONE

INTRODUCTION

1. 1. Discovery of antibiotics

In 1928, when working in his laboratory Sir Alexander Fleming, the famous British scientist, observed that the mold *Penicillium notatum* destroyed colonies of the bacterium *Staphylococcus aureus*, proving that some chemical substance produced by the mould was capable of killing the disease-causing bacteria. At that time, nobody took notice of Fleming's discovery. The use of penicillin as a medicine had to wait until 1940s when Howard Florey and Ernst Chain prepared a powdery form of the antibiotic. The effectiveness of penicillin against bacterial infection had been first demonstrated in mice. Later sufficient material was prepared with great difficulty to treat a few human patients (Nayler, 1991a). It was indeed a significant finding that antibiotics could attack bacteria specifically and caused no harm to the organism that produced them.

Large-scale production of penicillin was a serious problem in the beginning. This was overcome by the selection of a strain Penicillium chrysogenum *which greatly increased the titres when grown in large fermentors. Large-scale fermentations also helped to identify a mixture of chemically related penicillins produced and it was demonstrated that the relative amounts of these naturally occurring penicillins depended on the composition of the fermentation medium (Vandamme & Voets, 1974). Subsequently, the selective fermentation of penicillin G (Pen G) was achieved by the addition of phenylacetic acid as an inducer into the fermentation medium. By using similar methods, another penicillin: the penicillin V (Pen V) was produced. Pen V was shown to be more suitable for oral administration on account of its greater stability in acid conditions.*

1. 2. Natural penicillins as antibiotics

Where before the discovery of penicillin, a slight scrape of a rusty nail or injury might lead to death; penicillin soon became the easy way to prevent injuries from getting

infected by bacteria. Following the discovery of penicillins many other antibiotics have also been discovered and have made it possible to cure diseases caused by bacteria such as pneumonia, tuberculosis, and meningitis, saving the lives of millions of people around the world.

Chemical foot printing has revealed that several classes of antibiotics (streptomycin, tetracycline, spectinomycin, edeine, hygromycin and neomycine) protect concise sets of highly conserved nucleotides in 16S ribosomal RNA when bound to ribosomes (Moazed & Noller, 1987). These findings have strong implications for the mechanism of action of these antibiotics.

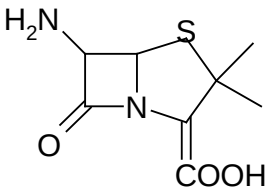

Figure 1. 1

The drawing of penam ring nucleus 6-APA, a common feature found in all natural penicillins.

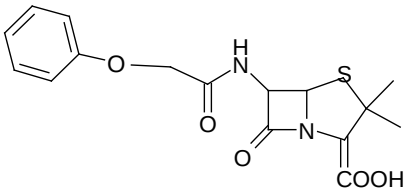

Penicillin V

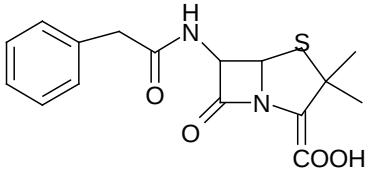

Penicillin G

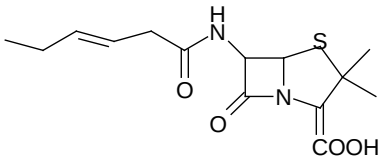

Penicillin F

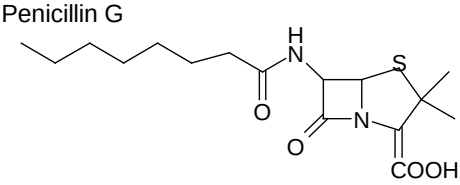

Penicillin K

Figure 1. 2

Figure showing naturally occurring penicillins: Penicillin V, G, F and K.

The first crystal structure of a naturally occurring penicillin, Pen G, was solved by Dorothy Hodgkin and colleagues (Crowfoot *et al.*,1949). It has also been established that several penicillins exist with different acyl side chains (RCH2CO) attached to a common bicyclic (penam ring) nucleus (Figure 1.1 and 1.2). The discovery that the nucleus 6-aminopenicillanic acid (6-APA) is common in different penicillins has lead to the development of semi-synthetic approaches towards preparing novel penicillins starting from 6-APA (Nayler, 1991a; Nayler, 1991b).

During the synthesis of bacterial cell wall the cross linking between two peptide chains attached to polysaccharide backbones is an important step. In such cross-linking, the terminal alanine from each peptide is firstly hydrolyzed and secondly one alanine is joined to lysine through an amide bond. This cross-linking is catalysed by the enzyme transpeptidase. Penicillin binds at the active site of the transpeptidase enzyme by mimicking the substrate D-alanyl-D-alanine. The inhibition carried out by antibiotics by reacting with a serine residue of the transpeptidase is irreversible. Thus, the growth of the bacterial cell wall is effectively prevented and at the same time the antibiotic molecule destroys its stability also.

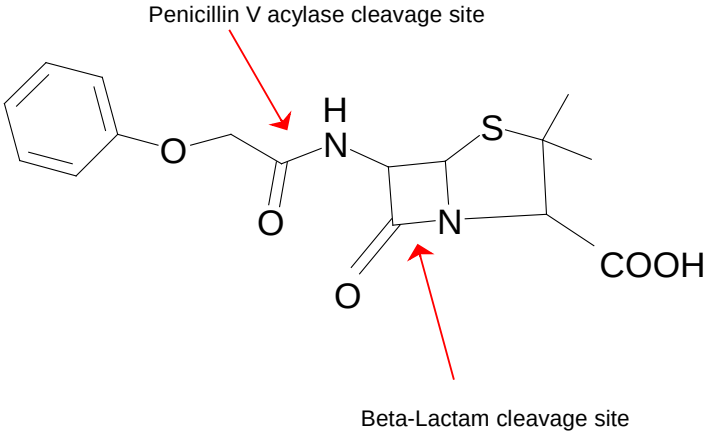

Figure 1. 3

The penicillin V molecule showing the respective hydrolytic bonds, the sites of action of penicillin acylase and β-lactamase.

Application of penicillin as antibiotic was a great discovery that helped save countless patients from death. But bacteria were quick to evolve. At first, the penicillin

was extremely effective against bacterial infections. However, natural selection in bacteria created resistant varieties. As a result the penicillin molecule became susceptible to hydrolytic cleavage not only at the amide bond connecting side chain but also at the β-lactam imide bond (Figure 1.3). β-lactamase is the enzyme capable of hydrolysing the β-lactam imide bond. Evolution and natural selection both are responsible for the changes that resulted from the past 85 years of interaction between bacteria and penicillin.

1. 3. β-lactam acylases

Classification of β-lactam acylases is based on their substrate specificities since their role *in vivo* is not known. They are broadly grouped into two classes; Penicillin acylases and cephalosporin acylases (Deshpande *et al*., 1994). Penicillin acylases (also known as penicillin amidases, penicillin amidohydrolases (EC 3.5.1.11) specifically hydolyse the amide bond connecting the β-lactam nucleus to the side chain of penicillins.

A. Penicillin acylases

Penicillin V acylase (type I)

Penicillin G acylase (type II)

Ampicillin acylase (type III)

Type I, the phenoxy-methyl-penicillin acylase has little activity towards Pen G or other derivatives. PVA occur mainly in moulds and actinomycetes, although bacterial PVA has been isolated from *Bacillus sphaericus*, *Erwina aroideae* and *Pseudomonas acidovorans* (Lowe *et al*., 1981; Olsson *et al*., 1985; Olsson & Uhlen, 1986). These PVAs are mainly intracellular enzymes. PVA from *Fusarium sp*. SKF 235 (Sudhakaran & Shewale, 1995) and Actinomycete *Streptomyces lavendulae* ATCC 13664 (Torres-Bacete *et al*., 2000a) are extracellular acylases.

Type II, the benzylpenicillin acylase or PGA has broader substrate specificity. In addition to Pen G they act on a range of N-phenyl acetyl compounds. PGAs are mainly found in bacteria as periplasmic enzymes. Bacterial PGAs also catalyse the reverse reaction i.e. the synthesis of penicillins from 6-APA and phenyl acetic acid and its derivatives.

Type III, ampicilin acylases have been found in *Pseudomonas melanogenum* (Kim & Byun, 1990). It has no action on pen V or Pen G or related compounds.

B. Cephalosporin acylase

Cephalosporin acylase (CPA)

Glutaryl –7-aminocephalosporanicacid acylase (Gl-7ACA acylase)

Much of the work reported on cephalosporin acylases is relatively recent and although the similarities between the penicillin and cephalosporin acylases will be highlighted, the main discussion will be limited to PVA.

1. 4. Semi-synthetic penicillin to overcome bacterial resistance

Despite the effectiveness of penicillin in curing a wide range of diseases, infections caused by certain strains of staphylococci cannot be cured because the latter produces an enzyme, penicillinase, capable of destroying the antibiotic. Moreover, the over-prescribing of the penicillin drugs led to the development of strains of infections resistant to current antibiotics. Enterococci and other bacteria known to cause respiratory and urinary tract infections were found intrinsically resistant to the action of penicillins.

In order to produce novel penicillins effective against resistant bacteria, a combined fermentation and chemical approach is used which leads to the production of semi-synthetic penicillins (Figure 1.4). Appropriate chemical treatment of a biological precursor to penicillin, isolated from bacterial cultures, resulted in a number of so-called semi-synthetic penicillins. After the mid 1950s a wide range of new penicillins has been developed this way.

Semi-synthetic penicillins exhibit enhanced properties - such as increased stability, easier absorption and fewer side effects - than Pen V and Pen G, and represent a practical solution to the problem of adaptive microbial resistance to antibiotics.

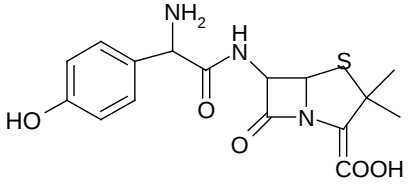

Amoxicillin

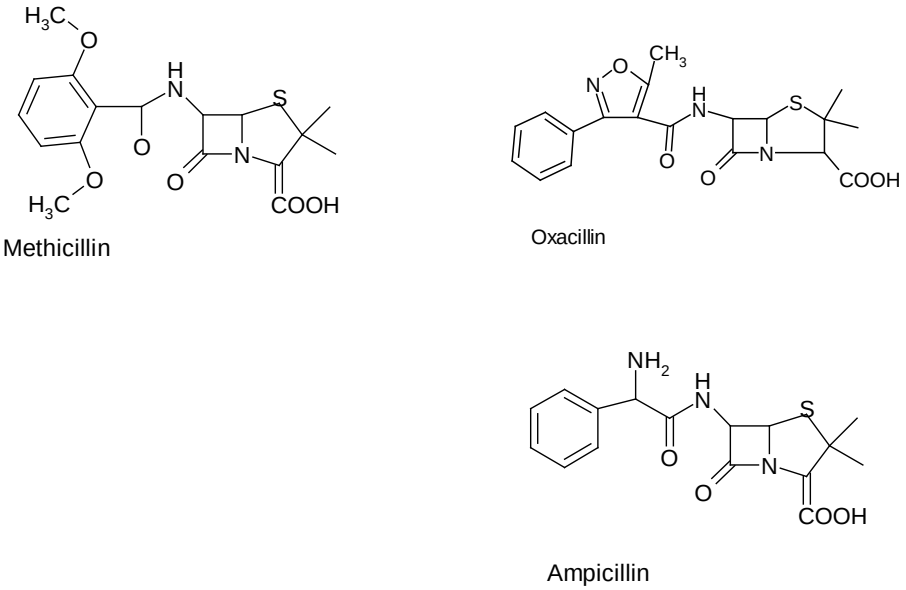

Figure 1. 4

Molecules of some semi-synthetic penicillins. Each of them has specific spectrum of activity against a wide range of organisms.

Ampicillin and amoxicillin are both active against most aerobic gram-positive cocci. *S. aureus* is usually resistant to ampicillin and amoxicillin. The anaerobic gram-positive cocci and rods are generally susceptible to ampicillin, so are some aerobic gram-negative bacilli such as *E. coli*, *Proteus mirabilis*, and *Haemophilus influenzae*. Ampicillin and penicillin are the drugs of choice for the treatment of infections caused by Group B streptococci. Ampicillin, when combined with an aminoglycoside, is effective in treating intra-amniotic infections. Oxacillin or Nafcillin are used in the treatment of complicated skin and skin structure infections.

Carbenicillin has a similar spectrum of activity as that of ampicillin but is also active against *Pseudomonas aeruginosa*. *Klebsiella pneumoniae* is resistant to carbenicillin. Ticarcillin is two to four times more potent than carbenicillin against *P. aeruginosa*. Piperacillin and mezlocillin have greater activity against gram-negative enteric organisms and also provide coverage against most anaerobes and enterococcus. Dicloxacillin is an orally-active semi-synthetic penicillin used to treat infections by bacteria such as *Staphylococcus aureus.*

The most important of these are methicillin and ampicillin, the former is remarkably effective against penicillinase-producing staphylococci and the latter is not only active against all organisms normally killed by penicillin, but also inhibits growth of

enterococci and many other bacteria. In fact, methicillin was the first successful semi-synthetic penicillin introduced in 1959 to overcome the problems that arose from the increasing prevalence of penicillinase-producing *S. aureus* (Livermore, 2000).

Table 1. 1
Semi-synthetic Penicillins

Amoxicillin	Dicloxacillin	Oxacillin
Ampicillin	Flucloxacillin	Piperacillin
Bacampicillin	Methicillin	Pivampicillin
Carbenicillin	Mezlocillin	Pivmecillinam
Cloxacillin	Nafcillin	Ticarcillin

In 1980s, CI-867, a semi-synthetic penicillin exhibited broad-spectrum activity *in vitro* against gram-positive cocci. It was active against *Pseudomonas aeruginosa* and *Klebsiella pneumoniae* (Weaver & Bodey, 1980). All of these newly prepared or identified antibiotics (Table 1.1) have varying effect on different types of microbial pathogens. This has provided evidence for the direct influence of the side chain on spectrum of penicillins and researchers started concentrating on the chemical structure of the side chain.

1. 5. Application of penicillin acylases in the production of semi-synthetic penicillins

The most common antibiotics used are based on the derivatives of 6-APA and 7-ACA, which are manufactured from penicillin. Penicillins are cleaved either chemically or enzymatically (using penicillin acylase) and the 6-APA obtained is then chemically attached with other side chains. In pharmaceutical industry, the enzymatic hydrolysis of Pen V / G and production of semi-synthetic penicillin are accomplished using immobilised penicillin acylase. This is carried out in both Batch Stirred Tank Reactor (BSTR) and Recirculated Packed Bed Batch Reactor (RPBR) on a larger level.

Chemical ring expansion of penicillin plus enzymatic removal of the phenylacetyl side chain is currently being used in industry to obtain 7-

aminodeacetoxycephalosporanic acid (7-ADCA) that is used for the manufacture of semi-synthetic cephalosporins. A biological route requiring only two enzymatic steps (ring expansion and deacylation) might replace this chemical process, thereby reducing costs and environmental problems.

Biotechnological processes for the large-scale production of semi-synthetic penicillins and cephalosporins are focused on the condensation of the appropriate d-amino acid derivative with a β-lactam nucleus catalysed by penicillin acylases (Bruggink *et al.*, 1998; Hoople, 1998; Wegman *et al.*, 2001). The simplest strategy for the enzymatic synthesis of β-lactam antibiotics is the use of equilibrium control or thermodynamically controlled synthesis. This method involves the direct acylation of an appropriate nucleophile such as 6-APA, 7-ACA (7-aminocephalosporanic acid) or 7-ADCA (7-aminodeacetoxycephalosporanic acid) by free acids at low pH values, i.e., conditions under which most of the substrate is present in the non-dissociated form. Water-organic solvent mixtures can be used to bring about an improvement in the direct synthesis of β-lactam antibiotics. As a matter of fact, a high solvent concentration is used to achieve a substantial decrease in the ionized form of the substrate in order to favor the synthetic process. In addition the pK value of substrates and products may be increased, resulting in an increased solubility of the non-dissociated form of the acids (Schroen *et al.*, 1999). For instance, immobilized PGA from *E. coli* and *Kluyvera citrophila* have been successfully employed in the synthesis of antibiotics in non-conventional media containing 50% (v/v) organic solvent (Fernandez-Lafuente *et al.*, 1991; 1996a). Generation of an artificial microenvironment around the immobilized enzyme molecules has proved to increase the stabilizing effect in the presence of high concentrations of organic cosolvents with a minimal loss of catalytic activity (Fernandez-Lafuente *et al.*, 1999; Abian *et al.*, 2001). The combined application of an immobilized biocatalyst (Fernandez-Lafuente *et al.*, 1995), optimized pH value of the reaction medium (Ospina *et al.*, 1996), addition of a suitable solvent (Rosell *et al.*, 1998), and a high concentration of activated side chain donor and β-lactam nucleus (Kaasgaard & Veitland, 1992) have together achieved the best results. Kinetically controlled strategy has proved equally successful for the synthesis of a wide number of different antibiotics such as pivampicillin (Kim & Lee, 1996), amoxicillin (Diender *et al.*, 2000), ampicillin (Illanes

& Fajardo, 2001; Illanes *et al*., 2002; Youshko *et al*., 2002), cephaloglycin (Fernandez Lafuente *et al*., 1996b), cephalexin (Hernandez-Justiz *et al*., 1999; Schroen *et al*., 2001; Aguirre *et al*. 2002), cefazolin (Park *et al*. 2000) and cephalotin (Shaw *et al*., 2000). A remarkable synthesis of different β-lactam antibiotics catalysed by PGA in ice at -20 °C has been reported (Van Langen *et al*., 1999). The synthesis of ampicillin, cephalexin, amoxicillin and cefadroxil catalysed by the soluble enzyme in a frozen medium achieved better results than those obtained in solution at 20 °C. However, immobilized PGA displayed a hydrolytic activity under such conditions.

It should be noted that the search for new variants of β-lactam acylases is an ongoing process, especially within industry where improved catalytic efficiency is the driving force. Penicillin acylase is expected to provide a strong biochemical support to the semi-synthetic penicillin industry.

1. 6. Penicillin G acylases (PGA)

Among all penicillin acylases, PGA (penicillin amidohydrolase, E.C. 3.5.1.11) is the most thoroughly studied and the widely used one by industry. The study of PGA remained the basis for all research on penicillin acylases. It is found in several bacteria as well as in fungi (Vandamme & Voets, 1973; 1974). The synthetic pathway and characteristics of PGA from the Bro1 mutant of *Providencia rettgeri* are similar to those of other PAs from Gram-negative bacteria (Schumacher *et al*., 1986; Thöny-Meyer *et al*., 1992). The catalytic serine is located at the N-terminus of the β-subunit created by the post-translational processing. It is also implied that the substrate specificity is associated with the hydrophobic phenyl moiety of Pen G and not with the β-lactam core.

1. 7. Cephalosporin acylases (CPA)

Like penicillin acylases are useful in the production of 6-APA, cephalosporin acylases are valuable in the production of 7-ACA, which can be used to synthesize semi-synthetic cephalosporins. Irrespective of the low sequence similarity between PAs and CPAs the structural homology at their active sites are impressive. However, despite this

structural conservation, they catalyse very different substrates. Several genes encoding cephalosporin acylases from different sources have been isolated (Matsuda & Komatsu, 1985; Matsuda *et al*., 1987; Aramori *et al*., 1991a; Aramori *et al*., 1991b; Ishii *et al*., 1994; Ishiye & Niwa, 1992; Yang & Yun, 1991; Yang *et al*., 1991). The gene encoding a cephalosporin acylase from *Pseudomonas sp*. 130 (CA-130) has been expressed in *Escherichia coli* and properties of the enzyme have been studied (Zhou *et al*., 1997; Li *et al*., 1998; Chen *et al*., 1998).

The semi-synthetic cephalosporins represent one of the commonly prescribed antibiotics classes. Consequently, there is huge demand for the intermediates of semi-synthetic cephalosporins, 7-ACA and 7-ADCA (Oh *et al*., 2003). In order to meet this need, alternative routes for the production of the intermediates are investigated to replace the currently used processes (Bruggink *et al*., 1998). One of these alternative routes comprises a one-step enzymatic deacylation of either the fermentation product adipyl-7-ADCA (Crawford *et al*., 1995) to 7-ADCA or the fermentation product Cephalosporin C (CPC) to 7-ACA by cephalosporin acylases. However, in spite of the fact that the available cephalosporin acylases are highly efficient in the deacylation of glutaryl-7-ACA, they are much less efficient in deacylating adipyl-7-ADCA and upfront inefficient for the hydrolysis of CPC (Shibuya *et al*., 1981; Kim *et al*., 1999; Li *et al*., 1999).

Figure 1. 5

A PVA monomer is shown with αββα core structure, a characteristic of Ntn-hydrolase family members.

1. 8. Acylases/amidases as members of Ntn-hydrolase family

The traditional classification of proteinases and other amidohydrolases has been based on the residue that acts as the nucleophile. The α/β-hydrolases share a common fold in which the position of the nucleophilic residue is conserved, but not the residue itself. Another exception to the rule came from the observation of chymotrypsin fold in viral 3C proteinases that possessed a cysteine in the place of serine as the nucleophile. Thus, it had been proposed that a more appropriate classification should be the one based on the protein fold and the location of the catalytic group (Murzin, 1996).

The core αββα-structure, the N-terminal nucleophile, and the topology of secondary elements are characteristic features of proteins belonging to N-terminal nucleophile (Ntn) hydrolase superfamily (Brannigan *et al*. 1995). The members of the Ntn-hydrolase family consist of aspartylglucosaminidase (AGA) (Oinonen *et al*., 1995), glutamine phosphoribosyl-pyrophosphate (PRPP) amidotransferase (Smith *et al*., 1994), PGA (Duggleby *et al*., 1995), the 20S subunit of the proteasome (Löwe *et al*., 1995), glucosamine-6-phosphate synthase (Isupov *et al*., 1996), penicillin V acylase (Suresh *et al*., 1999), glutaryl 7-aminocephalosporanic acid acylase (Lee *et al*., 2000a; 2000b) and cephalosporin acylase (Kim *et al*., 2000). Their structures have similar architecture and topology consisting of two layers of β-sheets sandwiched by layers of α-helices (Figure 1.5). On the basis of structural similarity and the observed common location of the catalytic nucleophile (cysteine, serine or threonine) it is suggested that Ntn-hydrolases are evolutionarily related, although the sequence similarities between different sub-families are poor. Their structures show variability in the number of secondary structural elements and the details of arrangement (Brannigan *et al*., 1995; Oinonen & Rouvinen, 2000). However, the common connectivity of sequential elements of secondary structure in these enzymes suggests that the Ntn-hydrolases have diverged from a common ancestor (Brannigan *et al*., 1995). The evolutionary relationship between these hydrolases, although hidden by the absence of sequence similarity, has thus been unveiled on determining their structures. The side chain of the nucleophile residue catalyses the hydrolysis of substrate's amide bond and each enzyme has its own substrate specificity.

Table 1. 2

Ntn-hydrolase family members (PVA: Penicillin V Acylase; PGA: Penicillin G Acylase; CPA: Cephalosporin Acylase; AGA: Aspartylglucosaminidase; GAT: Glutamine amido transferase; GCA: Glutaryl 7-aminocephalosporanic acid acylase).

	PVA	**PGA**	**CPA**	**Proteasomes**	**Human AGA**	**Bacterial AGA**	**GAT**	**GCA**
Structure	Homo-tetramer	αβ-dimer	αβ-dimer	7-member ring?	(αβ)2 hetero-tetramer	(αβ)2 hetero-tetramer	Homotetramer	(αβ)2 hetero-tetramer
Source	Bacterial, fungal,	Bacterial	Bacterial	Archaea yeast	Human	Bacterial	Bacterial	Bacterial
Catalytic function	Penicillin V Acylase	Penicillin G Acylase	Deacylation of Cephalosporin	Protease	Glycosyl-asparaginase	Glycosyl-asparaginase	Amidotransferase	Deacylation of Cephalosporin
Activation	Propeptide removal	Cleaveage in to subunits	Cleaveage in to subunits	Propeptide removal	Cleaveage in to subunits	Cleaveage in to subunits	Propeptide removal	Cleaveage in to subunits
WT structure PDB code	2PVA, 3PVA	1PNK, 1GK9	1FM2, 1GK0, 1GK1	1PMA	1APY, 1APZ	1AYY, 2GAW	1GPH, 1ECF	1OR0
Nucleophile	C1	S264	S1β	T1	T206	T152	C1	S170
Activation site	L2 – G1 – C1	T262-G263-S264	Q168α-G169α-S1β	L2 – G1 – T1	H204-D205-T206	H150-D151-T152	E2 – E1 – C1	Q168-G169-S170
Oxyanion hole in Catalysis	Asn175, Tyr82	A331, N504	N244β, V70β	-	T257, G258	T203, G204	N101, G102	H192, water
Precursor structure PDB code	-	1E3A	1KEH	1RYP	-	9GAA, 9GAC, 9GAW, 1P4K. 1P4V	-	1OQZ
Oxyanion Hole in Autocatalysis	Asn175, Tyr82	A332, N504	Water, H23β	-	T224	T170, water	N101, G102	N413, H192
Proposed general base in autocatalysis	-	Water	Water	Water	Water/D205	D151	Water	Water
Conformational Strain	Yes	Probable	Probable	γ-turn	Probable	Yes	Probable	Yes
Extra cleavage	-	Y260-P261	-	-	Q189-D191, E197-T198	-	-	G160-D161

During post-translational activation of Ntn-hydrolases such as AGA, PGA, cephalosporin acylase, and glutaryl 7-aminocephalosporanic acid acylase, the precursor polypeptide undergoes cleavage removing a spacer chain that results in the chain splitting into two parts in the processed protein, whereas in PVA, proteasome and glutamine PRPP amidotransferase, the activation is achieved by the removal of a small propeptide. This autocatalytic processing considered a common feature of Ntn-hydrolases, is absent in the newly added member - conjugated bile salt hydrolase (BSH). Sequence shows that it is produced with the nulcleophile residue present at the second position in the N-terminus, which gets exposed after enzymatic removal of initiation formyl-methionine without the aid of any autocatalytic processing.

According to the MEROPS database (Rawlings *et al*., 2004) classification, the Ntn-hydrolases form the peptidase clan PB, which is the only clan with three different catalytic types. Ntn-hydrolases represent a superfamily of amidohydrolases that have developed great divergence in sequence, structure, and substrate specificity (Table 1.2). Recently the addition of a new subfamily, peptidase family U34, to the Ntn-hydrolase superfamily is reported (Pei & Grishin, 2003).

A range of autocatalytic processing events proceed *via* protein splicing (Perler *et al*. 1994), where the initial steps are thought to involve an N à S or N à O acyl rearrangement to generate a branched intermediate (Shao *et al*., 1996). The hydrolysis of the peptide bond preceding the N-terminal nucleophile residue in Ntn-hydrolases is similar to the initial step in the protein splicing pathway observed in RecA from *M. tuberculosis* (Davis *et al*., 1992) and TFPI from Yeast (Cooper *et al*., 1993). The acyl rearrangement is strongly pH-dependent with acidic conditions favoring the ester formation and the alkaline conditions the amide formation. It is predicted that in Ntn-hydrolases the nucleophile residue responsible for enzyme catalysis also acts as the nucleophile for the autocatalytic processing (Schmidtke *et al*., 1996; Lee & Park, 1998; Li *et al*. 1999; Hewitt *et al*. 2000; Kim *et al*. 2002). Other residues also may be taking part in both the catalytic and autocatalytic reactions. In the work reported here we would be concentrating exclusively on the specific roles of residues surrounding the catalytic nucleophile Cys1 in PVA.

1. 9. Structural studies on PGA from *Escherichia coli*

Penicillin G acylase (PGA) is a heterodimeric enzyme synthesized as a single-polypeptide precursor that undergoes autocatalytic processing to remove an internal spacer peptide to produce the active enzyme. Intracellular proteolytic degradation of the newly synthesized *E. coli* PA precursor and translocation through the plasma membrane were determined to be the main post-translational processes limiting enzyme production (Ignatova *et al*., 2003). It was also established that simultaneous co-expression of the OmpT pac (penicillin acylase gene) with some proteins of the Sec export machinery of the cell resulted in up to threefold-enhanced PA production. Flores *et al*., (2004) have constructed a single-chain PGA (from *E. coli*) not dependent on autoproteolytic processing. The mature sequence of the β-domain was expressed as the N-terminus of a new polypeptide, connected by a random tetra-peptide to the α-domain, to afford a permuted protein. Active site titration experiments showed that the single-chain protein displayed similar k_{cat} values as the ones obtained with the wild-type enzyme. To test the choice of nucleophile in PGA, when the N-terminal serine of PGA was changed to cysteine both by chemical means (Slade *et al*., 1991) and by site-directed mutagenesis (Choi *et al*., 1992) the enzyme activity was completely abolished.

It has been noted that the PGA gene (pac) is located downstream of a gene cluster encoding the 4-hydroxyphenylacetic acid degradative pathway of *E. coli* W (Prieto *et al*., 1996). The authors proposed that the presence of pac in the proximity of the 4-HPA cluster could mean *that* PGA was a recent acquisition to improve the ability of *E. coli* W to metabolise a wider range of substrates, enhancing its catabolic versatility and at the same time supported the role of PGA as a scavenger enzyme for phenylacetylated compounds (Merino *et al*., 1992). Kinetic experiments with a series of substrates of phenylacetyl-arylamides have shown that at least one polar group in the amine moiety is required for the proper orientation of the substrate in the large nucleophile-binding subsite of penicillin acylase of *E. coli* (Guncheva *et al*., 2004). It has also been shown that in the case of substrates lacking local symmetry, the productive binding implies two nonsymmetrical arrangements with respect to the two positively charged guanidinium residues of ArgA145 and ArgB263. This indicates a crucial role for the specific arginine pair in the substrate-binding and stereoselectivity of penicillin acylase. Alkema *et al*.,

(2000) have characterized the β-lactam binding site of PGA of *E. coli* by structural and site-directed mutagenesis studies.

The crystal structure of PGA from *E. coli* was reported to 1.9 Å resolution (Duggleby *et al.*, 1995). The structure is pyramidal in cross section with a deep cone-shaped depression harboring the active site. The two chains of the heterodimer are closely intertwined, with no obvious discrete domains (Figure 1.6), the α chain is predominantly α-helical with the β chain organized into three regions of which the largest is a β-sandwich motif flanked by α-helices. One side of the sandwich is essentially a flat sheet formed by six anti-parallel strands, with two α-helices packed against it; the other side is a twisted sheet of seven anti-parallel β-strands with a second pair of flanking α-helices. The second domain (B:294-B:439) in the β chain is α-helical where six helices are arranged in two layers, three in the upper and three in the lower, whilst the third domain (B:74-B:142) is a seven stranded anti-parallel β-barrel. Absence of any catalytic base residue at the active site of *E. coli* PGA led to hypothesis that penicillin acylase has a single-amino-acid catalytic centre (Duggleby *et al.*, 1995). Structure of a slow processing precursor of *E. coli* penicillin acylase has revealed that the linker peptide of pro-enzyme blocks the active site cleft (Hewitt *et al.*, 2000). Kasche *et al.*, (1999) have shown that the maturation of penicillin amidase is initiated by intramolecular autoproteolysis.

1. 10. Other penicillin G acylases

Penicillin G acylase from *E. coli* is the mostly studied PA. This protein has guided research on PA from other organisms. Crystal structure of PGA from the *Providencia rettgeri* has been characterized and found similar to other Gram-negative bacterial PAs (McDonough *et al.*, 1999). PA from *Kluyvera citrophila* has been inactivated by N-ethoxycarbonyl-2-ethoxy-1,2-dihydroquinoline (Martin *et al.*, 1993a). Immobilisation of PA from *Streptomyces lavendulae* has been reported by Torres-Bacete *et al.*, (2000a). PA from *Alcaligenes faecalis* has been studied in silico (Braiuca, *et al.*, 2003). Kasche *et al.*, (2003) have shown that fragments of propeptide can activate PA of *Alcaligenes faecalis.*

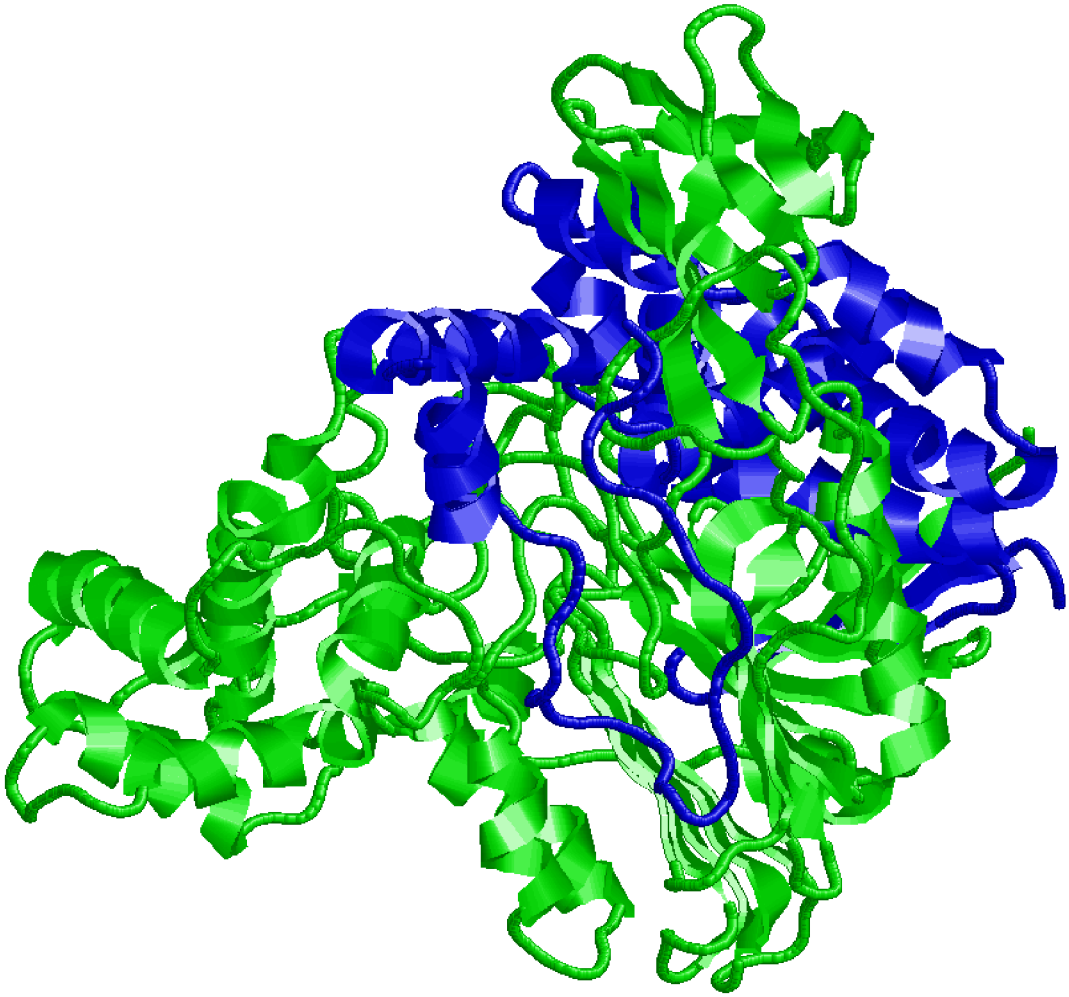

Figure 1. 6

The three-dimensional structure of heterodimeric penicillin G acylase from E. Coli. Chain α, mostly α-helical, has been shown in blue. Chain β which comprises the major part of structure is shown in green.

Some unpublished research has shown evidence of PGA activity in extremely halophilic microorganisms belonging to halophilic archea group. In addition, MEROPS database (Rawlings *et al*., 2004) also shows presence of penicillin acylase homolgues in *Sulfolobus solfataricus*, *Aeropyrum pernix*, *Pyrobaculum aerophilum*, *Archaeoglobus fulgidus*, *Thermoplasma acidophilum* and *Thermoplasma volcanium*.

PGA has been isolated from two fungal sources, *Aspergillus fumigatus* H/6.17.3 and *Mucor griseocyanum* H/55.1 (Jose *et al*., 2003). PGA from *Bacillus megaterium* has been cloned (McCullough, 1983) and being used in industry for chemical synthesis. PGA from *Providencia rettgeri* has been expressed in yeast (Sevo *et al*., 2002; Ljubijankic *et al*., 2002). A thermostable PGA from *Achromobacter xylosoxidans* has been cloned and characterized. (Cai *et al*., 2004). The study has suggested that the increased number of buried ion pair networks, lower Asn and Gln contents, excessive Arg residues, and remarkably high content of Pro residues in the structure of PGA can contribute to its high thermostability. The presence of protein-coding genes of penicillin acylase in *Bacillus anthracis* has been predicted by analytical work of Read *et al*., (2002).

1. 11. Structural studies on cephalosporin acylases (CPA)

Kim *et al*., (2000; 2002) have reported the crystal structures of both the inactive precursor and the active, mature CPA of *Pseudomonas diminuta* (pdb, 1KEH and 1FM2). The core of the enzyme has Ntn-hydrolase fold, and the active site has resembled that of penicillin acylase, otherwise CPA and PGA have no similarity. Kim & Hol (2001) suggested that by mutating bulky residues in the binding site to smaller ones the activity on CPC could be increased. From structures of CPA with bound phosphate and ethylene glycol and with bound glycerol, Fritz-Wolf *et al*., (2002), also proposed mutations that should allow CPA to act more efficiently on CPC.

There is a report suggesting that the recombinant strains of *Acremonium chrysogenum* might produce deacetoxy CPC by fermentation, which can be subsequently converted to 7-ADCA using enzymatic conversion by CPA (Velasco & Barredo, 2000). Otten *et al*., (2002) have changed *pseudomonas SY-77 CPA* into a more efficient adipyl acylase for the conversion of adipyl-7-ADCA into the free cephalosporin nucleus 7-ADCA by the selection of clones from a library of mutants.

.

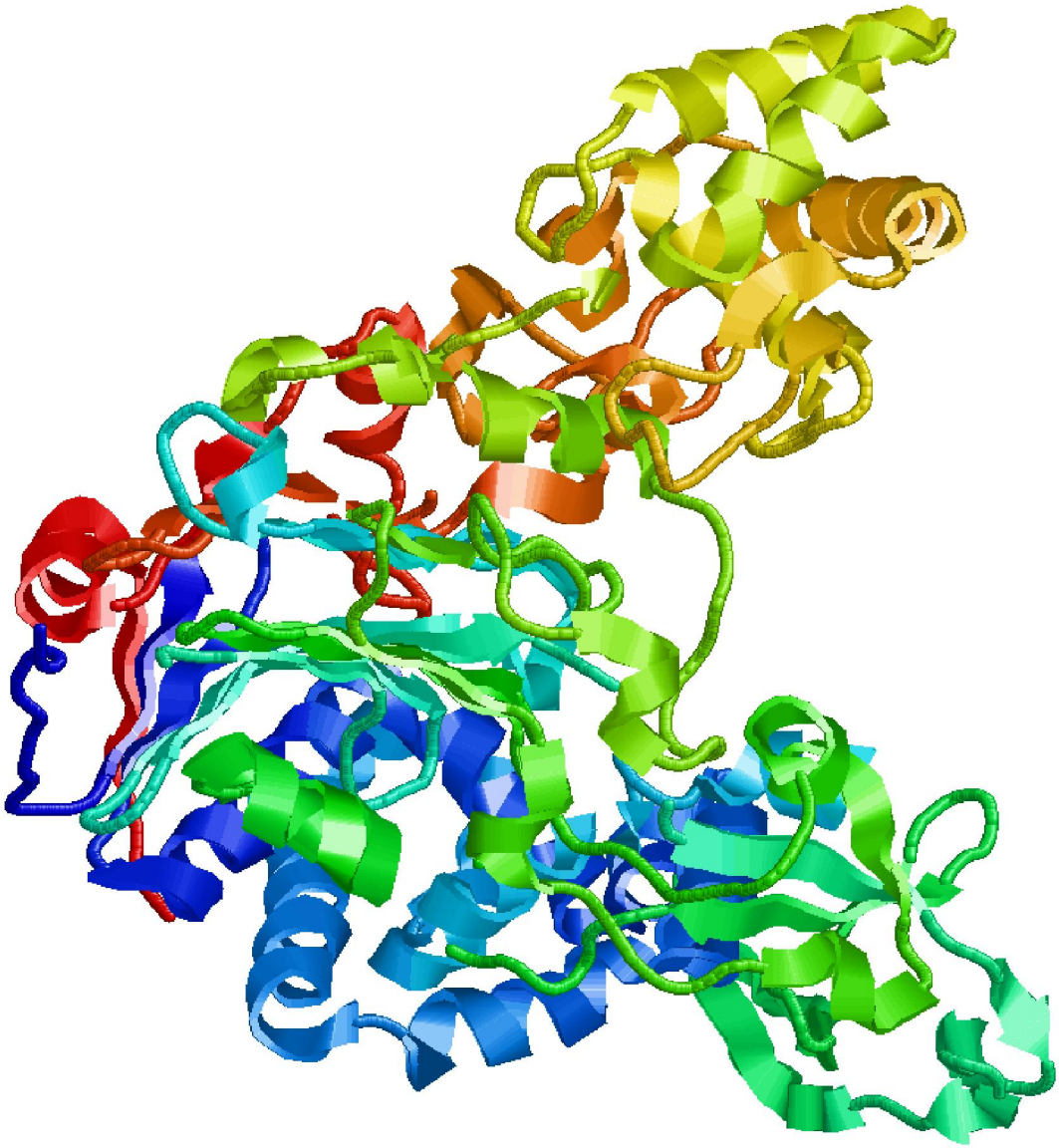

Figure 1. 7

Cephalosporin acylase from Brevundimonas diminuta shows αββα *core structure (pdb, 1FM2).*

Cephalosporanic acylase is a member of the N-terminal nucleophilic hydrolase family of enzymes. The crystal structure of the acylase reveals there is a Ser-His-Glu motif composed of Ser1β, His23β, and Glu455β near the active site. This mimics the catalytic triad of Ser-His-Asp in serine proteases. Experiments have proved that maturation of this enzyme involves autoproteolysis. It has been shown that Ser1β is the catalytic residue for the autoproteolysis and catalytic reaction (Kim *et al*., 2002; 2003a).

The precursor structure of a class I CPA from *Pseudomonas diminuta* reported by Kim *et al*., (2002) at 2.5-Å resolution showed a conserved water molecule, stabilized by four hydrogen bonds in unusual pseudotetrahedral geometry, which plays a key role to assist the O^{γ} atom of Ser1 to generate a strong nucleophile. The crystal structure of cephalosporin acylase in complex with glutaryl-7-aminocephalosporanic acid and glutarate show extensive interactions between the glutaryl moiety of GL-7-ACA and the seven residues that form the side chain binding pocket (Kim & Hol, 2001). These interactions explain why the D-K-aminoadipyl side chain of CPC yields a poorer substrate than GL-7-ACA. It has been suggested that the active site residues of cephalosporin acylase are critical not only for enzymatic catalysis but also for post-translational processing (Kim & Kim, 2001).

Fusion proteins of D-amino acid oxidase and glutaryl-7-aminocephalosporanic acid acylase have been designed to simplify the bioconversion process of cephalosporin C to 7-aminocephalosporanic acid (7-ACA), which is conventionally produced in a two-step enzymatic process (Lowe *et al*., 1995).

Deacylation activity of cephalosporin acylase to cephalosporin C has been improved by changing the side chain conformations of active site residues (Oh *et al*., 2003). Oh *et al*., (2004) has modified the substrate specificity of PGA to cephalosporin acylase by mutating active site residues. Residue Phe375 of cephalosporin acylase has been identified as one of the residues that is involved in substrate specificity (Sio *et al*., 2003).

1. 12. Penicillin V Acylase (PVA)

Random Screening has resulted in the isolation of several microorganisms expressing PVA (Table 1.3) which is contrary to the earlier assumption that PVA is produced mainly by fungus (Hamilton-Miller, 1966). From the early work on 6-APA it has been known that among the actinomycetes *Streptomyces lavendulae* BRL 198 ATCC 13644 can produce PVA (Batchelor *et al*., 1961, Rolinson *et al*., 1960). *Streptomyces ambofaciens* SPSL-15 is reportedly produce an intracellular penicillin G acylase and an extracellular PVA (Nara *et al*., 1971a; Nara *et al*., 1971b). Most of the actinomycetes also produce PVA constitutively (Vandamme *et al*., 1971a; Vandamme, 1980).

Aerobic culture of *Chainia*, a sclerotial *Streptomyces* was reported to produce PVA (Chauhan *et al*., 1998a, 1998b). Similarly, bacteria such as *B. Subtilis, Erwinia aroideae* (Vandamme & Voets, 1975), *Beijierinckia indica* var. *Penicillanicum* (Ambedkar *et al*., 1991), *Arthrobacter sp*. and *B. sphaericus* (Carlsen & Emborg, 1982) are also sources of penicillin acylase. Enzyme production in all these cases has been reported to be from β-lactamase-negative strains. Phenoxyacetic acid has been reported to induce enzyme production.

Among the yeasts, *Candida*, *Rhodotorula*, *Torula*, *Trichosporon* and *Saccharomyces* have been reported to produce PVA (Batchelor *et al*., 1961; Cole, 1966; Vandamme & Voets, 1973). Several genera of fungi have been reported to be producers of PVA (Vandamme & Voets, 1974; Sudhakaran & Borkar, 1985). Enzyme production in most cases is associated with the mycelia, the activity being produced intracellularly. The enzyme from *Pleurotus ostreatus* (*Bovista plumbea*) (Stoppock *et al*., 1980) has been used in the industrial production of 6-APA from Pen V (Savidge, 1975). Several strains of *Fusarium* have been reported to produce PVA (Doctor *et al*., 1964; Lowe *et al*., 1986; Vandamme, 1980; Thadani *et al*., 1972; Sudhakaran & Shewale, 1993a). The enzyme activity has been reported to be present in the spores of *Fusarium conglutinans* (Singh *et al*., 1969) and of *F. moniliforme* (Vandamme *et al*., 1971a, b).

1. 12. 1. Structure of PVA Gene and its organization

Most of the β-lactam acylases are apparently composed of two dissimilar subunits. The only exceptions known so far are PVA from *Bacillus sphaericus*

(homotetramer) and ampicillin acylase from *P. melanogenum* (homodimer). Ampicillin acylase is so referred because of its preferred substrate specificity but in fact it is very similar to α-amino acid ester hydrolase.

Table 1. 3 **List of PVA producing Microorganism**

Organism	References
Bacteria	
Escherichia coli	Cole (1964)
Beijierinckia indica var *penicillianicum*	Ambedkar *et al*.,(1991)
Bacillus sphaericus NCTC 10338	Carlsen & Emborg (1982)
Erwinia aroideae	Vandamme & Voets (1974)
Pseudomonas acidovorans	Carlsen & Emborg (1982)
Pseudomonas diminuta	Carlsen & Emborg (1982)
Micrococcus ureae KY 3769	Nara *et al*. (1971a, 1971b)
Streptomyces lavendulae BRL 198	Batchelor *et al*. (1961)
Streptomyces ambofaciens SPSL-15	Nara *et al*. (1971a, 1971b)
Nocardia globerula KY 3901	Nara *et al*. (1971a, 1971b)
Yeast/Fungus	
Rhodotorula glutinis	Vandamme & Voets (1973)
Saccharomyces	Batchelor *et al*. (1961)
Zygosaccharomyces, Debaromyces, Torula	Cole (1966)
Fusarium sp. SKF 235	Sudhakaran & Shewale (1993a)
Fusarium semitectum	Brandl (1972); Waldschmidt-Leitz & Bretzen (1964)
Fusarium moniliformae AYF 255	Vandamme & Voets (1974)
Pleurotus ostreatus NRRL, 3501, 3824 (*Bovista plumbea*)	Schneider & Roehr (1976)
Penicillium chrisogenum Q 176	Sakaguchi & Murao (1950)
Penicillium chrisogenum Q 9342	Claridge *et al*. (1963)
Penicillium chrisogenum Q 49408	Erickson & Bennett (1965)

Cephalosporium species	Cole (1966)
C. acremonium ATCC 11550	Dennen *et al*. (1971)
Aspergilus niger sp.	Vandamme & Voets (1974)
Emercellopsis minim (stolk) IMI 69015	Cole & Rolinson (1961)
Botrytis cinerea	Batchelor *et al*. (1961)
Gibberella fugikuroi	Vasilescu *et al*. (1966)

In the crystal structure of PVA a cysteine was observed at the N-terminal, whereas the gene sequence predicts an N-terminal sequence of Met-Leu-Gly-Cys-Ser. This finding shows that the three amino acids are processed and removed from the precursor N-terminus to unmask a nucleophile with a free α-amino group. By comparison with other Ntn-hydrolases the N-terminal cysteine in PVA is identified as the catalytic residue (Suresh *et al*., 1999).

1. 12. 2. PVA relation with U34 family

Pei & Grishin (2003) have proposed a sub-family of Ntn-hydrolase, PVA/U34 family which includes peptidase family U34 because of their basic similarities with PVA. The most striking conserved feature in the PVA/U34 family is the catalytic cysteine residue (Figure 1.8 and 1.9). The side chain of the cysteine serves as the nucleophile and the free α-amino group serves as the proton donor and acceptor in the catalytic process. For all Ntn-hydrolases, the nucleophile residue is uncovered in the active enzyme by the removal of the residues on the N-terminal side of it. There is different ways to achieve this in the U34 family proteins (Pei & Grishin, 2003). The acid ceramidases usually have a relatively long sequence of residues at the N-terminal before the nucleophile cysteine. The removal of this N-terminal peptide may be an autoproteolytic process, like in many other Ntn-hydrolases.

The strongest sequence signal for comparison of all PVA/U34 family proteins resides in the motif containing the catalytic cysteine residue and corresponds to the N-terminal β-hairpin in the structure of *B. sphaericus* PVA. Other common features in this motif include the hydrophobic pattern and positions occupied mainly by small residues

near the catalytic cysteine. The β-hairpin motif is longer in the close homologs of U34 family dipeptidases than in the close homologs of PVAs. Two other residues (Arg17 and Asp20) are also highly conserved in most of the PVA/U34 proteins. In the crystal structure of PVA, Arg17 makes hydrogen bonds with atoms belonging to the opposite β-sheet, two with the main chain carbonyl oxygen of Tyr68 and Met80 and one with the side chain carboxyl of Asp69. Considering the interactions, Arg17 should be important in maintaining the overall stability of the structure. A positively charged residue occupies the Arg17 position in PVA/U34 homologues (Figure 1.8 and 1.9). The side chain of Asp20 is hydrogen bonded to free backbone amino group of the catalytic cysteine.

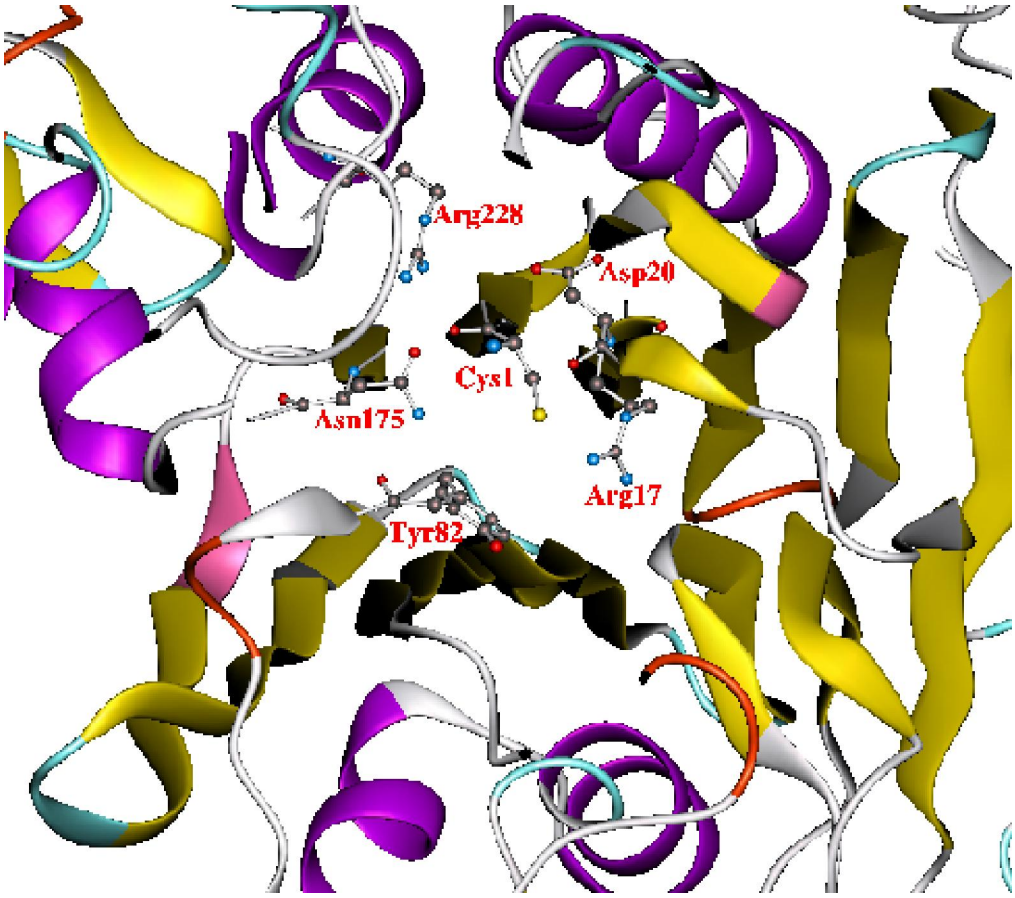

Figure 1. 8

Catalytic pocket of penicillin V acylase showing active site residues Cys1, Asp20, Asn175, Arg228, Tyr82 & Arg17.

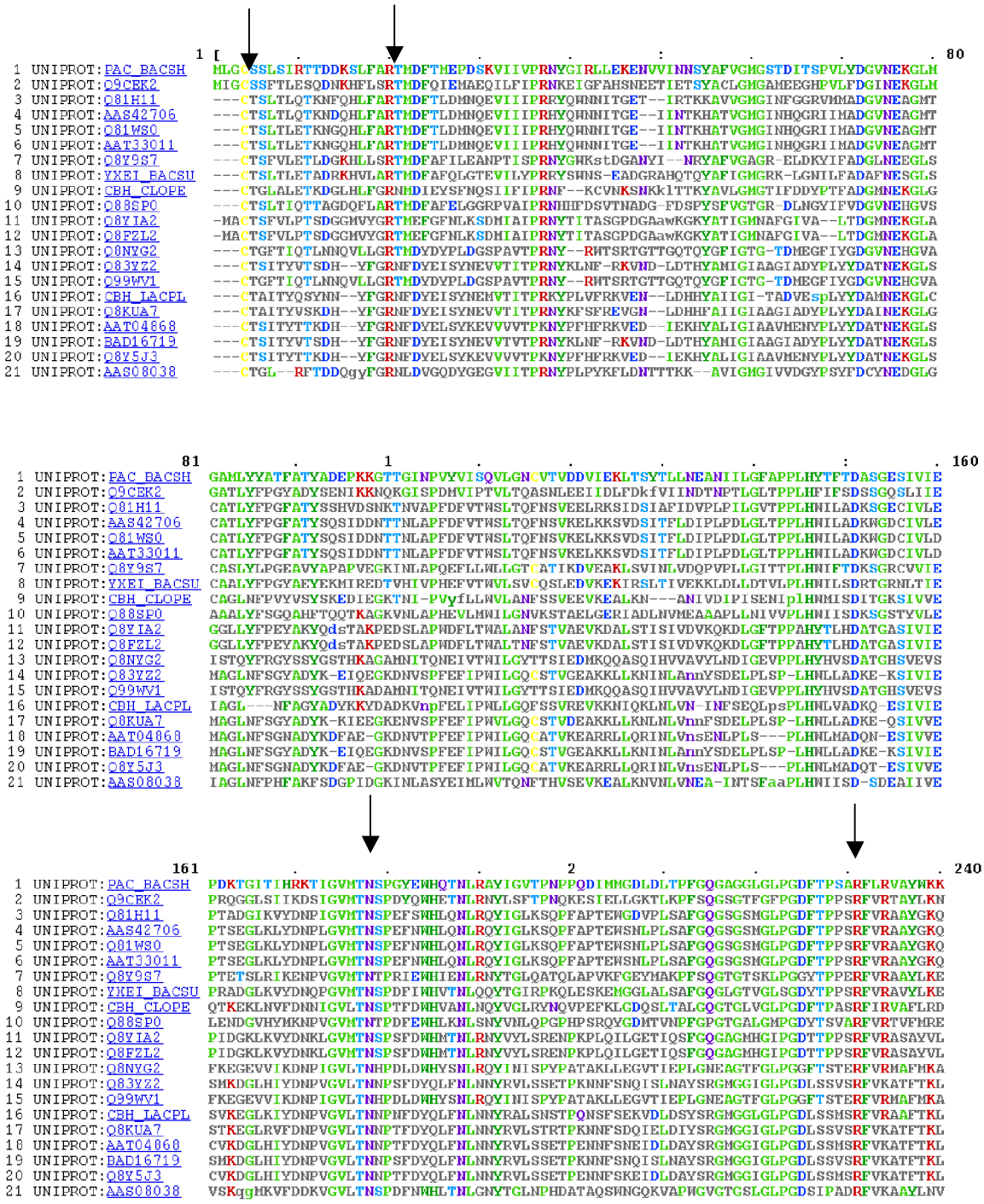

Figure 1. 9 (continued on next page)

Figure 1. 9 (Continued from previous page)

Comparison of PVA and related sequences. Multiple protein sequence alignment is presented to show that corresponding residuesin catalytic site are conserved. Amino acids Cys1, Arg17, Asn175 and Arg228 have been shown at the active site of PVA in figure 1.8.

This interaction is critical for maintaining the orientation of the cysteine residue for catalysis. Conservation of Arg17 and Asp20 is unique in the PVA/U34 family, compared with some of the other Ntn-hydrolase families.

PSI-BLAST alignments of the PVA/U34 homologs are usually restricted to the very N-terminal conserved β-hairpins, not covering the position of Asn175, the oxyanion hole. This indicates that the rest of the sequences are fairly diverse among different PVA/U34 subgroups, which is consistent with the broad spectrum of substrates that different subgroups of these enzymes can accommodate.

Structural comparison has revealed the great diversity in the placement of active site components in different Ntn-hydrolases (Oinonen & Rouvinen, 2000). Even in the PVA/U34 family, a few diverse subgroups have different conservation patterns of residues in the β-hairpin motif.

1. 13. Biochemical studies on PVA from *Bacillus sphaericus*

PVA from *B. sphaericus* has been reported to be a homotetramer (Mr 150 kDa) assembled from four identical subunits of Mr 37.5 kDa containing 338 amino acid residues (Olssen & Uhlen, 1986). The amino acid sequence of PVA has no detectable homology with that of heterodimeric penicillin G acylases. The specific activity of the purified enzyme has been estimated to be 29 $\mu mol.min^{-1}$ mg^{-1} at pH 5.8 and 40 ºC. K_m for the hydrolytic cleavage of Pen V was found to be 10 mM at pH 5.8 and 40 ºC. Regarding the specificity of PVA, it hydrolyses β-lactam antibiotics with preference towards Pen V (100%). Activities for other substrates are penicillin G (6.7%), carbenicillin (1%), cloxacillin (0.8%), dicloxacillin (2%). Beside these penicillin V sulfoxide (15%) and phenoxy acetamide (40.7%) also gets hydrolyzed relatively prominently.

The substrate specificity of this enzyme has been studied in detail (Pundle & SivaRaman, 1997) though not as much as PGA. The enzyme exhibited comparatively high specificity for Pen V. Pen G, and other related compounds were hydrolyzed at less than 10% of the rate of Pen V. High rate of hydrolysis was observed when the side chain of the substrate molecule was unsubstituted. Unlike PGA, which is capable of hydrolysing a diverse range of amides, PVA is active primarily on Pen V.

1. 13. 1. Chemical modification and related functional studies

No specific information is available in the literature on the mechanism of action and the active site residues of PVA. PGA has been investigated in greater detail. A number of residues and residue types important for enzyme function have been implicated in the case of PVA. This identification is based on sequence information and random chemical modification to more precise and intuitive mutagenesis experiments. Our own experiments have now clearly implicated certain residues in PVA activity.

Incubation of PVA from *B. sphaericus* with the lysine-modifying reagent, 2,4,6-trinitrobenzene sulfonic acid resulted in inactivation (Pundle & Sivaraman, 1997). The kinetics of inactivation indicated the presence of a single essential lysine moity per active unit of the enzyme. Pen V fully protected the enzyme against inactivation whereas phenoxyacetate and 6-APA did so partially. A comparison of the far-UV CD spectra of the modified enzyme showed no changes in its gross conformation. This result indicated that a putative single essential lysine residue is present at or near the active site of each subunit of the homotetrameric enzyme. The crystal structure, however, did not show any lysine at the immediate vicinity of the active site. There are few lysine residues near (though not very adjacent to) the active site. A possible explanation will be that the reaction has detected free N-terminal α–amino group rather than lysine ε-amino group.

The serine-modifying reagent phenylmethanesulfonyl fluoride (PMSF) also inactivated the PVA enzyme. Kinetics of the inactivation indicated the presence of a single essential serine per active unit of enzyme. Pen V partially protected the enzyme against inactivation while phenoxyacetate decreased inactivation to a much lower extent, indicating the possible presence of the serine residue at the catalytic site (Pundle & Sivaraman, 1997). It shall be noted that, the serine reagent phenylmethylsulfonyl fluoride, structurally resembles the side chain of Pen G, which in turn may have inactivated the PVA.

Organic solvents were found to modulate the hydrolytic activity of PVA from *Streptomyces lavendulae*. On one hand, the addition of water soluble co-solvents increased the catalytic activity up to a critical concentration of the non-aqueous solvents, further increase of the latter led to protein denaturation. For alcohols and aprotic polar solvents, there is linear correlation between the critical concentration of water miscible co-solvent and the dielectric constant of the co-solvents added. On the other hand, water-immiscible solvents showed activating or inhibitory effects that might be related to interactions between the structure of the solvent and the enzyme.

Understanding the molecular mechanisms involved in the regulation of the biosynthesis of penicillin acylase is important not only from a molecular biology point of view but also for the enzyme's commercial applications. A greater understanding would be beneficial for improving the cost efficiency of acylase production. Despite the amount

of work carried out in this area it is still not fully understood. It is a fact that the regulation of acylase production varies greatly from organism to organism.

1. 14. Structural studies on *B. sphaericus* PVA

The crystal structure of PVA has been determined to establish the nature of its catalytic mechanism and to identify its biochemical and structural relationships with PGA and other Ntn-hydrolases (Suresh *et al*., 1999). The PVA molecule is a well-defined tetramer with 222 organization made from two dimers (A and D) and (B and C), which generates a flat disc-like assembly. The X-ray analysis revealed that the PVA monomer contains two layers of central anti-parallel β-sheets, above and below which is a pair of anti-parallel helices. There are two extensions, one from the upper pair of helices and the other at the C-terminal segment, that interact with the neighbouring monomers in the tetramer and help stabilize it. The β-sheet and helix organization and connectivity are characteristic of members of the Ntn-hydrolase family (Suresh *et al*., 1999).

1. 14. 1. Residues thought to be important for catalysis and autoproteolysis

The PVA and PGA enzymes, although sequentially unrelated, share a distinctive structural core. Both PVA and PGA have approximately the same angle (+30°) between the β-strands of the two layers of β-sheets, which are decorated by the active site residues as in other Ntn-hydrolases. Use of these β-sheets for structural alignment reveals that the catalytic regions of PVA and PGA overlap with a root mean square (r.m.s.) deviation of 0.46 Å for the catalytic atoms. The oxyanion hole in PVA consists of ND2 atom of Asn175 and the NH of Tyr82, which can be compared with the corresponding atoms ND2 of Asn B241 and NH of Ala B69 of PGA. Other overlapping residues of the active sites of PVA and PGA include those of arginine (residue 228 in PVA and B263 in PGA), and the oxygens of Asp20 and Asn175 in PVA and Gln B23 and Asn B241 in PGA, which are critical for positioning the lone pair of the unprotonated N-terminal α-amino group (Suresh *et al*., 1999). This comparative study helped in predicting the active site residues thought to be important in activity. The selected residues for site directed mutagenesis studies were Cys1, Asp20, Asn175 and Arg228. Although Tyr82 has been

identified as an important residue in oxyanion hole, no mutation was attempted on it, as its main chain N atom only is involved in oxyanion hole formation.

1. 15. PVA as bile salt hydrolases (BSH)

Since the bile acid hydrolases (BSH) have extensive sequence similarity to PVA (Christiaens *et al*., 1992) and typically have an N-terminal methionine followed directly by cysteine, these enzymes have been assigned to the Ntn-hydrolase family (Suresh *et al*., 1999). By analogy with PVA it had been proposed that Cys2 is the active residue in BSH, that is, the active residue is revealed by simple processing of the initiation formyl-methionine (Suresh *et al*, 1999). This is equivalent to the process seen in the Ntn-hydrolase glutaminase domains of *E. Coli* glucosamine-6-P-synthase (Isupov *et al*., 1996) and glutamine PRPP amidotransferase (Kim *et al*., 1996). The relationship of PVA to the choloylglycine hydrolase enzymes sub-family may well help define the real physiological role of penicillin acylases. In addition, PVA and BSH are a fresh test-bed for protein engineering experiments to address the pharmaceutical need to enlarge penicillin specificity to cephalosporins. Indeed, there are natural antibiotics (collectively known as cephalosporin P) (Burton & Abraham, 1951), which are elaborations of the C27 steroid cholesterol nucleus of conjugated bile acids, hinting at a possible distant evolutionary link between antibiotics and cell signaling molecules.

1. 16. *In vivo* role of penicillin acylases

The question of the physiological role of penicillin acylase has been overshadowed by the attention paid to its industrial applications. The question still remains essentially unanswered although evidence suggests that the PVA gene is related to pathways involved in the assimilation of aromatic compounds as carbon sources.

It was suggested that penicillin acylase is involved in the degradation of phenoxyacetylated compounds for the generation of phenoxyacetic acid, which may be used as a carbon source and could act as an inducer of the degradative pathway (Valle *et al*, 1991). Since its initial suggestion, the location of penicillin acylase gene in *E. coli* near a gene encoding for an aromatic hydroxylase has been discovered (Prieto *et al*., 1993). Later the nucleic acid sequence of a 14855 base pair region that contains the complete gene cluster encoding 4-hydroxyphenylacetic acid degradative pathway of *E.*

coli W ATCC 11105 was determined (Prieto *et al*., 1996). The gene cluster is located in a region close to the gene encoding for PGA.

It has been therefore suggested that PGA is present in *E. coli* W to improve its ability to metabolize a wider range of substrates. Penicillin acylases are able to hydrolyze phenylacetylated compounds, the products that may then be fed into 4-hydroxyphenylacetic acid degradative pathways, thus enhancing the catabolic versatility of *E. coli*.

Although evidence presents this role for penicillin acylase, this pathway is of little use when *E. coli* lives as a parasite, since usually richer carbon sources will be then readily available. Nevertheless, when *E. coli* moves into its free living state, for example in soil, the utilisation of alternative carbon sources becomes necessary. Phenyl acetic acid derivatives would be available abundantly in this kind of nonparasitic environment (Burlingame & chapman, 1983).

PVA expression in *Vibrio cholerae* has been found to link with pathogenesis in response to cell density (Kovacikova *et al*., 2003). AphA, activator of a virulence operon, has a second binding site upstream of gene encoding PVA. It has been recognised as a negative regulator of PVA (Kovacikova *et al*., 2003). High levels of AphA represses the expression of PVA and activates tcpPH expression and the rest of the virulence cascade.

Kovacikova *et al*, (2003) showed that AphA (activator of virulence operon) negatively regulates PVA gene expression in both the classical and El Tor biotypes of *V. cholerae* by binding to a site virtually identical to a promoter, which overlaps with the PVA transcriptional start site. In El Tor strain C6706, the PVA gene is also regulated by quorum sensing such that its expression is reduced at low cell density. Since PVA does not appear to play a role in virulence, the ability of AphA to oppositely regulate PVA expression compared to virulence gene expression may provide *V. cholerae* with advantages in different environmental niches.

1. 17. Applications of PVA

In the 1950's it had been shown that an enzyme, later named as penicillin acylase, could hydrolyze penicillin (Sakaguchi & Murao, 1950; Murao, 1955). Later Rolinson *et*

al. (1960) demonstrated the practical importance of this enzymatic reaction, in which 6-APA was produced through the hydrolysis of natural penicillin, providing an elementary starting point for the production of semi-synthetic penicillins. Indeed the naming of penicillin acylase has been a reflection of this reaction and its industrial application in the synthesis of antibiotics.

The enzymatic cleavage of natural penicillins that was initially performed using cell free extracts was not found commercially competitive with the more efficient chemical deacylation process. The introduction of immobilized enzymes, which allows multiple use of the catalyst, is now the method of choice. Immobilized penicillin acylases are currently used in the industrial production of 6-aminopenicillanic acid (6-APA), the key intermediate of semi-synthetic penicillins (Sudhakaran & Shewale, 1993b).

1. 17. 1. 6-APA production

The worldwide demand for semi-synthetic penicillins, as the most successful and cost-effective antibiotics, has brought 6-APA into central position as a major pharmaceutical product (Lowe *et al*., 1981). Historically the β-lactam nucleus 6-APA was first isolated on an industrial scale from fermentation by *penicillium chrysogenum* (Ballio *et al*., 1961; Batchelor *et al*., 1959, 1961). It was then produced by the enzymatic synthesis of the precursor Pen V or Pen G by the supplementation of phenoxyacetate or phenylacetate, respectively to commercial Penicillium chrysogenum fermentation (Carrington, 1971; Claridge *et al*., 1960; Claridge *et al*., 1963; Kaufmann & Bauer, 1964; Rolinson *et al*., 1960) and then by the removal of their side chain either by chemical splitting or enzyme catalysed cleavage. Industrially, the removal of the acyl side chain group is currently carried out by means of immobilised PA (Savidge & cole, 1975; Shewale *et al*., 1990; Sudhakaran & Shewale, 1993b). Immobilized PGA is mainly utilized in this process, which accounts for 88% of the worldwide production of 6-APA.

Nevertheless, the use of PVA has been reported to be more advantageous in 6-APA production when using Pen V as a substrate (Shewale & Sudhakaran, 1997). The 6-APA can then be utilised to produce a wide range of semi-synthetic penicillins by attaching different side chains. This addition of side chain can again be achieved by chemical or enzymatic means. PVAs can be made to catalyse the acylation of 6-APA for

which immobilised acylases have been successfully used. However, its commercial application has been limited by low yields and due to availability of other simple acylation procedures. It is hoped that by understanding more about the structure of penicillin acylases and details of interaction with side chain ligands, one can suggest ways of increasing the efficiency of the enzyme catalysis and its acceptability in future for the production of new penicillins.

Over the years much effort has been put in the search for penicillins, which have better therapeutic properties (Nayler, 1991a & b). This has been achieved by changing the properties of the molecule by altering the side chain. For example, the stability at low pH can be increased by introducing an electron withdrawing group into α-position of the side chain e.g. α-phenoxyethylpenicillin. This is especially beneficial when the antibiotic is administered orally since it acquires greater resistance to degradation by acids in intestine. Antibiotics have also been found which are resistant to β-lactamase degradation e.g. triphenylmethylpenicillin. It has been suggested that the steric hindrance around the side chain amide group leads to a diminished affinity for β-lactamase.

1. 17. 2. Ring expansion

The manufacture of therapeutically important cephalosporins can be achieved also by a chemical ring expansion of the thiozolidine ring to a dihydrothiazine in Pen V or Pen G (Verweij & de Vroom, 1993). During the course of this reaction the amino group remains protected as phenoxyacetyl or phenylacetyl amide which is finally removed by PVA or PGA. Of particular importance is the choice of a suitable protecting function for the COOH group. It must be stable during the ring expansion but could be removed without damaging the cephalosporin nucleus. This has been achieved using phenylacetyloxymethylene (Baldaro *et al*., 1988).

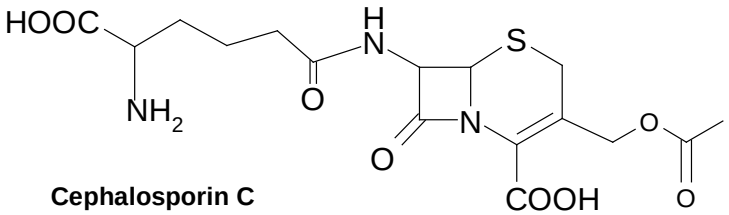

Cephalosporin C

Figure 1. 9

The thiozolidine ring in penicillin V can be expanded into a dihydrothiazine by ring expansion. Latter one is the nucleus for the cephalosporins.

1. 17. 3. Altering substrate specificity

In addition to the applications of PVA already described for penicillin acylases expanding the range of substrates which the enzyme can accept and also increasing its catalytic efficiency towards those substrates will further benefit its industrial use. The most common approach followed today is the site directed mutagenesis; this will be more effective if prior knowledge of the three-dimensional structure of the protein or of the position of residues, which are important for catalysis and binding, are known. The method of selective pressure or directed evolution is an alternate method.

Selective pressures have been used previously to direct the evolution of enzymes. This approach has been successfully used to alter the substrate specificity of aliphatic amidase (Betz *et al*., 1974), ribitol dehydrogenase (Mortlock, 1982), β-lactamase (Hall & Knowles, 1976), β-galactosidase (Campbell *et al*., 1973) and alcohol dehydrogenase (Wills, 1976). The use of selective pressure to alter the enzyme characteristics offers the advantage that only catalysts with greater effectiveness are obtained and prior knowledge of the enzyme structure or enzyme-substrate interaction is not needed. This approach provides a useful method to identify the amino acid residues and the protein domains that affect the substrate binding and catalysis and can lead to the development of improved enzymes.

In a similar study it was shown that substrate specificity could be altered to hydrolyze substances with α-aminophenylacetyl moieties at relatively low pH (6.5) by using the substrate D(-)phenylacetyl-L-leucine (Forney & Wong, 1989). This is important for two reasons: the first is that this substrate has cephalexin side chain, cephalexin being another very important commercial antibiotic. The second is that the catalytic efficiency of the enzyme will increase if it could work at pH where the α-amino group is in

protonated state. Mutants showed increased catalytic efficiency for the substrate compared to the wild type enzyme.

1. 18. Scope of the thesis

Analysis of structural and mechanistic information, sequence comparisons, and site-directed mutagenesis continue to provide basis for the rational design of new protein functions and the alteration of existing functions. Random mutagenesis and 'directed evolution' approaches are one way of fine-tuning of properties such as substrate specificity of enzymes. The rational design of an enzyme's catalytic site requires extensive knowledge of the catalytic mechanism and enzyme structure. For this reason, it is imperative to study the role of individual active site residues in the autoproteolysis and catalysis. Information on the functional relationship of individual residues would help in predicting their putative role in the enzyme catalysis.

The study is aimed at understanding the post-translational processing and catalytic mechanism of PVA mainly using X-ray crystallographic and mutational studies. The putative active site of PVA has been identified based on structural comparison with PGA. The residues that are expected to play a role in catalysis have also been identified. Here our strategy is to prepare and study the crystal structure of site directed mutants of the PVA, mutated at these residues. Most of these mutants show loss of activity for which the three-dimensional crystal structure tells whether the mutant is catalytically inactive or the activity is suppressed due to lack of autoprocessing. This observation has helped to distinguish between the residues important for processing of the precursor and the residues that are directly involved in catalysis.

A careful study of mutants prepared based on available information, has helped to identify some of the active site functional groups and their role in catalysis. The truncated inactive mutant mimics the active form and had been used for binding the substrate to produce enzyme substrate complex.

Another objective of this thesis is to investigate the interaction of penicillin acylase with its substrate Pen V. This is also undertaken by combining the techniques of mutagenesis and X-ray crystallography. A series of PVA mutants have been crystallised for studying the post-translational processing, substrate specificity and mechanism of

enzyme activity. The interaction and packing of PVA in different crystal structures have been investigated. We have also encountered twinning in some of the crystals.

We envisage that our study has thrown light on the mechanism of autoprocessing and the substrate specificity of the PVA. Some interesting crystallographic problems like twinning have been resolved. It is hoped that the contribution arising from the work described in this thesis will be useful in the long-term goal of engineering PVA to recognise cephalosporin molecules which are fermentation products to use them in the preparation of semi-synthetic cephalosporin antibiotics.

CHAPTER – TWO

MATERIALS AND METHODS

2. 1. Introduction

A wealth of information regarding enzyme function can be extracted using the combined approaches of biochemical characterization, mutagenesis and structural analyses. This chapter describes the methods employed in the study of post-translational processing and catalytic activity of penicillin V acylase (PVA) from *Bacillus sphaericus* combining the techniques of genetic engineering and X-ray crystallography.

Structure-based study is one component of multidisciplinary design cycles, as illustrated in Figure 2.1. In case of proteins the protein engineering cycle is of value. In this cycle, the protein is cloned, expressed and characterized kinetically, and the three-dimensional structure is explored, preferably as a complex with an inhibitor, ligand or a pseudo-substrate. The three-dimensional structure of a protein-ligand complex is used as the basis to elaborate the chemical mechanism of the reaction taking place at the active site of protein. In most cases, we may have to go round the cycle several times to study the influence of a particular design on the electronic balance of catalytic site and hence the reaction catalysed in the present conformation. Rational approach to study the protein PVA is organized as design cycle shown in Figure 2.1, where repeated cycles of the procedure provide further understanding of the role of individual residues at the catalytic pocket in the functioning of PVA.

The entry to the cycle is usually by obtaining protein by identifying and cloning the gene followed by expression and purification of the recombinant protein. After the biochemical characterization of the protein, its three-dimensional structure can be determined using X-ray analysis provided the protein can be crystallised. PVA has been extensively characterized in solution and its crystal structure determined. The structure has provided the platform to pursue more incisive and focused experiments, and at the same time allowing the interpretation of previous experimental observations. Once the structure has been determined, a more hypothetical and uncertain step is the introduction of a mutation to test hypotheses about parameters related to the crucial role of certain residues and the overall fold of protein in its function. The knowledge of the active site architecture certainly can provide a better starting point to identify possible candidates for mutagenic studies. The next step in the cycle is to test

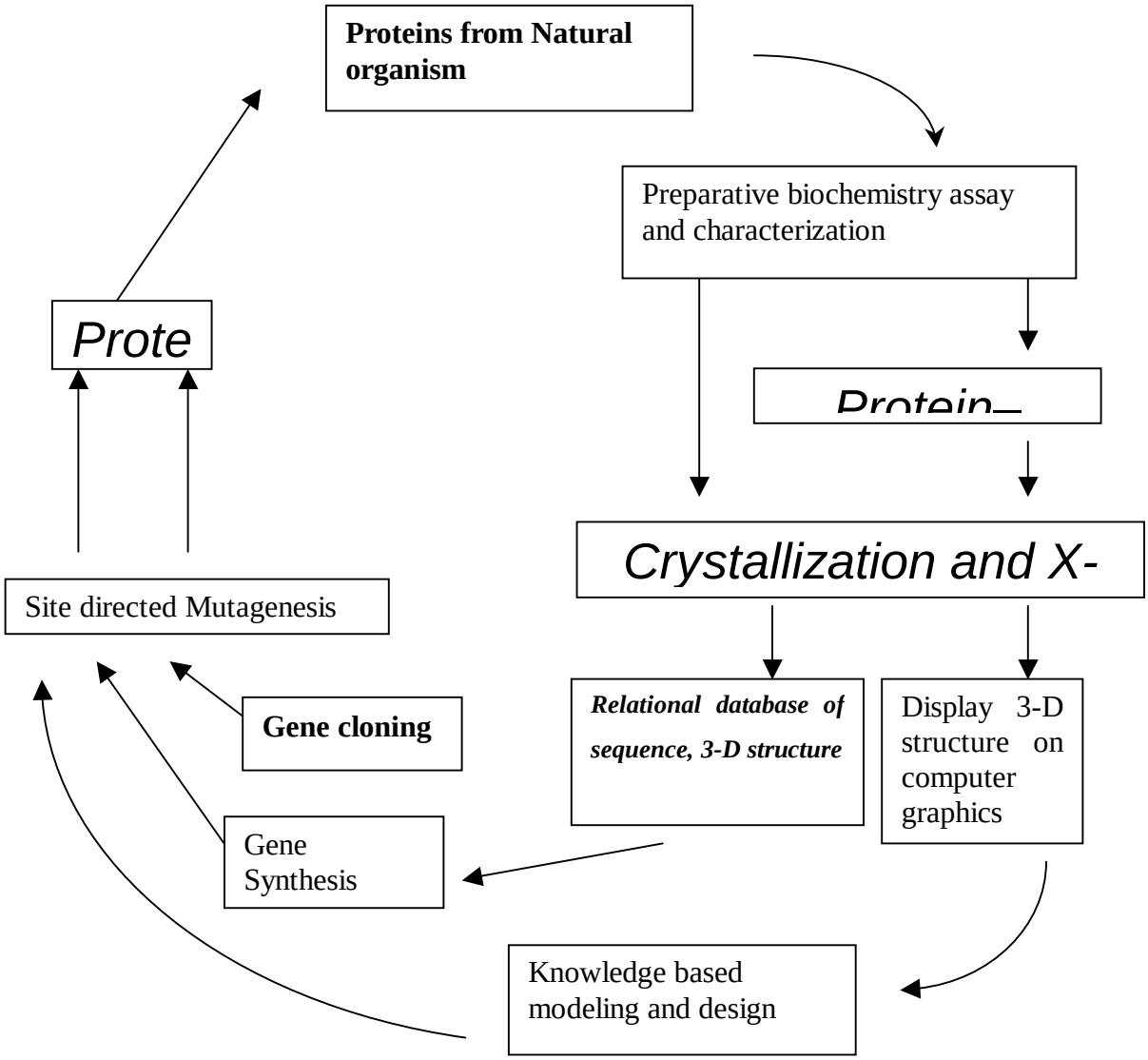

Figure 2. 1

Design cycle to illustrate the structure based study of proteins. In most cases, we may have to go round the cycle several times to study the influence of a particular design (adapted from Blundell et al., 1989).

the design hypothesis using site-directed mutagenesis followed by expression, biochemical characterization and structure determination of the mutant protein. The ability to modify protein molecules through site-directed mutagenesis plays a major part in addressing the many questions posed. The three-dimensional structure of a protein-ligand complex can help to unravel the key interactions and mechanism involved in enzyme catalysis and specificity. The methods involved in X-ray analysis and structure determination will be described in more detail later.

2. 2. Materials

Chemicals used in fermentation and protein expression were Yeast Extract, Tryptone, Sodium Chloride (NaCl), Ampicillin, Kanamycin, Isopropyl β D-thiogalactopyranoside (IPTG).

Purification of PVA mutant proteins from crude extract of cells to homogeneous protein solution involved chemicals such as Trizma, di-Potassium hydrogen phosphate, Potassium Hydrogen Phosphate, Ethylenediaminetetraacetic acid (EDTA), Streptomycin sulfate, Ammonium sulfate (AS), Imidazole, Sodium acetate, Nickel chloride, Glycerol, β-mercapto-ethanol, Bromo-phenol-blue (BPB), Acrylamide, N,N'-methylene bis-acrylamide, Sodium dodecyl sulfate (SDS), Acetic acid, Methanol, TEMED (N,N,N',N'-Tetramethylethylenediamine), Ammoniumpersulfate (APS), Molecular weight marker kits for SDS-PAGE etc, were purchased from Sigma chemical company, St. Louis, USA. The slab gel electrophoresis unit was purchased from Biotech, India.

Following chemicals were used extensively in the crystallization trials: Sodium-cacodylate buffer, Magnesium Chloride hexahydrate ($MgCl_2.6H_2O$), Nickel chloride ($NiCl_2$), Polyethylene glycol (PEG 20K, 4K), Lithium sulfate (Li_2SO_4).

Crystallization additives tried for improvement of diffraction quality were Isopropanol, Dioxan, Dimethyl formamide (DMF), Dimethyl Sulfoxide (DMSO), Glycerol, Ethelene Glycol, NDSB-195, NDSB-201 (Non-Detergent Sulfobetaines), trimethylamine N-oxide (TMAO), Poly oxy ethylene 5-octyl ether, 2-ethoxyethanol (ethyleneglycol monoethyl ether, Cellosolve), Maltose, sucrose. Several cryo-protectents were tried to flash cool the crystals of PVA mutants. Glycerol and 1,2,6-Hexanetriol were found most effective. Later it was used in most of the cases.

Multiwell trays used in crystallization were bought from Becton Dickson and Company or Falcon. All chemicals used were of analytical grade.

Silicon graphics Octane workstation was used for graphics display, for running the crystallographic programs and for related calculations. Programs from 'CCP4 suite' (Collaborative Computational Project, Number 4., 1994) were used extensively. The program QUANTA (Accelrys) was used for visualization of protein and model building.

2. 3. Site directed mutations

The site-directed mutagenesis is carried out to evaluate the effect of a particular mutation on the function of the enzyme or its structure. Site-directed mutagenesis technique can be employed to incorporate the desired mutations *in vitro* in a cloned plasmid DNA gene. Oligonucleotide-directed mutagenesis is by far the most commonly used method. An oligonucleotide encoding the desired mutation(s) is annealed to one strand of the DNA of interest and serves as a primer for initiation of DNA synthesis. In this manner, the mutagenic oligonucleotide is incorporated into the newly synthesized strand.

A number of methods introduce genetic manipulations to improve mutagenesis efficiency. These selection and enrichment methods include use of a uracil-containing DNA strand which can be selectively degraded *in vivo*, and the incorporation of dNTP analogue can render one strand of heteroduplex DNA impervious to digestion.

The PVA gene from *Bacillus sphaericus* NCIM 2478, inserted into the plasmid pBSK(+/-) was used as template for the preparation of precursor mutants pre-Asn175Ala, pre-Cys1Ser and pre-Cys1Ala. Truncated (processed form) mutants were cloned in pET vectors. The mutant Cys1Ala was cloned in pET-28a, whereas the mutants Asn175Ala and Cys1Ser were cloned in pET-26b. The QuickChange site-directed mutagenesis kit (Stratagene) was used for preparing mutants. The nicked vector DNA prepared with desired mutation was used in transforming competent cells and further used for protein production with IPTG induction.

The clone for the mutants Cys1Ala was constructed by PCR amplification of the PVA gene, introducing the mutation in the upstream oligonucleotide, and inserting it into

pET-28a vector. The construct was cloned in *E. coli* XL–1 Blue cells and subsequently transformed into BL-21 cells for hyper expression.

A histidine tag at the C-terminal end of PVA coding region was included in the case of truncated mutants Asn175Ala, Cys1Gly and Cys1Ser.

Table 2. 1

The plasmid and antibiotic pressure used in PVA mutants (pre: precursor, nCys: PVA without propeptide, deletion mutant)

Mutant	Plasmid	Antibiotic	His-tag
Native PVA	pBSK(+/-)	Ampicillin	No
pre-Cys1Ala	pBSK(+/-)	Ampicillin	No
pre-Cys1Ser	pBSK(+/-)	Ampicillin	No
pre-Asn175Ala	pBSK(+/-)	Ampicillin	No
pre-Arg228Ser	pBSK(+/-)	Ampicillin	No
pre-Asp20Asn	pBSK(+/-)	Ampicillin	No
nCys	pet-28a	Kanamycin	Yes
Cys1Ala	pet-28a	Kanamycin	No
Cys1Gly	pet-28a	Kanamycin	Yes
Cys1Ser	pet-26b	Kanamycin	Yes
Asn175Ala	pet-26b	Kanamycin	Yes
Arg228Ser	pet-26b	Kanamycin	Yes

2. 4. Expression and purification of Penicillin V acylase

Penicillin V acylase from *Bacillus sphaericus* is a cytoplasmic protein. The Gene for PVA protein has been cloned in *E. coli*. All studies reported here had been done on PVA site directed mutants. Mutant proteins were expressed in *E. coli* cells grown on Luria-Bertani (LB) media in the presence of appropriate antibiotic (ampicillin or kanamycin), depending on the construct used in the mutagenesis, (Table 2.1). When the OD_{660} of the culture medium reached about 0.6, IPTG was added to a final concentration of 1.0 m*M* to induce protein expression. After induction, the cells were harvested at the end of four hours by centrifugation at 8,000 g for 30 min in a Sorvall RC-5B refrigerated centrifuge at 10 °C. Cells were washed with 0.05 M potassium phosphate buffer, pH 7.5. All subsequent steps were carried out at 4 ºC. Cells were suspended in 0.05 M potassium phosphate buffer, pH 6.5, containing 10 mM EDTA (3 $ml.g^{-1}$ packed cells) and disrupted

by sonication in an ice bath, 2 min each for five times on a Biosonic III sonic oscillator (Bronwill Scientific Co., USA) at 20 KHz and 300 W. Cell debris were removed by centrifugation at 10,000 g for 20 min.

2. 4. 1. Treatment with Streptomycin Sulfate

The cell-free extract was treated with streptomycin sulfate under stirring to a final concentration of 1% (w/v). The stirring was continued for a period of 1 h, after which the precipitated nucleic acids were removed by centrifugation at 10,000 g for 30 min.

2. 4. 2. Ammonium Sulfate Fractionation

The supernatant from the streptomycin sulfate treatment step was subjected to fractional precipitation by slow addition of finely ground ammonium sulfate (AS) under stirring. The protein fraction which precipitated at 0.8 saturation (56%, w/v) of AS was collected by centrifugation at 10,000 g for 20 min. The supernatant was discarded and the precipitate was dissolved in a minimum volume of 0.05 M potassium phosphate buffer, pH 6.5, containing 10 mM EDTA and dialyzed overnight with one change against 100 times volume of 0.05 M potassium phosphate buffer, pH 6.5, containing 10 mM EDTA. AS was added to this to final concentration of 24% (w/v). The undissolved solids in the mixture were removed by centrifugation.

2. 4. 3. Hydrophobic Column Chromatography using Octyl-Sepharose

The clear, centrifuged dialyzate with 24% AS was loaded on the Octyl sepharose column (2.5x 10 cm), pre-equilibrated with 24% AS in 0.05 M potassium phosphate buffer, pH 6.5, containing 10 mM EDTA. The column was washed with 5 times its volume of the phosphate-EDTA buffer at a flow rate of 8 $ml.h^{-1}$. The elution was performed using gradient of AS (24 to 0 %). Fractions (3 or 4 ml) were collected on an automatic fraction collector at a flow rate of 15 $ml.h^{-1}$.

The aliquots of the fractions were checked for the presence of PVA using SDS-PAGE. Since the site directed mutations selected were to block the enzyme activity either fully or partially, the fractions could not be assayed and hence could be checked for the presence of PVA and its homogeneity only by SDS-PAGE run. Fractions containing

PVA mutant were pooled. The pooled fractions were concentrated by lyophilization. The purified enzyme was stable when stored at -20°C.

2. 4. 4. Purification of PVA mutants having His-Tag

To facilitate protein purification codons for hexa-histidine was included at the C-terminal end of PVA coding region in the case of truncated mutants Asn175Ala, Cys1Gly and Cys1Ser. The concept of this type of purification is rather simple. A gel bead is covalently modified so that it displays a chelator group for binding a heavy metal ion like Ni^{2+} or Zn^{2+}. The design of the chelating group on the gel bead is such that it provides only half the ligands needed to hold the metal ion. So when a protein with metal binding site finds the heavy metal, the protein will bind by providing ligands from its metal binding site to attach to the metal ion displayed on the chelator arm of the gel bead. It has been shown that an amino acid sequence consisting of 6 or more His residues in a row can act as a metal binding site. The number of purification steps will be reduced in His-tagged proteins. All steps prior to treating with 0.8 saturation (56%, w/v) of ammonium sulfate has been excluded by using His-tag. The crude cell extract after sonication was centrifuged to remove cell debris. The supernatant was then loaded on to the metal-chealating Ni^{+2} column. Pure protein was eluted from the column using 500 mM Imidazole solution. All the buffers used in this method of purification were at pH 6.4 and free from chelating agent EDTA.

2. 5. Assay for PVA activity

Bomstein and Evans (1965) devised a specific assay for 6-APA, which depended on the reaction of the 6-amino group with p-dimethylaminobenzaldehyde to form a colored Schiff base, which is estimated colorimetrically. The chromogen is stable only for a very short time.

The determination of PVA activity was carried out at pH 6.4 and 37 ºC using 2% (w/v) pen V as described by Olsson et al. (1985). The 6-APA formed was estimated spectrophotometrically by the p-dimethylaminobenzaldehyde method of Bomstein and Evans (1965) as modified by Shewale *et al.* (1987). A total of 10µl of the purified PVA was mixed with 990µl of a solution of the potassium salt of penicillin V (20mg/ml)

prepared in 50mM sodium phosphate buffer at pH 7.5. The reaction mixture was incubated for 30 minute at 37 °C. The reaction was stopped by the addition of 3ml of 300mM citric acid in 50mM Phosphate buffer (CPB) at pH 2.5. The 6-APA formed in the reaction mixture was estimated spectroscopically at wavelength 415 nm by the addition of 1 ml of a 5% (w/v) solution of p-dimethylaminobenzaldehyde in methanol (Shewale *et al*., 1987). One unit (U) of activity of the enzyme is defined as the amount of enzyme catalysing the hydrolysis of 1 µmole of the substrate in 1 min under the assay conditions.

2. 6. SDS - polyacrylamide gel electrophoresis (SDS-PAGE)

The purity of PVA preparation was checked on a 12% sodium dodecyl sulfate-polyacrylamide gel (SDS-PAGE), according to Laemmli (1970). The gel was prepared using the Biorad SDS-PAGE apparatus with 1 mm spacers and the samples electrophoresed alongside molecular weight markers applying voltage 200 V for 1 h. Protein bands were visualized by staining the gel with 0.25% coomassie blue R in 10% (v/v) glacial acetic acid and 25% (v/v) isopropanol. The destaining solution contained 7% (v/v) glacial acetic acid and 5% (v/v) isopropanol. The PVA enzyme mutant expressed in *E. coli* was identified by the appearance of a band of molecular weight 37500 Dalton corresponding to the PVA monomer in the SDS-PAGE gel.

2. 7. Crystallographic methods

The methods in protein crystallography followed are graphically summarized in Figure 2.2. The methods employed starting from crystal to final model will be briefly discussed, emphasizing those methods specially used in research reported in this thesis, including crystallization, cryo-crystallography, data collection, molecular replacement and refinement.

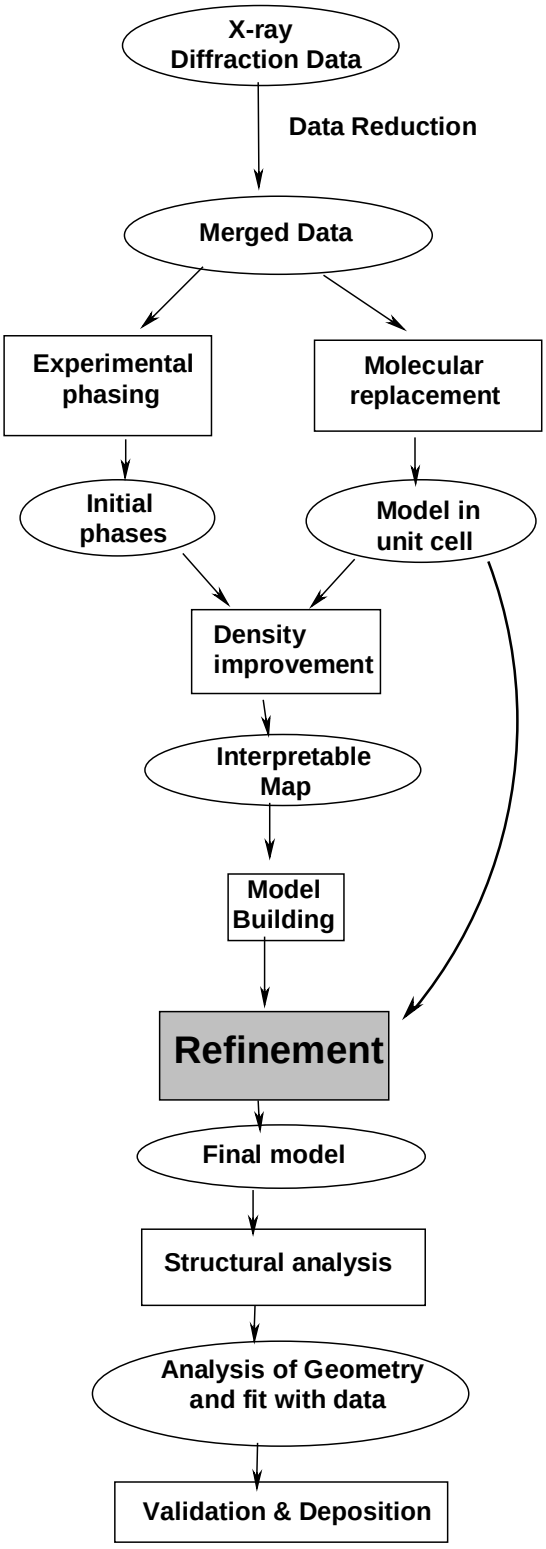

Figure 2. 2

A graphical summary of the methods used in protein X-ray crystallography. Structure refinement is an important step after structure solution. (Adapted from CCP4 tutorial)

2. 7. 1. Crystallization and Crystal growth

The first step considered crucial in protein structure determination is the availability of diffraction quality crystals. In the absence of any single concrete theory behind the mechanism of crystallization, protein crystallization is mainly considered as a trial and error procedure invoking experience and crystallization reports as guiding principles. It is accepted that the presence of impurities, ionic strength, pH, temperature, precipitating agent and several unspecified factors play role in crystallization process.

In crystallization experiments, a precipitant such as a salt or an organic solvent is diffused into a purified protein solution maintained at particular pH and temperature such that diffraction quality crystals of protein could grow from the protein solution (Drenth & Haas, 1998). Among various crystallization techniques known, hanging drop vapor diffusion method is widely adopted and has produced more protein crystals than all other methods combined (Chayen, 1998). This method is simple, consumes less protein and it is easy to monitor the progress of crystallization. In a typical experimental set up using multiwell tray (24 wells), 1 µl of protein solution was placed on a siliconized cover slip, mixed with 1 µl of the precipitant solution from the well and allowed to slowly equilibrate against ~1 ml reservoir solution of the precipitant.

Crystallization of proteins involves two critical steps, the nucleation and the growth of these nuclei. These two factors can influence the size and quality of the crystal finally grown (Weber, 1997). However, the degree of supersaturation required for stable nucleus to form is often higher than the optimal concentration necessary for its growth. Given that the ideal conditions for nucleation and growth vary, a logical crystallization strategy involves the independent optimization of these processes. This can be accomplished by seeding, a technique where crystals are transferred from nucleation conditions to those that will support growth. The technique of streak seeding as described by Stura and Wilson (Stura & Wilson, 1991) uses a needle to transfer seeds of crystals to a drop of non-nucleated protein. The needle is used to touch an existing crystal and dislodge seeds from it. Some of the seeds remain attached to the needle as it is drawn out of the solution, and these can be introduced into a pre-equilibrated drop which may support mainly growth. Seeding can be employed in situations where crystals are small and of poor quality, where they take too long to grow. Streak seeding also provides a

powerful tool for cross-seeding between macromolecular species, such as genetic variants (Stura & Wilson, 1990). Crystallization studies of PVA reported in this thesis have used hanging drop vapour diffusion method.

2. 7. 2. Characterization of crystals

Next step after crystallization is to proceed with X-ray diffraction experiments to measure intensities of Bragg reflections. The materials needed are a crystal, a X-ray source, an area detector (Image plate or CCD), cryostream, and a goniometer to orient and rotate the crystal. Protein crystals diffract poorly when compared with the small molecule crystals of the same size; hence the diffraction intensities will be relatively weak. Good quality X-ray data for protein crystals requires high intensity X-ray radiation source such as synchrotron and a high sensitivity area detector. Crystal testing at home source prior to actual data collection on synchrotron can assess the diffraction quality of the crystals.

The home tested good quality crystals were freezed in liquid nitrogen before taking them to synchrotron source. Each image collected has a size of ~10 MB. The whole process of data collection, exposure and acquisition of image, is fully automated.

All diffraction data collected from single crystals, described in this thesis are from synchrotron radiation sources at European Synchrotron Radiation Source (ESRF, Grenoble, France) and Synchrotron Radiation Source (SRS, Daresbury, Warrington, UK) recorded using CCD detectors. All data have been collected at 100K under liquid nitrogen jet by freeze cooling the crystal in 30% glycerol in some cases or 30% 1,2,6-Hexanetriol in others.

During data acquisition the crystals were oscillated about an axis perpendicular to the X-ray beam, with a chosen, relatively small angle of oscillation, close to 0.3 - 0.4 degree per frame. Crystal to detector distance is chosen, based on the longest unit cell dimension, mosaic spread etc., so that the intensity spots are well resolved, is approximately equal to the longest crystal cell dimension. The exposure time depended on the quality of the crystal and the oscillation range, larger the oscillation range longer the exposure time required. After indexing the initial images the module “strategy” of MOSFLM (Powell, 1999) was used to get the range of the rotation angles to be used to

acquire complete data. The “strategy” calculates parameter on the basis of space group of the crystal and its orientation in the X-ray beam. The program requires the crystal symmetry and orientation (which can be determined by auto-indexing a preliminary image) as input. On getting this information, the program determines the starting phi value and the total phi rotation required for collecting dataset with the highest completion possible.

2. 7. 3. Quality of Data

The general improvement in the quality of diffraction data collected in recent years can be attributed to the use of synchrotron radiation sources, and the application of sensitive two-dimensional CCD detectors, combined with the development of cryogenic freezing techniques.

The native structures, which sometimes cannot themselves provide any insight into the function of a protein, do at least provide a 'road map' for rational mutagenesis experiments that can indirectly link structure to function. To obtain the maximum information from an electron density map, the details should be clear and interpretable, and so the importance of good data obtained at as high a resolution as possible is crucial. This has a significant bearing on the rational design and engineering of proteins to understand and modify their functions. The problem for collecting high resolution data in the case of macromolecules lies with their inherent disorder. The irregular shape of molecules does not allow close packing in their crystals. As a result, intensities are also contributed by disordered solvent; the lattice forces are weak and often the surface residues of the protein show both static and thermal disorder.

Data at atomic resolution are available for an increasing number of proteins. The analysis of a structure at atomic resolution offers many advantages by revealing the finer details of protein structure. The information that can be unveiled is restricted by the limiting resolution (Table 2.2). The need for an accurate structure is particularly important and provides a standard by which meaningful comparisons with the structures of mutants and substrate complex could be achieved with a high degree of precision. It is hoped that a clear interpretation of structural differences can then be made, both substantial and, more importantly, subtle changes taken place at the active site.

Table 2. 2

The effects observed due to limitation of resolution in the refinement of protein structures. (from Dauter, 1997). Resolution of the X-ray diffraction data limits the identifiable features in protein structure.

Resolution (Å)	Protocol for refinement	Features identifiable
1.0	Full-matrix, anisotropic atoms	Fully resolved atoms
1.5	Border between isotropic/anisotropic	Hydrogens, disorder, ordered atom distinguished
2.0	Isotropic atoms, stereochemical restrains	Some disorder
2.5	Isotropic model starts to break down	Shape of small group
3.0	Rigid group, some constrains	Shape of fragments, e.g. helices
6.0	Complete domains as rigid bodies	Globular proteins

The X-ray detectors also play an important role in protein crystallography and a high sensitivity is demanded especially when the molecular weights of the proteins become larger and/or crystal sizes become smaller. The development of the charge coupled devise (CCD) detector has enabled protein crystallographers to obtain more accurate data with a reduced X-ray dosage and a shortened exposure time (Westbrook & Naday, 1997). The rapid scanning of the CCD detector in comparison to Image plate detectors has decreased the data collection time immensely. Reduction in exposure time and faster data acquisition minimizes the radiation damage to the crystals and their instability during X-ray exposure and provides a better signal-to-noise ratio due to high detective quantum efficiency (DQE) of CCD. A combination of synchrotron radiation and CCD has mutually enhanced their capabilities. The production of more intense X-rays by the use of insertion devices and bending magnets at synchrotron radiation sources is complemented by the high DQE of the CCD detectors.

2. 7. 4. Cryocrystallography

In recent years there have been many advancements and improvements in crystallization methods and data collection techniques in the field of cryocrystallography. Data are now routinely collected on macromolecular crystals at cryogenic temperatures. The crystals are prepared and rapidly flash cooled to prevent formation of ice lattice in the aqueous solvent inside and on the surface of the crystal. In the presence of cryoprotectant, instead of ice, glass forms, leaving the crystal lattice with little or no damage. Crystals are then maintained at a temperature of between 100-120K during data collection. This provides crystals with a sort of 'immortality' in the X-ray beam and enable better quality data with the capability for long-term storage and reuse of crystals and often extending the limit of resolution obtainable (Gamblin & Rodgers, 1993; Garman & Schneider, 1997; Rodgers, 1994; Watenpaugh, 1991). The intrinsic limitations with resolution due to diffraction quality had dramatically improved by cryotechniques. Many factors contribute to the improvement in data quality, including reduced thermal vibrations, decreased diffused scattering and reduced absorption due to absence of glass capillary and absence of excessive solvent surrounding crystal, enhancement of the signal-to-noise ratio, reduced conformational disorder and potentially improved limiting resolution. Another important effect is the prevention of radiation damage, permitting complete data collection from a single crystal that in turn eliminates errors from merging and scaling multiple data sets from different crystals. In effect these improvements can lead to enhanced contrast and sharpness in the electron density. If there is no undesirable increase in mosaicity, data collected at cryogenic temperatures are superior to data recorded at room temperature in many respects and facilitate smoother progress in structure solution and refinement. However, the use of cryocooling and cryoprotectants create an environment very different from that of its normal habitat and may induce some changes that can lead to complications later in structure solution and refinement (Garman & Schneider, 1997). Some changes can be induced by the binding of cryoprotectant molecules, especially when binding takes place in regions of particular interest. It should also be noted that, when data to only relatively low resolution are available, cryoprotectant molecules might not be identified as such in electron density maps and thus might lead to inaccuracies in the knowledge of the detailed protein structure.

The introduction by Teng (1990) of a loop mounting technique for flash cooling

of crystals was a major advancement in cryocrystallography. Loops are made of fine fibres, e.g. rayon, in which the crystal is scooped from the cryosolution and held within the loop suspended by a thin film of the solution. The loop is supported by a pin, which is itself attached to a steel base used for placing the assembly on a magnetic cap on the goniometer.

2. 7. 5. Diffraction data collection

The best strategy during X-ray diffraction data collection depends on qualitative factors, such as crystal quality and availability, type of X-ray source and detector, and time available, and quantitative ones, such as cell parameters, resolution limit, and crystal symmetry. Data were collected using the rotation method employing a range of crystal rotations based on resolution, crystal orientation and mosaicity and were processed using the HKL suite of programs (Otwinowski & Minor, 1997).

The processing of the diffraction data consists of the following steps:

1. Indexing of the diffraction pattern and determining of the crystal orientation
2. Refinement of the crystal and detector parameters
3. Integration of the diffraction intensities
4. Refining the relative scale factors between equivalent measurements
5. Precise refinement of crystal parameters using all the data
6. Merging and statistical analysis of the symmetry related reflections

First three steps are carried out by the program DENZO, while steps 4 to 6 are performed by the program, SCALEPACK.

One of the least defined criterion in data collection is the resolution limit of diffraction (Dauter, 1997). A useful guide is to restrict the resolution to the point below which more than half the reflection intensities are higher than 2σ. This assumes that the estimate of the errors in measurement of intensities is correct. The R_{merge} (also called Rsym) is the most widely accepted statistical parameter to indicate data quality in macromolecular crystallography and is defined as

$$\mathbf{R_{merge}} = \frac{\sum_h \sum_i |I_{hi} - \overline{I_h}|}{\sum_h \sum_i \overline{I_h}} \qquad (2.1)$$

where

I_{hi} is the intensity of i^{th} observation of h k l reflection, and

$\overline{I_h}$ is the mean intensity of all symmetry equivalents

Σ h is taken over all reflections

Σ i is taken over all observations of each reflection

R_{merge} is commonly used to guide decisions during data reduction, such as determining upto what resolution the data are reliable. Diederichs and Karplus (1997) have argued that R_{merge} is seriously flawed, because it has an implicit dependence on the redundancy of the data. The R_{merge} is less appropriate than the Chi-square, because of its dependency on the multiplicity of the data and on the symmetry of the crystal.

The desired crystal rotation per image is an important consideration during data collection. To prevent overlaps from successive zones, the crystal rotation per image must be selected depending on the resolution limit and the cell dimension along the beam direction. The rotation range should be reduced to allow for the crystal mosaicity and beam divergence. The effect of cell dimension along the spindle axis will be uniform, since the crystal is rotated around that axis and will never lie along the beam direction assuming the crystal is perfectly orientated in the beam.

2. 7. 6. Data Processing

Indexing, processing, scaling and merging of the raw X-ray data were carried out using the programs DENZO and SCALEPACK, respectively from HKL suit (Otwinowski & Minor, 1997). DENZO provides numerical analysis of each oscillation image, whereas SCALEPACK provides overall statistics for the whole data set. DENZO accepts peaks for autoindexing only from a single oscillation image and makes a

complete search of all possible indices of all reflections. The program calculates the distortion index for all 14 Bravais lattices, user is given the option to select the lattice and space-group. The interactive mode of indexing is also an option in DENZO. Our processing procedure involved interactive mode. The peaks were selected by defining overlapping boxes in case of crystals with huge unit cell. Spot overlap option was used in scaling of these images. The program SCALEPACK performs the scaling and merging of data from all images and does a global refinement of crystal parameters. The method used in SCALEPACK reduces the bias existing in other programs toward reflections with intensity below the average.

2. 7. 7. Matthew's number

Once the space group and unit cell dimensions of the crystal are known, it is possible to estimate the number of molecules in the crystallographic asymmetric unit and the solvent content of the protein crystals based on knowledge of the molecular weight of protein. The following equations (2.2 & 2.3) are used (Matthews, 1968).

$$V_m = \frac{\text{Unit cell volume}}{\text{Mol.Wt.} * n * z} \qquad (2.2)$$

$$V_{solv} = 1 - \frac{1.23}{V_m} \qquad (2.3)$$

Where V_m is the Matthew's number, n is the number of molecules per asymmetric unit and z is the Avagadro's number; V_{solv} is the fraction of unit cell volume occupied by solvent. The Matthew's number for all the crystal forms of PVA were calculated by assuming 37500 Dalton as the molecular weight of a monomer.

2. 7. 8. Structure solution

Multi-wavelength Anomalous Dispersion (MAD), Multiple Isomorphous Replacement (MIR) and Molecular Replacement (MR) are the three methods widely used

in protein crystallography to solve protein structures. MAD technique is currently the most popular one owing to the availability of variable wavelength synchrotron radiation sources and sensitive detectors like Image plate and CCD to collect anomalous data on selenium derivative that can be prepared using molecular biology techniques for any protein (Beauchamp & Isaacs, 1999). Another advantage is MAD needs only one heavy atom derivative compared to MIR technique that requires more than one. Molecular replacement technique is the simplest of all and can be used when a homologous protein with structural similarity is available in the database. The success of the MR method depends on the structural similarity between the search model and the unknown structure. The pioneering studies of Rossman & Blow (1962) laid the foundation for the successful use of MR method. With the rapid expansion of protein data bank and with the increase in the number of structures available MR method is now routinely used in protein structure determinations.

2. 7. 9. Molecular replacement method

The three-dimensional structure of PVA (pdb, 2pva ; Suresh *et al.*, 1999) has been used us model in molecular replacement method in the case of all mutants. The position of the molecular model in the unit cell of interest is defined in terms of three rotational and three translational parameters. The orientation and position of the molecules in the respective unit cell is determined by a Patterson search of the reciprocal space using cross-Patterson function by going through all possible orientations of the model and the correct orientation is selected based on the maxima of cross-Patterson using program *AMoRe* (Navaza & Saludjian, 1997).

The rotational parameters are first determined in terms of Eulerian angles from the rotation function, then placing the model in correct orientation the translational parameters are determined from the translation function. Eventually, the model obtained using rotational and translational solutions is refined using rigid body fit.

The MR calculations were carried out for mutants in different space groups ($P2_1$ form I & II, $P2_12_12_1$, $C222_1$) using the program *AMoRe* (Navaza & Saludjian, 1997). The coordinates of rigid body fitted model in the new unit cell was calculated using *LSQKAB* (Kabsch, 1976).

2. 7. 10. Refinement

The next step after getting the coordinates of a preliminary model using MR method is its refinement. Refinement is the process of fitting the parameters of the model to obtain a closer agreement between the calculated and observed structure factors. The refinement of the model is by incrementing the positional parameters and the temperature factors of the atoms keeping the stereochemical restraints on the structure. The numbers of atoms as well as the numbers of parameter to be refined are large in proteins. For PVA with ~10000 atoms, the refinement of three positional parameters (x, *y*, and z) and one isotropic temperature factor parameter (B) makes a total of ~40,000 parameters. Constraints are incorporated into the refinement in the form of stereochemical criteria deduced from data of small molecular structures of amino acids and peptides in which the bond lengths and angles have been determined to high precision (Engh & Huber, 1991). The stereochemical information can be applied in two different ways. For constrained refinement the geometry is considered as rigid which reduces the number of parameters to be refined. In contrast, when the stereochemical parameters are allowed to vary around a standard value, the refinement is restrained in which appropriate weights are applied between geometric parameters and X-ray terms. Restraints on bond lengths, bond angles, torsion angles, and Van der Waals contacts have the apparent effect of increasing the number of observations.

2. 7. 11. REFMAC5: program for Max-likelihood refinement

Refinement of structures were carried out using restrained maximum likelihood refinement implemented in the program REFMAC5 (Murshudov *et al.*, 1996; Murshudov, 1997). Each cycle of the program can be considered to carry out grossly two steps:

- Estimates the overall parameters of likelihood using the free set of reflections
- Uses these parameters to build the likelihood function and refine the atomic parameters. To refine the atomic parameters only a working set of reflections were used.

Maximum likelihood method of refinement performs the calculation of the first derivative and make an approximation of the second derivative of the likelihood function with respect to refinement parameters and then estimating the shifts to be added to the parameters.

The values of standard deviation are given for the geometric restraints used during the refinement. These values are also the estimated standard deviations that determine the relative weights of the corresponding restraints. The restraints used during refinement by REFMAC5 include distances, bond angles, torsion angles, peptide planarity, chiral volumes, Van der Waals radii and B values.

Model building and manual fitting were carried out using X-AUTOFIT module of QUANTA (Accelrys inc.) and the manual addition of waters was with X-SOLVATE, again of QUANTA.

2. 7. 12. Structure Refinement using SHELXL

SHELXL is another program for the refinement of crystal structures using diffraction data, and is originally intended for single crystal X-ray data of small molecular structures later modified for the refinement of macromolecules also. It uses a conventional structure factor summation, so it is much slower than standard FFT-based macromolecular programs. Polar axis restraints and special position constraints are generated automatically. SHELXL (Sheldrick, 1995) is the refinement program which both generates and inverts the matrix of second derivatives for many parameters, and thus give standard deviations of parameters. As the program can handle twinning it was used for the refinement of three mutant structures: pre-Cys1Ala, pre-Cys1Ser-II, Cys1Ser.

Twinned crystals were refined in SHELXL by the method of Pratt *et al* (1971). The sum of the Fc^2 values of the individual twin domains, each multiplied by its fractional contribution is fitted with the observed Fo^2.

2. 7. 13. Molecular modeling and energy minimization using CHARMM

The substrate Pen V was modelled in the PVA and energy minimized using CHARMM (Chemistry at HARvard Molecular Mechanics). Knowledge from PGA – Pen G complex structure was used to model pen V in PVA, which was energy minimized

using CharmM.

CHARMM is a program for macromolecular simulations, including energy minimization, molecular dynamics and Monte Carlo simulations. CHARMM uses an empirical energy function for energy minimization, molecular dynamics simulation, or vibrational analysis. With these major operations, CHARMM can efficiently calculate a wide range of molecular properties from simple peptide conformations to dynamic hinge-bending motions of large protein subunits. Moreover, intermolecular problems that underlie structure-activity relationships such as enzyme-substrate or receptor-ligand binding interactions can be addressed.

Energy minimization adjusts the structure of the molecule in order to lower the energy of the system. For small molecules, a global minimum energy configuration can often be found; for large macromolecular systems, energy minimization allows one to examine the local minimum around a particular conformation.

2. 8. Structure quality and validation

The cycle of rebuilding the model in QUANTA and restrained refinement in REFMAC5 are followed by structure validation. The correctness and precision of the atomic parameters in a structure need to be assessed thoroughly, both during and at the end of the refinement. An initial indication of the reliability of a protein crystal structure depends on the extent of resolution of the diffraction data used in refinement. The conventional R factor (R_{cryst}) is an indicator of the general fit of the crystal structure with observed data. However, it is not a reliable independent validator, since it can be biased by the exclusion or overfitting of the data. A better assessment of the fit between observed and calculated structure factors is provided by the *free R factor* (R_{free}) (Brunger, 1992). This is based on the general statistical principle of cross validation where the model is required not only to fit the experimental data included in its refinement but also should fit an excluded set. This is particularly valuable as it aids bias-free refinement by signaling any overfit. However, the R factor still can show only an overall structure quality and cannot point out local errors.

2. 8. 1. Estimate of coordinate precision

Isotropic temperature factors are related to the thermal vibrations of atoms and therefore to some extent a reflection of the precision with which these atomic positions can be measured. It has been demonstrated that precision of atomic positions are strongly depended on magnitudes of B values (Daopin *et al.*, 1994).

The program PROCHECK (Laskowski *et al.*, 1993) and SFCHECK (Vaguine *et al*., 1999) have been used to examine the stereochemistry of the final refined models. PROCHECK calculates the phi-psi angles and plots them on a two dimensional plot (Ramachandran plot). It estimates the percentage of residues within or outside the allowed or partially allowed regions in Ramachandran plot. The program output a detailed list of the extend of deviations from the ideal geometry for residues along with corresponding plots of the parameters.

CHAPTER – THREE

CRYSTALLIZATION AND X-RAY DATA COLLECTION

3. 1. Introduction

In 1912, a German physicist named Max Von Laue became interested in the way that light and crystals interacted with each other. He realized that the regular arrangement of atoms in crystals should provide about the right spacing (about 10^{-10} m) to produce an interference pattern on a photographic plate when X-rays pass through such a crystal. He knew that the X-rays must have a short enough wavelength in order to create a diffraction pattern from the crystal. He used an X-ray generator to do this and sure enough the crystal diffracted X-rays, but the resulting pattern was of no use because no information could be obtained from it. Later, an X-ray diffractometer was designed to further study the interaction patterns between light and crystalline structures. In the diffractometer a well-grown crystal was placed on a platform. X-rays were aimed at it by rotating the crystal and studying the resultant "powder pattern". This gave a much clearer understanding of the interaction between light and crystals. Slowly, the methods to interpret the results to determine the structure were worked out. With the development of computers and other emerging technologies, the ability to determine the structure has become relatively easy. X-ray crystallography has come a long way since its discovery, and has become an essential technique for determining the three-dimensional structures.

The single crystal X-ray diffraction experiment involves growing a diffraction quality single crystal of reasonable size (0.2 - 0.5 mm) of the molecule of interest and collecting full diffraction data on it. Most potential structure determinations were thwarted by lack of suitable single crystals. This chapter discusses the experiments carried out to obtain good quality crystals as well as collection of high resolution single crystal X-ray diffraction data on mutant PVA crystals.

3. 1. 1. Crystallization theory

Crystallization is one of the several means (including nonspecific aggregation/precipitation) by which a metastable supersaturated solution can reach a stable lower energy state by reduction of solute concentration (Weber, 1991). The general processes by which substances crystallise are similar for molecules of both microscopic (salts and small organics) and macroscopic (proteins, DNA, RNA) dimensions. There are three stages of crystallization common to all systems: nucleation, growth, and cessation of growth. Nucleation is the process by which molecules or noncrystalline aggregates

(dimers, trimers, etc.) that are free in solution come together in such a way as to produce a thermodynamically stable aggregate arrangement in a repeating lattice. Crystallization is known to lower the free energy of proteins by ~3-6 kcal/mole relative to the solution state (Drenth & Haas, 1992). The formation of crystalline aggregates from supersaturated solutions does not however necessitate the formation of macroscopic crystals. Instead, the aggregate must first exceed a specific size (the critical size) defined by the competition of the ratio of the surface area of the aggregate to its volume (Feher & Kam, 1985; Boistelle & Astier, 1988). Once the critical size is exceeded, the aggregate becomes a supercritical nucleus capable of further growth. If the nucleus decreases in size so that it is smaller than the critical size, spontaneous dissolution will occur. The process of formation of nonspecific aggregates and noncrystalline precipitation from a supersaturated solution does not involve competition between surface area and volume (*n*-mers add to the aggregate chain in a head to tail fashion forming a linear arrangement), and thus generally occurs on a much faster time scale than crystallization.

3. 1. 2. Crystallizing proteins with Salt

Salts like ammonium sulfate (AS) are by far the most common precipitant used to crystallise macromolecules. Historically they have been the most effective precipitants tried, although, there are few other options also existed (McPherson, 1991). Unfortunately, salts generally have the drawback of increasing the mean electron density of the crystallization solution which decreases the signal to noise ratio for crystallographic data. Salts also have a tendency to interact strongly with heavy atom compounds, making crystal derivatization for Multiple Isomorphous Replacement (M.I.R.) phasing difficult.

3. 2. Crystals of wild PVA

The native PVA crystals grew in two forms (Suresh *et al.*, 1999), hexagonal form (2pva) has its catalytic cysteine oxidized to cysteine sulfonic acid whereas triclinic (3pva) has S^{γ} atom of terminal cysteine in the reduced form. The well solution of the hanging drop contained 700 µl, 0.2 M sodium phosphate buffer at pH 6.4, 5 mM dithiothreitol (DTT), 300 µl saturated AS and 100 µl 10% (w/v) sucrose solution. Triclinic crystals were obtained when the protein was mixed with phenylacetic acid in 0.2 M Na_2HPO_4.

Synthetic crystallization solution containing glycerol (30% v/v) was used as cryoprotectant for freezing triclinic crystal.

3. 3. Crystals of PVA mutant

Site directed mutants have been prepared to study the autoproteolytic and catalytic mechanism of PVA. The selected targets for site directed mutation include N-terminal nucleophile Cys1, oxyanion hole residue Asn175, Arg228 and Asp20. Cys1 has been mutated in to alanine (pre-Cys1Ala), to remove nucleophilic S^{γ}-atom. Cysteine has been mutated to serine (pre-Cys1Ser) to test the efficiency of serine having an O^{γ} atom as nucleophile. Another mutant pre-Asn175Ala has been prepared to assess the role of this residue in oxyanion hole and in autoproteolysis.

3. 3. 1. Pre-Cys1Ala

Crystallization experiments with pre-Cys1Ala mutants gave crystals with AS as precipitant in 4-5 days. Diffraction quality of the crystals had improved only when sucrose and maltose were together used as additives. In the presence of maltose the crystals took longer time to grow, but helped in improving diffraction quality. Cryoprotectant 1,2,6-hexane-triol (HXT) was used at 30% (v/v) to flash cool the crystals in liquid nitrogen cryostream.

X-ray diffraction data were collected for pre-Cys1Ala at beam-line ID-14.1, ESRF. Preliminary indexing using DENZO of HKL suite programs suggested that the crystal belonged to monoclinic $P2_1$ with unit cell dimensions a = 103.30, b = 89.88, c = 103.60 Å, β = 100.56°. Crystal was exposed for 1 s with 0.4° oscillations per frame. A total of 360 frames were collected (Table 3.1). The crystal diffracted upto 2.5 Å resolution. Intensities of indexed spots were scaled using program SCALEPACK of the HKL suite (Otwinowski & Minor, 1997). Out of a total of 100565 reflections collected 72123 were unique. Data was 93.3 % complete with an overall R_{merge} of 7.8 % (Table 3.2).

Table 3. 1

X-ray data collection details

	Oscillation per image	Exposure time (seconds)	Total frames	Distance (mm)	Wavelength (Å)
Pre-Asn175Ala	0.5	2	255	180	0.870
Asn175Ala	0.3	1	615	162	0.934
Pre-Cys1Ser-I	0.5	5	360	184.08	0.978
Pre-Cys1Ser-II	0.5	5	360	200	0.933
Cys1Ser ($P2_1$)	0.5	1	360	183.63	0.934
Cys1Ser ($P2_12_12_1$)	0.5	3.0	180	173	0.934
Pre-Cys1Ala	0.4	1	300	200	0.934
Cys1Ala (pv)	0.5	1.5	270	210	0.97903
Cys1Ala (PAA)	0.5	1	300	190	0.97903
Cys1Gly (pv)	0.3	2	277	250.14	0.933

3. 3. 2. Truncated Cys1Ala

The cysteine at the N-terminal is mutated to alanine in this mutant and the N-terminal tri-peptide is excluded from the cloning sequence. Crystals of Cys1Ala were grown against well solutions containing 320 µl saturated AS mixed with 680 µl of 0.2M phosphate buffer prepared at pH 6.4. Crystals usually appeared within a week. The crystallization temperatures were 292K. 30% (v/v) glycerol along with the crystallization solution was used as cryoprotectant. These crystals diffracted upto 2.1 Å resolution at ESRF beam-line ID-14.4. The unit cell dimentions of crystals in monoclinic space group $P2_1$ were a = 47.86, b = 381.89, c = 102.89 Å, β = 94.1°. The numbers of total and unique reflections were 206635 and 196267, respectively. Data were 97.1 % complete with R_{merge} of 9 % (Table 3.2).

The same mutant crystallised in orthorhombic apace group $P2_12_12_1$ when AS was used in combination with PEG 4K. Two such data sets were collected at ESRF. Either Pen V or phenoxy acetic acid was present in the crystallization drops of the second form (Table 3.2).

Table 3. 2

X-ray data collection and processing statistics. [a]Final shell in parentheses. [b]Rsym = ∑|I-<I>|/∑I. * Twinned.

	Pre-Cys1Ser-I	*Pre-Cys1Ser–II* *	**Cys1Ser (pv)**	**Cys1Ser ***	**Pre-Asn175Ala**	**Asn175Ala**
Unit cell	102.64 90.09 102.27	102.76 90.48 102.69	90.93 129.42 158.78	102.34 90.70 102.32	103.66 92.52 103.84	47.29 379.39 102.01
β (°)	102.13	101.81	90.00	102.15	101.79	93.51
Space group	$P2_1$ (form II)	$P2_1$ (form II)	$P2_12_12_1$	$P2_1$ (form II)	$P2_1$ (form II)	$P2_1$ (form I)
Data collection statistics[a]						
Max Resolution (Å)	2.5	2.2	1.95	2.0	2.0	1.7
Observed reflections	236110	341910	470208	463873	1130879	1293348
Unique reflections	62997	91743	132141	121040	129730	370615
Completeness	99.9 (99.4)	98.7 (83.1)	96.7 (97.9)	98.2 (95.4)	99.0 (94.7)	94.6 (64.7)
Mosaicity	0.50	0.523	0.45	0.58	0.58	0.48
R_{sym}[b]	8.6 (29.2)	6.9	11.8 (72.8)	9.4 (58.5)	9.2 (46.6)	6.9 (48.6)
Unit cell volume	931873.4	953389.6	1867113.0	928476.96	969527.125	1825765.5
Mathews cofficient (V_m) ($Å^3\,Da^{-1}$)	3.21	3.18	3.11	3.09	3.23	3.04
Solvent content (%)	61.66	61.30	60.47	60.26	61.64	59.58

Table 3. 2 (continued)

	Pre-Cys1Ala *	**Cys1Ala**	**Cys1Ala (pv)**	**Cys1Ala(PAA)**	**Cys1Gly**	**Cys1Gly (pv)**
Unit cell	103.30 89.88 103.60	47.86 381.89 102.89	91.18 129.49 159.01	90.90 129.53 158.77	91.76 130.71 158.71	129.73 158.89 90.74
β (°)	100.56	94.1	90.00	90.00	90.00	90.00
Space group	$P2_1$ (form II)	$P2_1$ (form I)	$P2_12_12_1$	$P2_12_12_1$	$P2_12_12_1$	$C222_1$
Data collection statistics[a]						
Max Resolution (Å)	2.5	2.1	2.3	2.0	1.8	2.5
Observed reflections	150271	206635	421814	331607	166177	78639
Unique reflections	72123	196267	81103	120425	155411	28157
Completeness	93.3 (79.8)	97.1 (86.4)	96.9 (97.5)	95.1 (92.8)	99.04 (100)	85.7 (52.2)
Mosaicity	0.64	0.50	0.53	0.73	0.55	0.59
R_{sym}[b]	7.8 (48)	9.0 (16.0)	18.7 (89.9)	10.4 (53.6)	10.9 (55.2)	13.0 (49.8)
Unit cell volume	945672.9	1873651.8	1877414.88	1869401.96	1903559.74	1870405.44
Mathews cofficient (V_m) ($Å^3 Da^{-1}$)	3.15	3.12	3.13	3.12	3.17	3.12
Solvent content (%)	60.98	60.61	60.69	60.52	61.23	60.54

Table 3. 3

Crystallization experiments, combinations, cryoprotectant and data collection dates

Crystal	**Crystallization combination (in μl)**	**cryoprotectant**	**data collection (dd.mm.yy)**

Pre-Asn175Ala	650 PB, 350 AS, 100 S,	30 % HXT	SRS, 9.6, 30.04.01
Asn175Ala	750 PB, 250 AS, 100 S, 25 NC	30 % HXT	ESRF, ID-14.3, 13.04.03
Pre-Cys1Ser-I	700 PB, 300 AS, 100 S, 50 DMSO	30 % HXT	SRS, 14.2, 05.05.01
Pre-Cys1Ser-II	700 PB, 300 AS, 100 S	30 % HXT	ESRF, ID-14.3, 08.10.01
Cys1Ser ($P2_1$)	700 PB, 300 AS, 100 S,	30 % Glycerol	ESRF, ID-14.3, 22.10.02
Cys1Ser ($P2_12_12_1$)	750 PB, 250 AS, 100 S, 3 pv	30 % HXT	ESRF, ID-14.3, 13.04.03
Pre-Cys1Ala	700 PB, 300 AS, 100 S, 50 ML	30 % HXT	ESRF, ID-14.1, 08.03.03
Cys1Ala	700 PB, 300 AS, 100 S	30 % Glycerol	ESRF, ID-14-EH4, 22.02.99
Cys1Ala (form 2)	425 PB, 75 AS, 50 S, 200 PEG 4K 50%, 2 pv	30 % HXT	ESRF, ID-29, 15.05.03
Cys1Ala (form 3)	425 PB, 75 AS, 50 S, 200 PEG 4K 50%, 2 PAA	30 % HXT	ESRF, ID-29, 15.05.03
Cys1Gly	830 SCB, 100 MC; 70 PEG 20K 5% (w/v)	30 % Glycerol	ESRF, Grenoble, Dec, 1999
Cys1Gly (pv)	700 PB, 300 AS, 100 S, 2 pv	30 % HXT	ESRF, ID-14.1, 08.03.03

PB : Phosphate Buffer, 200 mM, pH 6.4
AS : Ammonium sulfate saturated
S : Sucrose 10% (w/v)
ML : Maltose 2M
DMSO : di-methyl sulfoxide
NC : Nickel chloride 2M in PB
HXT : 1,2,6-Hexane tri-ol
pv : 1 M Penicilllin V
PAA : 1M Phenoxy Acetic Acid
SCB : Sodium Cacodylate Buffer, 0.1M, pH 6.13
MC : 2M Magnesium Chloride

3. 3. 3. Pre-Cys1Ser-I

Crystallization trials with AS as precipitant gave crystals of pre-Cys1Ser. The quality of these crystals could be improved by the addition of di-methyl sulfoxide (DMSO). These crystals were more stable also. The optimum conditions resulted in plate-like crystals of approximately 0.3 x 0.3 x 0.1 mm size. The crystals belonged to the monoclinic space group $P2_1$, with unit-cell parameters a = 102.64, b=90.09, c=102.27 Å, β=102.13°. The crystals diffracted to 2.5 Å resolution using synchrotron X-ray source at Daresbury, beam-line 14.2. As in the previous case 30 % (v/v) HXT prepared in crystallization solution provided cryoprotectant for data collection at 100 K in the liquid nitrogen stream.

An oscillation range of 0.5° and 5 s exposure time per frame was used to collect 360 frames (Table 3.1). A total of 236110 reflections were collected of which 62997 were unique (Table 3.2). Running SCALEPACK on the data gave 99.9 % completion with R_{merge} of 8.6 %.

Another X-ray data set (pre-Cys1Ser-II) for the similar mutant was collected at ESRF. It was different from the earlier one as the crystal grew without DMSO. The unit cell dimensions were a=102.76, b=90.48, c=102.69 Å, β = 101.81°. The maximum resolution reached was 2.2 Å. 360 frames were collected, each given 0.5° oscillation and 5 s exposure time. Out of 341910 reflections recorded 91743 were unique. The data were complete by 98.7 % and R_{merge} was 6.9 % (Table 3.2). Later the crystal was confirmed to have merohedral twinning with twin fraction of 0.49579 (Table 6.6).

3. 3. 4. Truncated Cys1Ser

Complementary to the studies on pre-Cys1Ser, a processed form of the same mutant was prepared and crystallised. Assay showed this mutant inactive towards Pen V. The crystals (Cys1Ser pv) belonged to orthorhombic space group $P2_12_12_1$. These crystals grew only when Pen V (5.42 mM) was also present in the hanging drop. These crystals diffracted to 1.9 Å at ESRF beam-line ID-14.3. The cell dimensions were a = 90.93, b = 129.42, c = 158.78 Å. Data were 96.7 % complete with R_{merge} 11.8 %. Out of a total of 470208 reflections 132141 were unique (Table 3.2).

Another crystal form (Cys1Ser) of this mutant belonging to monoclinic space group $P2_1$ also grew from AS, which was confirmed to have merohedral twinning. These crystals diffracted upto 2 Å resolution at ESRF. A total of 360 diffraction frames were collected with 0.5º oscillation and 1s exposure time. The data was 98.2 % complete for 121040 unique reflections out of a total of 463873. Data merged in monoclinic space group $P2_1$ gave R_{merge} 9.4 % (Table 3.2).

3. 3. 5. Pre-Asn175Ala

The mutant pre-Asn175Ala also gave crystals belonging to monoclinic space group $P2_1$ like the two precursor mutants already described (Figure 3.1). Structural comparison between native and precursor proteins showed differences in intermolecular interactions that could influence the crystal packing. This has been discussed in detail in chapter 6.

Good crystals were grown using hanging drop method against precipitant solution containing saturated AS (350 µl), 200 mM phosphate buffer at pH 6.4 (650 µl) and 100 µl sucrose 10 % (w/v) as additive. Cryo-protectant was 30% HXT.

X-ray diffraction data were collected using charge-coupled device (CCD) camera on beam-line 9.6 at SRS, Daresbury, from a crystal freezed at 100 K. The unit cell dimensions were a=103.66, b=92.52, c=103.84 Å, β = 101.79°. The maximum resolution reached was 2 Å. 255 frames were collected, each given 0.5° oscillation and 2 s exposure time. Diffraction images were indexed, integrated and scaled using the HKL program suite. Out of 1130879 reflections recorded 129730 were unique. The data were complete by 99 % and R_{merge} was 9.2 % (Table 3.2).

3. 3. 6. Truncated Asn175Ala

This particular mutant was included to study the catalytic efficiency of PVA in the absence of Asn175, prepared by omitting the precursor peptide and retaining the N-terminal methionine. It is expected that this Methionine residue essential for initiation of protein translation will be removed on completion of translation.

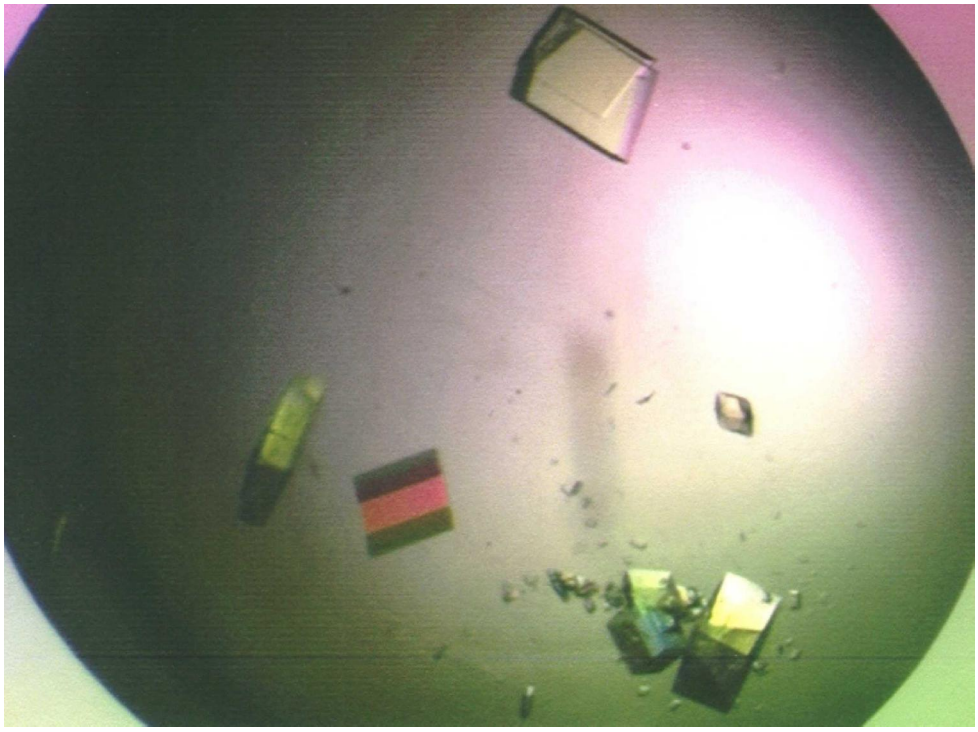

(a)

(b)

Figure 3. 1
(a) Monoclinic (form II) crystals of Pre-Asn175Ala precursor and (b) (form I) crystals of Asn175Ala mutant proteins of PVA.

No crystals of satisfactory quality could be grown using AS as precipitant and additives such as sucrose and maltose used in the crystallization of other mutants were also ineffective. Trials with more additives finally yielded good diffraction quality crystals with AS and sucrose in the presence of 44.44 mM nickel chloride. The crystals belonged to monoclinic space group $P2_1$ with a large b axis (a = 47.29, b = 379.39, c = 102.01 Å, β = 93.51°). Data were collected at ESRF beam-line ID-14.3 on a crystal at 100 K, flash-frozen in liquid nitrogen stream. The cryoprotectant was 30 % (v/v) HXT prepared in crystallization solution. The crystals diffracted to 1.7 Å. Out of 1293348 reflections recorded 370615 were unique (Table 3.2). The completion of data was 94.6 % and R_{merge} 6.9 %. This new monoclinic form will be denoted as $P2_1$ (form I).

3. 3. 7. Truncated Cys1Gly

Crystals of truncated mutant Cys1Gly were grown from a solution of PEG 20K in sodium cacodylate buffer at pH 6.13. The well solution in this case was prepared by mixing 70µl of 5% (w/v) PEG 20K, 830µl of 100mM sodium cacodylate buffer at pH 6.13 and 100µl of 2M $MgCl_2$. The orthorhombic crystals had space group $P2_12_12_1$. To freeze the crystals in cryostream 30% (v/v) glycerol prepared in crystallization solution was used. Crystals diffracted upto 1.8 Å. The total number of reflections collected were 166177, out of which 155411 were unique (Table 3.2). The data set was 99.04 % complete with R_{merge} of 10.9 %. The solvent content was calculated to be 61.23 %.

3. 3. 8. Cys1Gly co-crystal

After several trials with precipitants and additives as well as soaking experiments only a successful data collection on a co-crystal of Cys1Gly and Pen V could be accomplished. Soaking of Cys1Gly crystal always resulted in crystals cracking within fraction of seconds after soaking. Those survived showed only diffused and poor diffraction.

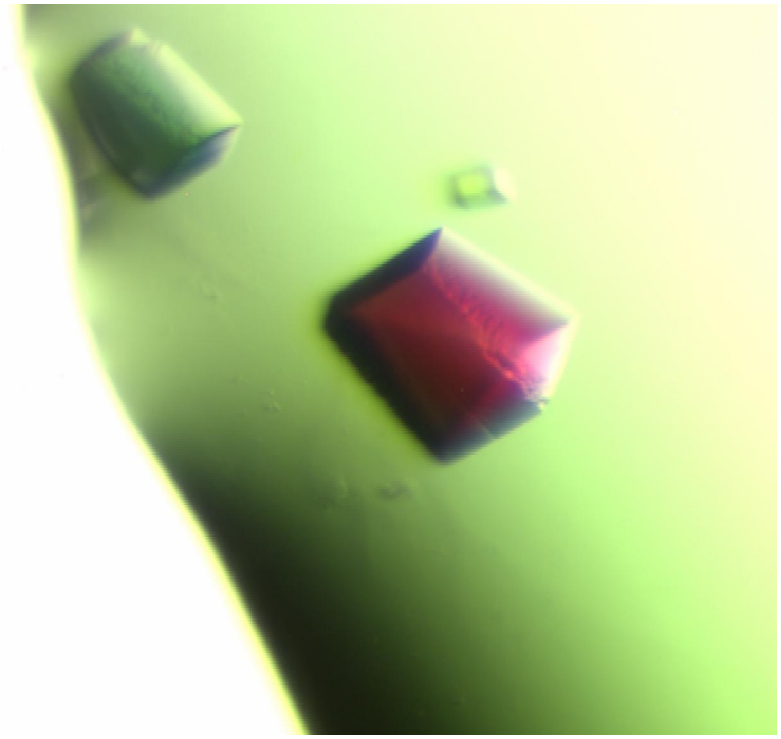

Figure 3. 2 *Orthorhombic crystal of Cys1Gly mutant - substrate Pen V complex.*

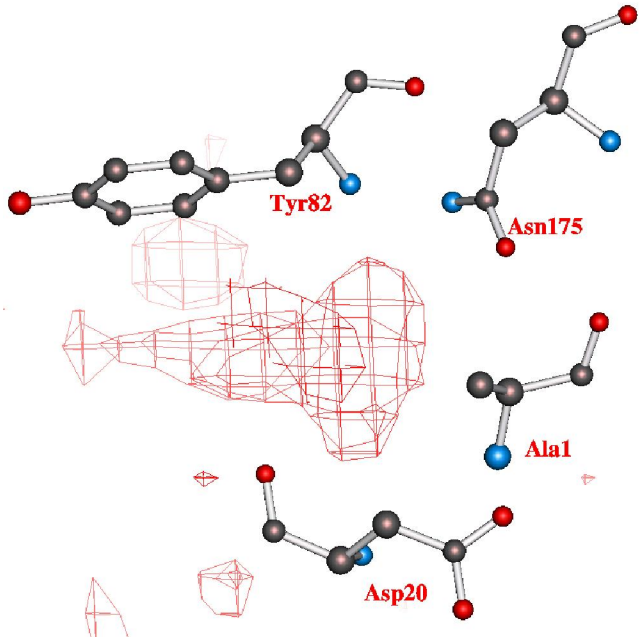

Figure 3. 3 *An unidentified electron density has been found in mutants Cys1Ala and Cys1Gly occupying the oxy-anion hole.It is shown with F_o-F_c difference electron density map (3σ).*

The crystals of Cys1Gly co-crystallised with Pen V grown from a solution of AS as precipitant and sucrose as additive. The crystal took more than a month to grow. The concentration of Pen V used in the experiment was 1.5 mM. The crystals were very tiny (0.1 X 0.1 X 0.1 mm) (Figure 3.2). 30% (v/v) HXT was used as cryo-protectent. Data upto 2.5 Å resolution was collected at ESRF beam-line ID-14.1. The data was indexed in spacegroup $C222_1$, a new spacegroup irrespective of the similar conditions used previously for crystallization of this mutant.

Indexing and merging of the co-crystal data set suggested a similar pattern of pseudo- symmetry in this data too. Careful observation has brought to notice some significant differences in behavior of this crystal. The crystal morphology is very distinct than the true monoclinic form (Figure 3.2). As opposed to $P2_1$ form which grows in 3 to 4 days this crystal takes more than one month to grow. The refinement pattern in $C222_1$ space group is very encouraging, as the R factor has come down to 24.6 %. It should be noted that the R factor for refinement in $C222_1$ in other problematic data sets never reached below 38%.

3. 4. An unidentified electron density at the active site of mutants

Initially, two inactive truncated PVA mutants Cys1Gly and Cys1Ala were crystallised for co-crystallization studies with substrate. In their crystal structures both these mutants showed similar unidentified electron density at the active site (Figure 3.3). These were in the preformed oxyanion hole near the nucleophile. It is thought that a small molecule might have got incorporated into the protein from either the fermentation media or during purification or from crystallization buffers. No chemical that could be thought of as can be present in fermentation, purification or crystallization media could be fitted into the electron density. Other possibility is that it has got incorporated in the active site from the cell metabolism itself. A hydrophobic patch exists in the vicinity of the nucleophile in PVA. Any mutation of N-terminal cysteine in to a non-polar residue extends this hydrophobic region. In such a case any molecule with hydrophobic tail and polar (negatively charged) head group can bind strongly in the oxyanion hole. This perhaps mimics the stabilization of partial negative charge on the carbonyl group of scissile bond. The affinity of mutant enzyme for the substrate Pen V has decreased to

such an extent that a high concentration of substrate or substrate derivative (Pen V, cephalosporin C, 7-amino cephalosporanic acid, 6-amino penicillanic Acid) could not displace this molecule from the oxyanion hole. Combination of all these factors together made co-crystallization with substrate Pen V a formidable task.

To obtain a co-crystal with substrate Pen V, it is important that the oxyanion hole is freely accessible and not permanently blocked. To remove the blocking molecule from the substrate binding site, protein was subjected to vigorous dialysis in denaturing conditions. Dialysis in 4 M urea (in 50mM phosphate buffer) overnight was tried. The concentration of urea in dialysate was increased gradually in steps of 0.5 M every 3 hours. After that, the dialysed protein was again renatured slowly. The concentration of urea in dialyzate was decreased gradually in steps of 0.5 M every 3 hours. This dialyzed protein sample was used for co-crystallization with substrates Pen V, cephalosporin C, 7-Amino cephalosporanic acid and 6-Amino penicillanic Acid (data not shown). Unfortunately, the unidentified electron density was still found in the same original place in the denatured and renatured protein even without soaking in any ligands.

Prior to denaturation-renaturation experiment, truncated mutant Cys1Ala had crystallised using AS in monoclinic space group $P2_1$. Dialyzed protein, crystallised from a solution containing both AS and PEG. The crystals belonged to orthorhombic space group $P2_12_12_1$ with unit cell dimensions a=91.18, b=129.49, c=159.01 Å.

3. 5. Conclusions from crystallization experiments

Native PVA had been crystallised with AS as precipitant. The basic problem of crystals of mutants grown with AS was their poor quality of diffraction. It was almost impossible to get high resolution data from these crystals. Moreover, the mosaicity of the crystals was beyond the tolerance limit.

A variety of conditions were tried to improve the diffraction quality of the crystals. Crystallization trials using hampton screen and CSS-I & CSS-II (Brzozowski & Walton, 2001) kits gave morphologically well formed crystals. The conditions for better crystals narrowed down to two. Crystals from lithium sulfate were excellent morphologically and sufficient in size (0.2 X 0.2 X 0.2) (Figure 3.4). Unfortunately, their diffraction was not upto the expectation. Improvement tried with several additives

[Isopropanol, Dioxan, Dimethyl formamide (DMF), Dimethyl Sulfoxide (DMSO), Glycerol, Ethelene Glycol, NDSB-195, NDSB-201 (Non-Detergent Sulfobetaines), trimethylamine N-oxide (TMAO), Polyoxyethylene 5-octylether, 2-ethoxyethanol (ethyleneglycol monoethyl ether, Cellosolve)] did not yield satisfactory results.

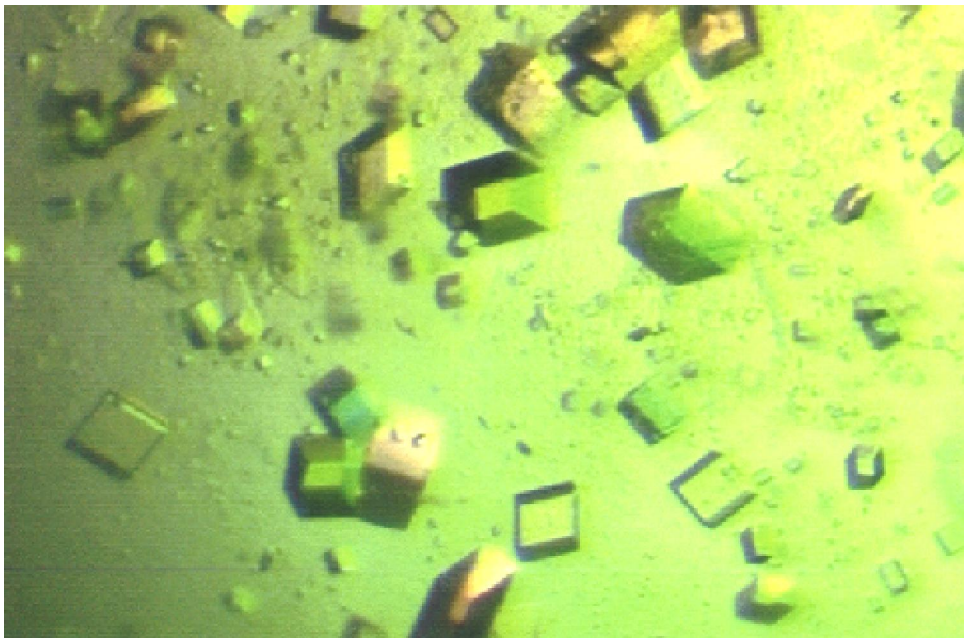

Figure 3. 4

Crystals of pre-Asn175Ala mutant grown with Lithium sulfate as precipitant. These morphologically excellent crystals did not diffract.

Finally, PEG turned out to be a good precipitant. Cys1Gly mutant gave good quality crystals with sodium cacodylate buffer. The crystals diffracted to 1.8 Å at ESRF. However, the same conditions failed to give crystals of other PVA mutants such as pre-Cys1Ala, pre-Cys1Ser and pre-Asn175Ala. It was then hoped that perhaps AS with some additives could help. Several additives were tried which resulted in better crystals in individual cases. For example, DMSO helped to grow crystals of pre-Cys1Ser, Maltose improved crystals of pre-Cys1Ala and Nickel chloride helped to grow Asn175Ala crystals.

3. 5. 1. Synchrotron Data collection

The benefits of having high resolution data include bringing greater precision in the analysis of the structure and higher reliability of atom positioning and geometry. A high resolution structure of PVA is important for locating every atom or groups at the active site, since the primary objective of this research is to understand the autocatalytic processing and enzyme catalysis. High resolution data would enable to draw clear distinctions between the interacting atoms of active site residues observed in the wild type PVA, the unprocessed and processed mutants and the substrate complex of mutant enzyme.

It is always mentioned that synchrotron sources are beneficial for X-ray data collection. But there are some disadvantages also. Fast crystal death is an obstacle towards collecting full data from one crystal alone in the case of delicate crystals. Beam lines at ESRF, France are one of the most intense synchrotron sources available. PVA crystals of pre-Cys1Ala and co-crystal of Cys1Gly with Pen V were tiny (or delicate) and died prematurely in the beam leaving the data incomplete. Pre-Cys1Ala data is only 93.3 % complete whereas data from co-crystal of Cys1Gly with Pen V is only 89.7 % complete. Interestingly, it is reported the crystal decay can be used to derive phases to determine the structure (Ravelli *et al.*, 2003).

3. 5. 2. Orientation of longest axis in data collection strategy

Crystals of Asn175Ala mutant grew in monoclinic form $P2_1$ (form I) when crystallised with nickel chloride as additive (Figure 3.1). These crystals took 10-15 days to grow and diffracted to 2.1 Å on home source. One of the cell dimensions turned out to be much larger (~380 Å) than the other two. The requirement for data collection from this kind of crystal demands optimizing the crystal orientation. It is advantageous if longest cell axis is aligned along the spindle axis. Crystals often grow slowest along the direction of the longest axis and because of that it provides the thinnest dimension also of the crystal. Invariably the crystal need to be remounted in the loop with changed orientation so as to bring the thinnest dimension (corresponding to the largest axis) along the spindle axis. Then, comparatively high resolution data can be collected on such crystals in one setting.

CHAPTER - FOUR

THE STUDIES ON THE AUTOPROTEOLYTIC ACTIVATION OF PENICILLIN V ACYLASE FROM *BACILLUS SPHAERICUS*

4. 1. Introduction

There have been several studies in higher eukaryotes and animal viruses where proteolytic production of functional proteins from polypeptide precursors is encountered, but only few such cases have been encountered in bacteria (Thony-Meyer *et al*., 1992). Variety of them has been found to activate by self-catalysed peptide bond rearrangements from single-chain precursors. These protein systems are modified by intramolecular and/or intermolecular cleavages of precursors to become active enzymes.

The interaction with damaged DNA initiates a cascade of proteolytic cleavage steps linked with auto-activation of p53 protein (Okorokov & Milner, 1997; Molinari *et al.*, 1996). Several serine protein convertase are secreted as zymogens and activated by autoproteolysis in endoplasmic reticulum and golgi apparatus (Nakayama, 1997). After translocation from cytosol to the membrane the enzyme calpain undergoes two N-terminal autoproteolytic events to form two smaller subunits (Croall & DeMartino, 1991). Rosenblum & Blobel (1999) have molecularly characterized an autoproteolytic cleavage in conserved nuclear pore complex proteins essential for the biogenesis of two nuclear pore complex proteins in mammals and yeast. Ornithine acetyltransferase undergoes autoproteolytic cleavage between the alanine and threonine to yield two subunits that assemble into a heterotetramer in prokaryotes (Marc *et al*., 2000; 2001) and heterodimer in yeast (Abadjieva *et al*., 2000). Similarly, autoprocessing is an essential step for the activation of Human immunodeficiency virus type 1 protease (Wang *et al*., 1986). Autoproteolysis in hedgehog leads to mature protein (Perler, 1998a). From the application part, targeting of proteins to membranes can be used through hedgehog autoprocessing (Vincent *et al*., 2003). The fact that these proteins can self-process at these scissile peptide bonds suggests that these are not typical peptide bonds (Qian *et al*., 2003).

It is known in the literature from the three-dimensional structures of proteins identified as members of the Ntn-hydrolase family such as penicillin G acylase (PGA) (Duggleby *et al* 1995), cephalosporin acylase (Kim *et al*, 2000), glycosyl asparaginase (Oinonen *et al*, 1995), glutamine amidotransferase (Smith *et al*, 1994), proteasome (Groll *et al*, 1997; Löwe *et al*, 1995; Bochtler *et al*, 1999) all posses an N-terminal residue either a Cys, Ser or Thr that act as both nucleophile and base for autoproteolysis. By now it is

well recognised that the post-translational cleavage of peptide bond can be considered as a chosen method of biological systems to activate molecules participating in many diverse biological processes. Very often these processes are regulated by external factors or induced by environmental changes. Recent findings in the case of Ntn-hydrolases (Zwickl *et al*., 1994; Brannigan *et al*., 1995; Aronson, 1996; Guan *et al*., 1996; Schmidtke *et al*., 1996), pyruvoyl-dependent enzymes (Recsei *et al*., 1983), Hedghog proteins (Lee *et al*., 1994) and in the case of protein splicing (Paulus, 1998; Perler, 1998a) have confirmed that it is an intramolecular autoproteolysis that activates these proteins.

N-terminal nucleophile hydrolases form a novel class of hydrolytic enzymes that are activated from an inactive precursor polypeptide by autoproteolytic processing, generating a new N-terminal residue. It is known that the intramolecular proteolysis proceeds through an N à O or N à S acyl shift (Tikkanen *et al*., 1996; Schmidtke *et al*., 1996; Guan *et al*., 1998; Perler, 1998b) and leads to an ester or thioester that is subsequently hydrolysed to a carboxyl and an amino group probably by the attack of a nucleophilic water molecule. As a result of this cleavage a free alpha amino group is generated which has to become an essential component of the enzyme's active centre. The resulting N-terminal residue becomes comparatively more exposed to solvent and plays the role of the nucleophile in Ntn-hydrolases (Brannigan *et al*., 1995; Murzin, 1996; Xu *et al*., 1999). The members of the Ntn-hydrolase family possess S^{γ} of the cysteine or the O^{γ} of the serine or threonine as the nucleophile atom. These hydrolases act on a range of substrates to cleave an amide or an ester bond by a nucleophilic reaction. The autocatalytic mechanism that activates the enzyme is also hypothesized to be a common feature in all Ntn-hydrolases (Zwickl *et al.*, 1994; Kasche *et al*., 1999; Lee *et al*., 2000b; Hewitt *et al.*, 2000).

In this chapter, we analyse precursor structures of PVA site directed mutants, from which the mechanism of autoproteolytic reaction of PVA could be deduced. The crystal structure analyses of these mutants have given insights into the self catalysed intramolecular proteolytic processing of PVA. It has revealed the importance of cysteine residue at the processing site, revealed the strained geometry of the scissile peptide bond and has eventually captured an intermediates generated during the processing event of

PVA. The mutant pre-Asn175Ala structure presents direct evidence for the N à S acyl shift during autoproteolysis. A detailed inspection of the scissile peptide bond and its environment in the mutated precursor molecule is an obvious step towards understanding the chemistry of the reaction. But the PVA precursor structures analysed are not that of the truly native molecule; there is a mutation at one of the critical residues closer to the linker peptide. It is possible that the conformations of local side chains and possibly that of main chain and the surrounding water structure might have been altered by this mutation. Nonetheless some careful comparisons can be made and it is possible to arrive at some conclusions on the reaction mechanism.

4. 2. Studies of post-translational processing in PGA and CPA

The gene coding for the open reading frame of *B. sphaericus* penicillin V acylase has bases coding for a tri-peptide Met-Leu-Gly in front of the N-terminal cysteine. Post-translational processing removes these three amino acids from the precursor N-terminus to unmask the nucleophile cysteine and to generate its own free α-amino group. This processing is different from those of penicillin G acylase (PGA) and cephalosporin acylase (CPA), where the open reading frame consists of a signal peptide followed by an α-subunit, a spacer sequence, and a β-subunit. The genes of PGA & CPA are translated into an inactive single chain precursor peptide that is post-translationally modified into active enzyme having two chains, one for α-subunit and other for β-subunit (Brannigan *et al*, 1995). The nucleophile is the N-terminal residue of β chain. Serine is the nucleophile in PGA that carries out both autoproteolysis and enzymatic deacylation whereas cysteine has replaced serine in PVA. Unlike the heterodimeric PGA which requires minimum two clevages to autocatalyse and generate α and β-subunits, the autoproteolysis of PVA resulting in a single shortened chain can be accomplished in a single cleavage.

The essential role of the α-amino group of N-terminal serine in β-subunit for enzyme catalysis and autoproteolytic activation has been identified (Lee *et al*., 2000b). It has been shown that the autocatalytic processing of the glutaryl 7-aminocephalosporanic acid acylase is a two-step reaction (Lee & Park, 1998). In the case of cephalosporin

acylase also it has been concluded that the active site residues are critical for catalysis as well as for post-translational modification (Kim & Kim, 2001).

4. 3. Mechanism proposed for autoproteolysis in PGA and CPA

On the basis of precursor structure, an activation mechanism for PGA and CPA during autoproteolysis has been proposed (Hewitt *et al*., 2000; Kim *et al*., 2002; Kim *et al*., 2003b; Lee & Park, 1998) that utilizes an N à O acyl shift. A sequestered solvent water molecule underneath the cleavage site of spacer peptide is held by pseudo-tetrahedral hydrogen bonded geometry. It is postulated that one of the hydrogen bonds could be created by a peptide flip under the influence of the conformational constraints within the spacer peptide. Water is positioned to act as a general base and can deprotonate the hydroxyl group of serine to enhance its nucleophilicity. The nucleophilic attack on the scissile carbonyl carbon of glycine by Ser O^{γ} would result in producing a transition state of the hydroxazolidine ring stabilized by oxyanion hole. Collapse of the transient hydroxazolidine shifts the scissile bond from an amide to an ester bond intermediate (N à O acyl shift), completing the acylation step of the primary processing. A bound water molecule carries out the second nucleophilic attack on the carbonyl carbon of the newly formed ester intermediate to start the deacylation step. After the second nucleophilic attack, the same oxyanion hole residues stabilize the tetrahedral intermediate. Finally, the ester intermediate collapses, resulting in a free N-terminal serine residue and the C-terminus of glycine.

Once the mobile end of the spacer peptide moves out of the autoproteolytic site it is now ready for the secondary processing. It is unlikely that the terminal serine can perform a direct nucleophilic attack on the secondary cleavage site, the distal peptide bond, since in protein like GCA it is 24 Å away from the primary autoproteolytic site. In the case of CPA the discharge of the spacer peptide resulting in the clearance of substrate binding pocket and the consequent introduction of solvent molecules in this space are prerequisite for its activity. The similarity in folding of the chains α and β in precursor as well as in mature protein, together with the burial of active site by the linker peptide, are conclusive evidence for the occurrence of an intramolecular autocatalytic mechanism of activation. The analysis of a mutant precursor of PGA has revealed firstly that there is

cleavage of 260–261 peptide bond and secondly that the Ser264 could lie in a position so as to make a nucleophilic attack on the 263–264 peptide bond. There are no nearby groups that can act as base and it can only be assumed that steric interactions, particularly those at the oxyanion hole, are sufficient to help this reaction (Burgi *et al*., 1973). In the deacylation step, the newly generated α-amino group presumably activates the water molecule hydrogen bonded to the O^{γ} involved in the second nucleophilic attack.

4. 4. The pre-processed/partially processed mutants of PVA

4. 4. 1. The role for a propeptide in PVA

The protection of cysteine from oxidation: A characteristic of cysteine and methionine containing proteins is the tendency of these residues to get oxidized (Stadtman, 1993). Susceptibility to oxidation of these residues is sequence-dependent and sometimes even minimal exposure to air can lead to oxidation. Once N-terminal cysteine gets oxidized the enzyme becomes catalytically inactive. In the crystal structures of precursor PVA, the tri-peptide acquires a folded arrangement such that Met–3 comes closer at one side of Ser1 in Pre-Cys1Ser (or beside Ala1 in Pre-Cys1Ala) mutant. The accessible molecular surface area of S^{γ} atom of Cys1 is obviously higher in the absence of Met –3 than in its presence. Decreasing the accessibility of Cys1 is thought to be a method to protect this residue from getting oxidized and inactivated. Methionine is also considered to be an antioxidant, protects other important amino acids against oxidation (Levine *et al*., 1996).

Regulating catalytic activity: From the crystal structure of unprocessed mutants it is apparent that the precursor peptide occupies the catalytic pocket. As long as the covalently linked precursor peptide is present it is impossible for substrate to access the catalytic cleft of PVA, resultantly there will be no enzyme activity. This could be a way of regulating the activity of PVA enzyme by the cellular system.

Any other advantage of the propeptide present: Precursor peptides, supposedly, have a probable role in the folding of the protein. The propeptides can help to achieve proper folding by the protein, i.e. it may work as a chaperon (Marie-Claire *et al*., 1999;

Bissonnette *et al*., 2004) and guide the protein towards right fold or perhaps keeps the polypeptide unfolded in certain instances. These proteins (eg. subtilisin) once fully unfolded cannot be renatured. These proteins are usually synthesized as preproteins that are later post-translationally activated by cleavage of the propeptide. Two types of experiments might help in the study of understanding the usefulness of precursor tri-peptide in PVA. One is the structural comparison and the other is probing the biochemical activity. All three pairs of PVA mutants were studied in this manner. The Cys1Ala mutation removes the nucleophile atom thereby suppressing both autoproteolytic processing and the enzyme catalysis. Thus the pre-Cys1Ala has the precursor tri-peptide at the N-terminus and Cys1Ala mimics the processed form but is inactive. A comparison of the secondary structural organization of precursor, truncated mutant and native PVA suggests that all three forms share the common fold. Irrespective of whether the propeptide is present or not PVA protein has folded correctly as in native (Table 6.3). Thus the role of extended tri-peptide in PVA may be only to regulate enzyme's self-activation.

4. 4. 2. Studies on *E. coli* PGA helped in selecting residues for mutagenesis

It is indeed very interesting to note the structural and mechanistic similarities between PVA and PGA even when their amino acid sequences completely differ. They also share the distinctive core structure of αββα motif, characteristic of Ntn-hydrolase family members. Both PVA and PGA have approximately the same angle (+30°) between the β-strands of the two β-sheets decorated by their active site residues. When these β-sheets were used as reference for structural alignment, the catalytic regions of PVA and PGA overlapped with a root mean square (r.m.s.) deviation of 0.46 Å for the putative catalytic atoms. The residues thus identified at the catalytic pocket were the targets of site directed mutagenesis studies. Structural comparison with PGA also led to the identification of atoms forming the oxyanion hole Nδ2 of Asn175 and the NH of Tyr82 in PVA, corresponding to Nδ2 of AsnB241 and NH of Ala B69 in PGA. Preparation of specific site directed mutants of PVA were directed at getting an understanding of autocatalytic processing also.

4. 4. 3. Slow self-activating mutants

To study the maturation process of PVA we sought mutations in PVA gene that retard or eliminate processing. The mutations selected are on the residues Cys1, Asp20, Asn175, Arg228, mutated to Ala or Ser using quick change mutagenesis. The crystal structures of the precursors of PVA have been determined that reveal the probable stereochemistry prior to autocatalytic cleavage of the residues sequentially or spatially close to the scissile peptide bond.

It was known that in the place of S^{γ} atom of cysteine residue the O^{γ} atom of serine or threonine can also act as nucleophile in enzyme activity as well as processing of Ntn-hydrolases. We decided to investigate the capability of serine to act in place of cysteine as nucleophile in PVA. Clone constructs for two mutants, one including the nucleotides for the extra tri-peptide at the N-terminal (pre-Cys1Ser) and the other excluding this peptide, to mimic the native form of PVA except that the N-terminal cysteine was mutated to serine (Cys1Ser), were prepared.

It is known that an asparagine residue similar to AsnB241 in PGA found in the oxyanion hole of Ntn-hydrolases stabilizes the tetrahedral reaction intermediate (Dodson, 2000). The mutation of this asparagine to alanine was introduced in a pair of mutants, one with the N-terminal tri-peptide present (pre-Asn175Ala) and another without it (Asn175Ala). The mutants crystallised in two different monoclinic unit cells (Chapter 6) different from $P6_5$ and P1 of wild type PVA, using crystallization conditions similar to that of latter (Chandra *et al*., 2005).

Pre-Cys1Ala

The obvious strategy of this mutation is to strip the N-terminal residue of its nucleophilicity. Importance of nucleophile cysteine for catalysis is indisputable, however, its importance in autocatalysis is unclear. Does PVA use the same residues for both autoproteolysis and catalysis? Whether PVA will be able to undergo post-translational modification in the absence of N-terminal nucleophile? The answers to these questions were expected to come from the analysis of pre-Cys1Ala. Biochemical assay carried out on this point mutant showed zero acylase activity towards substrate Pen V. This could be anticipated due to the absence of nucleophile atom. The difference in molecular weights

of pre-enzyme and processed mutants is not sufficiently large to distinguish their post-translational status in a SDS-PAGE experiment. Further information came from N-terminal protein sequencing of the mutant PVA. N-terminal sequencing of this point mutant (MLG**A**SS…) showed the presence of intact precursor tri-peptide. This result is an affirmation on the role of Cys1 in autocatalysis also. X-ray crystal structure of the pre-Cys1Ala showed continuous electron density for the extended precursor peptide. These observations have clearly answered the questions on the role of Cys1 in catalysis and autoproteolysis. Details of putative mechanism involving cysteine will be discussed later in this chapter.

Pre-Cys1Ser

The role of Cys1 as nucleophile is ascertained from the analysis of pre-Cys1Ala. Although Ntn-hydrolases share a common core structure αββα fold, they differ in the choice of residue that acts as N-terminal nucleophile. Moreover, invariably the nucleophile is very specific for a set of closely related enzymes irrespective of the source organism. Serine has been found in every PGA and CPA, whereas it is threonine in proteasomes. Here the question arises about the exclusiveness of cysteine in its N-terminal position in PVA. Is cysteine at this position indispensable for PVA processing and activity? Can serine substitute for the role of cysteine? To answer these questions we prepared the pre-Cys1Ser mutant. Biochemical assay of pre-Cys1Ser showed no penicillin V acylase activity. Now the question remains whether this lack of activity is due to insufficiency of serine as nucleophile in catalysis or due to the unprocessed protein. The N-terminal sequence of pre-Cys1Ser was determined as MLG**S**SS indicating a halt to autoprocessing happened in this mutant. Next, whether serine is sufficient as nucleophile for catalysis of Pen V can be ascertained independently from the processed mutant Cys1Ser.

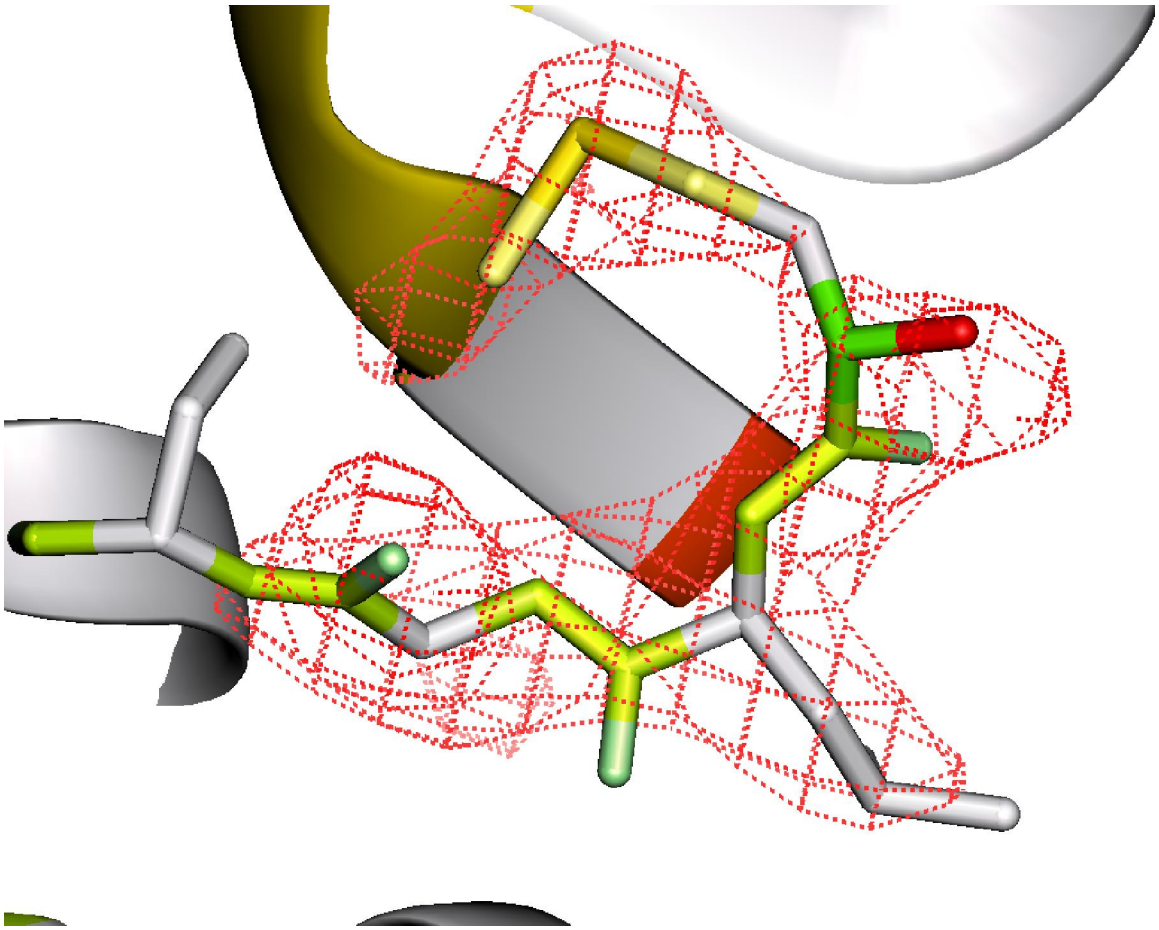

Figure 4. 1

Precursor peptide in the mutant Pre-Cys1Ser. Replacement of Cys1 by Ser made the mutant autoproteolytically inactive. The propeptide is shown with F_o-F_c difference electron density map (2.5 σ).

Pre-Asn175Ala

The oxyanion hole identified first in serine proteases, has been inferred to stabilize the tetrahedral complex formed during the catalysis. The oxyanion hole in PVA consists of main chain NH of Tyr82 and side chain Nδ2 atom of Asn175. The residue Asn175 has been mutated to Ala to investigate the importance of this residue in

autoprocessing. This will also tell whether NH of Tyr82 alone in the oxyanion hole can stabilize the tetrahedral complex even if Nδ2 is absent.

The pre-Asn175Ala mutant failed to show catalytic activity. N-terminal sequencing suggested partial processing at the N-terminus near nucleophile Cys1. In fact, two sequences were co-sequencing together in a proportion 50 : 50. The two sequences were MLG**C**SS.. and **C**SSL.. (Table 4.1). This co-sequencing could be due to partial processing of PVA. The absence of a complete oxyanion hole has obviously slowed down the process of autocatalysis but not completely eliminated it. In the X-ray crystal structure of pre-Asn175Ala unusual and different geometries have been seen for the scissile carbonyl carbon in different monomers of the tetramer (Figure 4.4). This is distinct from other precursor mutants (Figure 4.3). These different geometries observed can be associated with the dynamics of autocatalysis. Extremely weak hydrogen bonds are also present at the autocatalytic site of slow processing mutant pre-Asn175Ala. This also establishes the requirement for strong H-bond for fast processing to take place. The stereochemistry of the unusual geometry at the scissile carbonyl of Gly –1 in pre-Asn175Ala has been discussed later. The structure can be considered as an example to demonstrate how a nucleophilic side chain attacks the scissile peptide bond at the immediate upstream backbone carbonyl carbon and thus provides an understanding to the structural basis for peptide bond cleavage via an N à S acyl shift, a common mechanism in all intramolecular proteolytic autoprocessing.

Pre-Arg228Ser

Arg228 is a conserved residue at the active site of penicillin acylases. There are evidences that in the case of PGA arginines correspond to Arg228 and another one, presumably Arg17 in PVA, are crucial for catalysis. We also wanted to know the effect of mild change in charge rather than drastic change in hydrophobicity at this position. Hence this residue was substituted by a hydrophilic serine residue. There was no PVA activity for this mutant. N-terminal sequencing has shown its unprocessed state, irrespective of the fact that Arg228 is positioned ~6 Å away from the autoproteolytic centre (carbonyl carbon). This larger distance suggest perhaps only an indirect role for

Arg228 in autoproteolysis. Still its crucial role is established by unprocessing of this mutant. However, repeated attempts to crystallise this mutant have not succeeded.

Table 4. 1

Listing of the N-terminal sequences of PVA mutants and their activity. "Pre-" indicates the presence of precursor tri-peptide. Pre-Asn175Ala showed ~50 % processing activity based on the products detected by N-terminal sequencing. The proteins were pre-derivatised with acrylamide to allow detection of a stable Cys-adduct. The site of mutation at the N-terminus is highlighted in bold. $_{f}$Met indicates that processing had occurred, probably by simple removal of the initiator methionine residue.

PVA /mutant	N-terminal sequence		Activity	
	cloned gene	mature peptide	processed	Catalytic
Native	MLG**C**SS…	**C**SS…	Yes	Yes
Pre Cys1Ala	MLG**A**SS…	MLG**A**SS…	No	No
Pre Cys1Ser	MLG**S**SS…	MLG**S**SS…	No	No
Pre Asn175Ala	MLG**C**SS…	MLG**C**SS…+ **C**SS…	50%	No
Cys1Ser	M**S**SS…	**S**SS…	$_{f}$Met	No
Cys1Ala	M**A**SS…	**A**SS…	$_{f}$Met	No
Asn175Ala	M**C**SS…	**C**SS…	$_{f}$Met	No
Pre Arg228Ser	MLG**C**SS…	MLG**C**SS…	No	No
Pre Asp20Asn	MLG**C**SS…	MLG**C**SS…	No	No
nCys	MCSS…	CSS…	$_{f}$Met	Yes

Pre-Asp20Asn

The proximity of the carboxyl group of Asp20 to the free α-amino group of N-terminal residue suggests a major role for it in PVA reaction chemistry. In PGA GlnB23 occupies the corresponding position. Similarly, HisB23 sits at this position in CPA. It has been mutated to an amide group residue Asn to mimic GlnB23 of PGA while holding the same chain length as Asp20. No PVA activity could be detected in pre-Asp20Asn mutant. Not surprisingly, the subsequent N-terminal sequencing has showed it to be unprocessed.

Table 4. 2

X-ray data and refinement statistics for precursor and the corresponding truncated mutants. Penicillin V was present in the crystallization drop of Cys1Ser (pv).

	Pre-Cys1Ala	**Cys1Ala**	**Pre-Cys1Ser-I**	**Cys1Ser (pv)**	**Pre-Asn175Ala**	**Asn175Ala**
Unit cell (Å) *a* *b* *c*	103.30 89.88 103.60	47.86 381.89 102.89	102.64 90.09 102.27	90.93 129.42 158.78	103.66 92.52 103.84	47.29 379.39 102.01
β (°)	100.56	94.1	102.13	90	101.79	93.51
Space group	$P2_1$ (form II) *	$P2_1$ (form I)	$P2_1$ (form II)	$P2_12_12_1$	$P2_1$ (form II)	$P2_1$ (form I)
Refinement statistics						
R_{factor} [a] (%)	21.21	16.19	20.07	23.69	19.43	17.76
R_{free} (%)	25.61	20.45	24.74	27.88	23.44	20.36
Mean B factor (Å^2)	53.18	18.22	26.37	23.33	21.93	14.2
Bonds (Å)[b]	0.34	0.02	0.02	0.02	0.02	0.02
Angle (Å)[b]	2.60	1.46	2.03	2.20	2.53	2.18
Ramachandran plot[c]	82.4/16.3/1.3/0	91.2/8.1/0.7/0	87.7/10.4/1.6/0	90/9.5/0.5/0	90/9.2/0.6/0	90.9/8.5/0.6/0

[a]Rfactor = $\sum||F_{obs}| - |F_{calc}||/\sum|F_{obs}|$.

[b]Root-mean-square error.

[c]Percentage of residues in most favored/additionally allowed/generously allowed/disallowed region.

*Twinned

From a structural comparison with cysteine proteases and serine proteases a significant role for aspartate can be illustrated solely based on its position near catalytic base (Stopbauer *et al*, 1999). In these class of proteins the aspartate residue (pK_r=3.65) has been located near the base histidine (pK_r=6.00) to keep the base in a protonated state. Asp in PVA and His in CPA can be expected to assume similar roles of keeping the α-amino group protonated.

4. 5. The processed type mutants

The PVA gene sans the code for tri-peptide was cloned for assessing the influence of the tri-peptide on the folding and for understanding the environmental effects of the mutation in the processed form. The activity of the expressed protein was checked. The activity was not different from that of the enzyme obtained from native organism. Thus the role of propeptide in the case of PVA may be only to protect the active site till the maturation of the enzyme.

The processed mutants prepared were Cys1Gly, Cys1Ala, Cys1Ser, Asn175Ala and Asp20Asn. Among these, we could crystallise Cys1Gly, Cys1Ala, Cys1Ser and Asn175Ala mutants. The core of these structures, especially active site, superpose on native PVA with only insignificant r.m.s. deviation between atoms showing no major changes at macroscopic level has taken place, though the wild type and mutants have crystallised in different space groups and unit cells. From these experiments, it was concluded that the same residues in PVA are responsible for mediating autoproteolytic as well as catalytic activity.

4. 6. The role of Cys1 in autoproteolysis

As already stated PVA from *Bacillus sphaericus* is synthesized as a precursor protein with additional three residues at the N-terminus. The activation of PVA is by the removal of the above, which is linked to the N-terminal nucleophile residue in the inactive precursor molecule. Facilitated by various functional groups surrounding the autoproteolytic site, the side chain of Cys1 acts as a nucleophile to activate the immediate upstream peptide bond to substitute the peptide bond with more reactive intermediates.

All mutations replacing cysteine have deleterious effect on autoproteolytic and catalytic capabilities of PVA.

PGA (Hewitt *et al*., 2000) and subtilisin (Li & Inouye, 1994) lost activity (60-80% in subtilisin) when their respective nucleophile serines were substituted by cysteines. Mutating cysteine to serine in PVA suppressed its autoprocessing. The difference between Cys and Ser is only in their nucleophilic strength. Their mechanism of attack could remain same. The environments for the two enzymes are very different and resultantly the ineffective path for proton translocation could be the limiting factor.

4. 7. The effectiveness of serine as a nucleophile in the place of Cys1 in PVA

4. 7. 1. Serine is not sufficient as nucleophile in PVA

The serine O^{γ} atom acts as nucleophile in PGA and CPA. It was reasonable to expect Ser to work in place of Cys1 in PVA. However, such a mutation, surprisingly suppressed both the autoprocessing and catalysis. A possible explanation is that thiol group of cysteine is intrinsically a better nucleophile than hydroxyl group of serine (Kahyaoglu *et al*., 1997). In all precursor structures of PVA, the electron density for the propeptide has been found disordered.

It is interesting to note that in PGA when nucleophile serine was replaced by cysteine (SerB1Cys), autoprocessing still proceeded but not catalytic action on Pen G (Hewitt *et al*., 2000). Similarly SerB1Cys mutant of cephalosporin C acylase showed partial autoprocessing (only first step) but had no catalytic activity (Kim & Kim, 2001).

N-terminal sequencing of protein has shown that mutant Cys1Ser is unprocessed. In its crystal structure a non-catalytic conformation of serine has been observed. In addition to autoprocessing experiments a truncated mutant Cys1Ser was also prepared to confirm the catalytic efficiency of serine in PVA. It has been cloned excluding the precursor peptide sequence, so that the enzyme is produced in processed form. This truncated Cys1Ser mutant also failed to show PVA activity although the protein has folded in native conformation (Table 6.3). The proper folding of Cys1Ser was confirmed by X-ray crystal structure.

4. 7. 2. Interaction between Cys1 and Arg17: role of pK_R

During evolution proteins from related families can diverge beyond recognition, but still conserve their overall structural features and catalytic residues. In PVA, the role of Arg17 has been predicted to be important based on its proximity to the nucleophile residue (Pei & Grishin, 2003). Moreover, in a group of hydrolases also (U34 peptidase), an Arg has been identified near the nucleophile cysteine. It should be noted that Arg17 of PVA is not conserved in other Ntn family members that have Ser or Thr as nucleophile residue. The electronic effects of this conserved Arg in PVA are evident from site directed mutagenesis studies. In PVA Arg17 flanks nucleophile residue Cys1. Its disposition is conducive for the proton translocation in the direction of Cys à Arg, as Arg has higher pK_R value compared to Cys (Table 4.3). This can result in an unprotonated cysteine. The presence of Arg17 in PVA related proteins and simultaneous absence in PGA has conveyed the importance of this residue in the presence of cysteine residue. In PVA its role has been proved further by site directed mutagenesis studies.

Table 4. 3

Significance of Arg17 proximity on the protonation status of nucleophile cysteine and serine in PVA. pK_R values are taken from Principles of Biochemistry (Second edition) by Lehninger, Nelson, Cox.

Residue	**pK_R value**	**Direction of proton translocation**	**Nucleophiile**
Cys	10.28	From Cys to Arg	Cys unprotonated
Arg	12.48	-	-
Ser	13.6	From Arg to Ser	Ser protonated

In Cys1Ser mutant the terminal nucleophile residue Ser in combination with Arg (pK_R = 12.48) fails to undergo reaction. This is because of the shift in direction of proton translocation in Ser-Arg combination compared to Cys-Arg. In the former combination, the pK_R of Ser (13.6) is higher than that of Arg (12.48). So in pre-Cys1Ser mutant, Ser

will exist in protonated form and can neither catalyse nor autoproteolyse through a nucleophilic reaction.

Any reaction that inhibits Arg17 (specifically) would perhaps be able to bring reaction ability back to Cys1Ser mutants. Inspection of the environment near the Sγ in precursor structures shows that no group that can act as a base to extract the proton from nucleophile exists. In PGA, this reaction is presumably driven by the physical approach of the Oγ to the peptide bond brought about by the local structure (Hewitt *et al*., 2000; Bürgi *et al*., 1973).

4. 8. The role of Asn175 in autoproteolysis

4. 8. 1. Asn175Ala mutation affects catalysis more than autoproteolysis

The hydrolytic enzymes generally hold the catalytic group called the charge-relay system, or the catalytic triad consisting of His-Cys-Asp(Asn) or His-Ser-Asp first observed in papain and chymotrypsin, respectively. The nucleophilic capacity of Cys or Ser in hydrolytic enzymes is generated by a precise stereochemical arrangement of the interacting side chain and main chain groups. In the catalytic triad hydrogen bonds (H-bond) and electrostatic interactions promote nucleophilic capacity of the nucleophile residue in a range of cysteine and serine hydrolases.

Relatively, the side chains of the active site residues have distinct properties and functions. The carboxylate group of Asp20 forms a H-bond with the free α-amino group and the free α-amino group acts as a base to accept proton from the Cys1; the cysteine becomes a powerful nucleophile on losing this proton. When the substrate binds to the enzyme it is positioned through contacts mediated by the specificity pocket and active site, to favour attack by the nucleophilic S^{γ}. In this complex several events happen in concert. The proton leaves the S^{γ} and the scissile bond moves into the transition state conformation. The peptide bond is then broken down into the acyl (thioester) intermediate which in turn is attacked by a water that is activated by the aspartate : free α-amino group structure, still in place. Once the second tetrahedral intermediate collapses, the product leaves and the free enzyme gets regenerated.

Similar events are expected to take place during autoproteolytic as well as catalytic reaction in PVA, the availability of already formed free α-amino group is an

additional advantage in case of catalysis. It is strange to note that Asn175Ala mutation could retain 50% autoproteolytic capability (at least) but failed to perform catalytic activity after attaining truncated form (Table 4.1). On the catalytic front both precursor as well as truncated PVA are found inactive. The reason for lack of catalytic activity in the processed Asn175Ala may be attributed to the improper positioning of substrate in the pocket in the absence of Asn175. It is obvious that the positioning of the carbonyl carbon of Gly –1 with respect to nucleophile in autoproteolysis is relatively easier because the connectivity of the substrate through the amide bond whose α-amino group (of Cys1) is to be freed subsequently after processing. During catalysis proper alignment of the substrate may be difficult in the absence of all atoms of the oxyanion hole required for the stabilization of the electronic charge developed on carbonyl oxygen.

4. 8. 2. Impaired oxyanion hole slows the reaction

Reactivity was expected from pre-Asn175Ala mutant as autoprocessing events are taking place, very slowly. N-terminal sequencing has shown that the protein is 50% processed and the remaining 50% is unprocessed (Table 4.1). The lack of catalytic activity by the 50% processed proteins was not surprising in the context that truncated Asn175Ala mutant also showed no activity. It can be inferred from these two mutants that the modification at the oxyanion hole, although only partially affects the autoprocessing, completely suppresses the enzymatic activity.

The autoproteolytic mechanism involves two tetrahedral intermediates. As oxythiazolidine anion, the first tetrahedral intermediate, is short lived and unstable in the absence of a complete oxyanion hole, the reaction has become substantially slower. This is evident from the crystal structure of Asn175Ala mutant. The slow reaction rate in turn can perhaps be associated with weak hydrogen bonds at the autocatalytic pocket. Indeed, in the absence of Asn175 the carbonyl of the thioester is relatively poorly hydrogen bonded (3.11 Å) to NH of Tyr82. This might have halted the reaction at the autoproteolytic intermediate product. This was one of the aims of site directed mutation, to bring down the speed of reaction partially or fully, so as to ascertain the role of mutated residue in autoproteolysis.

The tetrahedral intermediate could not be obtained because the carboxyl group of Asp20 positioned near the scissile peptide bond is capable of donating a proton to promote the oxythiazolidine anion intermediate to turn it in to the thioester product (Figure 4.9a). It is imperative that to catch the tetrahedral intermediate the surrounding condition should be conducive for stabilizing the intermediate structure.

4. 8. 3. Abstraction of proton from S^{γ} is also dependent on Asn175

In pre-Asn175Ala structure thioester as well as precursor structure has been obtained in separate monomers of the tatramer. Although, the electro-chemical establishment at the autoproteolytic site is equal in all four monomers, the existence of distinct events modulates the possible mechanism. If the abstraction of proton from S^{γ} is independent of Asn175, all four monomers in the crystal structure should have snapped up at the thioester stage. Simultaneous presence of thioester as well as precursor form suggests the involvement (though not irreplaceable) of Asn175. Partial reaction could be attributed to some form of co-operativity among the monomers or could be the influence of random molecular dynamics. The pairs of monomers which have related configuration are A and C as well as B and D (Figure 5.6). It should be noted that an extension loop comprising of ~30 residues from each chain cuddles up with a neighbour. Interestingly, this extended loop reaches up to the autoprocessing site of neighbouring monomer.

4. 9. The participation of water molecule in autoproteolysis and acylase activity

4. 9. 1. Water occupies the space vacated by carbonyl oxygen of scissile bond

In several chemical reactions catalysed by enzymes, water molecule takes a central role for the efficient translocation of protons. Prior to the autoprocessing in Ntn-hydrolases the terminal α-amino group is unavailable to act as a base in nucleophilic attack. In autoproteolytic reaction of CPA, where serine is the nucleophile, the presence of a water molecule close to the autoproteolytic site is shown (Kim *et al*., 2002). According to the mechanism described for CPA, this water molecule mimics the base group and facilitates the nucleophilic attack on the carbonyl carbon. Considering the mechanistic similarity of autoprocessing in Ntn-hydrolases, a water molecule as found in others could be expected in PVA also. Absence of any such water molecule at the autoproteolytic site of PVA suggests that the requirements are different when cysteine is

the nucleophile residue. This has implications also to the combination of Arg17-Cys1 found in PVA active site.

The water, which occupies the position vacated by scissile carbonyl oxygen of Gly –1 influences the positions of other atoms also. Slight but important changes in the localization of atoms at the autocatalytic pocket because of Asn175Ala mutation involve a 0.57 Å movement of the main chain N of Asn175. Modelling the Asn to mimic its position in native PVA creates a short contact of 2.0 Å between Asn175 side chain and the autocatalytic water in pre-Asn175Ala (Figure 4.2).

Chemically, the deacylation step of the acyl-enzyme intermediate is unusually slow. Therefore the acyl-enzyme intermediate has accumulated in the crystal structure. Besides the absence of oxyanion hole residue Asn175, the reason for slow deacylation is the localisation of the attacking water in the sub-optimal location away from scissile carbonyl carbon. Like deacylation, acylation step also has been affected adversely, probably because the same residues are involved in both the reactions. The attacking water occupies the sub-spatial position earlier occupied by the scissile carbonyl oxygen of the propeptide. Water molecules at this sub-position in the structures of truncated mutants act as a bridge between the nucleophile and the free α-amino group.

4. 10. The geometry of residues at autoproteolytic site

4. 10. 1. Orientation of Gly -1 carbonyl group influences autoproteolysis

It is known from literature that Gly –1 is a conserved residue in many autocatalytic processing proteins (Albert *et al.* 1998; Schmidtke *et al.*, 1996; Hall *et al.* 1997; Perler *et al.* 1994; Porter *et al.*, 1995; Xu *et al.*, 1993). In two inactive precursor mutants pre-Cys1Ala and pre-Cys1Ser of PVA, the carbonyl oxygen of Gly –1 has been found interacting with NH of Asp20 (Figure 4.3). However, in the crystal structure of pre-Asn175Ala a distinct conformation of Gly –1 carbonyl is observed. In this case, carbonyl oxygen is weakly H-bonded to the oxyanion hole atom N of Tyr82 (Figure 4.4). The relationship of carbonyl conformation and the autoproteolytic processing in the mutants reported here suggests the importance of correct carbonyl positioning in the oxyanion hole for effective autocatalysis.

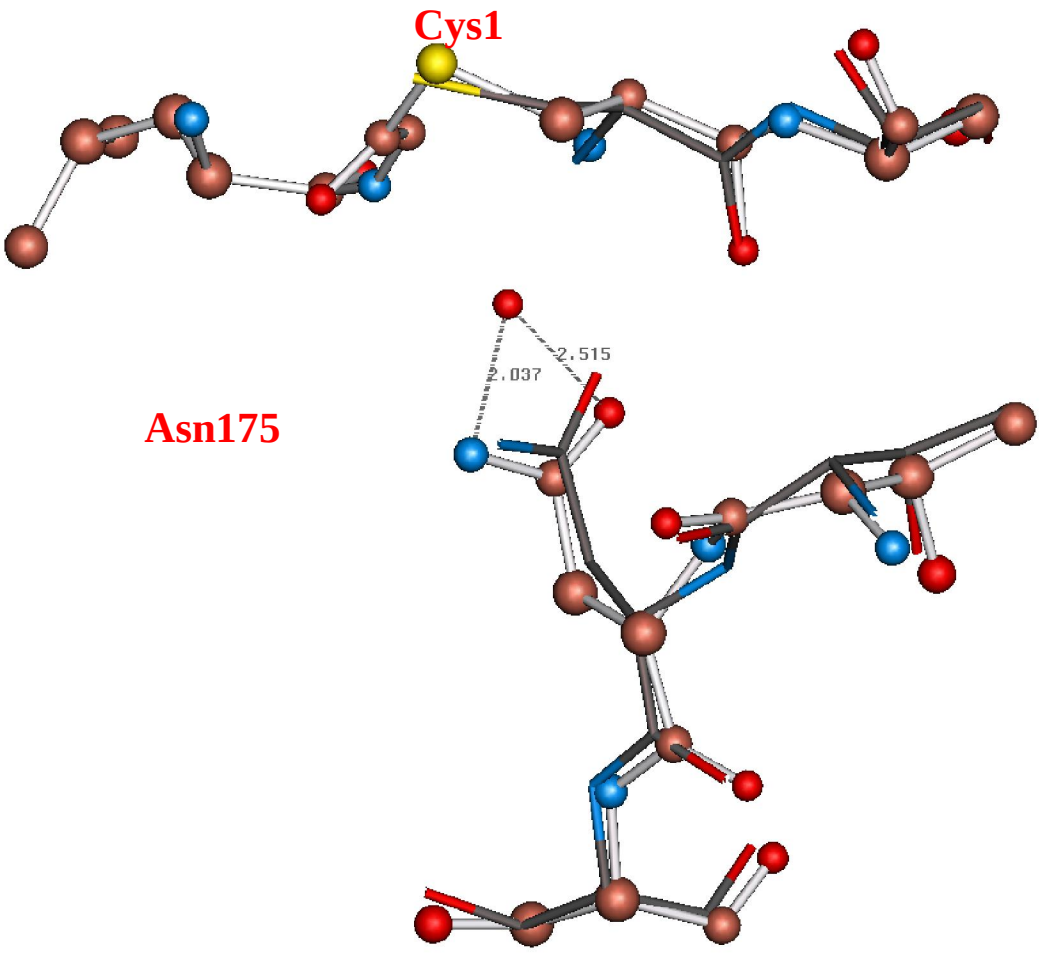

Figure 4. 2

Active site residues of pre-Asn175Ala mutant (white backbone, ball and sticks) superimposed on native PVA (red colour stick). Residue Ala175 in the mutant has been back- modelled as Asn as in the native structure 3PVA. The back-modelled residue Asn175 makes a short contact with the water molecule.

Figure 4. 3

Autoprocessing site in pre-Cys1Ser showing the conformation of carbonyl of Gly -1. Like pre-Cys1Ala this mutant is also autocatalytically inactive. The carbonyl conformation of the Gly –1 also overlaps in them. The electron density shown is 2Fo-Fc map at 2σ level.

All the three situations obtained from the three point-mutant-structures conclude that carbonyl oxygen interacts with main chain NH of Asp20 in the absence of sufficient nucleophilic capacity. In the presence of favourable nucleophilic residue its orientation is in the opposite direction and is stabilised by the oxyanion hole. This circumvolution brings the carbonyl of Gly–1 to an active conformation for autocatalysis. In this

conformation, the atoms of the oxyanion hole will balance the negative charge developed on carbonyl oxygen.

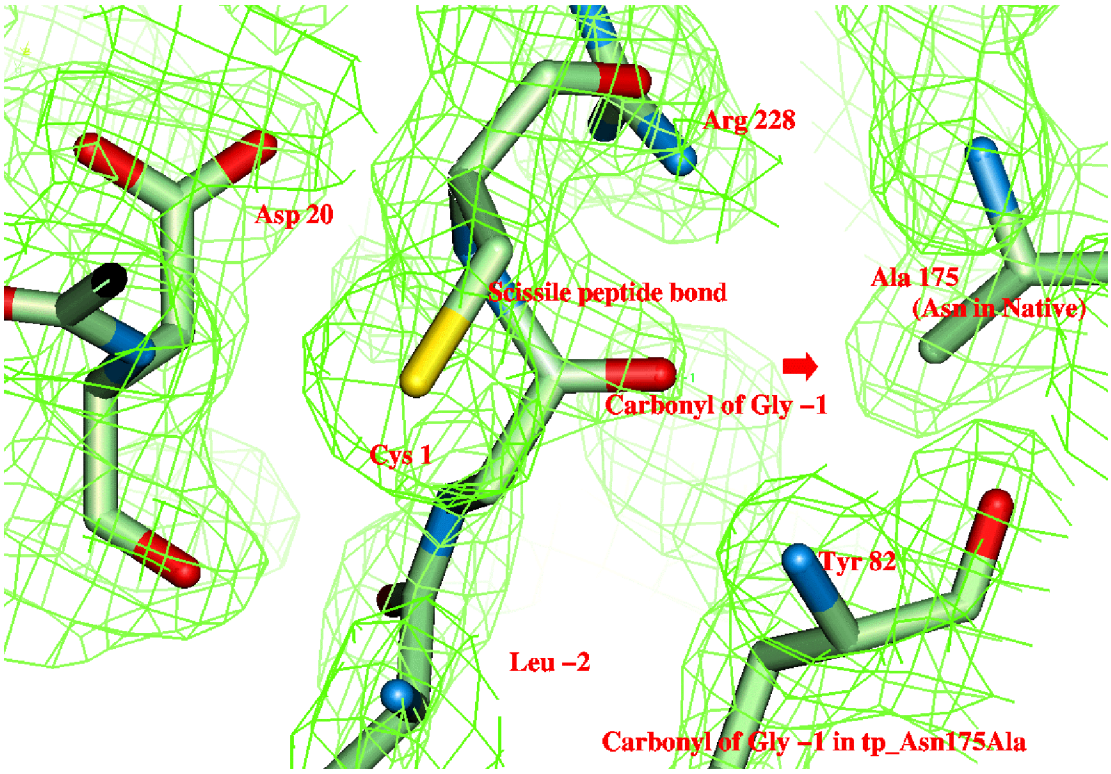

Figure 4. 4

Autoprocessing site in pre-Asn175Ala showing the conformation of carbonyl of Gly -1. Unlike others this mutant is 50% autocatalytically active. N-terminal sequencing also suggests partial processing. The electron density map shown is 2Fo-Fc map at 2σ level.

4. 10. 2. Distinct electron density at the autoproteolytic site of each monomer

The different conformations of amino acid residues at autoproteolytic site between monomers in pre-Asn175Ala mutant represent significant local structural

differences in the four monomer molecules of the tetramer. These differences can be related to the kinetic and allosteric properties of the enzyme.

In two monomers B and D, the propeptide has been found intact under normal conditions with carbonyl carbon of Gly-1 linked to N of Cys1 *via* a peptide bond. Though the strain on the peptide is evident from the χ^1 and φ values of Cys1. The favoured conformations of cysteine side chain are with χ^1 values 60, 180 and -60^o , and φ value range is -50 to –150^o (Figure 4.5). When pdb data were randomly scanned, we could identify some cysteins lying outside this conformation. After manually checking these deviating ones, it has been concluded that most of such cysteines are involved in di-sulfide bridges. Several of them belong to structures determined through NMR. In a few cases heavy metal (eg. Hg in 1ARO) is forcing cysteine to acquire positive φ values. In two structures, pdb: 1AYL and 1BSG they are found at the putative active site.

Eventually, the detailed knowledge of the differences in the conformations of the cleavage site cysteine in various precursor structures are helpful in understanding the relevance of this conformation for self processing. In Asn175Ala, Cys1 at the scissile peptide has a positive φ (89.7). This conformation of cysteine is not common when searched through the PDB files.

The connecting amino acid Gly–1 and the scissile peptide are in different conformations in different structures. The entrapped autoproteolytic site in PVA provides a convincing structural evidence to show that the processing is autocatalytic. Moreover, these structures observed for the first time in any Ntn-hydrolase family member provide clues to decipher the mechanism of autoproteolysis in them.

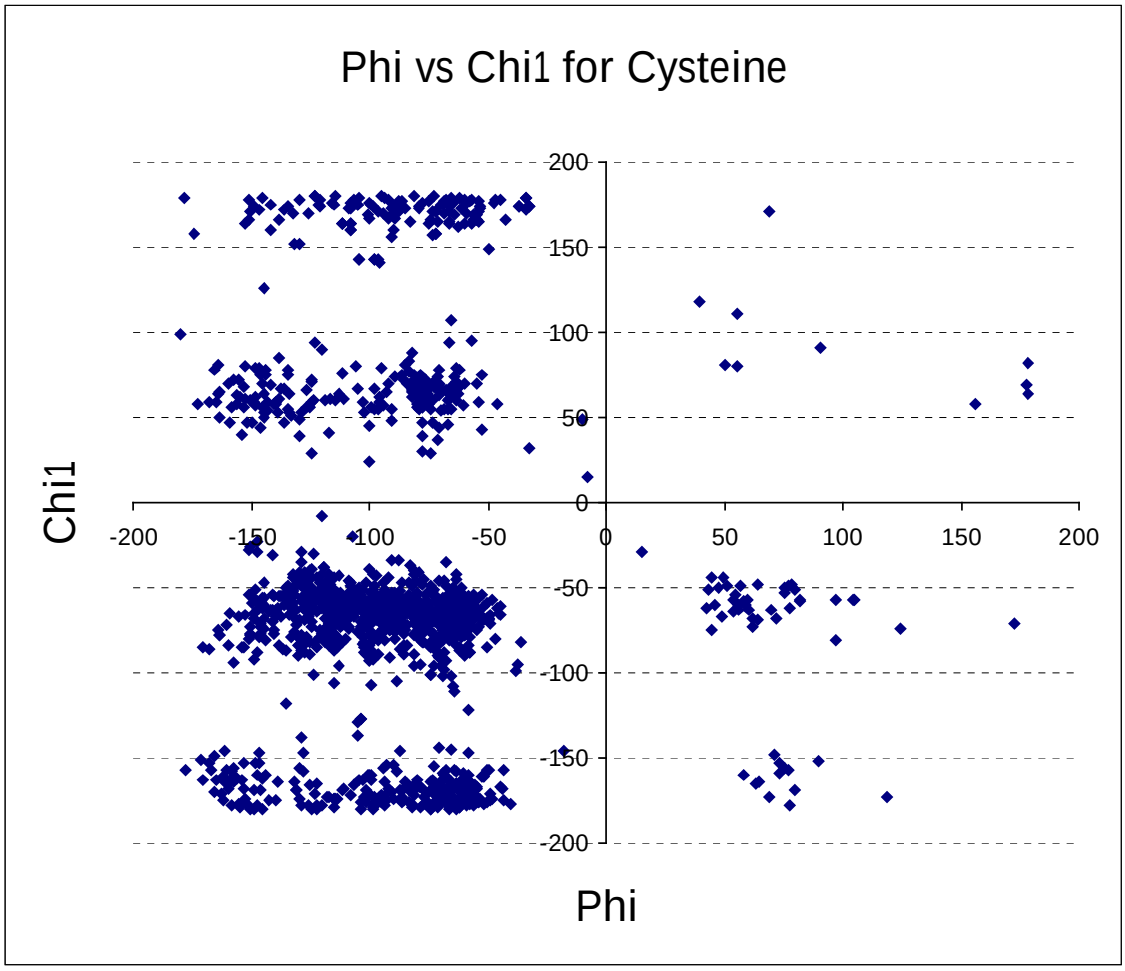

Figure 4. 5

Phi (ϕ) vs Chi1 (χ^1) distribution for Cysteine in a random set of proteins from PDB. All cysteines lying in the positive side of ϕ are either in disulphide bridges or interacting with metals. Only two of them are in active site.

4. 11. The enzyme active site and the autoproteolytic site

4. 11. 1. Propeptide occupies the catalytic pocket

Analysis of precursor structures and co-crystal structure of Cys1Gly mutant with bound Pen V has shown that the catalytic pocket is initially occupied by the propeptide in precursor structures. The positioning of substrate in modelled complex and the occurrence of propetide in precursor PVA both almost coincide. Hence, no catalysis and substrate binding is expected to take place in unprocessed enzyme. The mutational analysis of the active site residues has also suggested that the same catalytic centre is responsible for the cleavage of propeptide as well as the catalysis of substrate. Earlier, in the structure of a slow processing precursor of PGA also the blocking of active site cleft by spacer peptide similar to our observation in PVA has been reported (Hewitt *et al*., 1999).

4. 11. 2. Flexibility of adjoining loops and autoproteolysis

As could be expected, some rearrangements of the residues and solvent molecules could be observed in the structure of precursor type mutants compared to the processed type mutants in the vicinity of N-terminus. PVA active site pocket is flanked by two loops *viz*. 21-26 and 132-139. These two stretches are found extremely mobile in the crystal structures. This is interesting in the context that the side chain of Asp20 interacts with the free α-amino group of nucleophile residue Cys1. Comparison of the precursor structures with the corresponding truncated structures shows that these zones have moved inside to occupy the place vacated by the precursor peptide after autoprocessing has taken place (Figure 4. 6 and 4. 7). In studies on PVA modelled with the substrate molecule Pen V, this zone has moved a little bit inwards toward the catalytic pocket, similar to what found in processed structures.

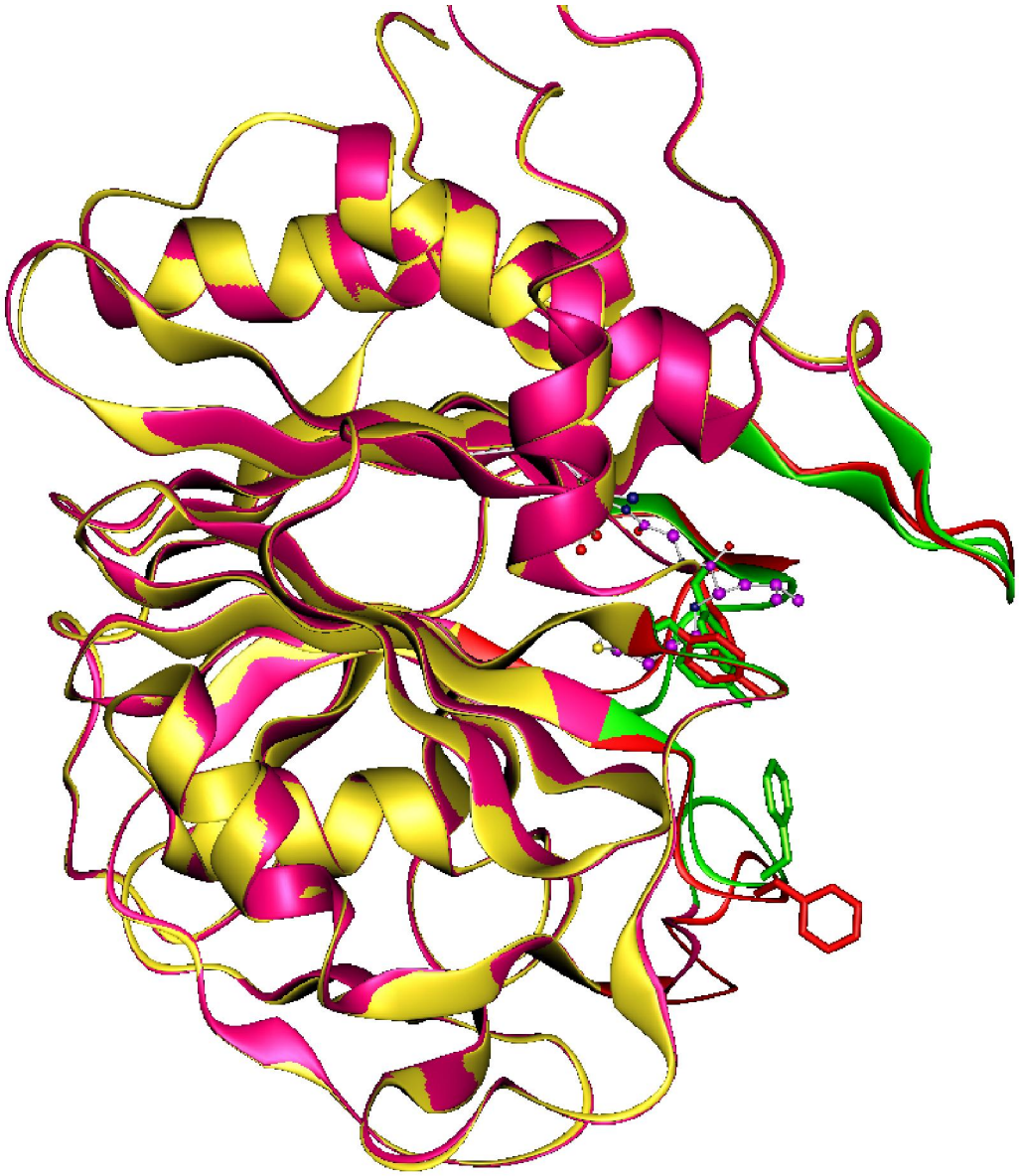

Figure 4. 6

Pre-Cys1Ser (red) superimposed on processed Cys1Ser mutant (Green in the flexible zone). Phe21 and Phe138 have been shown moved from their position in the two

structures. Precursor peptide is shown in ball and stick. In the absence of propeptide, the surrounding residues have moved in to occupy the space vacated by the propeptide

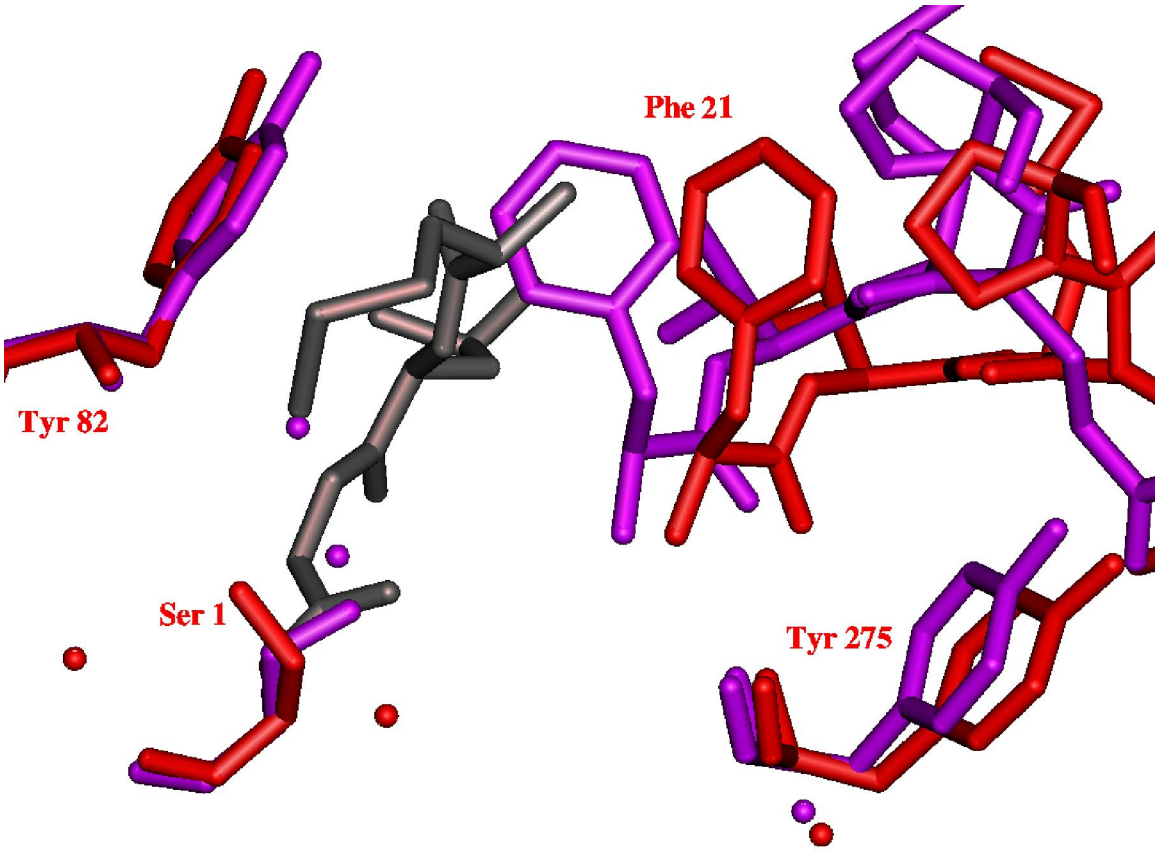

Figure 4. 7

Truncated mutant Cys1Ser (magenta) superimposed on pre-Cys1Ser (red). Surrounding residues in the processed mutant have moved in to the space vacated by propeptide (black).

Superposing the four monomers of pre-Cys1Ser reveals the flexibility of these zones between the monomers of the same tetramer. The r.m.s. deviation for Cα atom of residue Ile135 [138 (n+3) in the pre-Cys1Ser] in two monomers C and D is 4.18 Å.

Phe21 side chain, which moves inside in case of processed structure has been seen static at the same position in all four chains. This observation is in line with the lack of activity of Cys1Ser mutant to autoprocessing itself. In pre-Asn175Ala structure, Phe21 has moved inward in the autocatalytic pocket. The Met residue modelled in the electron density at the N-terminal end has short contact with the side chain of Phe21 in chain C. From the N-terminal sequencing result it has been concluded that this mutant could process itself partially (Table 4.1). The two observations imply that the inward movement of Phe21 takes place subsequent to autoproteolysis.

4. 12. Suggested mechanism of autoproteolysis in PVA

Based on the atomic model of PVA precursor mutants having Cys and Ser as the nucleophile we propose the following detailed steps in the molecular mechanism of autoproteolysis that utilizes N à S acyl shift. The study of PVA has revealed a new catalytic machinery for amide hydrolysis and identified a new environment capable of autocatalytic removal of its precursor peptide, different from PGA.

1. Initial precursor structure of PVA
2. Nucleophilic attack by Sγ of Cys1 on the carbonyl carbon of Gly near the N-terminal
3. Formation of thiazolidine ring tetrahedral intermediate
4. Rearrangement of the tetrahedral intermediate
5. N à S-acyl shifted thioester bond formation
6. Nucleophilic attack by water molecule on thioester
7. Formation of second tetrahedral intermediate
8. Rearrangement of the tetrahedral intermediate leading to the formation of processed protein

The possible mechanism for the autoproteolytic reaction involves direct attack by the Cys S^{γ} atom on to the scissile peptide's carbonyl C atom. The mechanism proposed for PGA invoking intermediate water molecule for nucleophilic attack, cannot be applied in the case of PVA because no electron density is present for water molecule at the

autoproteolytic site. The presence of C^{δ} of Met –3 at the location required for water molecule and the essential interactive contacts observed in pre-Cys1Ser mutant points to a slightly different mechanism for autoprocessing in PVA.

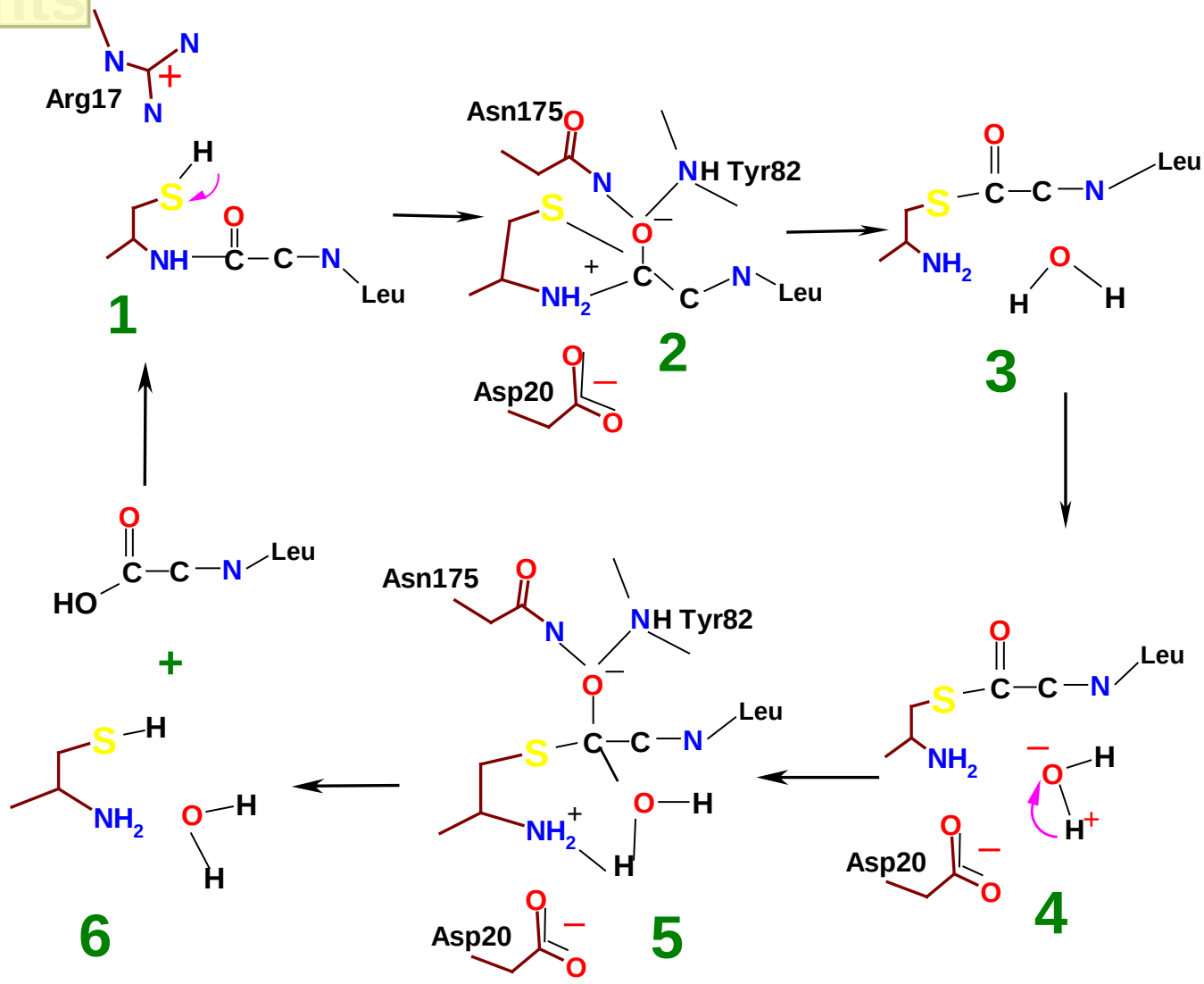

Figure 4. 8

Schematic diagram showing the proposed reaction mechanism of autoproteolysis in penicillin V acylase.

The steps involve two nucleophilic attacks resulting in two intermediate tetrahedral forms (iii) & (vii). The first attack mediated by S^{γ} atom of Cys1 leads to formation of thiazolidine ring that rearranges in to thioester. The second nucleophilic attack by a water molecule results in the cleavage of the thioester linkage between the residue Cys1 and Gly –1. In the crystal structure of slowly processing pre-Asn175Ala mutant a thioester intermediate as shown in scheme is trapped (Figure 4.8).

In summary, the reaction mechanism for autoproteolysis of PVA includes the nucleophilic attack resulting in a tetrahedral intermediate, which collapses into a covalently bound glycinyl-thioester intermediate. Hydrolysis of this intermediate by an activated water molecule, finally, removes the propeptide. Here, the third species in this pathway has been freezed in the structure, namely, the covalently bound thioester with already formed free α-amino group of Cys1.

4. 12. 1. N à S acyl shift resulting in thioester formation

The formation of thioester bond has been observed in several proteins as an intermediate in enzymatic reactions (Perler, 1998a; 1998b). There have been very few cases wherein the thioesters could be identified in the X-ray crystal structure itself (1A9X, Thoden *et al*., 1998). Complement proteins C3 and C4 have an internal thioester bond, which is available for nucleophilic attack (Law & Dodds, 1997).

During the activation of Gycosylasparaginase, it has been shown that a stable thioester intermediate is generated (Guan *et al*., 1996). The ubiquitin-proteasome mediated proteolytic pathways also involve formation of a high-energy ubiquitin–thioester linkage (Myung *et al*., 2001). Catalytic mechanism of Glutamate synthase, a Ntn-hydrolase member, involves a thioester-cysteine intermediate (Heuvel *et al*., 2004). In autoproteolytic mechanism of Ntn-hydrolases, (thio)ester formation is the step between two tetrahedral intermediates. First tetrahedral arrangement at carbonyl carbon is formed when the nucleophile S^{γ} atom attacks and covalently binds the carbonyl carbon. As the reaction progresses the second tetrahedral intermediate is formed when a water molecule under the influence of oxyanion hole and newly freed α-amino nitrogen attacks the carbonyl carbon. This step finally yields the mature protein. Both the tetrahedral intermediates are short-lived and unstable.

The electron density for the N-terminal tri-peptide could be clearly seen in the structures of pre-Cys1Ala, pre-Cys1Ser and pre-Asn175Ala, being clearer in the former two. The tri-peptide Met-Leu-Gly could be modelled into the extra difference density at the N-terminus of pre-Cys1Ser and pre-Cys1Ala structures. In the crystal structure of pre-Asn175Ala the autoproteolytic site in four monomers differ from each other. Electron density in two chains A and C could be interpreted as covalently bound glycinyl-thioester intermediate at Cys1. This structural investigation provides the first direct X-ray crystallographic observation of an autoproteolytic intermediate in the Ntn-hydrolase family. Shown in Figure 4.9 is a portion of the electron density map corresponding to thioester formed in chain C and Gly -1 and Cys1 in chain B of pre-Asn175Ala.

For the sake of simplicity the following discussion will refer only to monomer in chain C unless otherwise indicated. As can be seen, the electron density map is unambiguous and demonstrates the formation of glycinyl thioester intermediate in this chain. The thiol group of Cys1 is covalently bound (1.8 Å) to the carbonyl carbon of scissile peptide. The thioester obtained is in a highly distorted geometry and also in a partial tetrahedral conformation, interacting with a water molecule. The water molecule is positioned at 2.85 Å from free α-amino group and 2.50 Å from the scissile carbonyl carbon of thioester poised for nucleophilic attack. The nucleophilic water makes angle of 102, 90 & 106^{o} with O, C^{α} & S^{γ}, respectively at the scissile carbonyl carbon. The features of thioester are distinct than that of Cys and Gly in other monomers.

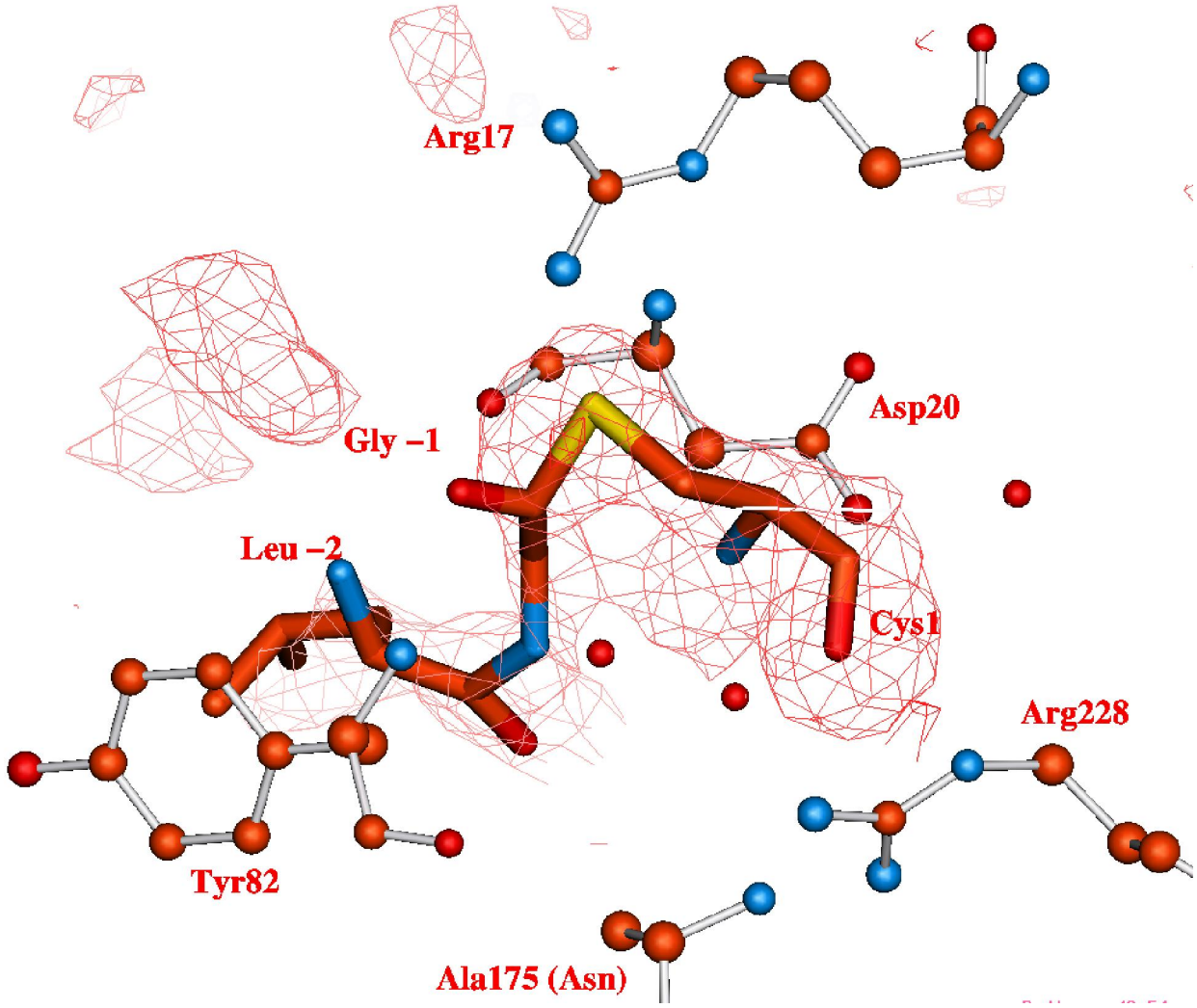

Figure 4. 9 a

The polypeptide chain showing the glycinyl thioester group in the chain C. The electron density map corresponds to F_o-F_c difference Fourier at 3σ level. The unoccupied density could be of terminal Methionine

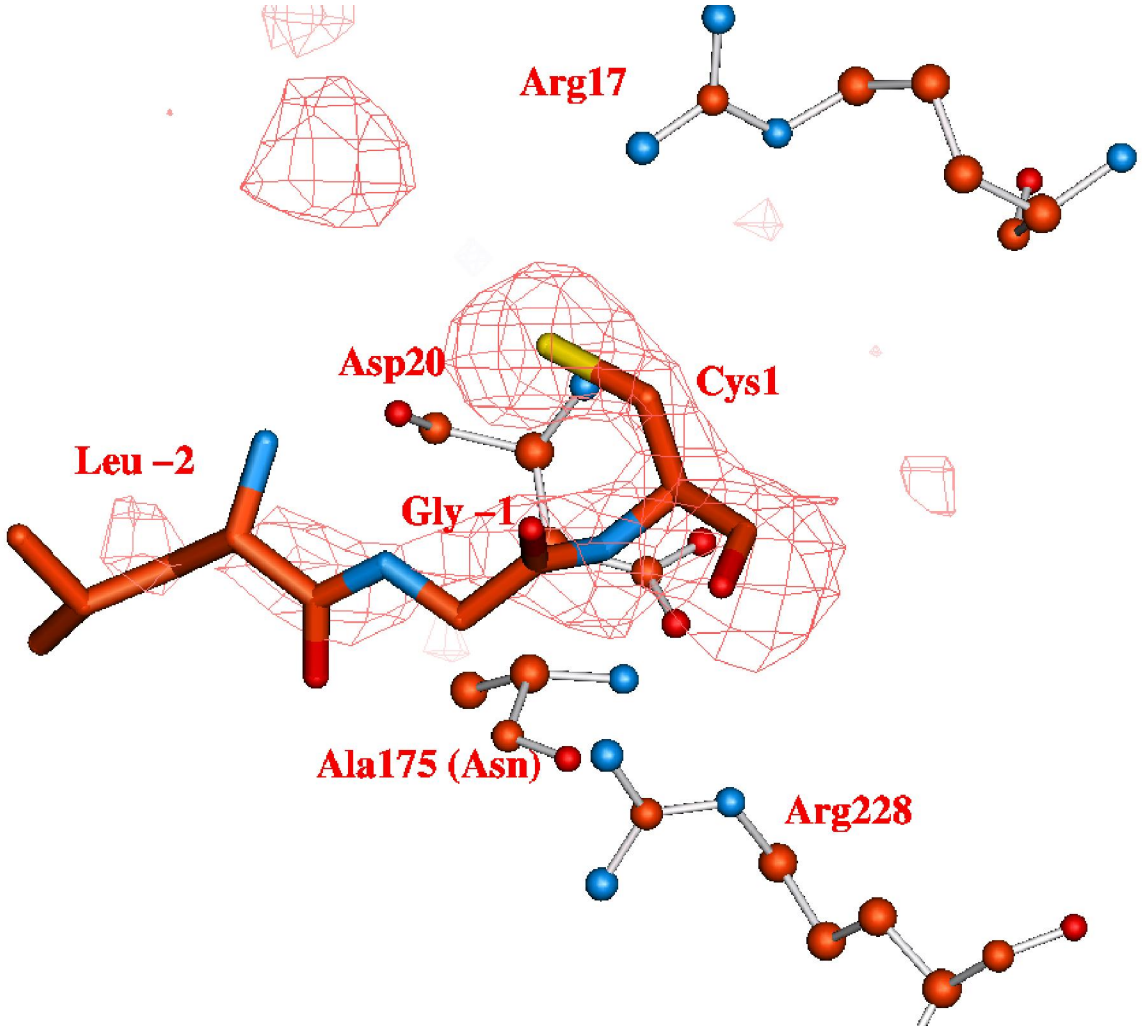

Figure 4. 9 b

The polypeptide chain showing the intact propeptide in the chain B. The electron density map corresponds to F_o-F_c difference Fourier at 3σ level. The unoccupied density could be of terminal Methionine.

The intermediate getting entraped in the crystals has been reported in the case of subtilisin carlsberg (Schmitke *et al*., 1998), carbamoyl phosphate synthetase (Thoden *et al*., 1998), porcine pancreatic elastase (Ding *et al*., 1994) and β-lactamase (Strynadka *et*

al., 1992). To our knowledge, the structure reported here represents the first structural evidence for the formation of a glycinyl thioester intermediate in any protein studied yet.

The autoproteolytic mechanism of the PVA proceeds via a tetrahedral intermediate indicated as in step 2 of Scheme (Figure 4.8). From the hydrogen-bonding interactions between the glycinyl thioester intermediate and the neighboring amino acids, it can be speculated that N^{δ} of Asn175 (as in the native structure) and the backbone amide hydrogen of Tyr82 both serve to position the carbonyl of the Gly –1 for nucleophilic attack. This in turn stabilises the partial negative charge developed on the scissile carbonyl oxygen during autoprocessing. This has already been predicted as the presumptive role of oxyanion hole residues Asn175 and Tyr82 (Suresh *et al.*, 1999). Besides Tyr82 and Asp20 the other specific side chain group interacting with the glycinyl thioester intermediate is that of Arg17 (3.11 Å). The distances between S^{γ} atom of Cys1 and carbonyl C atom of the Gly -1 of the four monomers A, B C & D are 1.82, 3.35, 1.80 and 2.85 Å, respectively. A search of the Cambridge Data Base reveals that the typical carbon-sulfur bond distances in such thioesters range from 1.74 to 1.78 Å.

One immediate question concerns the stability to hydrolysis of the glycinyl-thioester intermediate in this mutant. The simplest explanation perhaps may be that the small degree of ionization of Cys1 is sufficient to permit attack by the thiolate on the carbonyl carbon of Gly -1 to form the covalently bound intermediate. For the subsequent hydrolysis of thioester to occur, however, an activated water molecule is required, to carry out a nucleophilic attack at the carbonyl carbon of the thioester intermediate. By replacing Asn175 with an alanine, the chances of an appropriately placed nucleophilic water molecule are significantly reduced.

4. 12. 2. Breaking the scissile peptide bond

During rearrangement of the first tetrahedral intermediate, the amino group of original peptide bond picks up a proton. The carboxyl side of the original bond remains attached to the enzyme by covalently bonding through S^{γ} of Cys1. In the meantime, the carbonyl of Gly –1 moves closer to NH of Tyr82. A water molecule now occupies the position of carbonyl oxygen in chain C of pre-Asn175Ala. The strength of thioester intermediate demands a strong nucleophile to deacylate the enzyme and to accomplish

the processing reaction. A water molecule influenced by the oxyanion hole and the newly formed α-amino group is the only probable candidate.

According to the observed chemistry, a water molecule has diffused into the autocatalytic site, as mentioned above. This water molecule is bound to the enzyme in a specific way so that the required electron flow occurs. The free α-amino group acts as a base catalyst, drawing a proton from the water. Oxyanion hole helps in increasing the polarization of charge on the water molecule, which would initiate second nucleophilic attack. Having aspartate as an electron source and oxyanion hole as a massive electron sink on either side of the autocatalytic centre helps to polarize the nucleophile and the base in the terminal residue cysteine. Their roles seem similar during both autoproteolysis and catalysis.

4. 12. 3. N-terminal Methionine excision in PVA

Methionine is the universal initiating aminoacid in bacterial translation. The N-terminal methionine is removed from most mature proteins. During post-translational processing of PVA three residues Met-Leu-Gly at N-terminal before Cys are removed. Studies on point mutants prepared for autocatalytic studies have given rise to another question in this regard. If we look at the N-terminal sequences of mature mutants, the methionine removal seems to follow different pathways. From the present evidence it appears that it is closely linked to the autocatalytic removal of propeptide. In most of the mutants where autocatalytic processing fails, methionine is also found intact (Table 4.1).

The structure of the mutant pre-Asn175Ala turns out to be important because of the disruption of oxyanion hole by the Asn175 mutation. Here, the N-terminal sequencing showed two prominent components co-sequenced. This was interpreted as partial clipping/degradation at cysteine. This observation was in accordance with the slow processing of this mutant. Here also electron density for methionine was more or less present in all the chains, indicating no separate mechanism has worked for methionine removal.

In contrast to this, all the truncated PVA mutants were made with methionine as the starting residue at the N-terminus for translation initiation. In crystal structure as well as in N-terminal sequencing methionine was absent. Thus, methionine was found

removed in all truncated mutants, including in those devoid of the N-terminal nucleophile, indicating no role for terminal nucleophile in Met removal.

4. 12. 4. PVA is mechanistically similar to cysteine and serine proteases

In serine and cysteine proteases, the nucleophilic hydroxyl or thiol side chain of the respective active site residue serine or cysteine attacks the peptide bond of the substrate at the main chain carbonyl carbon. The nucleophilic attack results in the cleavage of the scissile peptide bond, with the release of the C-terminal cleavage product and formation of an acyl-enzyme intermediate comprising of the N-terminal peptide covalently attached to the enzyme as a (thio)ester. Hydrolysis of the (thio)ester linkage releases the N-terminal peptide and regenerates the active protease. The protease reaction is driven to completion by the hydrolysis of the acyl-enzyme intermediate. As a result, serine and cysteine proteases can act as peptide ligases if water is excluded from the reaction (Barbas *et al*., 1988) or if the active site nucleophile is mutagenized into a poor leaving group in the acyl-enzyme hydrolytic step (Nakatsuka *et al*., 1987; Abrahmsen *et al*., 1991).

By increasing both the electrophilicity of the substrate carbonyl group (by interaction of the carbonyl oxygen atom with adjacent positive charge, the “oxyanion hole”, in the transition state) and the nucleophilicity of the attacking hydroxyl or thiol group the efficiency of initial nucleophilic attack on the peptide bond can be enhanced (Fersht, 1985). The nucleophilicity is increased by a charge-relay system in which the proton of the attacking species is transferred to an adjacent histidine residue, which in turn has its pK_r (and thus basicity) raised by interaction with an adjacent aspartate (in serine proteases) or asparagine residue (in cysteine proteases) Warshel *et al*., 1989; Corey & Craik, 1992). This “catalytic triad” of Asp-His-Ser or Asn-His-Cys is the hallmark of all serine or cysteine proteases.

The substrates of Ntn-hydrolases vary considerably, from peptides (the proteasome), amino acid side chains, (Glutamine amido transferase), amidated sugars (Aspartyl glucosyl amidase) to amides (penicillin G amidase, penicillin V amidase). One member of Ntn-hydrolase family, Glycosylasparaginase has Thr152 as the nucleophile residue. The involvement of His150 and Thr/Ser/Cys152 in activation suggests that

autoproteolysis resembles proteolysis carried out by serine/cysteine proteases (Guan *et al.*, 1996). The free α-amino group and N-terminal residues Ser/Thr/Cys along with conserved Asp/Gln/Asn, residues in the Ntn-hydrolases reminds of protease catalytic triads, which led us to postulate similar functional roles for these residues in penicillin V acylase. Hence, mechanistically also we expect these enzymes to be similar.

CHAPTER – FIVE

THE STUDIES ON THE MECHANISM OF ACTIVITY OF PENICILLIN V ACYLASE

5. 1. Introduction

The manufacture of semi-synthetic penicillin antibiotics requires a cost effective process for the production of the starting compound 6-APA. The naturally available fermentation product penicillin V (Pen V) can be used for yielding 6-APA through a deacylation step by a good catalyst. PVA is identified as the enzyme that carries out the deacylation reaction. In an attempt to understand the catalytic mechanism of PVA several site directed mutants have been prepared and attempted to co-crystallise with substrate Pen V. Our studies have focused on the role of residues involved in binding the substrate or interacting with it and the actual process of binding the substrate. We have attempted to explain the unique features of PVA-catalysed reaction. It may be interesting to note that Pen V and Pen G have similar groups of atoms in their structure, however, the amidases show different specificities towards the two.

Locating a cysteine residue at the N-terminus of the protein in its crystal structure has helped to place PVA in the Ntn-hydrolase family. Using this residue as the reference the putative catalytic site and residues could be inferred by comparison with other members of the Ntn-hydrolase family, especially PGA. Mutations were directed at those residues identified as taking part directly or indirectly in the catalysis or interacting with the substrate. In fact, all site-directed mutants chosen were found to be catalytically inactive. In the absence of any kinetic data for the site-directed mutants, investigation using biochemical techniques on these mutants is ruled out. All those mutations, where nucleophile Cys1 has been replaced by residues such as Ala or Gly, have shown the presence of an unaccountable electron density which can accommodate a small organic molecule, occupied the position in the vicinity of mutated cysteine. Even in the co-crystal structure, the oxyanion hole has been found preoccupied with the unidentified moiety.

5. 2. Substrate binding studies

The main aim of this chapter is to identify the catalytically important residues in PVA and arrive at a putative mechanism based on the type of residues identified. Structural studies of PGA and CA showed them to have shallow, solvent-exposed active sites with relatively few residues that can act like protein functional groups in positions where they can successfully participate in catalysis (Duggleby *et al.*, 1995; Kim & Hol,

2001). In the structure of PGA mutant complexed with its substrate, the penam ring of substrate is loosely placed in the catalytic pocket without any interactions with the enzyme. The results from our study are in contrast with those from other Ntn-hydrolase members therein that the PVA has surface loops that close around the substrate, bringing a variety of residues into the active site and virtually surrounding the substrate. In the structure of PVA co-crystallised with Pen V or substrate modelled in the active site, in both the penam ring showed multiple interactions (Table 5.1).

The crystal structure of Cys1Gly mutant with bound Pen V molecule clearly revealed electron density corresponding to the ligand. The shortest contact, the substrate makes with free α-amino group is the one from C of phenyl ring (4.32 Å). The carbonyl carbon of the substrate is at 7.64 Å away from the free α-amino group of terminal residue. The binding site is formed mainly by the loops connecting β-strands and helixes. The penam ring and the atoms of the scissile bond make several hydrogen bonds with the protein (Figure 5.1 and 5.2). The key residue in substrate recognition could be Asp274. The residues Gln212, Glu270 & Asp274 cover the substrate-binding pocket, which form lid on the catalytic pocket.

5. 2. 1. Non-productive binding: A mode of recognition

The interaction between substrate and enzyme in solution, driven by collisions, may result in the formation of a number of different complexes. There has been reports of non-productive complexes of Methylmalonyl-COA mutase (pdb code 1E1C & 2REQ), Ribonuclease-A with Uridylyl (2',5') Guanosine (pdb code 1EOW), Ribonuclease T1/2',3'-Cgps (pdb code 7GSP).

Here the difference electron density of the co-crystal structure of PVA with Pen V showed density corresponding to substrate Pen V in the catalytic pocket. The disposition of Pen V in the active site of this structure turned out to be different from what was expected. (1) The placement of Pen V in PVA was totally different from that observed in the studies of PGA complexed with Pen G; (2) Scissile carbonyl carbon of Pen V which undergo nucleophilic attack is around 7.68 Å away from the actual position of nucleophile atom in wild protein. It is in all probability represents a non-productive complex; (3) None of the expected residues (Asn175, Arg228, Asp20) are in direct

contact with the substrate in this complex; (4) Inter molecular co-operation between monomers for binding substrate in the tetramer could be detected.

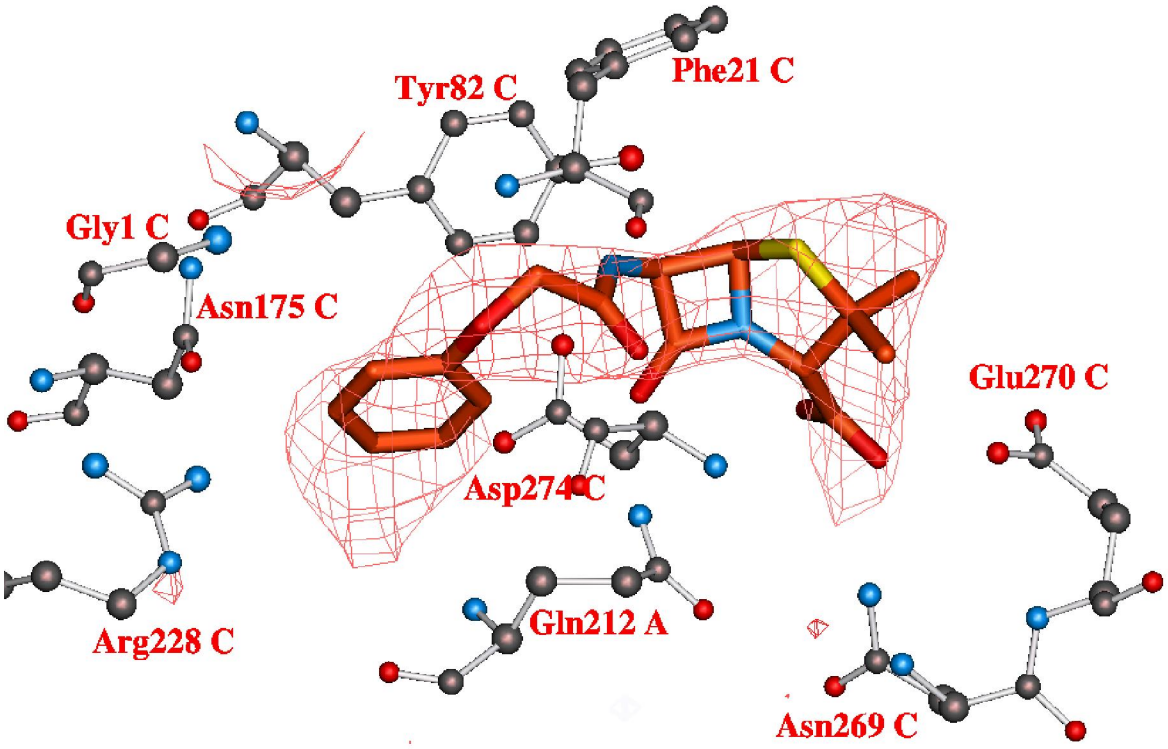

Figure 5. 1

The modeling of Pen V (liquoriced, red) into the difference electron density in the structure of PVA mutant Cys1Gly complexed with substrate penicillin V. The map of the electron density shown is Fo-Fc at 3 σ level.

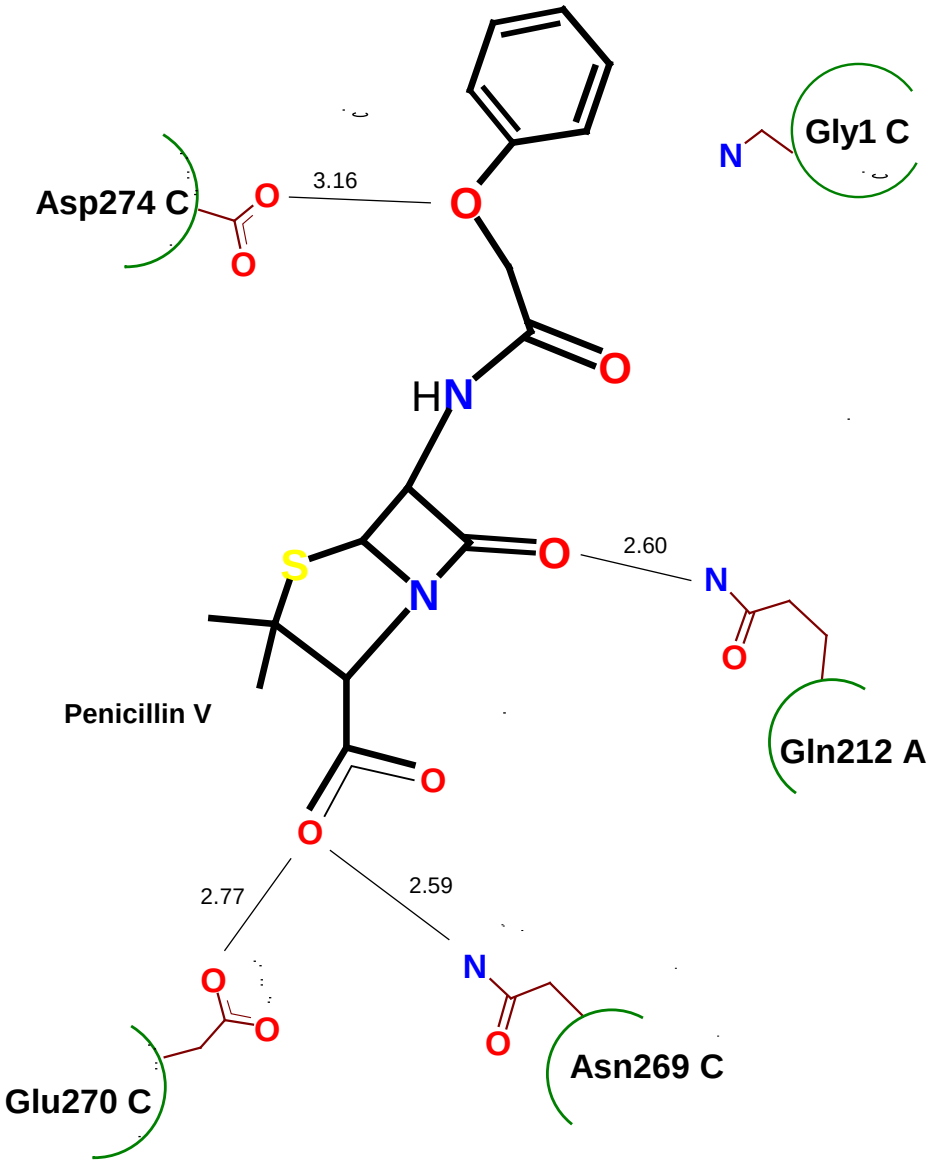

Figure 5. 2

A schematic diagram is presented to show the interaction between substrate penicillin V and active site residues of PVA in the structure of the complex. Asp274 is near phenoxy oxygen of the substrate. Gln212, which has contact with imide oxygen of penam ring, is part of a neighbouring monomer. Free α-`amino group of Gly1 is 7.64 Å away from the carbonyl carbon of substrate Pen V.

Oxyanion hole of the enzyme plays a significant role in the catalysis by PVA. In the co-crystal structure, the oxyanion hole has been occupied by unidentified chemical, which is supposedly from cellular metabolism. None of the chemicals used in protein purification and crystallization could be fitted into the electron density. It is reported that substrate binding is pre-requisite for the formation of oxyanion hole in Ntn-hydrolase family (Isupoh *et al*., 1996). It looks like that a pre-occupied oxyanion hole has obstructed the formation of productive complex between enzyme and substrate. Attempts to free the oxyanion hole were futile (Chapter 2). To remove unidentified molecule from the protein, Cys1Ala protein was subjected to gradual dialysis against 4 M urea overnight. Again the protein was re-natured gradually in 0.05 M phosphate buffer pH 6.4. Crystals grown from dialyzed sample of Cys1Ala still showed unidentified electron density at the same position (data not shown). Thus, it has been concluded that the affinity of the protein for substrate has decreased significantly due to the binding of unidentified molecule.

5. 2. 2. Modeling Pen V binding in the active site of PVA

Since we were not successful in getting a productive complex of PVA with Pen V it was decided to model and optimize the substrate binding in PVA using energy minimization techniques. The energy minimized structure placed substrate close to nucleophile with carbonyl oxygen of Pen V sitting in the oxyanion hole. This is in accordance with the already available structure of PGA substrate complex. The distance between the scissile carbonyl carbon atom and the nucleophile S^{γ} atom in the model structure has been 3.26 Å. The free α-amino group of terminal cysteine has interactions with imide (2.57 Å) as well as carboxyl oxygen (2.61 Å) of penam ring (Table 5.1). The residue Asp20 is positioned such as it can protonate the spliced amine group of penam ring in modelled structure. The oxygen of the phenoxy side chain of Pen V makes a short contact (3.09 Å) with S^{δ} of Met19.

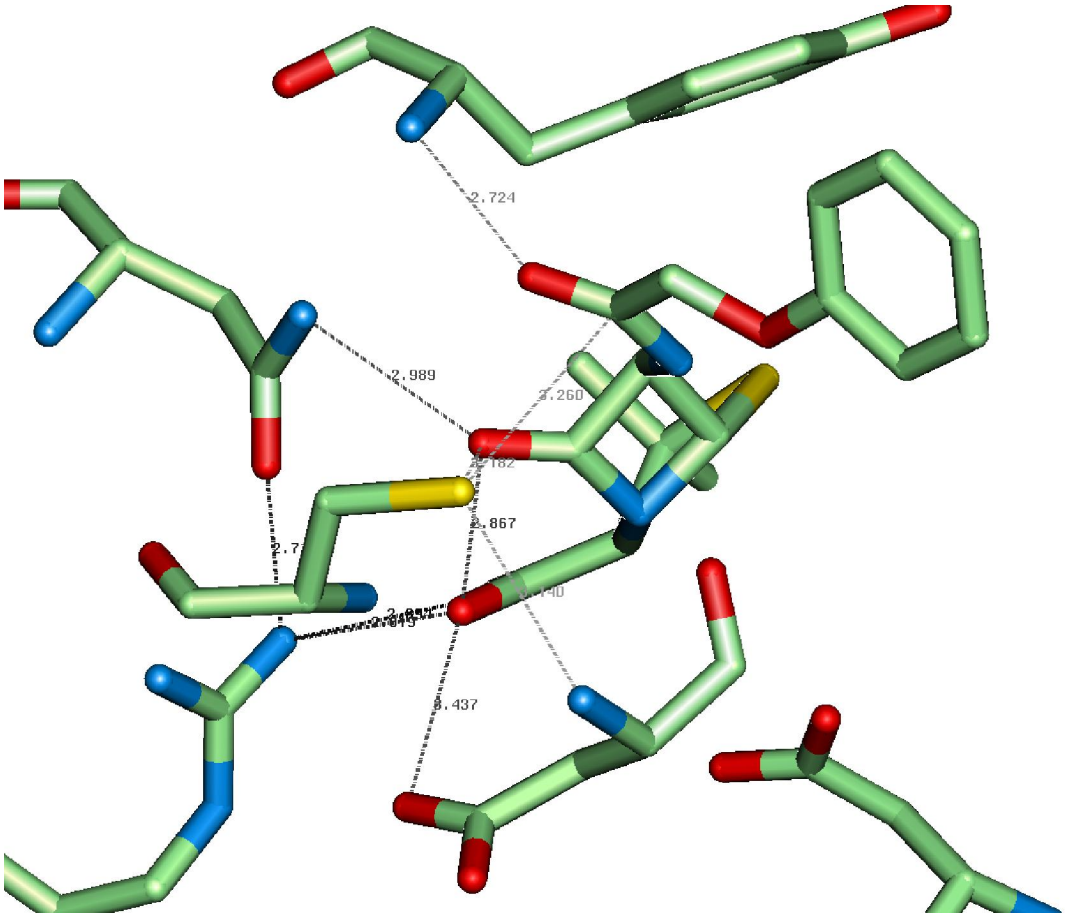

Figure 5. 3

The substrate penicillin V is modelled in PVA active site. In this modelled structure, substrate has extensive contacts with the Arg228 and oxyanion hole residues Tyr82 and Asn175.

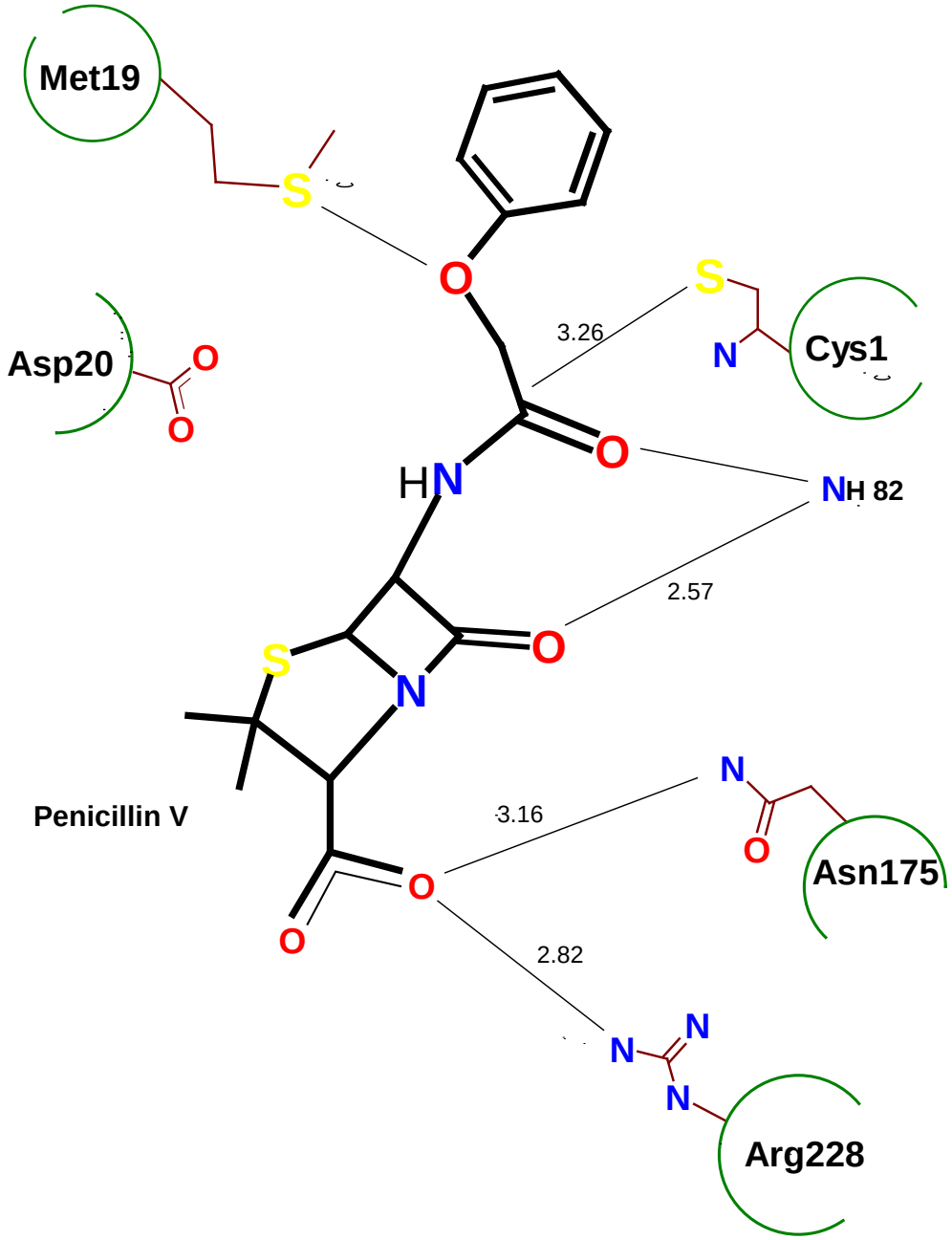

Figure 5. 4

A schematic diagram showing the interaction of substrate penicillin V with the active site residues in modelled structure. Distances between atoms are shown (in Å) with the broken line. There is an additional interaction of 2.61 Å between free α-amino N of Cys1 and carboxyl oxygen of penam ring of substrate, which is not shown here.

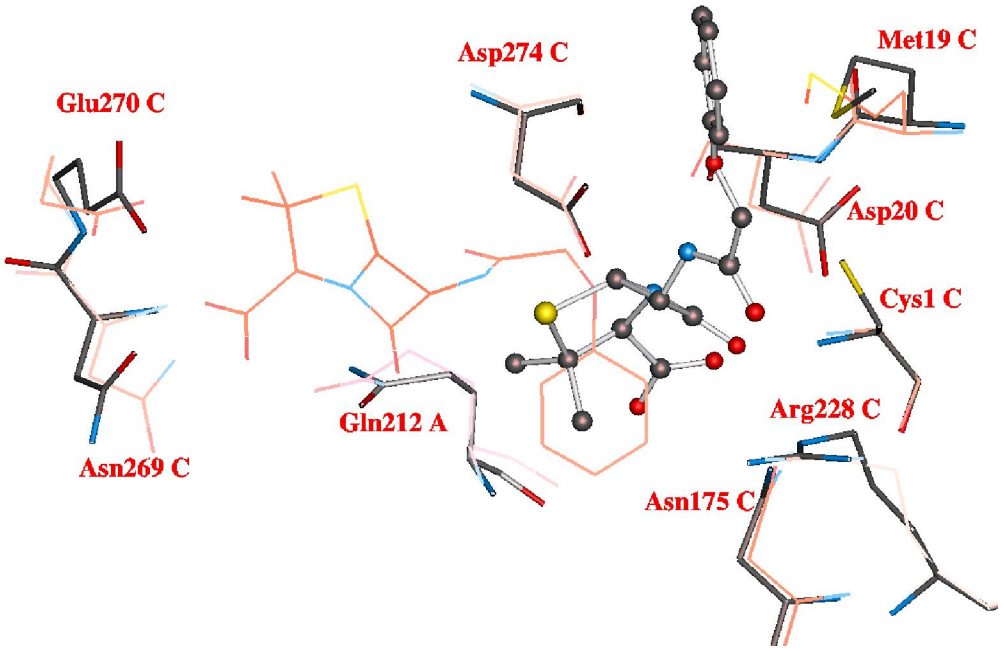

(a)

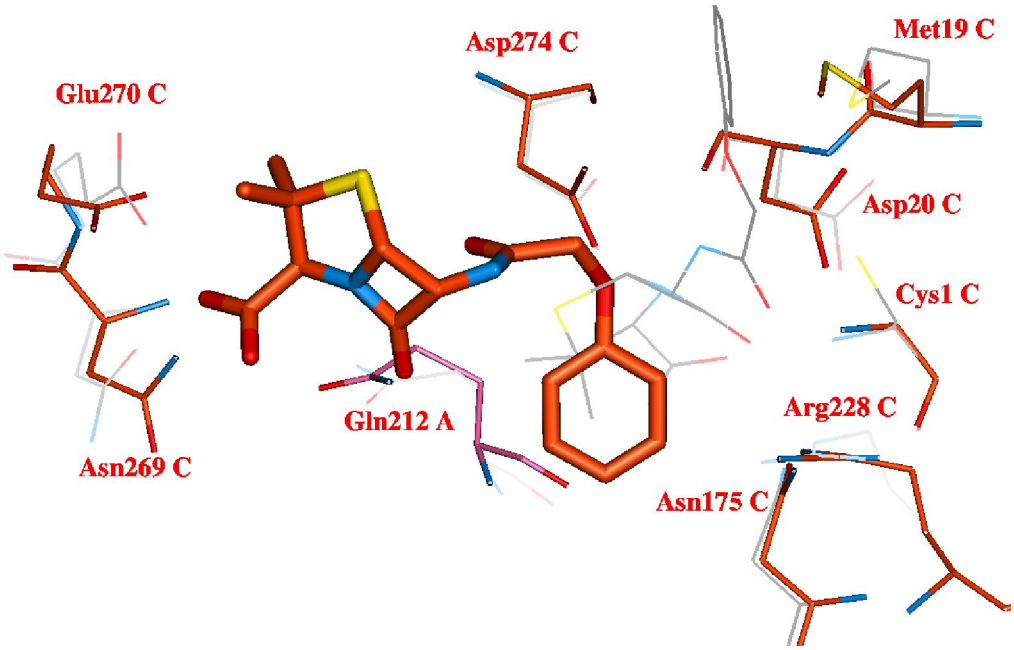

(b)

Figure 5. 5

Modelled PVA structure superposed on the co-crystal structure. (a) Modelled substrate is in ball and stick with co-crystal structure in background. (b) Substrate in co-crystal structure is in liquorice with modelled structure in background.

5. 2. 3. Comparison of modelled and crystallised complex

A comparison of PVA with PGA has predicted the involvement of Asn175 and Arg228 in the catalysis of PVA. However, the co-crystal structure of PVA with Pen V does not show any direct involvement of these residues in substrate binding (Figure 5.1). At the same time the truncated site directed mutants of these residues showed no enzyme activity. Whereas, modelled structure clearly indicated interaction of Asn175 as well as Arg228 with the substrate (Figure 5.5). It may be remembered that the nucleophile is suppressed in the crystallised complex. So modelled structure may provide a more realistic situation in actual catalysis.

During catalysis the carbonyl oxygen of Pen V has to be stabilized by the oxyanion hole residues. We have seen in the partially active precursor structure of a PVA mutant (pre-Asn175Ala) that the carbonyl oxygen of scissile residue Gly –1 is directed toward residues forming oxyanion hole, unlike in inactive precursor structure (pre-Cys1Ser). Here in the structure of co-crystal of Pen V – PVA also carbonyl oxygen of substrate Pen V is perversely directed away from the oxyanion hole. Modeling studies established such a requirement of carbonyl oxygen pointing in the direction of oxyanion hole for the catalysis to proceed by stabilizing the intermediate (Figure 5.3 and 5.4).

According to the hypothesized mechanism of action of Ntn-hydrolases, carbonyl carbon of the scissile bond has to be close to the nucleophile atom. In the crystal structure of the complex the distance between the carbonyl carbon and the N-terminal residue is around 7.64 Å, which indicates that it is placed in an unproductive mode of binding. Substrate recognition is pre-requisite to enzyme specificity. Moreover, a displacement of the substrate by around 2 Å is required as a next step after recognition for orienting for catalysis. Obviously, the specific interaction of the substrate Pen V with the residues in the PVA active site will be the basis for its preference by PVA. Comparison of the molecular structures of β-lactam antibiotics especially Pen V and Pen G reveals that mostly they are similar (Figure 1.2). The only difference between them lies with the extra oxygen atom in the side chain phenoxy ring of Pen V whereas it is benzyl ring in Pen G. This oxygen atom must be playing a significant role in substrate recognition at the PVA active site leading to catalysis. The crystal structure of Pen V - PVA complex has helped to explain the specificity question of PVA enzyme for substrate Pen V. The essential

contact between the oxygen of phenoxy group and Asp274 OD1 has been observed in the crystal structure of complex (Figure 5.1 and 5.2). This interaction could be the desired one for the Pen V specificity. On the basis of this, the specificity for Pen V can be explained. Appropriately mutating Asp274 residue to remove the carboxylate group may tilt the specificity of PVA towards Pen G. It is generally recognised that the residue that confer specificity to enzyme need not take part in its activity (Keck & Marqusee, 1996).

5. 3. Catalytic water molecule

In Ntn-hydrolases, N-terminal residue acts as both nucleophile and base, but a direct transfer of proton is unlikely from the point of view of bond angles and distance restrain between the two groups. A water molecule has always been located in an appropriate position where in the S^{γ} or O^{γ} atom and free α-amino group of cysteine/serine in PVA are in a skewed geometry. This catalytically conserved water is absent in the co-crystal structure of PVA-Pen V (Figure 5.1). The absence of the terminal nucleophile could be the reason for the absence of this water molecule in the mutant.

5. 4. Autoproteolysis *vs* catalysis in PVA

PVA monomer has a loop of around 30 residues consisting of residues 190 to 220, which extends out of the core of each monomer and reaches the active site of the neighbouring monomer in the quaternary structure and folds back to its own core (Figure 5.6). In the structure of PVA mutant – Pen V crystal the intermolecular co-operation between monomers of tetramer for the substrate binding is observed (Figure 5.1 and 5.2). This is different from the autoproteolysis of PVA where residues from same monomer only were actively involved. In the co-crystal structure, the penam ring of Pen V has been held by the side chains of Gln212, Asn269 and Glu270, where residue Gln212 has been provided by neighbouring monomer. This interaction could be part of intermolecular co-operativity in tetramer.

Table 5. 1

Comparison of contacts of substrate Pen V in Cys1Gly co-crystal and modelled structure

Contact		Cys1Gly chain C	Cys1Gly Chain A	Modelled PVA
Atom of substrate	**Atom of PVA**			
Carbonyl-C	**Cys1 S^{γ}**	-	-	3.26
Carbonyl-O	**Gln212 $N^{\varepsilon}2$**	3.80	3.42	11.87
Carbonyl-O	**Tyr82 N**	5.03	9.05	2.72
Scissile-N	**Asp20 O**	5.43	5.86	2.79
Penam-imide O	**Cys1 N**	9.82	10.48	2.57
Penam-imide O	**Gln212 $N^{\varepsilon}2$**	2.60	2.53	9.83
Penam-imide N	**Asp20 O**	5.43	8.60	2.99
Penam-carboxy-O1	**Glu270 $O^{\varepsilon}1$**	2.77	3.00	13.75
Penam-carboxy-O1	**Cys1 N**	14.14	14.47	2.61
Penam-carboxy-O1	**Arg228 $N^{\eta}2$**	13.65	13.18	2.82
Penam-carboxy-O1	**Asn269 $N^{\delta}2$**	2.59	3.82	14.25
Penam-carboxy-O2	**Arg228 $N^{\eta}2$**	12.96	14.34	2.89
Phenoxy-O	**Met19 S^{δ}**	8.01	8.14	3.09
Phenoxy-O	**Asp20 O**	3.45	3.41	3.78
Phenoxy-O	**Asp274 $O^{\delta}1$**	3.16	3.33	7.39

Figure 5. 6

In the homotetrameric structure of PVA, a loop of around 30 residues (eg. yellow) reaches near the active site of neighboring monomer (eg. green). During catalysis the substrate has inter-monomer contacts, whereas in autoproteolysis residues from the same monomer only participate.

5. 5. Putative mechanism of penicillin V hydrolysis by PVA

The mechanism, by which PVA cleaves Pen V to produce phenoxyacetic acid (PAA) and 6-aminopenicillanic acid (6-APA), proceeds *via* a mechanism similar to that of cysteine proteases but lacks the catalytic triad. However, PVA being the member of Ntn-hydrolase family has a cysteine residue at the N-terminus, which is the focal point of the catalytic centre. Consistent with all the previous evidence from the structures presented, it is possible for us to propose the essential role of the nucleophile in the acylase reaction mechanism. A possible catalytic model shown in Figure 5.7, to explain the inactivation of mutated residues, is based on the structural data on those mutants presented in this study.

From the analysis and comparison of the structures we conclude that the serine in the place of cysteine is unable to act as a nucleophile in PVA. The truncated mutant Cys1Ser did not act on Pen V as gathered from the negative result of biochemical assay. Asn175Ala mutation in PVA, though showed partial autoproteolysis, had no acylase activity. The soaking experiment with processed type Asn175Ala also did not yield a complex. Similarly, in the absence of the side chain Asn175 the conversion of the intermediate formed in the processing step is either retarded or blocked completely from processing further.

Just like the catalytic mechanism in other Ntn-hydrolase members, PVA cleaves the side chain of penicillin V by nucleophilic attack of the scissile cabonyl carbon by S^{γ} atom of Cys1. The putative base is the free α-amino group of the same terminal nucleophile residue. In autoproteolysis, where the amino group is blocked by the propeptide, it is possible that Arg17 causes deprotonation of the nucleophile atom S^{γ}. It has been already shown that Arg17 is conserved (in chapter 4) in members of Ntn-hydrolase family which use cysteine as nucleophile. It has been argued that an arginine is the bronsted base that abstracts the proton in the family Pel1A enzymes also (Jenkins *et al.*, 2004; Scavetta *et al.*, 1999). The argument for Arg17 as base in autoproteolysis is strongly supported by absence of any other base in the vicinity along with the recent Pel10A structure that has an active site arginine (Jenkins *et al.*, 2004; Scavetta *et al.*, 1999). Arginine acts as a base under physiological conditions; the double-bonded

nitrogen of guanidyl group at the end of the side chain readily captures a hydrogen ion and becomes positively charged.

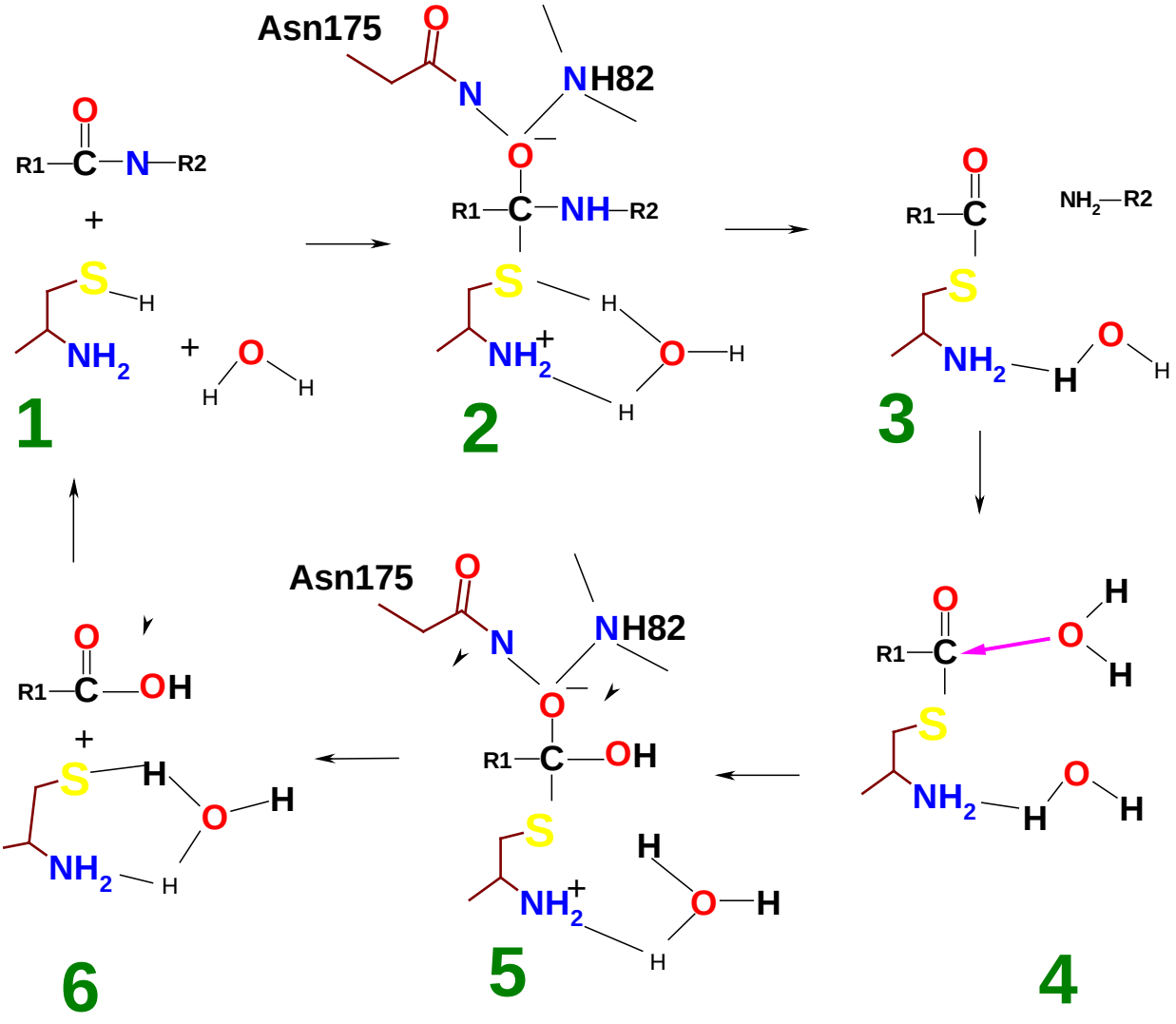

Figure 5. 7 *A schematic diagram to show the proposed catalytic mechanism of penicillin V acylase. The reaction is initiated by a general base, water (**1**), which receives the hydrogen atom from the side chain of Cys1, thus enabling a nucleophilic attack on the carbonyl carbon of Pen V and resulting in a tetrahedral intermediate (2). This tetrahedral intermediate decays to form a thioester releasing the leaving group (3). A water molecule hydrolyses the thioester bond (4) and a second tetrahedral intermediate is formed (**5**). The intermediate is resolved and Cys1 attains free amino and side chain groups, thus become ready for next cycle.*

In the catalytic structure, the obvious bronsted acid to protonate the spliced penam amine is Asp20, which has been found near scissile nitrogen in all the processed structures. The oxyanion hole formed by Tyr82 NH and Asn175 $N^{\delta}H2$ is expected to stabilize the departing phenoxy acetate anion.

Once the substrate is bound, the thiol group of Cys1 nucleophilically attacks the scissile carbonyl group. The thiol group is made nucleophilic by the free α-amino group of the same residue that extracts the thiol hydrogen, a process that is facilitated by the polarizing effects of Asp20 and Asn175 as in cysteine and serine proteases. A covalent bond forms between the cysteine and the substrate to yield a tetrahedral intermediate. The tetrahedral intermediate, which is also in the transition state, is stabilized by the oxyanion hole.

The tetrahedral intermediate quickly transforms back to a planar carbonyl group. This happens with the splicing of the bond with the amide nitrogen, releasing the penam ring part of the substrate while forming an ester linkage with the phenoxyacetate. This assembly is the acyl-enzyme intermediate. The breakage of ester bond of the acyl-enzyme is accomplished, in accordance with the established Ntn-hydrolase reaction mechanism (Dodson, 2000), by nucleophilic attack on the carbonyl group, most probably by a solvent water molecule which diffuses into the active site. The water would transfer one hydrogen to the free α-amino group while forming a covalent bond to the carbonyl carbon, as part of another tetrahedral intermediate, which gets stabilized in the oxyanion hole. This tetrahedral intermediate is freed by breaking the thioester bond to the thiol and releasing the phenoxyacetate. This final step regenerates the enzyme and opens the catalytic pocket for binding another substrate.

5. 6. Implications for future research in understanding PVA activity

The reported structure of PVA complexed with substrate Pen V has provided clear information on the mode of substrate recognition in the protein prior to catalysis. These results have opened up the door for the next generation of experiments with this pharmaceutically important enzyme. Attempts at altering the specificity of PVA by site directed mutagenesis would significantly benefit from the availability of this structural imformation. As we have already pointed out, removal of Asp274 carboxylate by site

directed mutation has potential to alter the PVA specificity in favour of Pen G. Shortening of the side chain of Glu270, i.e. Glu270Asp mutation may favor binding of a bigger antibiotic nucleus like 7-ACA. Increased flexibility of Arg228 during autoproteolysis is an indicator that a bigger substrate than Pen V can be accommodated without mutating this residue.

The information regarding the identities and individual functions of catalytically important residues in PVA can be used to guide structure-based design of catalytic pocket of PVA in which the enzyme would be modified to accept other substrates such as cephalosporins also. This may be achieved by targeting both conserved residues important strictly for catalysis and non-conserved residues important for binding of substrate and specificity identified in this study. Next immediate experiment would be to choose mutations that can cause the enzyme to accept 7-ACA or any other potential parent nucleus whose acylated product can move into semi-synthetic form for trials against a wide variety of viral and bacterial pathogens.

Table 5. 2

X-ray data and refinement statistics

	Cys1Gly (pv)	**Cys1Gly**
Unit cell (Å) *a b c*	129.73 158.89 90.74	91.76 130.71 158.71
Space group	$C222_1$	$P2_12_12_1$
Refinement statistics		
R_{factor} [a] (%)	23.88	20.08
R_{free} (%)	27.03	22.91
Mean B factor (Å^2)	46.45	21.31
Bonds (Å)[b]	0.054	0.012
Angle (Å)[b]	0.979	1.326
Ramachandran plot[c]	84.2/14.4/1.0/0	91.6/7.8/0.6/0

[a] Rfactor = $\sum||F_{obs}| - |F_{calc}||/\sum|F_{obs}|$.
[b] Root-mean-square error.
[c] Percentage of residues in most favored/additionally allowed/generously allowed/disallowed regions.

CHAPTER - SIX

THE POLYMORPHISM, PSEUDO-SYMMETRY AND TWINNING IN THE CRYSTALS OF PENICILLIN V ACYLASE

6. 1. Introduction: Polymorphism

Polymorphism means "many forms". In mineralogy it means that a single chemical composition can exist with two or more different crystal structures. Looking more closely at crystal structures, if the molecules to be crystallised are subjected to different environment of chemical pressures and temperatures, the spatial arrangement of molecule in crystal may vary, resulting in a different kind of space group packing. If the temperature of crystallization is increased, the molecule will tend to vibrate more and increase their effective size. In this case, a point may be reached where a less compact crystal structure is stabilized. Due to restriction of chirality, out of the 230 space groups proteins can crystallise only in 74 non-centrosymmetric ones. Padamaja *et al*. (1990) has analysed the distribution of organic crystal structures with more than one formula unit in the asymmetric unit listed in Cambridge Structural Database. From the analysis of the reported structures it was concluded that only 5 space groups (P1, $P2_1$, $P2_1/c$, C2/c, $P2_12_12_1$) are more frequent and account for over 75% of the structures reported. It seems that there is a preference for packing objects like proteins and other organic molecules in space. The structures of various mutants of T4 lysozyme determined in 25 non-isomorphous crystal forms provide an unusually diverse database. Zhang *et al*. (1995) have compared protein molecules in different crystal packing environments. A general rule observed is that the more tightly the molecules are packed their crystals diffract better. Thus in proteins a higher solvent content can lower the diffraction quality of the crystal.

6. 1. 1. Polymorphism in PVA

The tetramer assembly of PVA can be considered as a square disc of 100 Å sides and 45 Å thickness. The native PVA and mutants crystallised in five different space groups. Since the mutations applied are not on the surface of protein and crystal structures confirm correct folding of the mutants the various space groups in which the molecule has crystallised can be considered as polymorphism.

Two crystal forms of the native PVA have been previously reported (Suresh *et al*., 1999). In the first form which crystallised in the hexagonal space group $P6_5$ with unit cell

parameters a = b = 208.4, c = 96.3 Å (pdb code, 2PVA) the N-terminal cysteine was found oxidized into cysteine sulfonic acid. In the second form the N-terminal cysteine remained in the reduced form and the protein crystallised in the triclinic space group P1 with cell parameters a = 47.4, b = 129.6, c = 156.7, α = 88.3, β = 83.4, γ = 84.6° (pdb, 3PVA).

Table 6. 1

X-ray and refinement statistics of twinned structures. These two structures along with that of pre-Cys1Ala (Table 4.2) were refined using SHELXL.

	Cys1Ser	**Pre-Cys1Ser – II**
Unit cell (Å) ***a***	102.34	102.76
b	90.70	90.48
c	102.32	102.69
β (°)	102.15	101.81
Space group	$P2_1$	$P2_1$
Refinement statistics		
R_{factor} [a] (%)	23.22	24.20
R_{free} (%)	25.10	28.56
Mean B factor (Å^2)	39.3	35.89
Bonds (Å)[b]	0.023	0.022
Angle (Å)[b]	1.75	2.175
Ramachandran plot[c]	82.9/15.9/1.2/0	79/19.8/1.2/0

[a]Rfactor = $\sum||F_{obs}| - |F_{calc}||/\sum|F_{obs}|$.

[b]Root-mean-square error.

[c]Percentage of residues in most favored/additionally allowed/generously allowed/disallowed region.

Table 6. 2

X-ray and refinement statistics of the remaining truncated mutant structures not mentioned previously. Cys1Ala (pv) has penicillin V in the crystallization drop, whereas phenoxy acetic acid (PAA) was present in case of Cys1Ala (PAA).

	Cys1Ala (pv)	**Cys1Ala (PAA)**
Unit cell (Å) ***a***	91.18	90.90
b	129.49	129.53
c	159.01	158.77
β	90.00	90.00
Space group	$P2_12_12_1$	$P2_12_12_1$
Refinement statistics		
R_{factor} [a] (%)	22.09	22.25
R_{free} (%)	26.80	25.74
Mean B factor (Å^2)	9.47	15.592
Bonds (Å)[b]	0.024	0.021
Angle (Å)[b]	2.009	1.731
Ramachandran plot[c]	90.3/9.3/0.4/0	91.1/8.5/0.3/0

[a]Rfactor = $\sum||F_{obs}| - |F_{calc}||/\sum|F_{obs}|$.

[b]Root-mean-square error.

[c]Percentage of residues in most favored/additionally allowed/generously allowed/disallowed region.

Table 6. 3

Root Mean Square deviation of atom positions between PVA monomers in various structures. The numbers in bold refer to structures listed below. The letters A, B, C, D represent chain ID of monomers used in comparison. Pv indicates that the crystallization drop had penicillin V present.

1. pre-Asn175Ala A	5. Asn175Ala A	9. Asn175Ala A	13. pre-Cys1Ser-I A	17. Cys1Ser (pv) A	21. Cys1Ser A	25. pre-Cys1Ser-II A
2. pre-Asn175Ala B	6. Asn175Ala B	10. Asn175Ala B	14. pre-Cys1Ser-I B	18. Cys1Ser (pv) B	22. Cys1Ser B	26. pre-Cys1Ser-II B
3. pre-Asn175Ala C	7. Asn175Ala C	11. Asn175Ala C	15. pre-Cys1Ser-I C	19. Cys1Ser (pv) C	23. Cys1Ser C	27. pre-Cys1Ser-II C
4. pre-Asn175Ala D	8. Asn175Ala D	12. Asn175Ala D	16. pre-Cys1Ser-I D	20. Cys1Ser (pv) D	24. Cys1Ser D	28. pre-Cys1Ser-II D

Moving--> Fixed	**1**	**2**	**3**	**4**	**5**	**6**	**7**	**8**	**9**	**10**	**11**	**12**	**13**	**14**	**15**	**16**	**17**	**18**	**19**	**20**	**21**	**22**	**23**	**24**	**25**	**26**	**27**	**28**
1	0	0.19	0.27	0.18	0.35	0.35	0.33	0.32	0.35	0.34	0.35	0.37	0.37	0.37	0.56	0.41	0.31	0.34	0.32	0.35	0.46	0.43	0.44	0.43	0.43	0.47	0.53	0.53
2	0.19	0	0.28	0.22	0.37	0.32	0.34	0.31	0.33	0.29	0.30	0.38	0.32	0.40	0.56	0.44	0.33	0.35	0.32	0.34	0.48	0.41	0.46	0.42	0.43	0.52	0.56	0.54
3	0.27	0.28	0	0.33	0.46	0.45	0.43	0.39	0.43	0.39	0.43	0.48	0.38	0.39	0.48	0.48	0.41	0.44	0.42	0.45	0.55	0.51	0.53	0.52	0.47	0.51	0.50	0.56
4	0.18	0.22	0.33	0	0.31	0.32	0.33	0.33	0.37	0.33	0.33	0.37	0.37	0.36	0.57	0.35	0.32	0.35	0.31	0.34	0.45	0.42	0.43	0.41	0.43	0.48	0.56	0.50
5	0.35	0.37	0.46	0.31	0	0.22	0.22	0.23	0.26	0.25	0.25	0.22	0.32	0.36	0.57	0.32	0.22	0.25	0.22	0.24	0.35	0.31	0.32	0.30	0.38	0.43	0.54	0.47
6	0.35	0.32	0.45	0.32	0.22	0	0.21	0.19	0.23	0.18	0.16	0.26	0.27	0.35	0.56	0.34	0.24	0.26	0.20	0.22	0.36	0.30	0.34	0.30	0.38	0.46	0.53	0.47
7	0.33	0.34	0.43	0.33	0.22	0.21	0	0.18	0.20	0.22	0.23	0.21	0.32	0.35	0.56	0.36	0.20	0.23	0.22	0.23	0.34	0.32	0.33	0.31	0.38	0.46	0.51	0.48
8	0.32	0.31	0.39	0.33	0.23	0.19	0.18	0	0.16	0.19	0.17	0.21	0.25	0.33	0.53	0.36	0.19	0.22	0.20	0.22	0.36	0.30	0.33	0.31	0.37	0.45	0.49	0.48
9	0.35	0.33	0.43	0.37	0.26	0.23	0.20	0.16	0	0.23	0.19	0.24	0.30	0.39	0.58	0.42	0.22	0.23	0.22	0.23	0.38	0.32	0.34	0.33	0.39	0.48	0.53	0.53
10	0.34	0.29	0.39	0.33	0.25	0.18	0.22	0.19	0.23	0	0.19	0.26	0.26	0.35	0.53	0.38	0.25	0.29	0.23	0.26	0.38	0.32	0.37	0.32	0.37	0.47	0.51	0.48
11	0.35	0.3	0.43	0.33	0.25	0.16	0.23	0.17	0.19	0.19	0	0.26	0.26	0.36	0.56	0.37	0.23	0.25	0.20	0.22	0.37	0.30	0.35	0.30	0.37	0.47	0.53	0.49
12	0.37	0.38	0.48	0.37	0.22	0.26	0.21	0.20	0.24	0.26	0.26	0	0.34	0.38	0.61	0.37	0.23	0.24	0.26	0.27	0.37	0.31	0.34	0.33	0.39	0.48	0.56	0.52
13	0.37	0.32	0.38	0.37	0.32	0.27	0.32	0.25	0.30	0.26	0.26	0.34	0	0.29	0.46	0.32	0.29	0.32	0.28	0.31	0.44	0.36	0.40	0.37	0.36	0.44	0.46	0.45
14	0.37	0.4	0.39	0.36	0.36	0.35	0.35	0.33	0.39	0.35	0.36	0.38	0.29	0	0.42	0.27	0.34	0.38	0.35	0.39	0.44	0.41	0.42	0.41	0.41	0.40	0.44	0.42
15	0.56	0.56	0.48	0.57	0.57	0.56	0.56	0.53	0.58	0.53	0.56	0.61	0.46	0.42	0	0.49	0.55	0.57	0.56	0.59	0.64	0.62	0.64	0.62	0.58	0.56	0.53	0.59
16	0.41	0.44	0.48	0.35	0.32	0.34	0.36	0.36	0.42	0.38	0.37	0.37	0.32	0.27	0.49	0	0.34	0.38	0.35	0.38	0.45	0.43	0.43	0.42	0.45	0.43	0.49	0.42
17	0.31	0.33	0.41	0.32	0.22	0.24	0.20	0.19	0.22	0.25	0.23	0.23	0.29	0.34	0.55	0.34	0	0.14	0.16	0.18	0.35	0.30	0.31	0.30	0.38	0.43	0.5	0.48
18	0.34	0.35	0.44	0.35	0.25	0.26	0.23	0.22	0.23	0.29	0.25	0.24	0.32	0.38	0.57	0.38	0.14	0	0.19	0.16	0.36	0.29	0.30	0.31	0.39	0.44	0.53	0.50
19	0.32	0.32	0.42	0.31	0.22	0.20	0.22	0.20	0.22	0.23	0.20	0.26	0.28	0.35	0.56	0.35	0.16	0.19	0	0.15	0.35	0.29	0.32	0.29	0.38	0.44	0.52	0.47
20	0.35	0.34	0.45	0.34	0.24	0.22	0.23	0.22	0.23	0.26	0.22	0.27	0.31	0.39	0.59	0.38	0.18	0.16	0.15	0	0.36	0.29	0.32	0.30	0.40	0.44	0.54	0.50
21	0.46	0.48	0.55	0.45	0.35	0.36	0.34	0.36	0.38	0.38	0.37	0.37	0.44	0.44	0.64	0.45	0.35	0.36	0.35	0.36	0	0.37	0.38	0.36	0.45	0.48	0.57	0.53
22	0.43	0.41	0.51	0.42	0.31	0.30	0.32	0.30	0.32	0.32	0.30	0.31	0.36	0.41	0.62	0.43	0.29	0.29	0.29	0.29	0.37	0	0.36	0.31	0.39	0.48	0.58	0.50
23	0.44	0.46	0.53	0.43	0.32	0.34	0.33	0.33	0.34	0.37	0.35	0.34	0.40	0.42	0.64	0.43	0.31	0.30	0.32	0.32	0.38	0.36	0	0.35	0.45	0.47	0.57	0.53
24	0.43	0.42	0.52	0.41	0.30	0.30	0.31	0.31	0.33	0.32	0.30	0.33	0.37	0.41	0.62	0.42	0.30	0.31	0.29	0.30	0.36	0.31	0.35	0	0.41	0.48	0.59	0.48
25	0.43	0.43	0.47	0.43	0.38	0.38	0.38	0.37	0.39	0.37	0.37	0.39	0.36	0.41	0.58	0.45	0.38	0.39	0.38	0.40	0.46	0.39	0.45	0.41	0	0.46	0.52	0.52
26	0.47	0.52	0.51	0.48	0.43	0.46	0.46	0.45	0.48	0.47	0.47	0.48	0.44	0.40	0.56	0.43	0.43	0.44	0.44	0.44	0.48	0.48	0.47	0.48	0.46	0	0.51	0.50
27	0.53	0.56	0.50	0.56	0.54	0.53	0.51	0.49	0.53	0.51	0.53	0.56	0.46	0.44	0.53	0.49	0.50	0.53	0.52	0.54	0.57	0.58	0.57	0.59	0.52	0.51	0	0.55
28	0.53	0.54	0.56	0.50	0.47	0.47	0.48	0.48	0.53	0.48	0.49	0.52	0.45	0.42	0.59	0.42	0.48	0.50	0.47	0.50	0.53	0.50	0.53	0.48	0.52	0.50	0.55	0

Later on, PVA mutants were crystallised in monoclinic $P2_1$ and orthorhombic $P2_12_12_1$ forms. PVA in complex with pen V has been crystallised in $C222_1$ crystal form.

The PVA site directed mutants have crystallised in space groups different from those of the native enzyme. Interestingly, the site directed mutants, which remained as unprocessed precursors of PVA by mutation have all crystallised in monoclinic space group $P2_1$ (e.g. precursor-Cys1Ser - I, a = 102.64, b = 90.09, c = 102.27 Å, β = 102.13º). Truncated PVA mutants prepared for co-crystallization studies with pen V, crystallised in orthorhombic space group $P2_12_12_1$. (e.g. Cys1Gly mutant in processed form, a = 91.76, b = 130.71, c = 158.70 Å). Some other processed form of mutants had a different monoclinic cell with one cell dimension very long (eg. Asn175Ala, a = 47.29, b = 379.38, c = 102.01 Å, β = 93.5º).

Some of the cells are related by simple transformations (Figure 6.10) but with different symmetry. In a few cases the refinement of the structure itself turned out to be challenging due to the presence of pseudo-symmetry or twinning.

6. 2. Crystal packing

The densely packed environment of globular proteins in crystal structures is dissimilar from the environment in the natural state. Moreover, the protein structures vary among themselves too, depending upon their environment. In this chapter our aim will be to compare the structures of the mutants in different crystal forms. The pattern of crystal packing and the residues involved in packing interactions will be studied. While the environment is not expected to induce major changes in the fold, we do observe significant local differences between the structures. For example, the r.m.s. deviation of Cα atoms of some residues at certain flexible zones vary more than 3.0 Å.

Although the two monoclinic structures (pre-Asn175Ala and pre-Cys1Ser-I) have almost similar unit cell dimensions and are in $P2_1$ space group, the positions of their assymetric unit is different. Two cell dimensions in the monoclinic space group form II are almost equal ($a \approx c \approx 102$). The distinct handedness of these two structures about 2_1 screw is obvious from the packing of the mutants in their respective unit cells. Figure 6.1 shows the position of tetramers in overlapped unit cell.

Analysis of the crystal packing in different space groups suggest that layers of PVA molecules in crystals are similar in P1 (3PVA) (Figure 6.2a), $P2_1$ form II (pre-Cys1Ser-I), $P2_12_12_1$ (Cys1Gly) and $C222_1$ (Cys1Gly complex) (Figure 6.3 and 6.4). The crystal packing in the case of monoclinic crystal $P2_1$ form I is sort of wavy pattern (Figure 6.3a). Packing in 2PVA ($P6_5$) is unique among all crystals (Figure 6.2b). The interaction observed in $P6_5$ space group is also very different from that of others (Table 6.5). Hexagonal arrangement creates more channels between the molecules. As a result the solvent content is the highest in hexagonal crystals (69 %).

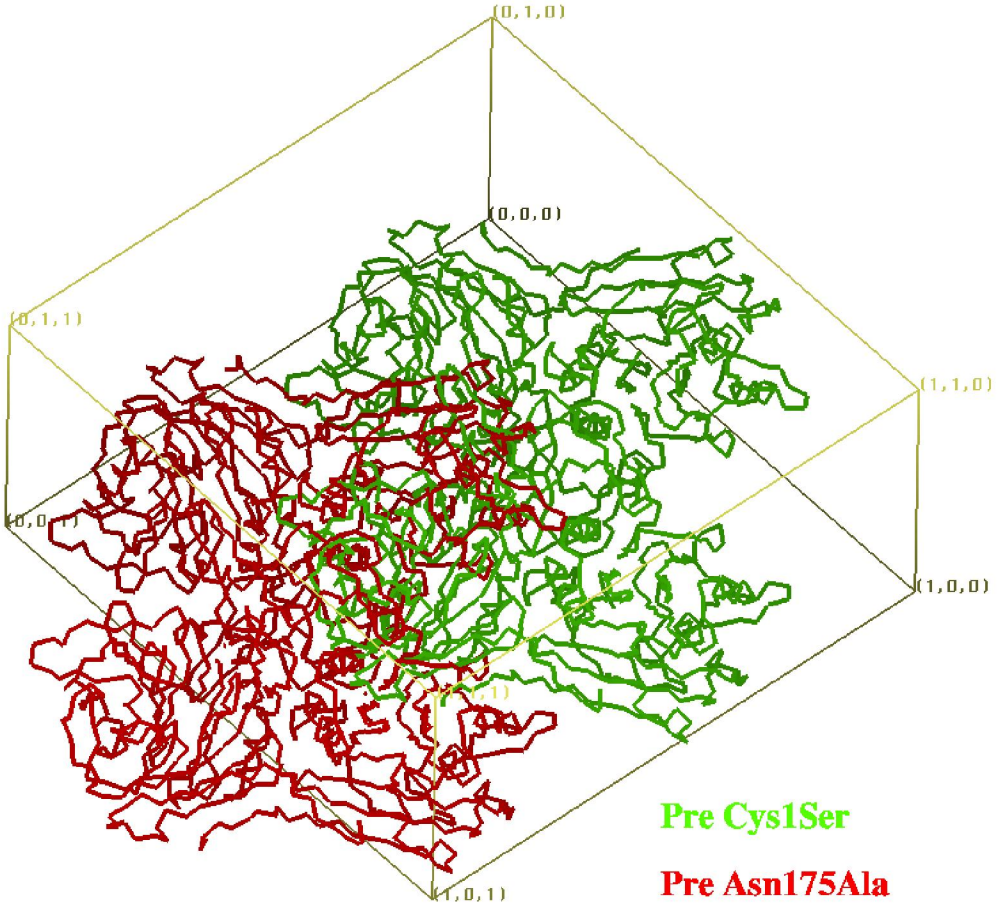

Figure 6. 1

Pre-Asn175Ala (red) and pre-Cys1Ser-I (green) have same unit cell dimensions but have opposite handedness. They occupy distinct locations in the monoclinic unit cell.

Table 6. 4
Different crystal systems in which PVA and its mutants crystallised.

	2PVA	**3PVA**	**Cys1Ala**	**Pre-Cys1Ser-I**	**Cys1Gly**	**Cys1Gly (pv)**
Description	Native PVA (Oxidized catalytic cysteine)	Native PVA (Reduced catalytic cysteine)	Truncated mutant Cys1Ala	Precursor Cys1Ser (with tri-peptide)	Truncated mutant Cys1Gly	Truncated Cys1Gly co-crystallised with PenV
Precipitant	Ammonium sulfate	Ammonium sulfate	PEG	Ammonium sulfate	PEG	Ammonium sulfate
Crystal system	Hexagonal	Triclinic	Primitive monoclinic	Primitive Monoclinic	Primitive Orthorhombic	C-centered orthorhombic
Space group	$P6_5$	P1	$P2_1$ form I	$P2_1$ form II	$P2_12_12_1$	$C222_1$
Unit cell dimension (Å & º)	a = b = 208.4, c = 96.3.	a = 47.4, b=129.6, c = 156.7, α= 88.3, β = 83.4, γ = 84.6	a = 47.86, b =381.89, c = 102.89, β = 94.1	a = 102.6, b= 90.0, c = 102.26, β= 102.13	a = 91.76, b = 130.71, c = 158.71	a = 129.730 b = 158.890 c = 90.742
Resolution (Å)	2.5	2.8	2.1	2.5	1.8	2.5

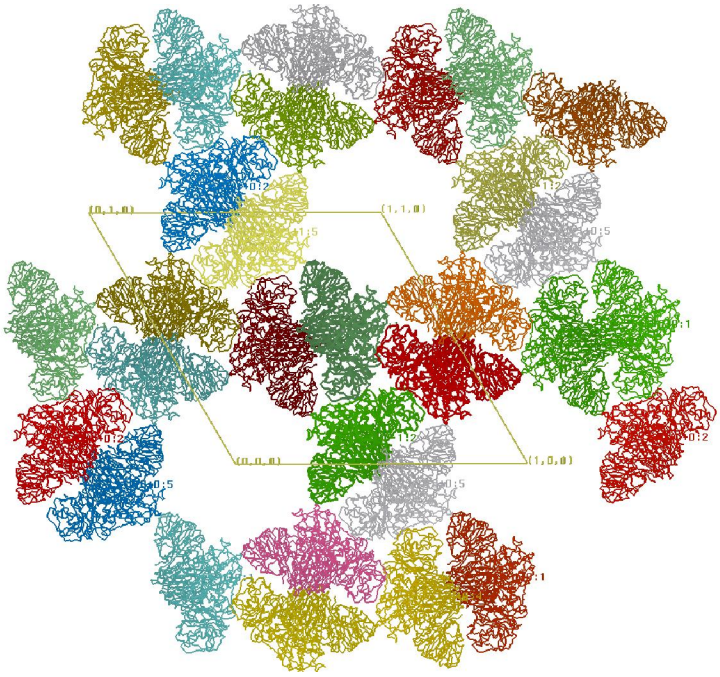

(a)

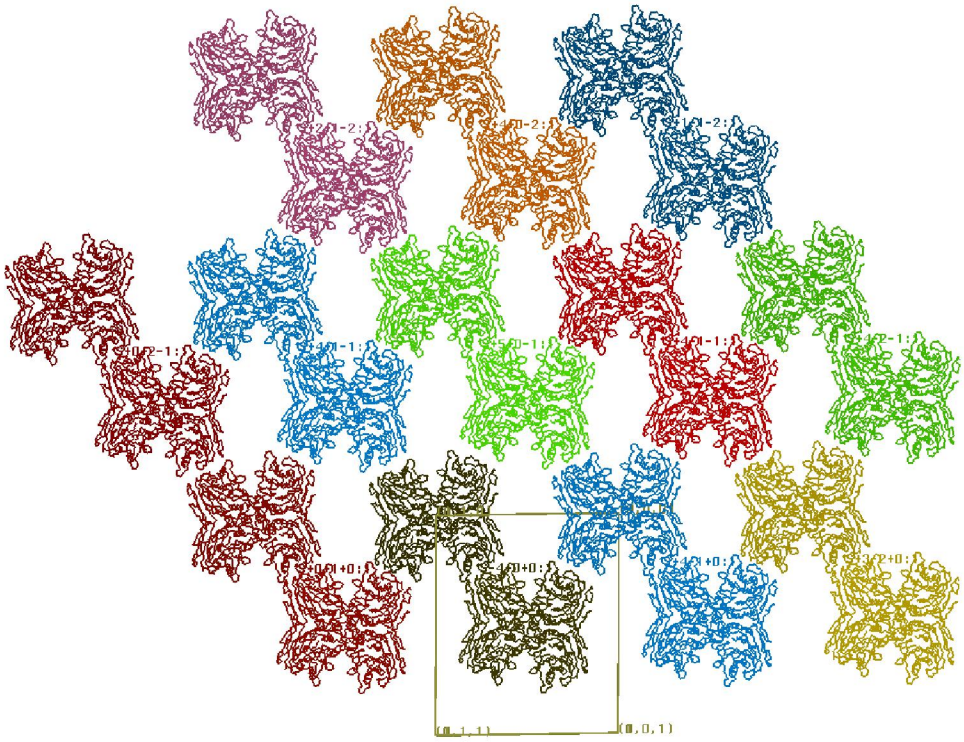

(b)

Figure 6. 2

Packing of molecules in the crystals of wild type PVA is shown. (a) View along c axis of hexagonal crystal, $P6_5$ (2PVA). (b) View along a axis of triclinic crystals, P1 (3PVA).

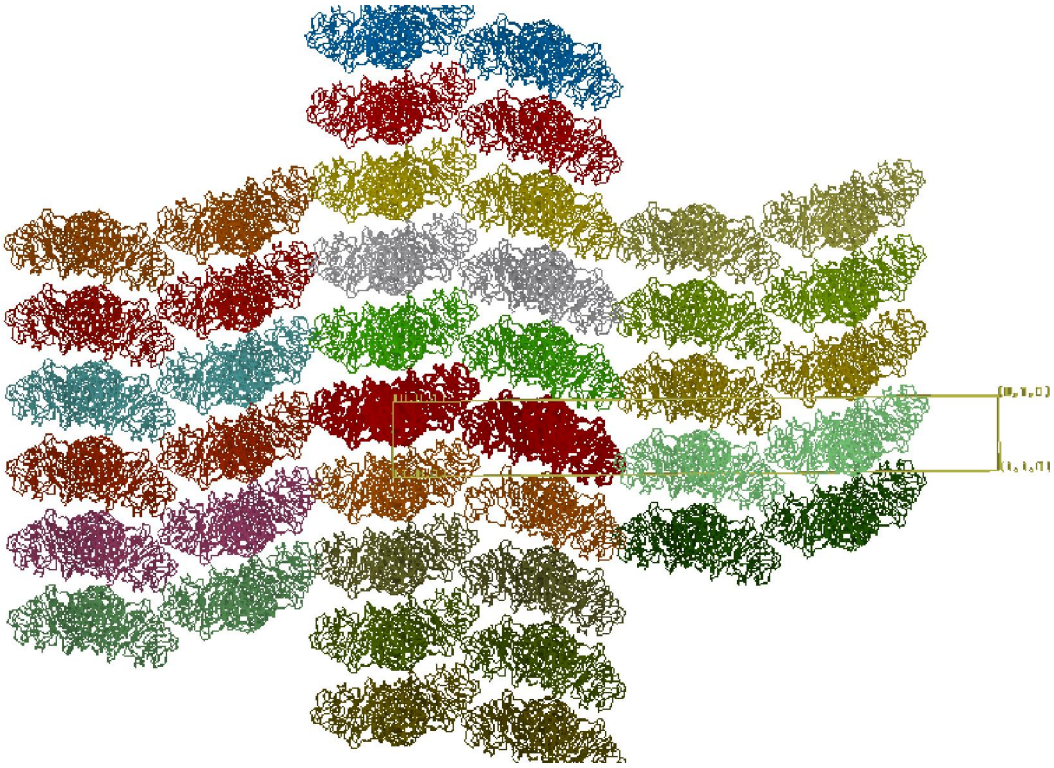

(a)

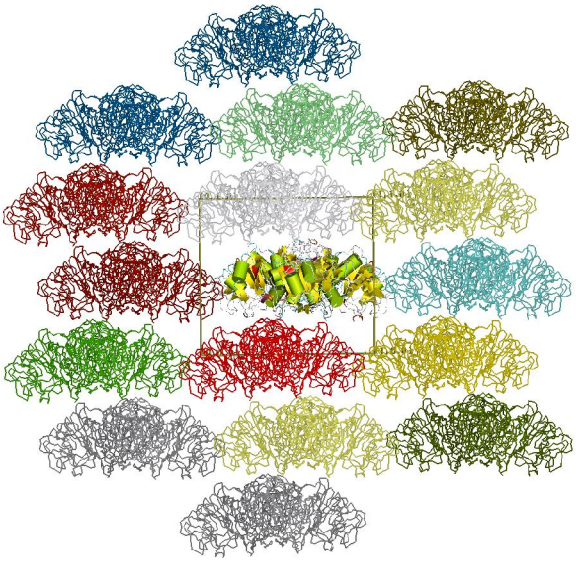

(b)

Figure 6. 3

Packing in monoclinic crystals of mutant PVA. (a) View along c direction of Asn175Ala in $P2_1$ form I (b) View along c axis of pre-Cys1Ser-I in $P2_1$ form II.

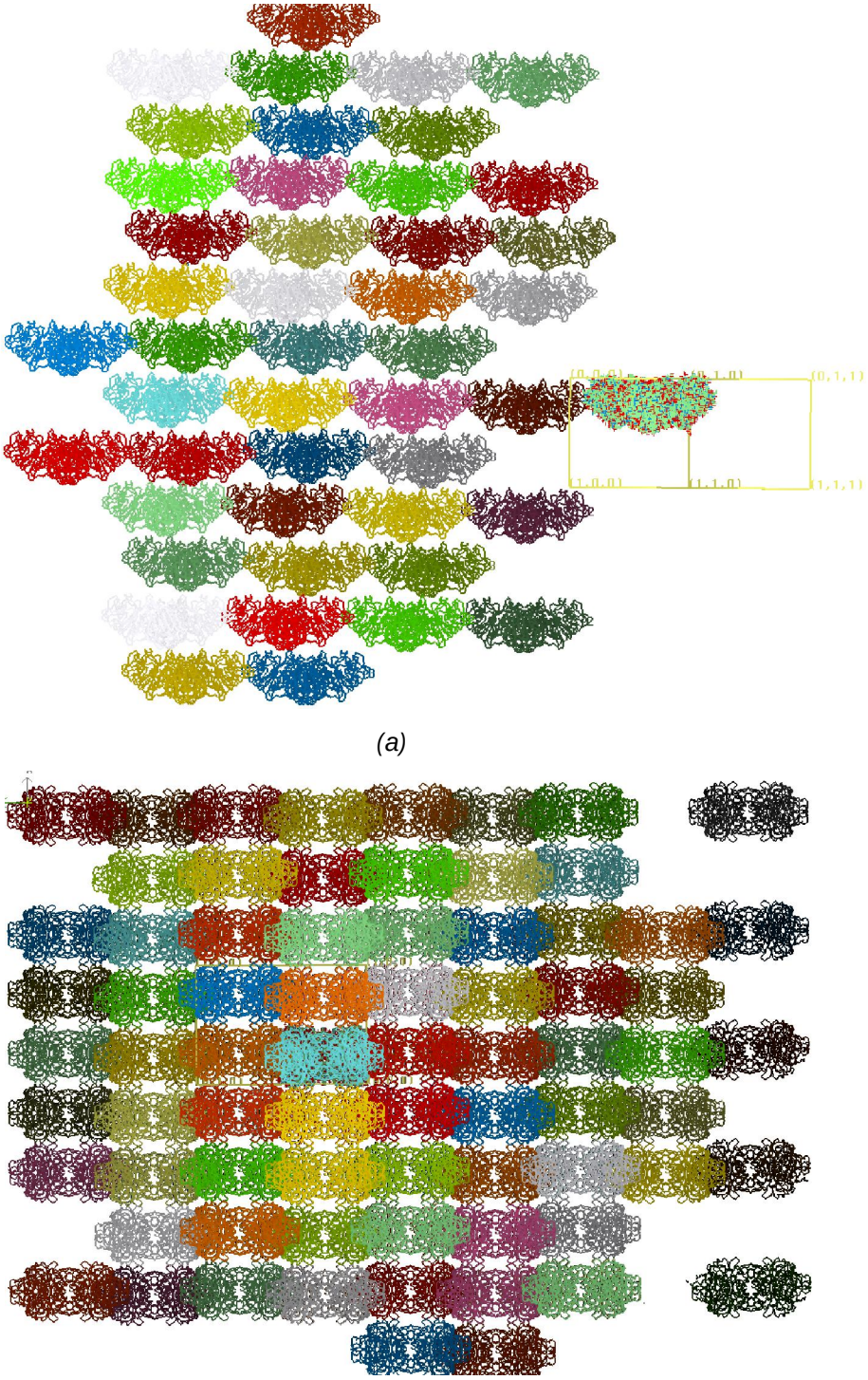

(a)

(b)

Figure 6. 4

Packing in orthorhombic $P2_12_12_1$ crystals of Cys1Gly (a) A view against the diagonal plane to show the packing (b) View along c direction

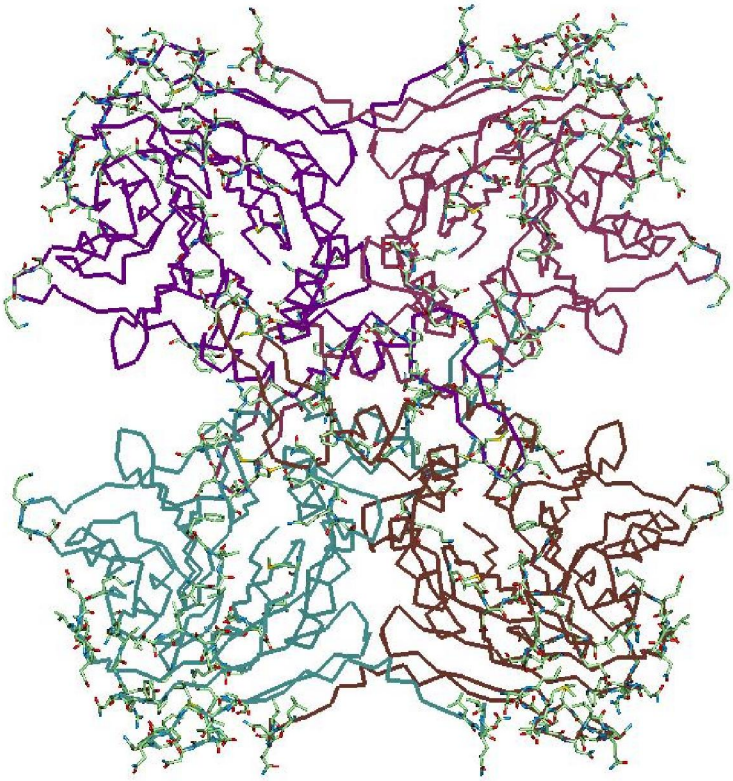

(a)

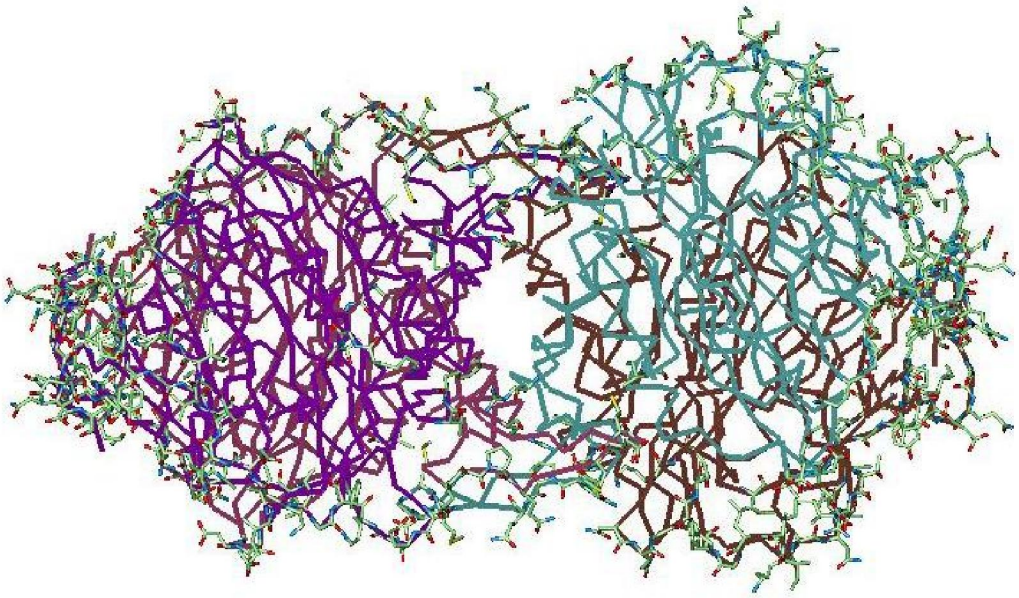

(b)

Figure 6. 5

Figure shows the residues (side chains in liquorice) which are involved in the packing in crystals of PVA (a) & (b).

Table 6. 5

Intermolecular interactions and short contacts found in different crystal structures (wild and mutants) of PVA.

	P1 (3PVA)	**$P6_5$ (2PVA)**	**$P2_1$ Form I (Asn175Ala)**	**$P2_1$ -form II (Pre-Asn175Ala)**	**$C222_1$ (Cys1Gly)**	**$P2_12_12_1$ (Cys1Ser)**
Thr9 to Thr9	X	X	X	4.5	3.8, 4.1	3.1
Thr9 to Asp10	X	X	X	3.86	X	X
Thr9 to Lys43	X	X	X	2.9	2.7	4
Thr9 to Ile134	3.1	X	X	X	X	X
Thr9 to Gly137	3.5, 3.2	X	2.74	X	X	X
Thr9 to HOH	3.54	X	2.94	3.91	X	2.49
Asp11 to Lys43	X	X	2.73	X	X	X
Asp11 to Ile134	3	X	X	X	X	X
Met23 to Ile135	X	3.07	X	3.9	3.4	X
Arg34 to Asp199	X	3.07	X	X	X	X
Asn35 to Arg98	X	X	2.76	4.4	3.57	3.2
Asn35 to Leu328	X	3.36	X	X	X	X
Tyr36 to Thr/Arg98	X	X	X	4.15	3.5	3.1
Arg39 to Asp313	X	3.13	X	X	X	X
Lys43 to Asp204	X	X	2.92	X	X	X
Lys43 to Glu240	X	X	X	4.4	3.3	3.1
Lys43 to Lys241	X	X	X	3.1	3.3	X
Lys43 to Lys247	X	X	X	3.3	4.65	X
Lys43 to Gln312	X	X	2.88	X	X	X
Asn45 to Asn45	2.7, 2.9	X	X	3.5, 2.6	2.9	2.9
Asn45 to Val46	X	X	X	3.5	3.83	3.8, 3.1
Asn45 to Val47	3.1, 3.3	X	2.76	3	4.11	3
Asn45 to Thr60	X	X	2.88	X	X	X
Asn45 to Thr63	X	X	2.81	X	X	X
Asn45 to Gln312	X	3.4	X	X	X	X
Asn45 to Asp313	X	3.32	X	X	X	X
Asn45 to Leu314	X	2.88	X	X	X	X
Val47 to Val46	3.4, 3.2	X	X	X	3.99	3.3
Val47 to Val47	2.7, 2.6	X	2.79	2.9	3.62	2.8
Val47 to Asn49	3	X	2.84	3	4.39	3
Val47 to Asp313	X	3.09	X	X	X	X
Val47 to Leu314	X	2.9	X	X	X	X
Val47 to Thr316	X	2.96	X	X	X	X

Asn49 to Val47	3.1	X	X	3	4.39	3
Asn49 to Ile48	3.3	X	X	4	4.28	X
Asn49 to Ile315	X	3.25	X	X	X	X
Asn49 to Thr316	X	2.98	X	X	X	X
Glu73 to Gln198	X	2.68	X	X	X	X
Thr85 to Arg187	X	X	X	X	2.8	X
Phe86 to Arg187	X	X	X	X	3.2	X

Table 6. 5 Continued.

Lys95 to Gln312	3.5, 3.2	X	X	4.9	4.84	3.78
Gly96 to Gln312	3, 2.8, 2.7	X	2.99	4.1	5.63	3.62. 3.56
Thr97 to Gln312	3, 2.7, 2.6	X	X	3.75	X	5.8
Ile134 to Lys241	2.8	X	X	X	X	X
Leu136 to Glu270	X	X	X	3.5	X	X
Leu136 to Lys272	X	X	X	3.4	4	3.6
Gly137 to Glu270	X	X	X	3.5	X	3.4
Gly137 to Gly271	X	X	X	3.4	X	3.9
Gly137 to Lys272	X	X	X	3.6, 5.4	3.5	3.4
Phe138 to Met201	X	X	2.97	X	X	X
Phe138 to Glu270	X	X	X	2.8	2.9	4
Phe138 to Gly271	X	X	X	3.5	3.2	3.5
Phe138 to Lys272	X	X	X	3.74	3.3	3.35
Ile170 to Met202	X	X	X	X	3.3	X
Asp199 to Asn310	X	3.24	X	X	X	X
Met201 to Glu270	2.8	2.8	X	X	X	X
Asp206 to Asn308	X	3.07	X	X	X	X

Asn269 to Gln198	X	X	2.86	X	X	X
Asn269 to Gly271	2.9, 3	X	X	X	X	X
Asn269 to Lys287	X	2.92	X	X	X	X
Asn269 to Met305	X	3.38	X	X	X	X
Glu270 to Asn195	X	X	2.99	X	X	X
Glu270 to Glu270	X	X	X	3.8	2.73	3.4
Glu270 to Gly271	3.2, 2.8	X	2.95	X	X	X
Glu270 to Gln285	X	3.39	X	X	X	X
Glu270 to Ser286	X	3.33	X	X	X	X
Glu270 to Ser303	X	2.98	X	X	X	X
Glu270 to Val331	X	2.57	X	X	X	X
Lys272 to Asp11	X	3.24	2.96	X	X	X
Lys287 to Asn269	X	2.92	X	X	X	X

6. 3. Molecular contacts

In pre-Asn175Ala ($P2_1$, form II), Asn45 is involved in specific interactions with Asn45, Val46 and Val47 of symmetrically related molecule replacing contacts with Gln312, Asp313, and Leu314 found in hexagonal form. An interaction between Lys241 and Ile134 (2.8 Å) in native triclinic replaces one between Lys241 and Lys43 (3.1 Å) in pre-Asn175Ala ($P2_1$ form II) (Table 6.5). This is again replaced by interaction between Lys241 and Lys43 (3.3 Å) in Cys1Gly complex ($C222_1$). Almost all the interactions found in truncated Asn175Ala ($P2_1$ form I) are stronger. This tight crystal packing also correlates with the good diffraction (resolution:1.7 Å) obtained from the crystal.

Carbonyl oxygen of Thr25 is hydrogen bonded to a (symmetrical) water molecule (3.3 Å); this interaction may be important for packing. This water (W117) in pre-Cys1Ser - I) has three interactions: with carbonyl oxygen of Thr22 chain C (3.37 Å), with main chain N of Thr273 chain C (2.91 Å), and with carbonyl oxygen of

Gly137 chain A (symmetry related) (2.49 Å). First two interactions hold the extended part of two loops *viz.* 22-26 & 132-136 together. The third contact is involved in packing.

6. 4. Indexing the diffraction data from twinned crystals and identifying type of twin

Several site-directed mutants have been prepared with the intention of studying the mechanism of autoproteolysis and catalysis of PVA, some of them could be successfully crystallised also. Five mutants: pre-Asn175Ala, pre-Cys1Ala, pre-Cys1Ser-I, pre-Cys1Ser-II, Cys1Ser have crystallised in monoclinic $P2_1$ for which X-ray data sets have been collected, indexed and scaled. Structures of two of them (pre-Asn175Ala, pre-Cys1Ser-I) could be determined and refined satisfactorily using REFMAC5 (Murshudov, 1997), but other three data sets could be hardly refined successfully.

The problem was felt, in the beginning itself when processing the first such diffraction data from pre-Asn175Ala using DENZO. The data could be indexed equally well in monoclinic space group as well as in orthorhombic space group $C222_1$. Finally space group $P2_1$ has been chosen for both pre-Asn175Ala and pre-Cys1Ser – I since scaling gave slightly more favourable R_{merge} in $P2_1$ than $C222_1$. The structure could be solved using molecular replacement (MR) method using PVA monomer (pdb, 2PVA) as model.

Subsequently, Cys1Ser and pre-Cys1Ser-II have also crystallised in the same unit cell. However, these two data sets scaled equally well in both $P2_1$ and $C222_1$ space groups, R_{merge} in both the space groups were nearly same. The space group $C222_1$ was chosen as being of higher symmetry. In this unit cell a dimer is the asymmetric unit related by a crystallographic symmetry rotation to the other dimer of tetramer.

However, the structure did not refine smoothly. Repeated manual refinement using QUANTA and restrained refinement using REFMAC5 has lead to no further decrease in R_{free} (~39) and Rfactor (~34). This came as a surprise, since the maps were looking good and model fitted well. The Ramachandran plots were quite reasonable. It has been reported (Vajdos *et al.*, 1997) that the correlation coefficient will be a more reliable indicator of the progress of refinement in the case of

problematic data. The structure solution using molecular replacement method was also not straightforward in the case of some of the problematic data sets.

The cumulative intensity distributions (CID) for the acentric reflections are non-sigmoid (Figure 6.6 & 6.7). The degree-of-sigmoidalness is also a point of concern, because another data set Asn175Ala has a more sigmoid CID curve (Figure 6.6c). But eventually, the refinement of this structure with the same data was smooth.

6. 5. Twinning

Twinning occurs when the crystal consists of multiple domains grown together, which are mutually reoriented according to a specific transformation that does not belong to the symmetry operations of the crystal point group but is related in some way to the crystal lattice. The domains in the crystal are inter-grown in such a way that at least some of their lattice directions are parallel. True merohedral twinning is possible when the twin operator is the twin operator of the crystal system and not belonging to its point group. For chiral molecules trigonal, tetragonal, hexagonal and cubic crystal systems belonging to point groups 3, 32, 4, 6, 23 etc. can display merohedral twinning. In cases where the twin operator belongs to higher crystal symmetry than the structure, it leads to pseudo-merohedry. A monoclinic system with certain special unit cells such as $a \approx c$, $\beta = 90^{o}$ or $c \cos\beta = -a/2$, all these can generate orthorhombic symmetry. Similarly in orthorhombic system possessing two equal unit cell axes also can have pseudo-merohedry. The reciprocal lattice of the twin domains in the case of merohedral twinning overlaps and hence the twinning cannot be detected directly from the diffraction pattern. The fractional contribution of each twin domain is defined as twin factor, which is also an estimate of the fraction of that twin domain in the crystal.

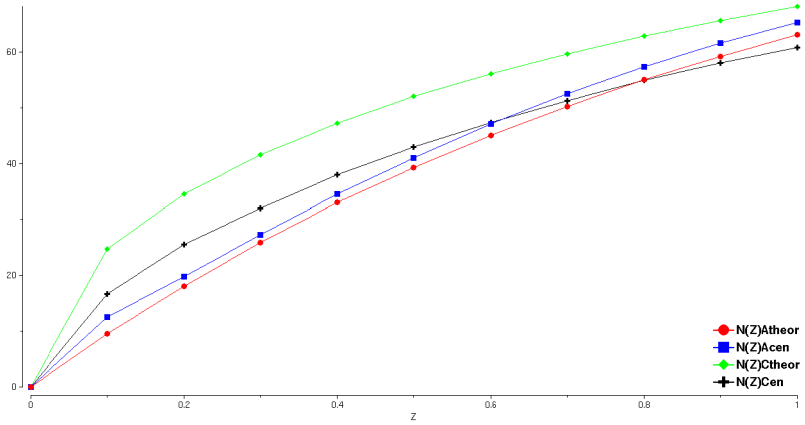

(a)

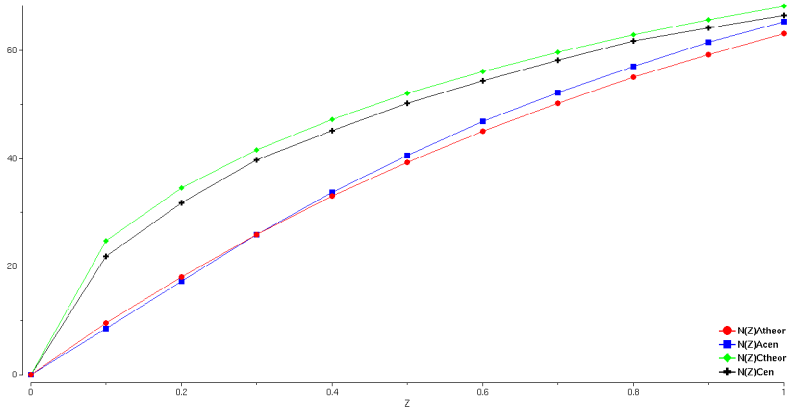

(b)

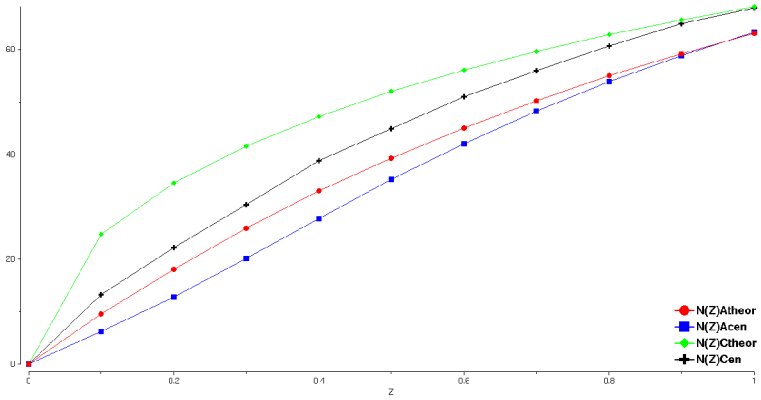

(c)

Figure 6. 6

Cumulative intensity distribution of three data sets which could be refined using REFMAC5. (a) Pre-Asn175Ala (b) Pre-Cys1Ser-I (c) Asn175Ala.

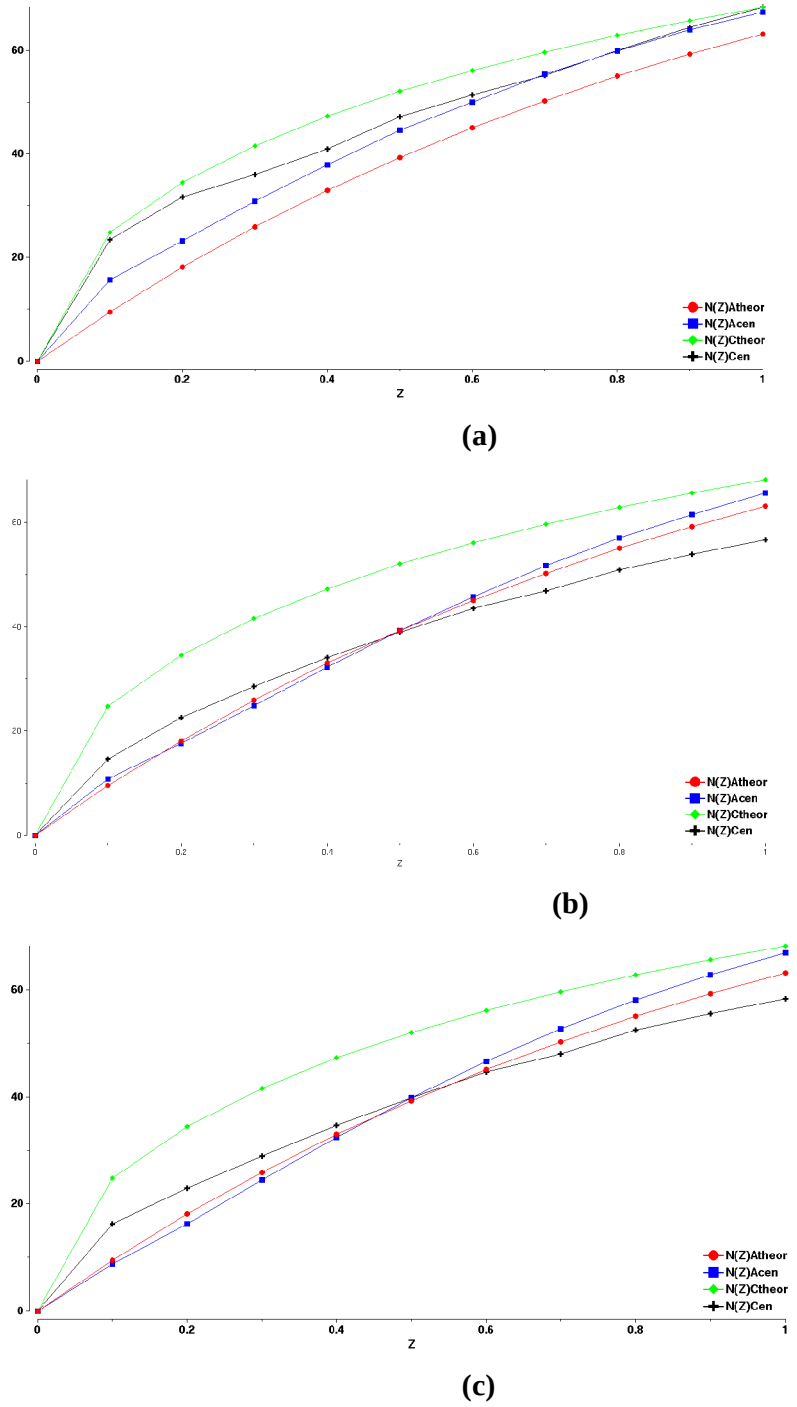

Figure 6. 7

Cumulative intensity distribution of twinned data sets. (a) Pre-Cys1Ala (b) Cys1Ser (c) Pre-Cys1Ser-II.

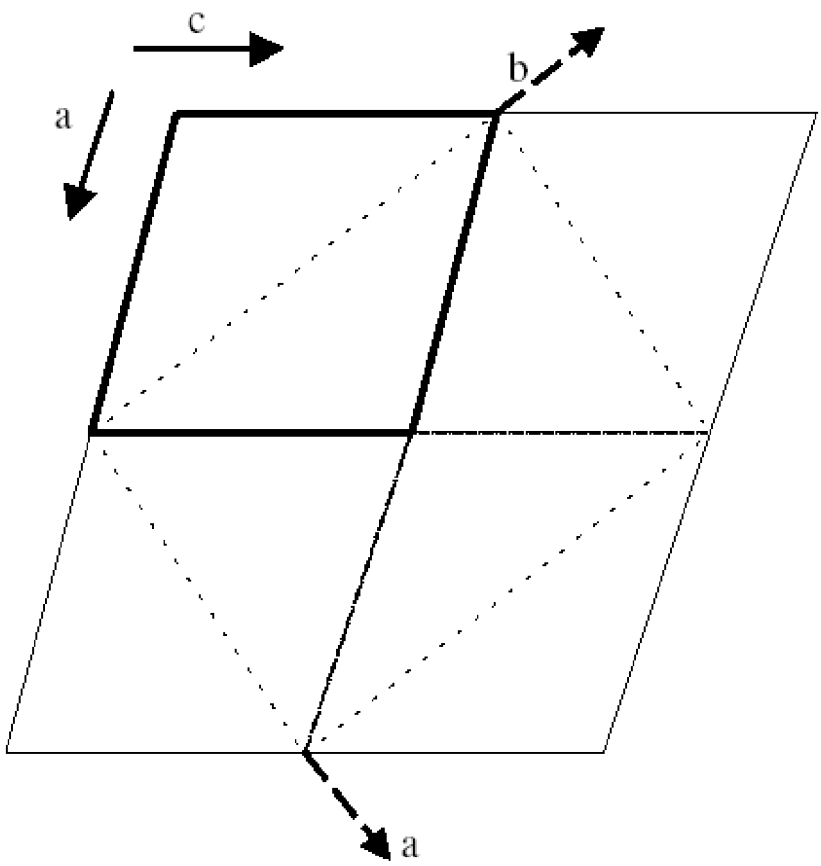

Figure 6. 8

Diagram showing conversion of monoclinic unit cell (in thick line) in to orthorhombic unit cell (broken line) for pre-Asn175Ala. The cell dimensions for monoclinic space group $P2_1$ is a = 103.59, b = 92.16, c = 103.74, β = 101.78; whereas for orthorhombic space group $C222_1$ it is a = 130.78, b = 160.88, c = 92.16.

6. 5. 1. Merohedral Twinning in PVA

Since some of the structures were not refining satisfactorily we had a fresh look at the data processing and tested the data for the presence of twinning. We realized that some typical symptoms of merohedral twinning were present.

Firstly, during data processing diffraction data was indexed in two equally probable unit cells, one monoclinic and the other C-centred orthorhombic. However, only in problematic data sets the R_{merge} has closely similar values in $C222_1$ and $P2_1$. The relationship between the two unit cells is shown in Figure 6.8. Secondly, in such cases the structure could be satisfactorily refined in none of the space groups chosen. In addition, the monoclinic lattice can generate merohedral twinning in the special case where two non-unique axes a and c have similar dimension. Thus, it became reasonably clear that the PVA crystals are twinned by the twinning operator (l,-k,h). The effect of this twinning is observed in the projection of hkl plots using program HKLVIEW (CCP4). The h k l plots are very similar to l -k h plots, in all twin cases (Figure 6.9). Pseudo 2-fold axes can exist along the diagonal directions parallel to a-c plane in the case of a perfect twin, where the twin-domains will be in the ratio 1:1.

α, the twin fraction, has been estimated by a statistical evaluation of the similarity between twin-related observations. But the presence of pseudo-symmetry or non-crystallographic symmetry can bring additional complication, as it tends to mimic twinning (at least at lower resolution) by leading to intensity similarity between crystallographically distinct reflections (Yeates, 1997). To obtain an accurate estimate of the twinning fraction, Britton plots (Britton, 1972) have been calculated (Figure 6.11). This plot shows the number of negative intensities after de-twinning as a function of the twinning fraction.

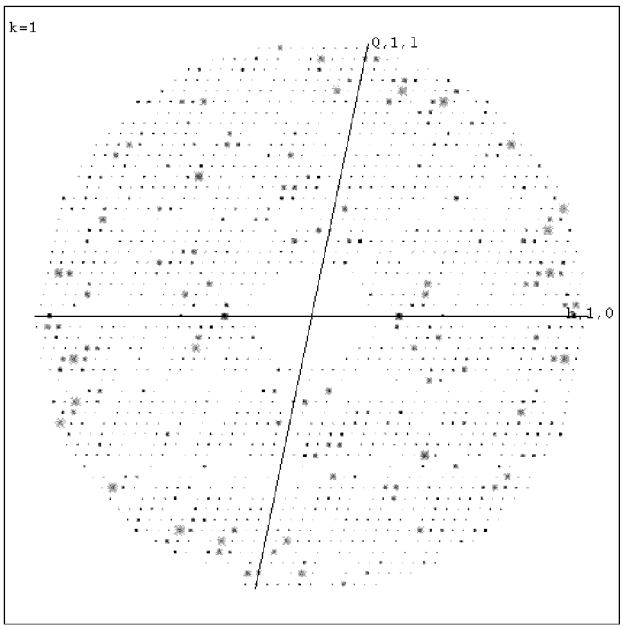

(a)

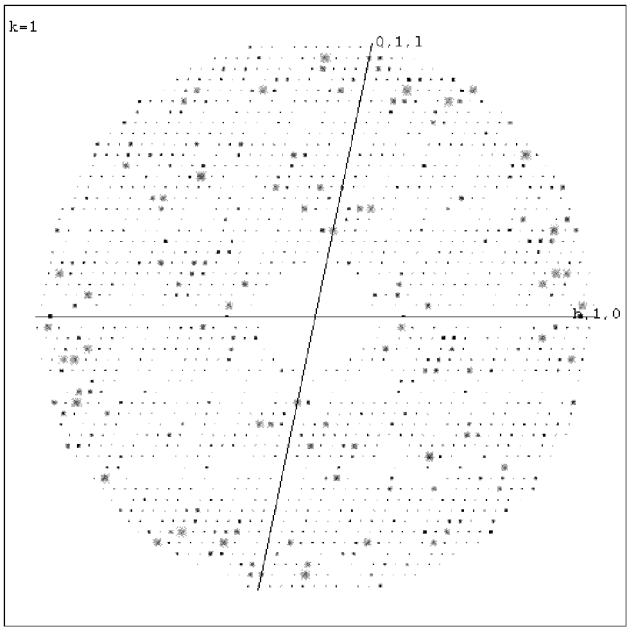

(b)

Figure 6. 9

HKLVIEW plots showing h1l plane for monoclinic pre-Cys1Ser- I indexed as $P2_1$ (a) and reindexed as l –1 h (b). Two dissimilar plots for this structure suggest absence of twinning. REFMAC5 refined this structure satisfactorily.

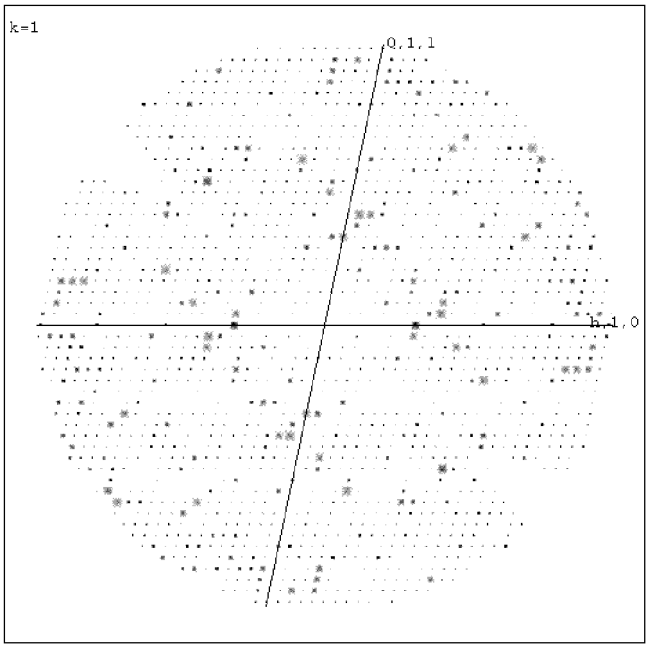

(a)

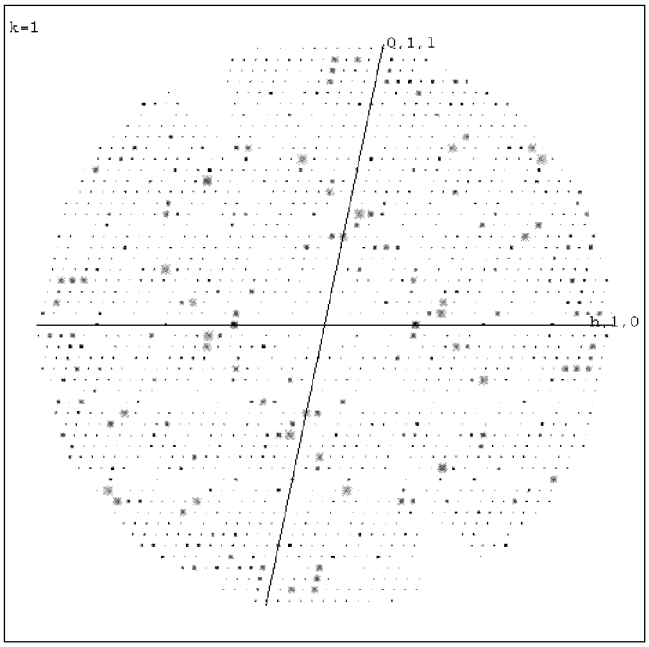

(b)

Figure 6. 10

HKLVIEW plots showing h1l plane for truncated Cys1Ser indexed as $P2_1$ (a) and reindexed as l –k h (b). Two similar plots suggest presence of twinning in this data.

Despite structure determination in $P2_1$ using molecular replacement method, refinement by REFMAC5 converged at unsatisfactorily high R and R_{free} values.

Further refinement, rebuilding of model or addition of water molecules resulted in intolerably large differences between R and R_{free}, indicating problems with the data. This problem has been reported with twinned data where the R_{free} does not correspond to the quality of the map calculated (Vajdos *et al.*, 1997). Strangely, the intensity statistics calculated for our data to check for merohedral twinning happened to be closer to values for normal crystals rather than for perfect twins.

The structures were refined in REFMAC5 till it converged. Unfortunately, the refinement programs of the CCP4 suite have no provision for handling twinned data. Hence, refinement against observed intensities with the inclusion of twin component was performed using SHELXL-97 (Sheldrick & Schneider, 1997; Herbst-Irmer & Sheldrick, 1998) inputting the refined REFMAC5 coordinates. The twin-refinement in SHELXL produced better R_{cryst} and R_{free} values and also output refined twin factor (Table 6.6). The twin factor was very close to 0.5 in all cases showing that the PVA mutant crystals provide cases of perfect twin.

Table 6. 6

Results of rfinement using REFMAC5 and SHELXL for twined data. Twin fraction has been obtained from SHELXL and Britton plot. R_{merge} for processing in $P2_1$ and $C222_1$ are also shown for comparison.

Structure	R_{merge}		Twin fraction		REFMAC5		SHELXL	
	$P2_1$	**$C222_1$**	**SHELXL**	**Britton plot**	**R_{cryst}**	**R_{free}**	**R_{cryst}**	**R_{free}**
Pre Cys1Ser-II	6.5	7.0	0.49579	0.42	0.2705	0.3274	0.2390	0.2854
Pre Cys1Ala	7.8	19.1	0.42897	0.24	0.2684	0.3120	0.2057	0.2561
Cys1Ser	9.4	10.7	0.46051	0.36	0.2723	0.3148	0.2322	0.2510

Table 6. 7

Various moments of intensity distribution, output by the program TRUNCATE (CCP4) for mutant structures.

	Acentric Moments			Centric Moments		
	Z2	**Z3**	**Z4**	**Z2**	**Z3**	**Z4**
Expected	2.00	6.00	24.00	3.00	15.00	105.00
Asn175Ala (pv)	1.93	5.96	27.36	2.58	11.70	78.40
Cys1Ser (pv)	6.11	78.37	1654.10	9.13	152.35	3446.51
Cys1Ala (pv)	4.78	45.31	667.94	7.55	100.03	1831.43
Cys1Ala (PAA)	4.99	48.39	720.99	7.22	87.87	1408.41
Cys1Gly (pv)	4.56	47.54	824.28	4.95	43.37	508.63
Pre-Asn175Ala	2.41	10.25	74.97	3.02	15.69	113.91
Pre-Cys1Ser-I	2.19	8.27	49.39	3.03	15.11	104.71
Pre-Cys1Ala (Twinned)	3.29	21.00	240.35	21.06	-142.62	74277.54
Pre-Cys1Ser–II (Twinned)	2.6	11.2	75.2	5.2	34.1	242.0
Cys1Ser (Twinned)	2.32	9.48	62.75	2.71	12.08	74.17

6. 6. Analysis of twin data using twinning indicators and intensity statistics

It is possible to detect twinning by observing intensity distribution of the observed reflections. Cumulative intensity distribution curves become sinusoidal in case of twinned data, instead of hyperbolic. The change in shape of the curve is accounted for by the overlap of weak reflections from different twin domains. This reduces the number of weak reflections and eventually also increases the number of strong reflections.

In PVA datasets, the cumulative intensity distribution does not show any significant sigmoidal shape (Figure 6.6 and 6.7) to indicate the presence of twinning. Moreover, moments are only higher than the theoretical value of 2.0 expected for normal crystals and not closer to 1.5 as can be expected for a twinned crystal.

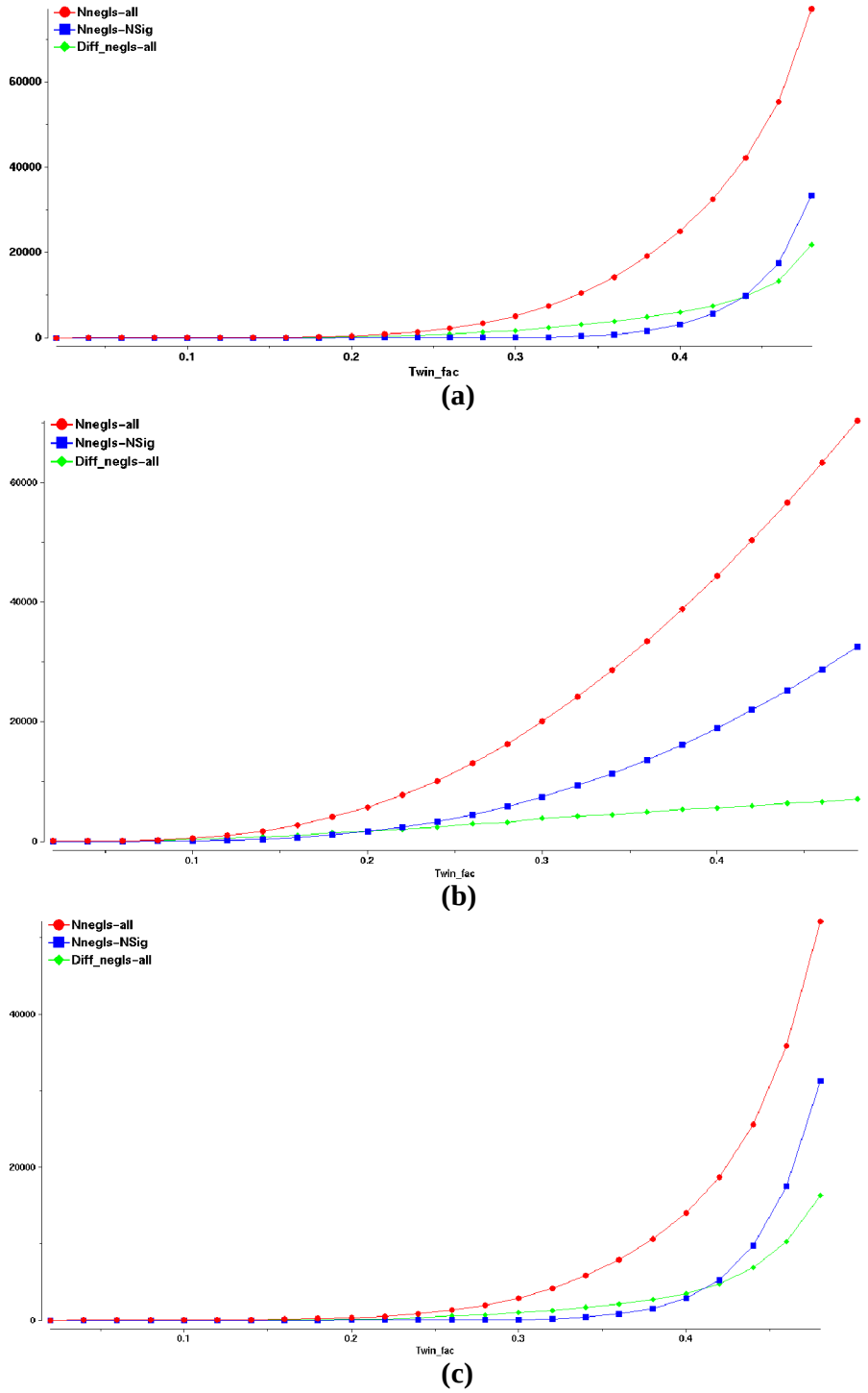

Figure 6. 11

Britton plots of (a)Cys1Ser, (b)pre-Cys1Ala and (c)Pre-Cys1Ser-II data to estimate twin factor

The Britton plot of data from Cys1Ser, pre-Cys1Ala and pre-Cys1Ser-II are shown in Figure 6.11. Using this plot, a twinning fraction was obtained by extrapolation of the linear part.

These plots suggest twin fractions of 0.24 for Pre-Cys1Ala, 0.42 for pre-Cys1Ser-II and 0.36 for Cys1Ser. These values of twin fractions predicted by Britton plots are lower than what obtained through SHELXL refinement (Table 6.6).

Keeping pre-Asn175Ala as master data, we compared few of the indexing for different mutant data sets. $P2_1$ data for pre-Cys1Ser - I gives Riso of 35 %. But if the same data is reindexed as l, -k, h, then the R_{iso} becomes 19%. And it has very similar spots as master data in certain regions (around hkl= 0.3, 1, 0). Orthorhombic $C222_1$ and monoclinic $P2_1$ data for Cys1Ser agree very closely (R_{iso} = 5%). This shows this data is definitely twinned. R_{iso} of Cys1Ser data with pre-Asn175Ala is 35 %.

Cys1Ser $P2_1$ data (hkl) and reindexed as l -k h (h1l view) are almost identical and shows a two fold symmetry in a diagonal directions to the reciprocal a and c axes (Figure 6.9b).

In conclusion, the structure determination of PVA mutants has shown pseudo-merohedral twinning generated because of the special arrangement of molecules in the lattice giving rise to a monoclinic cell of a and c axes having almost equal length. In our crystal structures we have come across each of the twin domains crystallised separately in different mutant crystals as well as they have grown together in closer to 1 : 1 ratio in the same crystals in the case of some other mutants. Although we have demonstrated that these twinned structures can be solved and refined, we have not proceeded with a complete refinement inputting solvent molecules etc. of these structures as we could derive the structural and packing information from corresponding untwined structures.

6. 7. Potential pseudo-merohedral twinned structures in Protein Data Bank (PDB)

As we have already discussed that a special unit cell with dimensions a≈c have potential to possess pseudo-merohedral twinning. Three cases of twinned data similar to that found here have been reported (Ito *et al*., 1995; Ban *et al.*, 1999; Yang *et al.*, 2000). All these structures have been solved and refined to descent R values albeit at different resolutions. However, when the presence of twinning goes undetected, the structure may be solved and refined but the R factors will remain at unacceptably high values. The protein data bank has been scanned for deposited structures belonging to monoclinic space group $P2_1$ satisfying condition a≈c and have high R factors. Interestingly, we could detect several of them. Some selected ones are listed in Table

6.8 along with their unit cell dimensions, R factor, R_{free} and resolution. From our experience with PVA mutant structures, described in this chapter, we are tempted to predict that these structures may possess potential twinning problems. However, this needs to be analysed to confirm the extent of twinning in each case.

Table 6. 8

This table lists monoclinic ($P2_1$) unit cells where cell dimension a ≈ c (the difference is less than 1 Å) and the R factor is high. These PDB structures might have a potential twinning problem.

PDB ID	β	a	b	c	R Value	R_{free}	Res [Å]	Reference
1JJK	115.300	115.500	149.000	115.600	0.344	0.344	3.000	-
2ER0	97.000	43.000	75.800	42.800	0.280	-	3.000	Cooper *et al*., (1989)
1KON	97.890	39.560	73.480	39.260	0.273	0.317	2.200	-
1XCF	91.480	71.087	52.695	71.518	0.261	0.289	1.800	Jeong *et al*., (2004)
1MQ2	106.100	55.200	81.000	55.600	0.257	0.317	3.100	Krahn *et al*., (2003)
1WP9	114.850	118.498	165.940	119.157	0.257	0.286	2.900	Nishino *et al*., (2005)
1G39	90.040	40.610	37.330	41.160	0.256	0.278	1.220	Rose *et al*., (2000)
1NT0	119.930	70.411	103.901	70.484	0.248	0.283	2.700	Feinberg *et al*., (2003)
1W6X	111.430	35.160	45.160	35.060	0.248	0.25	2.000	Massenet *et al*., (2005)
1A31	98.300	72.000	66.600	71.800	0.247	0.310	2.100	Redinbo *et al*., (1998)
1J38	99.390	94.912	121.223	94.740	0.246	0.281	2.600	Kim *et al*., (2003b)
1EGA	115.820	86.790	67.560	87.290	0.243	0.298	2.400	Chen *et al*., (1999)
1K7T	110.810	45.150	93.170	45.100	0.242	0.326	2.400	Muraki *et al*., (2002)
1K7U	110.130	44.720	91.550	44.760	0.242	0.306	2.200	Muraki *et al*., (2002)
1KX1	119.600	61.800	255.560	61.790	0.242	0.287	2.800	Ng *et al*., (2002)
1J37	99.390	94.912	121.223	94.740	0.241	0.283	2.400	Kim *et al*., (2003b)

In the special case of pseudo-merohedral twinning where the twinning factor is close to 0.5, one may miss the actual symmetry and choose the orthorhombic space group $C222_1$, as happened in twinned structures of PVA mutant. Hence, we have searched for such structures also in PDB. There are a few with high R factors. They are listed in table 6.9. They also may have potential twinning problem.

Table 6. 9

A list of selected PDB structures in space group $C222_1$ with high R factors which may posses potential twinning. Numbers are as reported in pdb file, without approximation.

PDB	a	b	c	R factor	Resolution	Reference

1JNV	180.68	197.52	237.9	0.416	4.4	Hausrath *et al.*, 2001
1D8S	180.68	197.52	237.9	0.404	4.4	Hausrath *et al.*, 1999
1GRL	178	203	278	0.326	2.8	Braig *et al.*, 1994
1QBE	477.8	295.2	477.8	0.304	3.5	Golmohammadi *et al.*, 1994
1RPQ	199.7	149.7	104.1	0.294	3	Stamos *et al.*, 2004
1NBS	126.5	145.3	144.6	0.282	3.15	Krasilnikov *et al.*, 2003
1DWI	134.3	136.4	80.3	0.28	2	Burmeister *et al.*, 2000
1YKE	121.46	128.86	170.16	0.279	3.3	Baumli *et al.*, 2005
1GXD	75.696	374.58	191	0.278	3.1	Morgunova *et al.*, 2002
1HV8	109.13	131.45	131.83	0.27	3	Story *et al.*, 2001
1IBU	98.283	119.04	203.8	0.27	3.1	Worley *et al.*, 2002
1JII	71.56	98.45	142.13	0.269	3.2	Qiu *et al.*, 2001
1JKR	86.087	82.708	44.865	0.269	2.28	Chiu *et al.*, 2002
1MQL	147.68	147.1	251.99	0.269	2.9	Ha *et al.*, 2003
1MQM	146.92	147.29	250.63	0.265	2.6	Ha *et al.*, 2003
1T2V	97.117	138.36	198.27	0.261	3.3	Williams *et al.*, 2004
1IBT	96.2	115.31	202.39	0.26	2.6	Worley *et al.*, 2002
1TZD	71.679	98.535	188.75	0.26	2.2	Miller & Hurley, 2004
1UPP	155.88	156.25	199.75	0.259	2.3	Karkehabadi *et al.*, 2003
1SMJ	107.31	166.89	224.94	0.258	2.75	Joyce *et al.*, 2004
1HE9	42.897	55.646	107.47	0.257	2.4	Wurtele *et al.*, 2001
1JIJ	70.09	98.93	143.14	0.257	3.2	Qiu *et al.*, 2001
1PZN	144.16	193.12	176.93	0.257	2.85	Shin *et al.*, 2003
1JKQ	85.158	82.656	45.124	0.256	2.86	Chiu *et al.*, 2002
1IAS	172.56	251.62	140.23	0.255	2.9	Huse *et al.*, 2001
1NOH	114.01	117.3	105.93	0.254	2.8	Morais *et al.*, 2003
1IY2	86.647	101.15	66.99	0.253	3.2	Niwa *et al.*, 2002
1FFK	211.66	299.67	573.77	0.252	2.4	Ban *et al.*, 1999
1JP7	102.1	174.31	86.97	0.251	1.8	Appleby *et al.*, 2001
1Q3S	207.43	236.23	234.11	0.251	3	Shomura *et al.*, 2004
1S77	127.74	141.84	142.86	0.251	2.69	Yin & Steitz, 2004
1TF0	96.295	134.8	122.46	0.251	2.7	Lejon *et al.*, 2004
1XOK	50.1	123	53.6	0.251	3	Guogas *et al.*, 2004
1M5N	92.792	105.45	146.74	0.25	2.9	Cingolani *et al.*, 2002
1OVU	89.78	147.72	37.6	0.25	3.1	Di Costanzo *et al.*, 2003

BIBLIOGRAPHY

- Abadjieva, A., Hilven, P., Pauwels, K. & Crabeel, M., (2000). The yeast ARG7 gene product is autoproteolyzed to two subunit peptides, yielding active ornithine acetyltransferase. *J. Biol. Chem.*, **275**; 11361–11367.

- Abian, C., Mateo, C., Fernandez-Lorente, G., Palomo, J. M., Fernandez-Lafuente, R. & Guisan, J. M., (2001). Stabilization of immobilized enzymes against water-soluble organic cosolvents and generation of hyper-hydrophilic microenvironments surrounding enzyme molecules. *Biocatal. Biotransform.*, **19**; 489–503.

- Abrahmsen, A., Tom, J., Burnier, J., Butcher K. A., Kossiaoff, A. & Wells, J. A., (1991). Engineering subtilisin and its substrates for efficient ligation of peptide bonds in aqueous solution. *Biochem.*, **30**; 4151-4159.

- Aguirre, C., Toledo, M., Medina, V. & Illanes, A., (2002). Effect of cosolvent and pH on the kinetically controlled synthesis of cephalexin with immobilized penicillin acylase. *Process Biochem.*, **38**; 351–360.

- Albert, A., Dhanaraj, V., Genschel, U., Khan, G., Ramjee, M. K., Pulido, R., Sibanda, B. L., von Delft, F., Witty, M., Blundell, T. L., Smith, A. G. & Abell, C., (1998). Crystal structure of aspartate decarboxylase at 2.2 A resolution provides evidence for an ester in protein self-processing. *Nat. Struct. Biol.*, **5**; 289-293.

- Alkema, W. B., Hensgens, C. M., Kroezinga, E. H., De Vries, E., Floris, R., Van der Laan, J. M., Dijkstra, B. W. & Janssen, D. B., (2000). Characterization of the β-lactam binding site of penicillin acylase of *Escherichia coli* by structural and site-directed mutagenesis studies. *Protein Eng.*, **13**; 857-863.

- Ambedkar, S. S., Deshpande, B. S., Sudhakaran, V. K. & Shewale, J. G., (1991). *Beijerinckia indica var. penicillanicum* penicillin V acylase: enhanced enzyme production by catabolite repression-resistant mutant and effect of solvents on enzyme activity. *J. Ind. Microbiol.*, **7**; 209-214.

- Appleby, T. C., Mathews, I. I., Porcelli, M., Cacciapuoti, G. & Ealick, S. E., (2001). Three-dimensional structure of a hyperthermophilic 5'-deoxy-5'-methylthioadenosine phosphorylase from Sulfolobus solfataricus. *J. Biol. Chem.*, **276**; 39232-39242.

- ***Aramori, I., Fukagawa, M., Tsumura, M., Iwami, M., Ono, H., Kojo, H., Kohsaka, M., Ueda, Y. & Imanaka, H., (1991a). Cloning and nucleotide sequencing of a novel 7b-(4-carboxybutanamido) cephalosporanic acid acylase gene of* Bacillus laterosporus *and its expression in* Escherichia coli *and* Bacillus subtilis. **J. Bacteriol.,** *173; 7848-7855.***

- Aramori, I., Fukagawa, M., Tsumura, M., Iwami, M., Isogai, T., Ono, H., Ishitani, Y., Kojo, H., Kohsaka, M., Ueda, Y. & Imanaka, H., (1991b). Cloning and nucleotide sequencing of new glutaryl 7-ACA and cephalosporin C acylase genes from *Pseudomonas strain*. *J. Ferment. Bioeng.*, **72**; 232-243.

- Aronson, N.N., Jr. (1996). Lysosomal glycosylasparaginase: a member of a family of amidases that employ a processed N-terminal threonine, serine or cysteine as a combined base-nucleophile cata- relyst. *Glycobiology*, **6**; 669–675.

- Baldaro, E., Faiardi, D., Fuganti, C., Grasselli, P. & Lazzarini, A., (1988). Phenylacetyloxymethylene, a carboxyl protecting group with immobilized penicillin acylase useful in benzyl penicillin chemistry. *Tetrahedron Letters*, **29**; 4623-4624.

- Ballio, A., Chain, E. B., Accadi, F. D. d., Mauri, M., Rauer, K., Schlesinger, J. & Schlesinger, S., (1961). Identification of a compound related to 6-aminopenicillanic acid, isolated from a culture media of *Penicillium chrysogenum. Nature (London)*, **191**; 909-910.

- Ban, N., Nissen, P., Hansen, J., Capel, M., Moore, P. B. & Steitz, T. A., (1999). Placement of protein and RNA structures into a 5 Å-resolution map of the 50S ribosomal subunit. *Nature*, **400**; 841-847.

- Barbas III, C. F., Matos, J. R., West, J. B. & Wong, C. H., (1988). A search for peptide ligase: cosolvent-mediated conversion of proteases to esterases for irreversible synthesis of peptides. *J. Am. Chem. Soc.*, **110**; 5162-5166.

- Batchelor, F. R., Doyle, F. P., Nayler, J. H. C. & Rolinson, G. N., (1959). Syntheses of penicillin : 6-aminopenicillanic acid in penicillin fermentations. *Nature (London)*, **183**; 257-258.

- Batchelor, F. R., Chain, E. B. & Rolinson, G. N., (1961). 6-Aminopenicillanic Acid 1. 6-Aminopenicillanic acid in penicillin fermentations. *Proc. Roy. Soc London Ser. B.*, **154**; 478-489.

- Baumli, S., Hoeppner, S. & Cramer, P., (2005). A Conserved Mediator Hinge Revealed in the Structure of the MED7/MED21 (Med7/Srb7) Heterodimer. *J. Biol. Chem.*, **280**; 18171-18178.

- Beauchamp, J. C. & Isaacs, N. W., (1999). Methods for X-ray diffraction analysis of macromolecular structures. *Curr. Opin. Chem. Biol.*, **3**; 525-529.

- Betz, J. L., Smyth, P. R. & Clarke, P. H., (1974). Evolution in Action. *Nature*, **247**; 261-264.

- Bissonnette, L., Charest, G., Longpre, J. M., Lavigne, P. & Leduc, R., (2004). Identification of furin pro-region determinants involved in folding and activation. *Biochem J.*, **379**; 757-763.

- Blundell, T. L., Elliott, G., Gardner, S. P., Hubbard, T., Islam, S. & et a. l., (1989). Protein engineering and design. *Philos. Trans.R. Soc. London Set. B*, **324**: 447.

- Bochtler, M., Ditzel, L., Groll, M., Hartmann, C. & Huber, R., (1999). The proteasome. *Annu. Rev. Biophys. Biomol. Struct.*, **28**; 295–317.

- Boistelle, R. & Astier, J. P., (1988). Crystallization mechanisms in solution. *J. Cryst. Growth*, **90**; 14-30.

- Bomstein, J. & Evans, W. G., (1965). Automated colorimetric determination of 6-aminopenicillanic acid in fermentation media. *Anal. Chem.*, **37**; 576-578.

- Braig, K., Otwinowski, Z., Hegde, R., Boisvert, D. C., Joachimiak, A., Horwich, A. L. & Sigler, P. B. (1994). The crystal structure of the bacterial chaperonin GroEL at 2.8 A. *Nature*, **371**; 578-586.

- Braiuca, P., Ebert, C., Fischer, L., Gardossi, L., Linda, P. A., (2003). A Homology model of penicillin acylase from *Alcaligenes faecalis* and in silico evaluation of its selectivity. *Chembiochem.*, **4**; 615-622.

- Brandl, E., (1972). Reactions of penicillins. 2. Behaviour toward penicillin amidase. *Sci. Pharma*., **40**; 1-12.

- Brannigan, J. A., Dodson, G., Duggleby, H. J., Moody, P. C., Smith, J. L., Tomchick, D. R. & Murzin, A. G., (1995). A protein catalytic framework with an N-terminal nucleophile is capable of self-activation. *Nature*, **378**; 416-419. Erratum in: *Nature*, (1995). **378**; 644.

- Britton, D., (1972). Estimation of twinning parameter for twins with exactly superimposed reciprocal lattices. *Acta Cryst*., **A28**; 296-297.

- Bruggink, A., Roos, E. C. & de Vroom, E., (1998). Penicillin acylase in the industrial production of β-lactam antibiotics. *Organic Process Research & Development*, **2;** 128-133.

- Brunger, A. T., (1992). Free R value: a novel statistical quantity for assessing the accuracy of crystal structures. *Nature*, **355**; 472-475.

- Brzozowski, A., M. & Walton, J., (2001). Clear strategy screens for macromolecular crystallization. *J. Appl. Cryst.*, **34**; 97-101.

- Bürgi, H. B., Dunitz, J. D. & Shefter, E., (1973). Geometrical reaction coordinates. II**.** Nucleophilic addition to a carbonyl group. *J. Am. Chem. Soc*., **95;** 5065–5067.

- Burlingame, R. & Chapman, P. J., (1983). Catabolism of Phenylpropionic Acid and its 3-Hydroxy Derivative by *Escherichia coli*. *J. Bacteriol.*, **155**; 113-121.

- Burmeister, W. P., (2000). Structural changes in a cryo-cooled protein crystal owing to radiation damage. *Acta Cryst*, **D56**; 328-341.

- Burton, H. S. & Abraham, E. P., (1951). Isolation of antibiotics from a species of *Cephalosporium*. Cephalosporins P1, P2, P3, P4 and P5. *Biochem. J.*, **50**; 168–174.

- Cai, G., Zhu, S., Yang, S., Zhao, G. & Jiang, w., (2004). Cloning, overexpression, and characterization of a novel thermostable penicillin G acylase from *Achromobacter xylosoxidans*: probing the molecular basis for its high thermostability. *Appl Environ Microbiol*., **70**; 2764–2770.

- Campbell, J. H., Lengyel, J. A. & Langridge, J., (1973). Evolution of a second gene for β-galactosidase in *Escherichia coli*. *Proc. Natl. Acad. Sci*., **70**; 1841-1845.

- Carlsen, F. & Emborg, C., (1982). *Bacillus sphaericus* penicillin acylase. I. Isolation and characterization. *J. Chem. Technol. Biotechnol*., **32**; 808-811.

- Carrington, T. R., (1971). The Development of Commercial Processes for the Production of 6-aminopenicillanic acid (6-APA). *Proc. Roy. Soc. London Ser. B.*, **179**; 321-333.

- Chandra, P. M., Brannigan, J. A., Prabhune, A., Pundle, A., Turkenburg, J. P., Dodson, G. G. & Suresh C. G., (2005). Cloning, preparation and preliminary crystallographic studies of penicillin V acylase autoproteolytic processing mutants. *Acta Cryst*., **F61**; 124-127.

- Chauhan, S., Nichkawade, A., Iyengar, M. R. & Chattoo, B. B., (1998a). Chainia penicillin V acylase: strain characteristics, enzyme immobilization, and kinetic studies. *Curr Microbiol.*, **37**; 186-190.

- Chauhan, S., Iyengar, M. R. S. & Chattoo, B. B., (1998b). Factors influencing the production of penicillin V acylase by *Chainia*, a sclerotial *Streptomyces*. *J. Basic Microbiol*., **38**; 173–179.

- Chayen, N. E., (1998). Comparative studies of protein crystallization by vapor diffusion and microbatch. *Acta Cryst*., **D54**; 8–15.

- Chen, J., Li, Y., Jiang, W., Yang, Y., Zhao, G. & Wang, E., (1998). Secretary expression of GL-7-ACA acylase. *Acta Biochim. Biophys. Sinica*., **30**; 393-396.

- Chen, X., Court, D. L. & Ji, X., (1999). Crystal structure of ERA: a GTPase-dependent cell cycle regulator containing an RNA binding motif. *Proc. Natl. Acad. Sci. U S A*, **96**; 8396-8401.

- Cingolani, G., Bednenko, J., Gillespie, M. T. & Gerace, L., (2002). Molecular basis for the recognition of a nonclassical nuclear localization signal by importin beta. *Mol. Cell.*, 10; 1345-1353.

- Chiu, T. K., Sohn, C., Dickerson, R. E. & Johnson, R. C., (2002). Testing water-mediated DNA recognition by the Hin recombinase. *EMBO J*., **21**; 801-14.

- Choi, K. S., Kim, J. A. & Kang, H. S., (1992). Effects of Site Directed Mutations on Processing and Activities of Penicillin G Acylase from *Escherichia coli* ATCC 11105. *J. Bacteriol.*, **174**; 6270-6276.

- Christiaens, H., Leer, R.J., Pouwels, P.H. & Verstraete, W., (1992). Cloning and expression of a conjugated bile acid hydrolase gene from *Lactobacillus plantarum* by using a direct plate assay. *Appl. Environ. Microbiol.*, **57**; 3792–3798.
- Claridge, C. A., Gourevitch, A. & Lein, J., (1960). Bacterial Penicillin Amidase. *Nature (London)*, 187; 237-238.

- Claridge, C. A., Luttinger, J. R. & Lein, J., (1963). Specificity of Penicillin Amidases. *Pro. Soc. Exp. Biol. Med.*, **113**; 1008-1012.

- Collaborative Computational Project, Number 4, (1994). The CCP4 suite: programs for protein crystallography. *Acta Cryst*., **D50**; 760-763.

- Cole, M., (1964). Properties of the Penicillin deacylase enzyme of *Escherichia coli*. *Nature (London)*, **203**; 519.

- Cole, M., (1966). Formation of 6-APA penicillin and penicillin acylase by various fungi. *Appl. Microbiol.*, **14**, 98-103.

- Cole, M. & Rolinson, G. N., (1961). 6-APA. III: Formation of 6.APA by *Emericellopsis minima* (stolk) and related fungi. *Proc. Roy. Sot.*, **B154**; 490-497.

- Cooper, A. A., Chen, Y., Lindorfer, M. A. & Stevens, T. H., (1993). Protein Splicing of the Yeast TFPI Intervening Protein Sequence: A Model for Self Excision. *EMBO J.*, **12**; 2525-2583.

- Cooper, J. B., Foundling, S. I., Blundell, T. L., Boger, J., Jupp, R. A. & Kay, J., (1989). X-ray studies of aspartic proteinase-statine inhibitor complexes. *Biochem.*, **28**; 8596-8603.

- Corey, D. R. & Craik, C. S., (1992). An investigation into the minimum requirements for peptide hydrolysis by mutation of the catalytic triad of trypsin. *J. Am. Chem. Soc.*, **114**; 1784-1790.

- Crawford, L., Stepan, A. M., McAda, P. C., Rambosek, J. A., Conder, M. J., Vinci, V. A. & Reeves, C. D., (1995). Production of cephalosporin intermediates by feeding adipic acid to

recombinant *Penicillium chrysogenum* strains expressing ring expansion activity. *Biotechnology N. Y.*, **13**; 58-62.

- Croall, D. E. & DeMartino, G. N., (1991). Calcium-activated neutral protease (calpain) system: structure, function, and regulation. *Physiol Rev.*, **71**; 813-847.

- Crowfoot, D., Bunn, C. W., Rogers-Low, B. W. & Jones, A. T., (1949). The Chemistry of Penicillin, Princeton University Press, p. 310.
- Daopin, S., Davies, D. R., Schlunegger, M. P. & Grütter, M. G., (1994). Comparison of two crystal structures of TGF-b 2: the accuracy of refined protein structures. *Acta Cryst.*, **D50**; 85-92.

- Dauter, Z., (1997). Data collection strategy. *Methods Enzymol.*, **276**; 326 - 344.

- Davis, E. O., Jenner, P. J., Brooks, P. C., Colston, M. J. & Sedgwick, S. G., (1992). Protein Splicing in the Maturation of *M. tuberculosis* RecA Protein: a Mechanism for Tolerating a Novel Class of Intervening Sequence. *Cell*, **71**; 201-210.

- Dennen, D. W., Allen, C. C. & Carver, D. D., (1971). Arylamidase of *Cephalosporium acremonium* and its specificity for cephalosporin C. *Appl. Microbiol.*, **21**; 907-915.

- Deshpande, B. S., Ambedkar, S. S, Sudhakaran, V. K. & Shewale, J. G., (1994). Molecular Biology of Beta Lactam Acylases. *World Journal of Microbiology and Biotechnology*, **10**; 128-138.

- Di Costanzo L, Forneris F, Geremia S, Randaccio L. (2003). Phasing protein structures using the group-subgroup relation. *Acta Cryst.*, **D59**; 1435-1439.

- Diederichs, K. & Karplus, P. A., (1997). Improved R-factors for diffraction data analysis in macromolecular crystallography. *Nat. Struct. Biol.*, **4**; 269-275.

- Diender, M. B., Straathof, A. J. J., van der Does, T., Zomerdijk, M. & Heijnen, J. J., (2000). Course of pH during the formation of amoxicillin by a suspension-to-suspension reaction. *Enzyme Microb. Technol.*, **27**; 576–582.

- Ding, X., Rasmussen, B. F., Petsko, G. A. & Ringe, D., (1994). Direct structural observation of an acyl-enzyme intermediate in the hydrolysis of an ester substrate by elastase. *Biochem.*, **33**; 9285-9293.

- Doctor, V.M. & Thadani, S.B., (1964). *Hind. Antibiot. Bull.*, **6**; 183.

- Dodson, G. G., (2000). Catalysis in penicillin G amidase – a member of the Ntn (N-Terminal Nucleophile) hydrolase family. *Croatica Chemica Acta*, **73**; 901-908.

- Drenth, J. & Haas, C., (1992). Protein crystals and their stability. *J. Cryst. Growth*, **122**; 107-109.

- Drenth, J. & Haas, C., (1998). Nucleation in protein crystallization. *Acta Cryst.*, **D54**; 867-872.

- Duggleby, H. J., Tolley, S. P., Hill, C. P., Dodson, E. J., Dodson, G. & Moody, P. C. E., (1995). Penicillin Acylase has a single amino-acid catalytic centre. *Nature*, **373**; 264-268.

- Engh, R. A. & Huber, R., (1991). Accurate bond and angle parameters for X-ray protein structure refinement. *Acta Cryst.*, **A47**; 392-400.

- Erickson, R. C. & Bennett, R. E., (1965). Penicillin acylase activity of *Penicillium chrysogenum*. *AppI. Microbiol*., **13**; 738-742.

- Feher, G. & Kam, Z., (1985). Nucleation and growth of protein crystals: general principles and assays. *Methods Enzymol*., **114**; 77-111.

- Fernandez-Lafuente, R., Rosell, C. M. & Guisan, J. M., (1991). Enzyme reaction engineering: synthesis of antibiotics catalysed by stabilised penicillin G acylase in the presence of organic cosolvents. *Enzyme Microb. Technol.*, **13**; 898–905.

- Fernandez-Lafuente, R., Rosell, C. M. & Guisan, J. M., (1995). The use of stabilised penicillin acylase derivatives improves the design of kinetically controlled synthesis. *J. Mol. Catal. A*, **101**; 91–97.

- Fernandez-Lafuente, R., Rosell, C. M. & Guisan, J. M., (1996a). Dynamic reaction design of enzymic biotransformations in organic media: equilibrium-controlled synthesis of antibiotics by penicillin G acylase. *Biotechnol. Appl. Biochem*., **24**; 139–143.

- Fernandez-Lafuente, R., Rosell, C. M., Piatkowska, B. & Guisan, J. M., (1996b). Synthesis of antibiotics (cephaloglycin) catalyzed by penicillin G acylase. Evaluation and optimization of different synthetic approaches. *Enzyme Microb. Technol*., **19**; 9–14.

- Fernandez-Lafuente, R., Rosell, C. M., Caanan-Haden, L., Rodes, L. & Guisan, J. M., (1999). Facile synthesis of artificial enzyme nanoenvironments via solid-phase chemistry of immobilized derivatives: dramatic stabilization of penicillin acylase versus organic solvents. *Enzyme Microb. Technol*., **24**; 96–103.

- Fersht, A. R., (1985). Enzyme structure and mechanism, W. H. Freeman, Reading.

- Flores, G., Soberon, X. & Osuna, J., (2004). Production of a fully functional, permuted single-chain penicillin G acylase. *Prot. Sci.*, **13**; 1677-83.

- Fomey, L. J. & Wong, D. C. L., (1989). Alteration of the catalytic efficiency of penicillin amidase from *Escherichia coli*. *Applied and Environmental Microbiology*, **55**; 2556-2560.

- Feinberg, H., Uitdehaag, J. C., Davies, J. M., Wallis, R., Drickamer, K. & Weis, W. I., (2003). Crystal structure of the CUB1-EGF-CUB2 region of mannose-binding protein associated serine protease-2. *EMBO J.*, **22**; 2348-2359.

- Fritz-Wolf, K., Koller, K. P., Lange, G., Liesum, A., Sauber, K., Schreuder, H., Aretz, W. & Kabsch, W., (2002). Structure-based prediction of modifications in glutarylamidase to allow single-step enzymatic production of 7-aminocephalosporanic acid from cephalosporin C. *Prot. Sci.*, **11**; 92-103.

- Gamblin, S. J. & Rodgers, D. W., (1993). Some Practical Details of Data Collection at 100 K. *Proceedings of the CCP4 Study Weekend. Data Collection and Processing*, edited by L. Sawyer, N. Isaacs & S. Bailey, 28-32.

- Garman, E. F. & Schneider, T. R., (1997). Macromolecular Cryocrystallography *J. Appl. Cryst*., **30**; 211-237.

- Golmohammadi, R., Fridborg, K., Bundule, M., Valegard, K. & Liljas, L., (1996). The crystal structure of bacteriophage Q beta at 3.5 A resolution. *Structure*, **4**; 543-54.

- Groll, M., Ditzel, L., Lowe, J., Stock, D., Bochtler, M., Bartunik, H. D. & Huber, R., (1997). Structure of 20S proteasome from yeast at 2.4 A resolution. *Nature*, **386**; 463-471.

- Guan, C., Cui, T., Rao, V., Liao, W., Benner, J., Lin, C. L. & Comb, D., (1996). Activation of glycosylasparaginase: formation of active N-terminal threonine by intramolecular autoproteolysis. *J. Biol. Chem.*, **271**; 1732–1737.

- Guan, C., Liu, Y., Shao, Y., Cui, T., Liao, W., Ewel, A., Whitaker, R. & Paulus, H., (1998). Characterization and functional analysis of the cis-autoproteolysis active center of glycosylasparaginase. *J. Biol. Chem.*, **273**; 9695–9702.

- Guncheva, M., Ivanov, I., Galunsky, B., Stambolieva, N. & Kaneti, J., (2004). Kinetic studies and molecular modelling attribute a crucial role in the specificity and stereoselectivity of penicillin acylase to the pair ArgA145-ArgB263. *Eur. J. Biochem.*, **271**; 2272-2279.

- Guogas, L. M., Filman, D. J., Hogle, J. M. & Gehrke, L., (2004). Cofolding organizes alfalfa mosaic virus RNA and coat protein for replication. *Science*, **306**; 2108-2111.

- Ha, Y., Stevens, D. J., Skehel, J. J. & Wiley, D. C., (2003). X-ray structure of the hemagglutinin of a potential H3 avian progenitor of the 1968 Hong Kong pandemic influenza virus. *Virology*, **309**; 209-218.

- Hall, A. & Knowles, J. R., (1976). Directed selective pressure on a β-lactamase to analyse molecular changes involved in development of enzyme function. *Nature*, **264**; 803-804.

- Hall, T. M., Porter, J. A., Young, K. E., Koonin, E. V., Beachy, P. A. & Leahy, D. J., (1997). Crystal structure of a Hedgehog autoprocessing domain: homology between Hedgehog and self-splicing proteins. *Cell*, **91**; 85-97.

- Hamilton-Miller, J. M. T., (1966). Penicillinacylase. *Bacteriological Reviews*, **30**; 761-771.

- Hausrath, A. C., Gruber, G., Matthews, B. W. & Capaldi, R. A., (1999). Structural Features of the Gamma Subunit of the *Escherichia Coli* F(1) ATPase Revealed by a 4.4-A Resolution Map Obtained by X-Ray Crystallography. *Proc.Nat.Acad.Sci.USA*, **96**; 13697-13702.

- Hausrath, A. C., Capaldi, R. A. & Matthews, B. W., (2001). The Conformation of the Epsilon-and Gamma-Subunits within the *Escherichia Coli* F1 ATPase. *J. Biol.Chem.*, **276**; 47227-47232.

- Herbst-Irmer, R. & Sheldrick, G. M., (1998). Refinement of twinned structures with SHELXL97. *Acta Cryst.*, **B54**; 443-449.

- Hernandez-Justiz, O., Terreni, M., Pagani, G., Garcia, J. L., Guisan, J. M. & Fernandez-Lafuente, R., (1999). Evaluation of different enzymes as catalysts for the production of β-lactam antibiotics following a kinetically controlled strategy. *Enzyme Microb. Technol.*, **25**; 336–343.

- Heuvel, R. H. H. V., Curti, B., Vanoni M.A. & Mattevi, A., (2004). Glutamate synthase: a fascinating pathway from L-glutamine to L-glutamate. *Cell. Mol. Life Sci.*, **61**; 669–681.

- Hewitt, L., Kasche, V., Lummer, K., Rieks, A. & Wilson, K. S., (1999). Crystallization of a precursor penicillin acylase from *Escherichia coli*. *Acta Cryst.*, **D55**; 1052-1054.

- Hewitt, L., Kasche, V., Lummer, K., Lewis, R. J., Murshudov, G. N., Verma, C. S., Dodson, G. G. & Wilson, K. S., (2000). Structure of a slow processing precursor penicillin acylase from *Escherichia coli* reveals the linker peptide blocking the active-site cleft. *J. Mol. Biol.*, **302**; 887-898.

- Hoople, D., (1998). Cleavage and formation of amide bonds. In: Kelly DR (ed) *Biotechnology*, vol **8a**. *Biotransformations* I. Wiley-VCH, Weinheim, 243–275.

- Huse, M., Muir, T. W., Xu, L., Chen, Y. G., Kuriyan, J. & Massague, J., (2001). The TGF beta receptor activation process: an inhibitor- to substrate-binding switch. *Mol. Cell.*, **8**; 671-682.

- Ignatova, Z., Mahsunah, A., Georgieva, M. & Kasche, V., (2003). Improvement of posttranslational bottlenecks in the production of penicillin amidase in recombinant *Escherichia coli* strains. *Appl. Environ. Microbiol.*, **69**; 1237-1245.

- Illanes, A. & Fajardo, A., (2001). Kinetically controlled synthesis of ampicillin with immobilized penicillin acylase in the presence of organic cosolvents. *J. Mol. Catal. B*, **11**; 587–595.

- Illanes, A., Anjari, S., Arrieta, R. & Aguirre, C., (2002). Optimization of yield in the kinetically controlled synthesis of ampicillin with immobilized penicillin acylase in organic media. *Appl. Biochem. Biotechnol.*, **97**; 165–179.

- Ishii, Y., Saito, Y., Fujimura, T., Isogai, T., Kojo, H., Yamashita, M., Niwa, M. & Kohsaka, M., (1994). A novel 7b-(4-carboxybutanamido)-cephalosporanic acid acylase isolated from *Pseudomonas strain C427* and its high-level production in *Escherichia coli*. *J. Ferment. Bioeng.*, **77**; 591-597.

- Ishiye, M. & Niwa, M., (1992). Nucleotide sequence and expression in *Escherichia coli* of the cephalosporin acylase gene of a *Pseudomonas strain*. *Biochim. Biophys. Acta*, **1132**; 233-239.

- Isupov, M. N., Obmolova, G., Butterworth, S., Badet-Denisot, M. A., Badet, B., Polikarpov, I., Littlechild, J. A. & Teplyakov, A., (1996). Substrate binding is required for assembly of the active conformation of the catalytic site in Ntn amidotransferases: evidence from the 1.8 Å crystal structure of the glutaminase domain of glucosamine 6-phosphate synthase. *Structure*, **4**; 801–810.

- Ito, N., Komiyama, N. H. & Fermi G., (1995). Structure of deoxyhaemoglobin of the antarctic fish *Pagothenia bernacchii* with an analysis of the structural basis of the root effect by comparison of the liganded and unliganded haemoglobin structures. *J. Mol. Biol.*, **250**; 648-58.
- Jenkins, J., Shevchik, V. E., Hugouvieux-Cotte-Pattat, N. & Pickersgill, R. W., (2004). The crystal structure of pectate lyase Pel9A from *Erwinia chrysanthemi*. *J. Biol. Chem.*, **279**; 9139–9145.

- Jeong, M. S., Jeong, J. K., Lim, W. K. & Jang, S. B., (2004). Structures of wild-type and P28L/Y173F tryptophan synthase alpha-subunits from *Escherichia coli*. *Biochem. Biophys. Res. Commun.*, **323**; 1257-64.

- Jose, L. M. H., Iliyna, A., Dominguez, M. L., Olga, S. C., Dustet, M. J. C., (2003). Partial characterisation of penicillin acylase from fungi *Aspergillus fumigatus* and *Mucor gryseocianum*. Moscow University Chemistry Bulletin. **44**; 53-56.

- Joyce, M. G., Girvan, H. M., Munro, A. W. & Leys, D., (2004). A single mutation in cytochrome P450 BM3 induces the conformational rearrangement seen upon substrate binding in the wild-type enzyme. *J. Biol. Chem.*, **279**; 23287-23293.

- Kaasgaard, S. & Veitland, U., (1992). Process for the preparation of β-lactams. *International Patent Application* WO 92/01061 Novo-Nordisk.

- Kabsch, W., (1976). A solution for the best rotation to relate two sets of vectors. *Acta. Cryst.*, **A32;** 922-923.

- Kahyaoglu, A., Haghjoo, K., Kraicsovits, F., Jordan, F. & Polgar, L., (1997). Benzyloxycarbonylprolylprolinal, a transition-state analogue for prolyl oligopeptidase, forms a tetrahedral adduct with catalytic serine, not a reactive cysteine. *Biochem. J.*, **322**; 839–843.

- Karkehabadi, S., Taylor, T. C. & Andersson, I., (2003). Calcium supports loop closure but not catalysis in Rubisco. *J. Mol. Biol.*, **334**; 65-73.

- Kasche, V., Lummer, K., Nurk, A., Piotraschke, E., Rieks, A., Stoeva, S. & Voelter, W., (1999). Intramolecular autoproteolysis initiates the maturation of penicillin amidase from *Escherichia coli*. *Biochim. Biophys. Acta*, **1433**; 76-86.

- Kasche, V., Galunsky, B. & Ignatova, Z., (2003). Fragments of propeptide activate mature penicillin amidase of *Alcaligenes faecalis*. *Eur. J. Biochem.*, **270**; 4721-4728.
- Kaufmann, W. & Bauer, K., (1964). Variety of Substrates for Bacterial Benzylpenicillin Splitting Enzyme. *Nature (London)*, **203**; 520.

- Keck, J. L. & Marqusee, S., (1996). The putative substrate recognition loop of *Escherichia coli* ribonuclease H is not essential for activity. *J. Biol. Chem.*, **271**; 19883–19887.

- Kim, D. J. & Byun, S. M., (1990). Purification and properties of ampicillin acylase from *Pseudomonas melanogenum*. Biochim Biophys Acta. **1040**; 12-18.

- Kim, D. W., Kang, S. M. & Yoon, K. H., (1999). Isolation of novel *Pseudomonas diminuta* KAC-1 strain producing glutaryl 7-aminocephalosporanic acid acylase. *Journal of Microbiology*, **37**; 200-205.

- Kim, H. M., Shin, D. R., Yoo, O. J., Lee, H. & Lee, J. O., (2003b). Crystal structure of Drosophila angiotensin I-converting enzyme bound to captopril and lisinopril. *FEBS Lett.*, **538**; 65-70.

- Kim, J. K., Yang, I. S., Rhee, S., Dauter, Z., Lee, Y. S., Park, S. S. & Kim, K. H., (2003a). Crystal structures of glutaryl 7-aminocephalosporanic acid acylase: insight into autoproteolytic activation. *Biochem.*, **42**; 4084-4093.

- Kim, M. G. & Lee, S. B., (1996). Penicillin acylase-catalyzed synthesis of pivampicillin: effect of reaction variables and organic cosolvents. *J. Mol. Catal. B*, **1**; 71–80.

- Kim, S. & Kim, Y., (2001). Active site residues of cephalosporin acylase are critical not only for enzymatic catalysis but also for post-translational modification. *J. Biol. Chem.*, **276**; 48376-48381.

- Kim, Y., Yoon, K., Khang, Y., Turley, S. & Hol, W. G., (2000). The 2.0 Å crystal structure of cephalosporin acylase. *Structure Fold. Des.*, **8**; 1059-1068.

- Kim, Y. & Hol, W. G., (2001). Structure of cephalosporin acylase in complex with glutaryl-7-aminocephalosporanic acid and glutarate: insight into the basis of its substrate specificity. *Chem. Biol.*, **8**; 1253-1264.

- Kim, Y., Kim, S., Earnest, T. N. & Hol, W. G., (2002). Precursor structure of cephalosporin acylase. Insights into autoproteolytic activation in a new N-terminal hydrolase family. *J. Biol. Chem.*, **277**; 2823-2829.

- Kovacikova, G., Lin, W. & Skorupski, K., (2003). The virulence activator AphA links quorum sensing to pathogenesis and physiology in *Vibrio cholerae* by repressing the expression of a penicillin amidase gene on the small chromosome. *J. Bacteriol.*, **185**; 4825-4836.

- Krahn, J. M., Beard, W. A., Miller, H., Grollman, A. P. & Wilson, S. H., (2003). Structure of DNA polymerase beta with the mutagenic DNA lesion 8-oxodeo-xyguanine reveals structural insights into its coding potential. *Structure (Camb)*, **1**; 121-127.

- Krasilnikov, A. S., Yang, X., Pan, T. & Mondragon, A., (2003). Crystal structure of the specificity domain of ribonuclease P. *Nature*, **421**; 760-764.

- Laemmli, U. K., (1970). Cleavage of structural proteins during the assembly of the Head Bacteriophage T4. *Nature*, **227**; 680-685.

- Laskowski, R. A., Macarthur, M. W., Moss, D. S. & Thomton, J. M., (1993). PROCHECK - A program to check the stereochemical quality of protein structures. *Journal of Applied Crystallography*, **26**; 283-291.

- Law, S. K. A. & Dodds, A. W., (1997). The internal thioester and covalent binding properties of the complement proteins C3 and C4. *Prot. Sci.*, **6**; 263-274.

- Lee, J. J., Ekker, S. C., von Kessler, D. P., Porter, J. A., Sun, B. I. & Beachy, P. A., (1994). Autoproteolysis in *hedgehog* protein biogenesis. *Science*, **266**; 1528–1537.

- Lee, Y. S. & Park, S. S., (1998). Two-step autocatalytic processing of the glutaryl 7-amino-cephalosporanic acid acylase from *Pseudomonas sp. strain GK16*. *J. Bacteriol.*, **180**; 4576-4582.

- Lee, Y. S., Kim, H. W., Lee, K. B. & Park, S. S., (2000a). Involvement of arginine and tryptophan residues in catalytic activity of glutaryl 7-aminocephalosporanic acid acylase from *Pseudomonas sp*. strain GK16. *Biochim. Biophys. Acta.*, **1523**; 123-127.

- Lee, Y. S., Kim, H. W. & Park, S. S., (2000b). The role of alpha-amino group of the N-terminal serine of beta subunit for enzyme catalysis and autoproteolytic activation of glutaryl 7-aminocephalosporanic acid acylase. *J. Biol. Chem.*, **275**; 39200-39206.

- Lejon, S., Frick, I. M., Bjorck, L., Wikstrom, M. & Svensson, S., (2004). Crystal structure and biological implications of a bacterial albumin binding module in complex with human serum albumin. *J. Biol. Chem.*, **279**; 42924-42928.

- Levine, R. L., Mosoni, L., Berlett, B. S. & Stadtman, E. R., (1996). Methionine residues as endogenous antioxidants in proteins. *Proc. Natl. Acad. Sci. USA*, **93**; 15036–15040.

- Li, Y., Chen, J., Jiang, W., Mao, X., Zhao, G. & Wang, E., (1999). *In vivo* post-translational processing and subunit reconstitution of cephalosporin acylase from *Pseudomonas* sp. 130. *Eur. J. Biochem.*, **262**; 713-719.

- Li, Y. & Inouye, M., (1994). Autoprocessing of prothiolsubtilisin E in which active-site serine 221 is altered to cysteine. *J. Biol. Chem.*, **269**; 4169-4174.

- Li, Y., Jiang, W., Yang, Y., Zhao, G. & Wang, E. (1998). Overproduction and purification of glutaryl 7-amino cephalosporanic acid acylase. *Protein Express. Purif.*, **12**; 233-238.

- Livermore, D. M., (2000). Antibiotic resistance in *staphylococci*. *Int. J. Antimicrob. Agents*, **16**; 3-10.

- Ljubijankic, G., Gvozdenovic, J., Sevo, M. & Degrassi, G., (2002). High-level secretory expression of penicillin amidase from *Providencia rettgeri* in *Saccharomyces cerevisiae*: purification and characterization. *Biotechnol. Prog*., **18**; 330-336.

- Lowe, D. A., Romanchik, G. & Elander, R. P., (1981). Penicillin acylases – a review of existing enzymes and the isolation of a new bacterial penicillin V acylase. *Developments in Industrial Microbiology*, **22**; 163-180.

- Lowe, D. A., Romancik, G. & Elander. R. P., (1986). *Biotechnol. Lett*., **8**; 151.

- Lowe, J., Stock, D., Jap, B., Zwickl, P., Baumeister, W. & Huber, R., (1995). Crystal structure of the 20S proteasome from the Archaeon *T. acidophilum* at 3.4Å resolution. *Science*, **268**; 533-539.

- Marc, F., Weigel, P., Legrain, C., Almeras, Y., Santrot, M., Glansdorff, N. & Sakanyan, V., (2000). Characterization and kinetic mechanism of mono- and bifunctional ornithine acetyltransferases from thermophilic microorganisms. *Eur. J. Biochem*., **267**; 5217–5226.

- Marc, F., Weigel, P., Legrain, C., Glansdorff, N. & Sakanyan, V., (2001). An invariant threonine is involved in self-catalyzed cleavage of the precursor protein for ornithine acetyltransferase. *J. Biol. Chem*., **276**; 25404–25410.

- Marie-Claire, C., Ruffet, E., Beaumont, A. & Roques, B. P., (1999). The prosequence of thermolysin acts as an intramolecular chaperone when expressed in trans with the mature sequence in *Escherichia coli*. *J. Mol. Biol*., **285**; 1911-1915.

- Martin, J., Mancheno, J. M. & Arche, R., (1993a). Inactivation of penicillin acylase from *Kluyvera citrophila* by N-ethoxycarbonyl-2-ethoxy-1,2-dihydroquinoline: a case of time-dependent non-covalent enzyme inhibition. *Biochem. J*., **291**; 907-914.

- Massenet, C., Chenavas, S., Cohen-Addad, C., Dagher, M. C., Brandolin, G., Pebay-Peyroula, E. & Fieschi, F., (2005). Effects of p47phox C terminus phosphorylations on binding interactions with p40phox and p67phox. Structural and functional comparison of p40phox and p67phox SH3 domains. *J. Biol. Chem*., **280**; 13752-13761.

- Matsuda, A. & Komatsu, K., (1985). Molecular cloning and structure of the gene for 7b-(4-carboxybutanamido) cephalosporanic acid acylase from a *Pseudomonas strain*. *J. Bacteriol*., **163**; 1222-1228.

- Matsuda, A., Matsuyama, K., Yamamoto, K., Ichikawa, S. & Komatsu, K. I., (1987). Cloning and characterization of the genes for two distinct cephalosporin acylases from a *Pseudomonas strain*. *J. Bacteriol*., **169**; 5815-5820.

- Matthews, B. W., (1968). The Solvent Content of Protein Crystals. *J. Mol. Biol*., **33**; 491-497.

- McCullough, J. E., (1983). Gene cloning in bacilli related to enhanced penicillin acylase production. *Nature Biotechnology*, **1**; 879 – 882.

- McDonough, M. A., Klei, H. E. & Kelly, J. A., (1999). Crystal structure of penicillin G acylase from the Bro1 mutant strain of *Providencia rettgeri*. *Prot. Sci*., **8**; 1971-1981.

- McPherson, A., (1991). A brief history of protein crystal growth. *J. Cryst. Growth*., **110**; 1-10.

- Merino, E., Balbas, P., Recillas, F., Becerril, B., Valle, F. & Bolivar, F., (1992). Carbon regulation and the role in nature of the *Escherichia coli* penicillin acylase (pac) gene. *Mol. Microbiol*., **6**; 2175–2182.

- Miller, G. J. & Hurley, J. H., (2004). Crystal structure of the catalytic core of inositol 1,4,5-trisphosphate 3-kinase. *Mol Cell*., **15**; 703-711.

- Molinari, M., Okorokov, A. & Milner, J., (1996). Interaction with damaged DNA induces selective proteolytic cleavage of p53 to yield 40 kDa and 35 kDa fragments competent for sequence-specific DNA binding. *Oncogene*, **13**; 2077–2086.

- Moazed, D., Noller, H. F., (1987). Interaction of antibiotics with functional sites in 16S ribosomal RNA. *Nature*, **327**; 389-394.

- Morais, M. C., Kanamaru, S., Badasso, M. O., Koti, J. S., Owen, B. A. L., McMurray, C. T., Anderson, D. L. & Rossmann. M. G., (2003). Bacteriophage phi29 scaffolding protein gp7 before and after prohead assembly. *Nat. Struct.Biol*., **10**; 572-576

- Morgunova, E., Tuuttila, A., Bergmann, U. & Tryggvason, K., (2002). Structural insight into the complex formation of latent matrix metalloproteinase 2 with tissue inhibitor of metalloproteinase 2. *Proc Natl Acad Sci U S A*. **99**; 7414-7419.

- Mortlock, R. P., (1982). .Metabolic acquisitions through laboratory selection. *Annu. Rev. Microbiol*., **36**; 259-284.

- Muraki, M., Ishimura, M. & Harata, K., (2002). Interactions of wheat-germ agglutinin with GlcNAcbeta1,6Gal sequence. *Biochim. Biophys. Acta*, **1569**; 10-20.

- Murao, S., (1955). Penicillin-amidase. III. Mechanism of penicillin-amidase on sodium penicillin G. *J. Agr. Chem. Soc. Japan*, **29**; 404-407.

- Murshudov, G. N., Dodson, E. J. & Vagin, A. A., (1996). Application of maximum likelihood methods for macromolecular refinement. *Proceedings of the CCP4 Study Weekend (Macromolecular Refinement)*, 93-104.

- Murshudov, G. N., (1997). Refinement of macromolecular structures by the maximum likelihood method. *Acta Cryst.*, **D53**; 240-255.

- Murzin, A. G., (1996). Structural classification of proteins: New superfamilies. *Curr. Opin. Struct. Biol*., **6**; 386-394.

- Myung, J., Kim, K. B. & Crews, C. M., (2001). The ubiquitin-proteasome pathway and proteasome inhibitors. *Medicinal Research Reviews*, **21**; 245-273.
- Nakatsuka, T., Sasaki, T. & Kaiser, E. T., (1987). Peptide segment coupling catalyzed by the semisynthetic enzyme thiosubtilisin. *J. Am. Chem. Soc*., **109**; 3808-3810.

- Nakayama, K., (1997). Furin: a mammalian subtilisin/Kex2p-like endoprotease involved in processing of a wide variety of precursor proteins. *Biochem. J*., **327**; 625-635.

- Nara, T., Misawa, M., Okachi, R. & Yamamoto, M., (1971a). *Agric. Biol. Chem*., **35**; 1676.

- Nara, T., Okachi, R. & Misawa, M., (1971b). *J. Antibiot*., **24**; 321.

- Navaza, J. (1994). AMoRe - An automated package for molecular replacement. *Acta Cryst.* **A50**; 157-163.

- Navaza, J. & Saludjian, P., (1997). AMoRe: an automated molecular replacement program package. *Methods Enzymol*., **276**; 581–594.

- Nayler, J. H. C. (1991a). Early discoveries in the penicillin series. *Trends in Biochemical Sciences*, **16**; 195-234.

- Nayler, J. H. C. (1991b). Semi-synthetic approaches to novel penicillins. *Trends in Biochemicals Sciences*, **16**; 234-237.

- Ng, K. K., Kolatkar, A. R., Park-Snyder, S., Feinberg, H., Clark, D. A., Drickamer, K. & Weis, W. I., (2002). Orientation of bound ligands in mannose-binding proteins. Implications for multivalent ligand recognition. *J. Biol. Chem*., **277**; 16088-16095.

- Nishino, T., Komori, K., Tsuchiya, D., Ishino, Y. & Morikawa, K., (2005). Crystal structure and functional implications of *Pyrococcus furiosus* hef helicase domain involved in branched DNA processing. *Structure (Camb)*, **13**; 143-153.

- Niwa, H., Tsuchiya, D., Makyio, H., Yoshida, M. & Morikawa, K., (2002). Hexameric ring structure of the ATPase domain of the membrane-integrated metalloprotease FtsH from *Thermus thermophilus* HB8. *Structure (Camb)*, **10**; 1415-1423.

- Oh, B., Kim, M., Yoon, J., Chung, K., Shin, Y., Lee, D. & Kim Y., (2003). Deacylation activity of cephalosporin acylase to cephalosporin C is improved by changing the side chain conformations of active-site residues. *Biochem Biophys Res Commun.*, **310**; 19-27.

- Oh, B., Kim, K., Park, J., Yoon, J., Han, D., Kim, Y., (2004). Modifying the substrate specificity of penicillin G acylase to cephalosporin acylase by mutating active-site residues. *Biochem. Biophys. Res. Commun*., **319**; 486-492.

- Oinonen, C., Tikkanen, R,, Rouvinen, J. & Peltonen, L., (1995). Three Dimensional Structure of Human Lysosomal Aspartyiglucosaminidase. *Nat. Struct. Biol.*, **2**; 1102-1108.

- Oinonen, C. & Rouvinen, J., (2000). Structural comparison of Ntn-hydrolases. *Prot. Sci*., **9**; 2329-2337.

- Okorokov, A. L. & Milner, J., (1997). Induced N- and C-terminal cleavage of p53: a core fragment of p53, generated by interaction with damaged DNA, promotes cleavage of the N-terminus of full length p53, whereas ssDNA induces C-terminal cleavage of p53. *EMBO J*., **16**; 6008-6017.

- Olsson, A., Hagstrom, T., Nilsson, B., Uhlen, M. & Gatenbeck, S., (1985). Molecular cloning of *Bacillus sphaericus* penicilim V amidase gene and its expression in *Escherichia coli* and *Bacillus subtilis. Applied and Environmental Microbiology.* **49**; 1084-1089.

- Olsson, A. & Uhlen, M. (1986). Sequencing and heterologous expression of the gene encoding penicillin V amidase from *Bacillus sphaericus. Gene.* 45; 175-181.

- Ospina S, Barzana E, Ramrez O. T. & Lopez-Munguia, A., (1996). Effect of pH in the synthesis of ampicillin by penicillin acylase. *Enzyme Microb. Technol.*, **19**; 462–469.
- Otten, L. G., Sio, C. F., Vrielink, J., Cool, R. H. & Quax, W. J., (2002). Altering the substrate specificity of cephalosporin acylase by directed evolution of the β-subunit. *J. Biol. Chem.*, **277**; 42121-42127.

- Otwinowski, Z. & Minor, W., (1997). Processing of X-ray diffraction data collected in oscillation mode. *Methods Enzymol.*, **276**; 307-326.

- Padmaja, N., Ramakumar S. & Viswamitra, M. A., (1990). Space-group frequencies of proteins and of organic compounds with more than one formula unit in the asymmetric unit. Acta Cryst., **A46**; 725.

- Park, C. B., Lee, S. B. & Ryu, D. D. Y., (2000). Penicillin acylase-catalyzed synthesis of cefazolin in water-solvent mixtures: enhancement effect of ethyl acetate and carbon tetrachloride on the synthetic yield. *J. Mol. Catal.* B, **9**; 275–281.

- Paulus, H., (1998). The chemical basis of protein splicing. *Chem. Soc. Rev.*, **27**; 375–386.

- Pei, J. & Grishin, N. V., (2003). Peptidase family U34 belongs to the superfamily of N-terminal nucleophile hydrolases. *Prot. Sci.,* **12**; 1131–1135.

- Perler, F. B, Davis, E. O., Dean, G. E., Gimble, F. S., Jack, W. E., Noren, C. J., Neff, N., Thomer, J. & Belfort, M., (1994). Protein splicing elements: inteins and exteins - a definition of terms and recommended nomenclature. *Nucl. Acids Res.*, **22**; 1125-1127.

- Perler, F. B., (1998a). Protein splicing of inteins and Hedgehog autoproteolysis: structure, function, and evolution. *Cell*, **92**; 1–4.

- Perler, F.B., (1998b). Breaking up is easy with esters. *Nat. Struct. Biol.*, **5**; 249–252.

- Porter, J. A., von Kessler, D. P., Ekker, S. C., Young, K. E., Lee, J. J., Moses, K. & Beachy, P. A., (1995). The product of Hedgehog autoproteolytic cleavage active in local and long-range signaling. *Nature*, **374**; 363-366.

- Pratt, C. S., Coyle, B. A. & Ibers J. A., (1971). Redetermination of the Structure of Nitrosylpenta-amminecobalt(III) Dichloride. *J. Chem. Soc.*, 2146 - 2151.

- Prieto, M. A., Perez-Aranda, A. & Garcia, J. L., (1993). Characterization of an *Escherichia coli* aromatic hydroxylase with a broad substrate range. *J. Bacteriol.*, **175**; 2162-2167.

- Prieto, M. A., Diaz, E. & Garcia, J. L., (1996). Molecular characterization of the 4-hydroxyphenylacetate catabolic pathway of *Escherichia coli* W: engineering a mobile aromatic degradative cluster. *J. Bacteriol.*, **178**; 111–120.

- Pundle, A. & SivaRaman, H., (1997). *Bacillus sphaericus* penicillin V acylase: purification, substrate specificity, and active-site characterization. *Curr. Microbiol.*, **34**; 144-148.

- Qian, X., Guan, C. & Guo, H. C., (2003). A dual role for an aspartic acid in glycosylasparaginase autoproteolysis. *Structure (Camb)*, **11**; 997-1003.

- Qiu, X., Janson, C. A., Smith, W. W., Green, S. M., McDevitt, P., Johanson, K., Carter, P., Hibbs, M., Lewis, C., Chalker, A., Fosberry, A., Lalonde, J., Berge, J., Brown, P., Houge-Frydrych, C. S. & Jarvest, R. L., (2001). Crystal structure of *Staphylococcus aureus* tyrosyl-tRNA synthetase in complex with a class of potent and specific inhibitors. *Protein Sci.*, **10**; 2008-2016.

- Ravelli, R. B., Schroder Leiros, H. K., Pan, B., Caffrey, M. & McSweeney, S., (2003). Specific radiation damage can be used to solve macromolecular crystal structures. *Structure (Camb)*, **11**; 217-24.

- Rawlings, N. D., Tolle, D. P. & Barrett, A. J., (2004). MEROPS: the peptidase database. *Nucleic Acids Res.*, **32**; Database issue, D160-D164.

- Read, T. D., Salzberg, S. L., Pop, M., Shumway, M., Umayam, L., Jiang, L., Holtzapple, E., Busch, J. D., Smith, K. L., Schupp, J. M., Solomon, D., Keim, P. & Fraser, C. M., (2002). Comparative genome sequencing for discovery of novel polymorphisms in *Bacillus anthracis*. *Science*, **296**; 2028-2033.

- Recsei, P. A., Huynh, Q. K. & Snell , E. E., (1983). Conversion of Prohistidine Decarboxylase to Histidine Decarboxylase: Peptide Chain Cleavage by Nonhydrolytic Serinolysis. *Proc. Natl. Acad. Sci. USA*, **80**; 973-977.

- Redinbo, M. R., Stewart, L., Kuhn, P., Champoux, J. J. & Hol, W. G., (1998). Crystal structures of human topoisomerase I in covalent and noncovalent complexes with DNA. *Science*, **279**; 1504-1513.

- Rodgers, D. W., (1994). Cryocrystallography. *Structure* **2;** 1135-1140.

- Rolinson, G. N., Batchelor, F. R., Butterworth, D., Cameron-wood, J., Cole, M., Eustace, G. C., Hart, V., Richards, M. & Chain, E. B. (1960). Fermentation of 6-Aminopenicillanic Acid from Penicillin by Enzymatic Hydrolysis. *Nature (London)*, **187**; 236-237.

- Rose, R. B., Endrizzi, J. A., Cronk, J. D., Holton, J. & Alber, T., (2000). High-resolution structure of the HNF-1 alpha dimerization domain. *Biochem.*, **39**; 15062-15070. Erratum in: *Biochem.*, (2001). **40**; 3242.

- Rosell, C. M., Terreni, M., Fernandez-Lafuente, R. & Guisan, J. M., (1998). A criterion for the selection of monophasic solvents for enzymatic synthesis. *Enzyme Microb. Technol.*, **23**; 64–69.

- Rosenblum, J. S. & Blobel, G., (1999). Autoproteolysis in nucleoporin biogenesis. *Proc. Natl. Acad. Sci. U S A*, **96**; 11370-11375.

- Rossmann, M. G. & Blow, D. M., (1962). The detection of sub-units within the crystallographic asymmetric unit. *Acta Cryst.*, **A15**; 24-31.

- Sakaguchi, K. & Murao, S., (1950). A preliminary report on a new enzyme, penicillin-amidase. *J. Agric. Chem. Soc. Jpn*., **23**; 411.

- Savidge, T. A. & Cole, M., (1975). Penicillin Acylase (Bacterial). *Methods Enzymol.*, **43**; 705-721.

- Scavetta, R. D., Herron, S. R., Hotchkiss, A. T., Kita, N., Keen, N. T., Benen, J. A. E., Kester, H. C. M., Visser, J. & Jurnak, F. (1999). Structure of a plant cell wall fragment complexed to pectate lyase C. *Plant Cell*, **11**; 1081–1092.

- Schmidtke, G., Kraft, R., Kostka, S., Henklein, P., Frommel, C., Lowe, J., Huber, R., Kloetzel, P. M. & Schmidt, M., (1996). Analysis of mammalian 20S proteasome biogenesis: the maturation of beta-subunits is an ordered two-step mechanism involving autocatalysis. *EMBO J.*, **15**; 6887–6898.

- Schmitke, J. L., Stern, L. J. & Klibanov, A. M., (1998). Comparison of x-ray crystal structures of an acyl-enzyme intermediate of subtilisin Carlsberg formed in anhydrous acetonitrile and in water. *Proc. Natl. Acad. Sci. U S A*, **95**; 12918-12923.

- Schneider, W. J. & Roehr, M., (1976). Purification and properties of penicillin acylase of *Bovista plumbea*. *Biochim. Biophys. Acta*, **452**; 117-185.

- Schroen, C. G. P. H., Nierstrasz, V., Kroon, P. J., Bosma, R., Janssen, A. E. M., Beeftink, H. H. & Tramper, J., (1999). Thermodynamically controlled synthesis of β-lactam antibiotics. Equilibrium concentrations and side chain properties. *Enzyme Microb. Technol.*, **24**; 498–506.

- Schroen, C. G. P. H., Mohy Eldin, M., Janssen, A., Mita, G. & Tramper, J., (2001). Cephalexin synthesis by immobilized penicillin G acylase under non-isothermal conditions: reduction of diffusion limitation. *J. Mol. Catal. B*, **15**; 163–172.

- Schumacher, G., Sizmann, D., Huang, H., Buckel, P. & Bock, A. (1986). Penicillin Acylase from *E. coli:* Unique Gene-Protein Relation. *Nucleic Acids Research*, **14**; 5713-5727.

- Sevo, M., Degrassi, G., Skoko, N., Venturi, V. & Ljubijankic, G., (2002). Production of glycosylated thermostable *Providencia rettgeri* penicillin G amidase in *Pichia pastoris*. *FEMS Yeast Res*., **1**; 271-277.

- Shao, Y., Xu, M. Q. & Paulus, H., (1996). Protein splicing: evidence for an N-O acyl rearrangement as the initial step in the splicing process. *Biochem.*, **35**; 3810–3815.

- Shaw, S. Y., Shyu, J. C., Hsieh, Y. W. & Yeh, H. J., (2000). Enzymatic synthesis of cephalotin by penicillin G acylase. *Enzyme Microb, Technol.*, **26**; 142–151.

- Sheldrick, G. M., (1995). SHELXL-93, a Program for the Refinement of Crystal Structures from Diffraction Data. Institut fuer Anorg.Chemie, Goettingenm Germany.

- Sheldrick, G. M. & Schneider, T. R., (1997). SHELXL: High-resolution refinement. *Methods Enzymol*., **277**; 319-343.

- Shewale, J. G., Kumar, K. K., Ambedkar, G. R., (1987). Evaluation of determination of 6-amino penicillanic acid by p-dimethyl-amino benzaldehyde. *Biotechnol, Techniques*, **1**; 69-72.

- Shewale, J. G., Deshpande, B. S., Sudhakaran, V. K. & Ambedkar, S. S., (1990). Penicillin Acylases - Applications and Potentials. *Process Biochem. Int.*, **25**; 97-103.

- Shewale, J. & Sudhakaran, V., (1997). Penicillin V acylase: its potential in the production of 6–aminopenicillanic acid. *Enzyme Microb. Technol*., **20**; 402–410.

- Shibuya, Y., Matsumoto, K. & Fujii, T., (1981). Isolation and properties of 7-β-(4-carboxybutanamido) cephalosporanic acid acylase-producing bacteria. *Agricultural & Biological Chemistry*, **45**; 1561-1567.

- Shin, D. S., Pellegrini, L., Daniels, D. S., Yelent, B., Craig, L., Bates, D., Yu, D. S., Shivji, M. K., Hitomi, C., Arvai, A. S., Volkmann, N., Tsuruta, H., Blundell, T. L., Venkitaraman, A. R. & Tainer, J. A., (2003). Full-length archaeal Rad51 structure and mutants: mechanisms for RAD51 assembly and control by BRCA2. *EMBO J*., **22**; 4566-4576.

- Shomura Y, Yoshida T, Iizuka R, Maruyama T, Yohda M, Miki K. (2004). Crystal structures of the group II chaperonin from *Thermococcus* strain KS-1: steric hindrance by the substituted amino acid, and inter-subunit rearrangement between two crystal forms. *J. Mol. Biol*., **335**; 1265-1278.

- Singh, K., Sehgal, S. N. & Vezina, C., (1969). Hydrolysis of phenoxymethyl penicillin into 6-aminopenicillanic acid with spores of *fusaria*. *Appl. Microbiol*., **17**; 643-644.

- Sio, C. F., Otten, L. G., Cool, R. H. & Quax, W. J., (2003). Analysis of a substrate specificity switch residue of cephalosporin acylase. *Biochem. Biophys. Res. Commun*., **312**; 755-760.

- Slade, A., Horrocks, J., Lindsay, C., Dunbar, B. & Virden, R., (1991). Site directed chemical conversion of serine to cysteine in penicillin acylase from *Escherichia coli* ATTCI 105. *Eur. J. Biochem.*, **197**; 75-80.

- Smith, J. L., Zaiuzec, E. J., Wery, J. P., Niu, L., Switzer, R. L., Zaikin, H. & Satow, Y., (1994). Structure of the Allosteric Regulatory Enzyme of Purine Biosynthesis. *Science*, **264**; 1427-1433.

- Stadtman, E. R., (1993). Oxidation of Free Amino Acids and Amino Acid Residues in Proteins by Radiolysis and by Metal-Catalyzed Reactions. *Annu. Rev. Biochem.*, **62;** 797–821.

- Stamos, J., Eigenbrot, C., Nakamura, G. R., Reynolds, M. E., Yin, J., Lowman, H. B., Fairbrother, W. J. & Starovasnik, M. A., (2004). Convergent recognition of the IgE binding site on the high-affinity IgE receptor. *Structure (Camb)*, **12**; 1289-1301.

- Stockbauer, K. E., Magoun, L., Liu, M., Burns, E. H. Jr, Gubba, S., Renish, S., Pan, X., Bodary, S. C., Baker, E., Coburn, J., Leong, J. M. & Musser, J. M., (1999). A natural variant of the cysteine protease virulence factor of group A Streptococcus with an arginine-glycine-aspartic acid (RGD) motif preferentially binds human integrins alphavbeta3 and alphaIIbbeta3. *Proc. Natl. Acad. Sci. U S A*, **96**; 242-247.

- Stoppok, E., Schomer, U., Segner, A., Mayer, H. & Wagner, F., (1980). Production of 6-aminopenicillanic acid from penicillin V and G by *Bovista plumbea* NRRL 3824 and *Escherichia coli* 5K (pHM 12). *Adv. Biotechnol*., **3**; 547 –552.

- Story, R. M., Li, H. & Abelson, J. N., (2001). Crystal structure of a DEAD box protein from the hyperthermophile *Methanococcus jannaschii*. *Proc Natl Acad Sci U S A*, **98**; 1465-1470. Erratum in: *Proc Natl Acad Sci U S A*, (2001). **98**; 3624.

- Strynadka, N. C., Adachi, H., Jensen, S. E., Johns, K., Sielecki, A., Betzel, C., Sutoh, K. & James, M. N., (1992). Molecular structure of the acyl-enzyme intermediate in beta-lactam hydrolysis at 1.7 Å resolution. *Nature*, **359**; 700-705.

- Stura, E. A. & Wilson, I. A., (1990). Analytical and production seeding techniques. *Methods*, **1**; 38-49.

- Stura, E. A. & Wilson, I. A., (1991). Applications of the streak seeding technique in protein crystallization. *J. Cryst. Growth*, **110**; 270-282.

- Sudhakaran, V. K. & Borkar, P. S., (1985). Phenoxymethyl penicillin acylase: sources and study-a sum up. *Hindustan Antibiot Bull.*, **27**; 44-62.

- Sudhakaran, V. K. & Shewale, J. G., (1993a). *World J. Microbial. Biotechnol*., **9**; 233.

- Sudhakaran, V. K. & Shewale, J. G., (1993b). Enzymatic splitting of penicillin V for the production of 6-APA using immobilized penicillin V acylase. *World J. Microbiol. Biotechnol*., **9**; 630-634.

- Sudhakaran, V. K. & Shewale, J. G., (1995). Purification and characterization of extracellular penicillin V acylase from *Fusarium sp*. SKF 235. *Hindustan Antibiot Bull.* **37**; 9-15.

- Suresh, C. G., Pundle, A. V., SivaRaman, H., Rao, K. N., Brannigan, J. A., McVey, C. E., Verma, C. S., Dauter,. Z., Dodson, E. J. & Dodson, G. G., (1999). Penicillin V acylase crystal structure reveals new Ntn-hydrolase family members. *Nat. Struct. Biol*., 6; 414-416.

- Teng, T. Y., (1990). Mounting crystals for macromolecular crystallography in a free-standing thin film. *J. Appl. Cryst.*, **23**; 387-391.

- Thadhani, S. B., Borkar, P. S. & Ramachandran, S., (1972). Structural requirements of inducer for the formation of penicillin acylase in *Fusarium sp. 7.5-5. Biochem. J.*, **128**; 49-50.

- Thoden, J. B., Miran, S. G., Phillips, J. C., Howard, A. J., Raushel, F. .M. & Holden, H. M., (1998). Carbamoyl phosphate synthetase: caught in the act of glutamine hydrolysis. *Biochem.*, **37;** 8825-8831.

- Thony-Meyer, L., Bock, A. & Hennecke, H., (1992). Prokaryotic polyprotein precursors. *FEBS Lett.*, **307**; 62–65.

- Tikkanen, R., Riikonen, A., Oinonen, C., Rouvinen, J. & Peltonen, L., (1996). Functional Analyses of Active Site Residues of Human Lysosomal Aspartyiglucosaminidase: Implications for Catalytic Mechanism and Autocatalytic Activation. *EMBO J.*, **15**; 2954-2960.

- Torres-Bacete, J., Arroyo, M., Torres-Guzmán, R., de la Mata, I., Castillón, M. P. & Acebal, C., (2000a). Covalent immobilization of penicillin acylase from *Streptomyces lavendulae*. *Biotechnol Lett.*, **22**; 1011-1014.

- Torres-Bacete, J., Arroyo, M., Torres-Guzmán, R., Mata, I. D. L., Castillón, M. P. & Acebal, C., (2000b). Optimization of 6-aminopenicillanic acid (6-APA) production by using a new immobilized penicillin acylase. *Biotechnol. Appl. Biochem.* **32**; 173–177.

- Vaguine, A. A., Richelle, J. & Wodak, S. J., (1999). SFCHECK: a unified set of procedure for evaluating the quality of macromolecular structure-factor data and their agreement with atomic model. *Acta Cryst.*, **D55**; 191-205.

- Vajdos, F. F., Yoo, S., Houseweart, M., Sundquist, W. I. & Hill, C. P., (1997). Crystal structure of cyclophilin A complexed with a binding site peptide from the HIV-1 capsid protein. *Prot. Sci.*, **6**; 2297-2307.

- Valle, F., Balbas, P., Merino, E. & Bolivar, F., (1991). The role of penicillin amidases in nature and in industry. *Trends Biochem Sci.*, **16**; 36-40.

- Vandamme, E. J. & Voets, J. P., (1973). Some aspects of the penicillin V-acylase produced by *Rhodotorula glutinis var. glutinis*. *Z Allg Mikrobiol.*, **13**; 701-710.

- Vandamme, E. J. & Voets, J. P., (1974). Microbial penicillin acylase. *Adv. Microbiol.*, **17**; 311-369.

- Vandamme, E. J., Voets, J. P. & Dhaese, A., (1971a). Study of penicillin-acylase produced by *Erwinia aroideae*. *Ann. Inst. Pasteur*, **121**; 435-446.

- Vandamme, E. J., Voets, J. P. & Beyaert, (1971b). *Meded Fae and bouwwetensch. Rijiks Univ. Gent.*, **36**; 577-605.

- Vandamme, E. J. & Voets, J. P., (1975). Properties of the purified penicillin V-acylase of Erwinia aroideae. *Experientia*, **31**; 140-143.

- Vandamme, E. J., (1980). Penicillin acylases and beta-lactamases. *Economic Microbiology*, (ed. Rose, A.H.) Academic Press, N.Y. Vol. **5**; pp. 468.
- Van Langen, L. M., De Vroom, E., Van Rantwijk, F. & Sheldon, R. A., (1999). Enzymatic synthesis of b-lactam antibiotics using penicillin G acylase in frozen media. *FEBS Lett.*, **456**; 89–92.

- Vasilescu, I., Vocia, M., Voinescu, R., Birladeanu, R., Sasarman, E. & Rafirotu, I., (1966).The synthesis of 6-APA by enzymatic hydrolysis of phenoxymethyl penicillin. *Antibiotics Adv. Res. Prod. Clin. Use* (Herold, M. and Gabriel, Z., Eds.). Butterworths, London, 518-520.

- Velasco, J. & Barredo, J. L., (2000). Environmentally safe production of 7-aminodeacetoxycephalosporanic acid (7-ADCA) using recombinant strains of *Acremonium chrysogenum*. *Nat. Biotechnol*., **18**; 857-861.

- Verweij, J. & deVroom, E., (1993). Industrial transformations of penicillins and cephalosporins. *Recl. Trav. Chim. Pays-Bas*, **112**; 66-81.

- Vincent, S., Thomas, A., Brasher, B. & Benson, J. D., (2003). Targeting of proteins to membranes through hedgehog auto-processing. *Nat. Biotechnol.*, **21**; 936-40. Erratum in: *Nat. Biotechnol.*, (2003). **21**; 1098.

- Waldschmidt-Leitz, E. & Bretzel, G., (1964). Ueber Penicillinamidase: Reinigung und Eigenschaften. *Z. Physiol. Chem*., **337**; 222-228.

- Wang, Q. C., Fei, J., Zhu, D. F. & Xu, L. G., (1986). Application of an immobilised penicillin acylase to the deprotection of N-phenylacetyl insulin. *Biopolymers*, **25**; 109-114.

- Warshel, A., Naray-Szabo, G., Sussman, F. & Hwang, J. K., (1989). How do Serine Protease Really Works? *Biochem*., **28**; 3629-3637.

- Watenpaugh, K. D., (1991). Macromolecular crystallography at cryogenic temperatures. *Curr. Opin. in Struct. Biol*., **1**; 1012-1015.

- Weaver, S. S. & Bodey, G. P., (1980). CI-867, a new semisynthetic penicillin: in vitro studies. *Antimicrob Agents Chemother*. **18**; 939-943.

- Weber, P. C., (1991). Physical principles of protein crystallization. *Adv. Prot. Chem.*, **41**; 1-36.

- Weber, P. C., (1997). Overview of protein crystallization methods. *Methods Enzymol*., **276**; 13-22.

- Wegman, M. A., Janssen, M. H. A., Van Rantwijk, F. & Sheldon, R. A., (2001). Towards biocatalytic synthesis of β-lactam antibiotics. *Adv. Synth. Catal.*, **343**; 559–576.

- Westbrook, E. M. & Naday, I., (1997). CCD area detectors. *Methods Enzymol.*, **276**; Sweet, R. M. and Carter, C., editors, Academic Press, Orlando, 244-268.

- Williams, R. S., Lee, M. S., Hau, D. D. & Glover, J. N., (2004). Structural basis of phosphopeptide recognition by the BRCT domain of BRCA1. *Nat. Struct. Mol. Biol*., **11**; 519-525.

- Wills, C., (1976). Controlling Protein Evolution. *Federation Proceedings*, **35**; 2098-2101.

- Worley, S., Schelp, E., Monzingo, A. F., Ernst, S. & Robertus, J. D., (2002). Structure and cooperativity of a T-state mutant of histidine decarboxylase from *Lactobacillus 30a*. *Proteins*, 46; 321-329.

- Wurtele, M., Renault, L., Barbieri, J. T., Wittinghofer, A. & Wolf, E., (2001). Structure of the ExoS GTPase activating domain. *FEBS Lett.*, **491**; 26-29.

- Xu, M., Southworth, M. W., Mersha, F. B., Hornstra, L. J. & Perler, F. B., (1993). *In vitro* protein splicing of purified precursor and the identification of a branched intermediate. *Cell*, **75**; 1371-1377.

- Xu, Q., Buckley, D., Guan, C. & Guo, H. C., (1999). Structural insights into the mechanism of intramolecular proteolysis. *Cell*, **98**; 651–661.

- Yang, F., Dauter, Z. & Wlodawer, A., (2000). Effects of crystal twinning on the ability to solve a macromolecular structure using multiwavelength anomalous diffraction. *Acta Cryst*., **D56**; 959-964.

- Yang, Y. L. & Yun, D. F., (1991). Cloning of GL-7-ACA acylase from *Pseudomonas sp*. 130 and its expression in *Escherichia coli*., *Chin. J. Biotech*., **7**; 99–107.

- Yang, Y., Yun, D., Guan, Y., Peng, H., Chen, J., He, Y. & Jiao, R., (1991). Cloning of GL-7-ACA acylase gene from *Pseudomonas sp.130* and its expression in *Escherichia coli*. *Chin. J. Biotech*., **7**; 99-107.

- Yeates, T. O., (1997). Detecting and overcoming crystal twinning. *Methods Enzymol*., **276**; 344-358.

- Yin, Y. W. & Steitz, T. A., (2004). The structural mechanism of translocation and helicase activity in T7 RNA polymerase. *Cell*, **116**; 393-404.

- Youshko, M. I., Van Langen, L. M., De Vroom. E., Van Rantwijk. F., Sheldon, R. A. & Svedas, V. K., (2002). Penicillin acylase-catalyzed ampicillin synthesis using a pH gradient: a new approach to optimization. *Biotechnol Bioeng*., **78**; 589–593.

- Zhang, X. J., Wozniak, J. A. & Matthews, B. W., (1995). Protein flexibility and adaptability seen in 25 crystal forms of T4 lysozyme *J. Mol. Biol*., **250**; 527-552.

- Zhou, H.,Wei, Z., Yang, Y. & Jiao, R. (1997). Studies on purification and properties of GL-7ACA acylase from CU334. *Acta Microbiol. Sinica*., **37**; 196-201.

- Zwickl, P., Kleinz, J. & Baumeister, W., (1994). Critical elelments in proteasome assembli. *Nat. struct. Biol*., **1**; 765-769.